AGE-RELATED CHANGES IN THE MORPHOPHYSIOLOGY OF THE TESTIS AND EPIDIDYMIS OF THE AFRICAN GREATER CANE RAT (*Thryonomys swinderianus* TEMMINCK, 1827)

BY

OMIRINDE JAMIU OYEWOLE

DVM, MSc. (Ibadan)

MATRIC NO: 101670

A Thesis in the Department of Veterinary Anatomy,

Submitted to the Faculty of Veterinary Medicine,

In partial fulfillment of the requirements for the degree of

DOCTOR OF PHILOSOPHY

of the

UNIVERSITY OF IBADAN

NOVEMBER, 2019

CERTIFICATION

I certify that this work was carried out by Dr. J.O Omirinde in the Department of Veterinary Anatomy, University of Ibadan, Ibadan, Nigeria.

_____

Major Supervisor

Professor B.O Oke

DVM, MSc., PhD (Ibadan), FCVSN

_____

Co-Supervisor

Dr S.G Olukole

DVM, MSc., PhD (Ibadan)

DEDICATION

This thesis is dedicated to my late father, Imam Abdul Wahab Ayinde Omirinde.

ACKNOWLEDGMENTS

All gratification is due to Almighty God, the most compassionate, the most merciful, for granting me a successful completion of this study. I also acknowledge Professor B.O Oke, my main supervisor, for his meticulous supervision. Sir, I am short of words to describe your mentorship that has dovetailed to father and son relationship. You are indeed a priceless gift to the Department and the University of Ibadan at large. I am also grateful to Dr. S.G Olukole, my co-supervisor, for his thoroughness as well as for his stimulating words that can encourage one to attempt lifting rock.

I am equally appreciative of the encouragements received from Prof. J.O Olopade (Dean, Faculty of Veterinary Medicine, University of Ibadan) in my starting the PhD programme. I say a big thank you sir. The moral support of Prof. P.C Ozegbe, Head of Department, Veterinary Anatomy, U.I is equally well acknowledged. I will not forget the support received from the academic staff of the Department; Drs O.O Aina, O Igado, M.O Akpan and M.A Essien. The assistance received from the technical staff is well appreciated. The contribution of postgraduate students was also significant and commendable. Special gratitude goes to Dr (Mrs) O.R Folarin for the technical assistance rendered in the preparation of fixatives for EM protocols.

The effort of Dr S.G Olukole in providing the linkage for carrying out the advanced aspects of my study (Electron-microscopy and Immunohistochemistry) at University of Pretoria, South Africa is also deeply appreciated. In this regard, I am grateful to Dr L. Du Plesis, The Manager of Electron-Microscopy unit, Department of Veterinary Anatomy and Physiology, UP for her painstaking efforts in taking me through EM protocols. The effort of her able assistant, Ms A. Lensik is also appreciated. The valuable assistance

rendered on immuno-histochemistry protocols by Mrs R. Phaswane of the Pathology Laboratory Unit is equally acknowledged.

My sincere gratitude goes to the Academic staff of University of Jos (UJ) more particularly the Dean of Faculty of Veterinary medicine, Prof. L.H Lombin, Head of Department, Dr. S.A Hena, academic and non-academic staff of the Department for their show of love. The moral and financial supports received from Drs B.S Audu (Dept. of Zoology) and S. Momoh (Dept. of Geology) of UJ is very much appreciated. It is important to show gratitude for the effort of Mr M.A Salawu, a final year student of Business Management, UJ in my Ph.D journey.

The duos of Drs. I Adeyemo and T.J Isola played significant role in the sourcing and transportation of the animals used for this study and I cannot hesitate to say thank you Sirs. In the same vein, the moral and kind support from Dr. F.M Lawal (Department of Veterinary surgery, UNILORIN), Dr. A.O Lawal (Veterinary and Livestock Services, Oyo State) and Dr. O.O Oloso are equally appreciated.

Finally, I want to record profound appreciation of my extended family, the Omirindes, including my mother, Alhaja F.A Omirinde, Mesr. Soliu, Ahmad, Monsur,Abdullahi, Ismail, Rasheedat, Moshood, Hafsat, Ismat and Mrs Toyin Adebiyi. I reserve my deepest appreciation to my rare gem, Mrs K. M Omirinde for her second to none perseverance during the course of this work and to my little kids, the triple F; Faezol, Farhan and Fahim. Your understanding is commendable. My sincere supplication is that God should grant us long life to be able to enjoy the fruits of our labour (Amen).

ABSTRACT

African Greater Cane Rat (AGCR) is a wild rodent currently being domesticated as an alternative source of animal protein in West African countries. Available research reports on the reproductive biology of the male AGCR have focused mainly on the adult without any information on age-related changes in the reproductive organs of the animal. This study was therefore designed to investigate age-related changes in the morphophysiology of the testis and epididymis of the AGCR.

Fifty-two AGCR of known ages obtained from a commercial farm were used for the study. The rats were randomly assigned into 4 groups (n=13). Group I [prepubertal: ≤4 months]; group II [pubertal: >4≤12 months]; group III [adult: >12≤30 months] and group IV [aged: >30 months]. All rats were acclimatised for 7 days. On day 8, blood samples were collected for serum hormonal assay [testosterone, Follicle Stimulating Hormone (FSH), Luteinising Hormone (LH) and oestrogen, and testis and epididymis were harvested. Semen characteristics (sperm motility, livability, sperm concentration) were studied from epididymal tissue. Light microscopy and transmission electron microscopy were used to study age-related morphological changes in testis and epididymis. Testicular and epididymal immunoreactivities to vimentin, S-100, neurofilament and Glial Fibrillary Acid Protein (GFAP) were also estimated using standard methods. Data were analysed using descriptive statistics and one-way ANOVA at $\alpha_{0.05}$.

There were significant increases in the concentration of testosterone (2.02±0.19, 3.85±0.29,4.12±0.15 ng/mL) and oestrogen (0.94±0.00, 1.48±0.4, 4.33±0.82 pg/mL) for prepubertal, pubertal and adult, respectively as age increases, while there were no significant differences in these hormones between adult and aged AGCR. The concentrations of FSH (12.33±0.83, 10.58±0.95, 9.250±0.6 mIU/mL)and LH (15.50±0.88, 12.83±1.20, 10.17±0.83 mIU/mL) decreased significantly for prepubertal, pubertal and adult, respectively, while the adult and aged were similar. No spermatozoa was observed for the prepubertal rats. Sperm motility and concentration (80.00±4.08%; 135.3±6.42 x 10^6 sperm/mL, respectively) significantly increased in adult rats compared to pubertal (62.50±4.79%; 101.50±7.96 x 10^6 sperm/mL) and aged rats (55.00±5.00%; 91.25±2.56 x 10^6 sperm/mL). However, sperm livability showed no significant difference

across pubertal, adult and aged rats. The canalisation of the seminiferous tubules was absent in prepubertal rats, while it showed significant increases from pubertal to aged. Spermatogonia and spermatocytes in prepubertal had more mitochondria compared to others. Sertoli cell nuclei were uniquely roundish in prepubertal compared to their triangular shape in pubertal, adult and aged. Also, epididymal epithelium changed from simple cuboidal in prepubertal to pseudostratified columnar in other groups. Vimentin, S-100, neurofilament and GFAP were markedly expressed in the testis and epididymis of adult AGCR compared to other groups.

Age-related morphophysiological changes in the testis and epididymis of African greater cane rats were established. Hence, the adult cane rat is recommended for breeding programme.

Keywords: African greater cane rat, Rat testis, Rat epididymis, Rat spermatozoa.
Word count: 444

TABLE OF CONTENT

Title Page		i
Certification		ii
Dedication		iii
Acknowledgments		iv
Abstract		vi
Table of Contents		viii
List of Figures		xv
List of Tables		xxiii
List of Abbreviations		xxiv
CHAPTER ONE		
1.0	INTRODUCTION	1
1.1	Background	1
1.2	Justification	3
1.3	Research Questions	4
1.4	Aim of the Study	5
1.5	Specific objectives	5
1.6	Significance of the Study	5
CHAPTER TWO		
2.0	LITERATURE REVIEW	6
2.1	Scientific Classification of African Greater Cane Rat	6
2.1.2	Distribution, Physical Features and Habitat	6
2.1.3	Economic, Nutritional and Research Potentials of Cane Rat	7
2.2	Male Reproductive Biology	10
2.2.1	Testicular Development	10
2.2.2	Testicular Morphology	12
2.2.2.1	Testicular Capsule and Peritubular (Boundary) Tissue	12
2.2.2.2	Testicular Germ Cells	13
2.2.2.3	Spermatogonia	15
2.2.2.4	Spermatocytes	15
2.2.2.4.1	Leptotene	16

2.2.2.4.2 Zygotene 16
2.2.2.4.3 Pachytene 16
2.2.2.4.4 Diplotene 17
2.2.2.4.5 Secondary Spermatocyte 17
2.2.2.5 Spermatids 17
2.2.2.6 Spermiogenesis 18
2.2.2.7 Spermiation 19
2.2.2.8 Spermatogenesis 20
2.2.2.9 Spermatozoa Structure 21
2.2.2.9.1 Spermatozoon head 21
2.2.2.9.2 Spermatozoon neck 22
2.2.2.9.3 Spermatozoon mid-piece 22
2.2.2.9.4 Spermatozoon tail 23
2.2.2.9.5 Spermatozoon axoneme structure 23
2.2.2.10 Sertoli Cell 24
2.2.2.11 Leydig Cell 26
2.3 Morphology of the Epididymis 27
2.3.1 Development of Epididymis 27
2.3.2 Gross Anatomy 28
2.3.3 Epididymal Histology and Ultrastructure 28
2.3.4 Specific Morphological Changes in the Testes and Epididymis with Age Advancement 31
2.3.5 Epididymal Function 32
2.3.6 Epididymal Sperm Storage 33
2.3.7.1Sperm Morphology 33
2.3.7.2 Sperm Morphometry 36
2.3.7.3 Sperm Motility 37
2.3.7.4 Sperm Concentration 37
2.4 Testicular and Epididymal innervations and astrocyte-likecell demonstration 37
2.4.1 Testicular and epididymal innervations 37

2.4.2 Astrocyte expression in the testes 41
2.5 The Physiology of S-100 and its Distribution in Mammalian Testis and Epididymis 41
2.6 Role and Distribution of Vimentin in Mammalian Testis and Epididymis 43
2.7 Sex hormone interplay in male mammals 44
2.7.1 Gonadotrophin Releasing Hormone 43
2.7.2 Luteinising Hormone 47
2.7.3 Follicle Stimulating Hormone 47
2.7.4 Testosterone 47
2.7.5 Estrogen 48
2.7.6 Progesterone 48
2.7.7 Age-Related Changes in the Hormonal Profile 50
CHAPTER THREE
3.0 **MATERIALS AND METHODS** 51
3.1 EXPERIMENT ONE 51
3.1.1 Gross morphological and MorphometricStudies of the Testis and Epididymis in Different Age-groups of The Cane Rat. 51
3.1.1.1 Experimental Animals 51
3.1.1.2 Experimental Design 51
3.1.1.3 Anaesthesia and Organ Excision 51
3.1.1.4 Determination of Testicular and Epididymal Morphometric Parameters 50
3.1.1.5 Statistical Analysis 52
3.2 EXPERIMENT TWO 53
3.2.1 Age-Related Changes in the Histology, Histochemistry, Morphometry and Ultrastructure of the Testis and Epididymis in African Greater Cane Rat 53
3.2.2 Experimental Animals 53
3.2.3 Experimental Design 53
3.2.4 Preparation of Secondary Fixative Solution for Light Microscopy 53
3.2.5 Preparation of Karnovsky Glutaraldehyde Fixative for Electron 53

Microscopy
3.2.6 Anaesthesia 53
3.2.7 Dissection and Perfusion 53
3.2.8 Organ Excision 54
3.2.9 Tissue Processing for Histology, Histochemistry and Histomorphometry 54
3.2.10 Processing of Cane rat Tissues for Electron Microscopy 55
3.2.11 Statistical Analysis 56
3.3 EXPERIMENT THREE 57
3.3.1 Age-Related Changes in the Sperm Parameters of the Testis and Epididymis in African Greater Cane Rat 57
3.3.2 Experimental Animals 57
3.3.3 Experimental Design 57
3.3.4 Anaesthesia and Organ Excision 57
3.3.5 Sperm Morphological Characteristics 57
3.3.6 Determination of Sperm Morphometrics 57
3.3.7 Evaluation of Sperm Motility 58
3.3.8 Determination of the testicular and epididymal sperm counts 58
3.3.9 Assessment of Livability (Live-dead) Ratio 58
3.3.10 Statistical Analysis 59
3.4 EXPERIMENT FOUR
3.4.1 Age-Related Changes in the Immunohistochemical Expression of Structural Proteins (Vimentin and S-100), Nerves (NF), Glial-like cells (GFAP) and Histochemical Demonstrations of Nerves Using Golgi-silver Techniques 60
3.4.2 Experimental Animals 60
3.4.3 Experimental Design 60
3.4.4 Anaesthesia and Perfusion 60
3.4.5 Tissue Processing for Golgi-Silver Staining Procedure 60

3.4.6 Tissue Processing for Immunohistochemical Localisation of Structural Protein as well as Nerve Fibres and Astrocyte-like Cells in the Testes and Epididymis of Cane Rat 61
3.4.7 Statistical Analysis 62
3.5 EXPERIMENT FIVE
3.5.1 Age-Related Changes in Serum Hormonal Profile of African Greater Cane Rat 64
3.5.2 Experimental Animals 64
3.5.3 Experimental Design 64
3.5.4 Anaesthesia 64
3.5.5 Blood Collection 64
3.5.6 Hormonal Assay Procedure 64
3.5.7 Statistical Analysis 65
CHAPTER FOUR
4.0 **RESULTS** 66
4.1 EXPERIMENT ONE 66
4.1.1 **Age-related Changes in the Testicular and Epididymal Gross Morphology and Morphometrics of African Greater Cane rat** 66
4.1.1.1 Testicular and Epididymal Gross Appearances in Different Age Groups of African Greater Cane Rat 66
4.1.1.2 Age-related Changes in the Morphometry of the Testis and Epididymis in African Greater Cane rat 69
4.2 EXPERIMENT TWO
4.2.1 **Age-related Changes in Histology, Histochemistry, Histomorphometry and Ultrastructure of the Testes and Epididymis of African Greater Cane Rat** 71
4.2.1.1 Histological Changes in the Testes of Different Age Groups of Cane rat 71
4.2.1.2 Masson Trichome and Periodic Acid Schiff Stainings of the Testes of Different Age groups of African Greater Cane Rat 71
4.2.3 Age-Related Changes in the Testicular Histomorphometry 72
4.2.3.1 Testicular Capsule Thickness and Percentage Capsular Tunic Thickness 72
4.2.3.2 Seminiferous Epithelial Height, Luminal Diameter and Tubular Diameter 72

4.2.4 Changes in the Testicular Ultrastructure with Age Advancement 89
4.2.4.1 Peritubular Tissue (Boundary Tissue) 89
4.2.4.2 Sertoli Cell 89
4.2.4.3 Spermatogonia 89
4.2.4.4 Spermatocyte 89
4.2.4.5 Leydig Cell 89
4.2.5 Histological Changes in the Epididymis of Different Age-groups of African Greater Cane Rat 104
4.2.6 Age-related Changes in the Content of Glycogen and Collagen Fibres in the Epididymis of the African Greater Cane Rat 104
4.2.7 Ultrastructural Changes in the Epididymis of African Greater Cane Rat 105
4.2.8 Age- related Changes in the HistomorphometricParameters of the Epididymis of the African Greater Cane Rat 146
4.2.8.1 Ductal Diameter 146
4.2.8.2 Ductal Luminal Diameter 146
4.2.8.3 Ductal Epithelial Height 146
4.2.8.4 Ductal Stereocilia Height 146
4.2.8.5 Periductal Muscle Coat Thickness 146
4.3 EXPERIMENT THREE 153
4.3.1 **Age-Related Changes in the Testicular and Epididymal Sperm Parameters in Cane Rat** 153
4.3.2 Spermatozoa Morphological Characteristics 153
4.3.3 Sperm Morphometrics 153
4.3.4 Sperm Motility 154
4.3.5 Testicular and Epididymal Sperm Count 154
4.3.6 Sperm Livability (Live-dead) Ratio 154
4.4 EXPERIMENT FOUR
4.4.1 Age-Related Changes in the Immunohistochemical Expressions of Structural Proteins (Vimentin and S-100) as well as Nerves and Glial Cells in the Testis and Epididymis 159
4.4.1.1 Immunohistochemical Expressions of Structural Protein (Vimentin and S-100)in the Testis and Epididymis 159

4.4.1.2 Histochemical and Immunohistochemical Demonstrations of Nerves and Glial-like Cells (Astrocyte-like) in the Testis and Epididymis by using Golgi-silver techniques, anti NF 20 and anti-GFAP 178

4.5 EXPERIMENT FIVE

4.5.1 Age-Related Changes in the Serum Hormonal Profile of African GreaterCane Rat 211

4.5.1.1 Serum Testosterone Level 211

4.5.1.2 Serum Luteinising Hormone Level 211

4.5.1.3 Serum Follicle Stimulating Hormone Level 211

4.5.1.4 Serum Estrogen Level 211

4.5.1.5 Serum Progesterone Level 211

CHAPTER FIVE

5.0 Discussion 219

5.1 Conclusion 232

5.2 Contribution to Knowledge 232

5.3 Further Research 233

REFERENCES 234

LIST OF FIGURES

Figure 2.1	Photograph of the African Greater Cane Rat.	9
Figure 2.2	Equine Seminiferous Tubule.	14
Figure 2.3	Morphological Appearances of Spermatozoa in Different Animals	35
Figure 2.4	Schematic Diagram of the Testicular Innervation of Rat.	38
Figure 2.5	Regulation of Hypothalamic-pituitary-testis	46
Figure 2.6	Stages Involved in Steroidogenesis	49
Figure 4.1	Photographs of the Male Reproductive Organs in Cane Rat in Situ	68
Figure 4.2	Photographs of the Epididymis in the African Greater Cane Rat	69
Figure 4.3	Photomicrographs of the Testes of Different Age Groups of African Greater Cane Rat with Their Capsular Coverings.	74
Figure 4.4	Age-related Changes in the Testicular Capsule Thickness of Different Age Groups of African Greater Cane Rat	75
Figure 4.5	Age-related Changes in the Percentage capsular Tunic Thickness of the Testes of Different Age Groups ofAfrican Greater Cane Rat.	76
Figure 4.6	Photomicrographs of the Testicular capsule of different age Groups of African Greater Cane Rat with their Capsular Coverings.	77
Figure 4.7	Age-related Changes in the Intensity of Masson Trichome Staining of the Testicular Capsule in African Greater Cane Rat.	78
Figure 4.8	Photomicrographs of the Testicular Capsule of Different Age Groups of African Greater Cane Rat with their Capsular Coverings.	79
Figure 4.9	Age-related Changes in Intensity of PAS Staining of the Testicular Capsule in African Greater Cane Rat.	80
Figure 4.10	Photomicrographs of the Testis of Different Age Groups of African Greater Cane Rat.	81
Figure 4.11	Photomicrograph of the Testis Of Pre-Pubertal (4-Month) Cane Rat.	82
Figure 4.12	Age-related Changes in the Testicular Histomorphometric	83

Parameters of African Greater Cane Rat

Figure 4.13 Masson's Trichome Staining of the Testis of Different Age Groups of AGCR 84

Figure 4.14 Age-related Changes in Staining Intensity of Masson Trichome Staining of the Testicular Parenchyma in African Greater Cane Rat. 85

Figure 4.15 PAS Stainings of The Testis of Different Age Groups of AGCR 86

Figure 4.16 Age-Related Changes in Staining Intensity of PAS Staining of the Testicular Parenchyma in African Greater Cane Rat. 87

Figure 4.17 Photomicrographs of the Testicular Interstitum of Different Age Groupsof AGCR. 88

Figure 4.18 Transmission Electron Micrographs of the Seminiferous Epithelium in the Testes of Different Age Groups of African Greater Cane Rat 91

Figure 4.19 Transmission Electron Micrographs of the Testicular Boundary Tissue of the African Greater Cane Rat. 92

Figure 4.20 Transmission Electron Micrographs of the Basal Aspect of Sertoli Cell of African Greater Cane Rat. 93

Figure 4.21 Transmission Electron Micrographs of the Perinuclear Area of Sertoli Cell of African Greater Cane Rat. 94

Figure 4.22 Transmission Electron Micrographs of the Testicular Type A pale Spermatogonium in Cane Rat. 95

Figure 4.23 Transmission Electron Micrographs of the Type B Spermatogonium in the Testis of the African Greater Cane Rat. 96

Figure 4.24 Transmission Electron Micrographs of the Intermediate Spermatogonium Type in the Testis of the African Greater Cane Rat. 97

Figure 4.25 Transmission Electron Micrographs of the preleptotene Spermatocytes of the African Greater Cane Rat. 98

Figure 4.26 The TEM of Leptotene Spermatocytes of Cane Rat. 99

Figure 4.27 The TEM of Zygotene Spermatocytes of Cane Rat. 100

Figure 4.28 The TEM of Pachytene Spermatocytes of Cane Rat. 101

Figure 4.29 The TEM of the Diplotene Spermatocytes of Cane Rat 102

Figure 4.30	Transmission Electron Micrographs of the Leydig Cells of the AGCR	103
Figure 4.31	Schematic Representation of the African Greater Cane Rat Epididymis Illustrating Partitioning by Connective Tissue Septae	106
Figure 4.32	Photomicrograph of the Subdivisions of the Initial Segment (IS) of the Epididymis in Pubertal AGCR.	107
Figure 4.33	Photomicrograph of the Epididymal Segments in Pubertal AGCR	108
Figure 4.34	Photomicrographs of the Proximal Initial Segment of the Epididymis in Different Age Groups of AGCR	109
Figure 4.35	Masson's Trichrome Staining of the Proximal Initial Segment of Epididymis in Different Age Groups of AGCR	110
Figure 4.36	Age-related Changes in Intensity of Masson Trichome Staining of the Proximal Initial Segment in AGCR.	111
Figure 4.37	PAS Staining of the Proximal Initial Segment of Epididymis in Different Age Groups of AGCR.	112
Figure 4.38	Chart Illustrating Age-related Changes in Intensity of PAS Staining of the Proximal Initial Segment in AGCR.	113
Figure 4.39	Photomicrographs of the Middle Region of the Initial Segment of Epididymis in Different Age Groups of AGCR	114
Figure 4.40	Masson's Trichrome Staining of the Middle Initial Segment of Epididymis in Different Age Groups of AGCR	115
Figure 4.41	Age Related Changes in Intensity of Masson Trichome staining of the middle initial segment in AGCR.	116
Figure 4.42	PAS Staining of the Middle Region of the Initial Segment of Epididymis in Different Age Groups of AGCR.	117
Figure 4.43	Age-related Changes in Intensity of Periodic Acid Schiff Staining of the Middle Initial Segment in AGCR.	118

Figure 4.44	Photomicrographs of the Distal Initial Segment of Epididymis in Different Age Groups of AGCR.	119
Figure 4.45	Masson's Trichrome Staining of the Distal Initial Segment of Epididymis in Different Age Groups of AGCR.	120
Figure 4.46	Age-related Changes in Intensity of Masson Trichome Staining of the Distal Initial Segment in AGCR.	121
Figure 4.47	PAS Staining of the Distal Initial Segment of Epididymis in Different Age Groups of AGCR.	122
Figure 4.48	Age-related Changes in Intensity of PAS Staining of the Distal Initial Segment in AGCR.	123
Figure 4.49	Photomicrographs of the caput Segment of Epididymis in Different Age Groups of AGCR.	124
Figure 4.50	Masson's Trichome Stainings of the Caput Segment of Epididymis in Different Age Groups of AGCR	125
Figure 4.51	Chart Illustrating Age-related Changes in Intensity of Masson's Trichome Staining of the Caput Segment in AGCR.	126
Figure 4.52	PAS staining of the Caput Segment of Epididymis in the Different Age Groups of AGCR	127
Figure 4.53	Age-related Changes in Intensity of PAS Staining of the Middle Caput Segment in AGCR.	128
Figure 4.54	Transmission Electron Micrographs of the Basal Aspect of Caput Epididymis of the African Greater Cane Rat.	129
Figure 4.55	Photomicrographs of the Corpus Segment of Epididymis in Different Age Groups of AGCR .	130
Figure 4.56	Masson's Trichrome Staining of the Corpus Segment of Epididymis in the Different Age Groups of AGCR .	131
Figure 4.57	Age-related Changes in Intensity of Masson Trichome Staining in the Corpus Segment of AGCR.	132

Figure 4.58	PAS Staining of the Corpus Segment of Epididymis in the DifferentAge Groups of AGCR .	133
Figure 4.59	Age-related Changes in Intensity of PAS Staining in the Corpus Segment of AGCR.	134
Figure 4.60	Transmission Electron Micrographs of the Corpus Epididymis of Cane Rat	135
Figure 4.61	Transmission Electron Micrographs of the Basal Aspect of the Principal Cell in Corpus Epididymis of Cane Rat	136
Figure 4.62	Transmission Electron Micrographs of the Perinuclear Aspect of the Principal Cell in Corpus Epididymis of Cane Rat.	137
Figure 4.63	Transmission Electron Micrographs of the Supranuclear Aspect of the Principal Cell in Corpus Epididymis of Cane Rat	138
Figure 4.64	Photomicrographs of the Cauda Segment of Epididymis in Different Age Groups of AGCR	139
Figure 4.65	Masson's Trichrome Staining of the Caudal Segment of Epididymis in the Different Age Groups of AGCR	140
Figure 4.66	Age-related Changes in Intensity of Masson's Trichome Staining in the Cauda Epdidymal Segment of AGCR.	141
Figure 4.67	PAS staining of the Caudal Segment of Epididymis in the Different Age Groups of the AGCR .	142
Figure 4.68	Age-related Changes in Intensity of PAS Staining in the Cauda Epididymal Segment of AGCR.	143
Figure 4.69	Transmission Electron Micrographs of the Perinuclear Aspect of the Cauda Epididymal Principal Cells in AGCR.	144
Figure 4.70	Transmission Electron Micrographs of the Supranuclear Aspect of Principal Cell of Cauda Epididymis in the Cane Rat.	145
Figure 4.71	Photomicrographs of the Cauda Epididymal Spermatozoa of the African Greater Cane Rat	155
Figure 4.72	Photomicrographs of Vimentin Expression in the Testis of DifferentAge groups of AGCR.	160
Figure 4.73	Age-related Changes in Intensity of Vimentin Expression in the Testicular Parenchyma in AGCR.	161
Figure 4.74	Photomicrographs of Vimentin Expression in the Proximal Initial Segment of Epididymis in AGCR.	162

Figure 4.75	Photomicrographs of Vimentin Expression in the Middle Initial Segment of Epididymis in AGCR.	163
Figure 4.76	Photomicrographs of Vimentin Expression in the Distal Initial Segment of Epididymis of AGCR.	164
Figure 4.77	Photomicrographs of Vimentin Expression in the Caput Epididymal Segment of AGCR.	165
Figure 4.78	Photomicrographs of Vimentin Expression in the Corpus Epididymal Segment of AGCR.	166
Figure 4.79	Photomicrographs of Vimentin Expression in the Cauda Epididymal Segment of AGCR.	167
Figure 4.80	Age-related Changes in intensity of VimentinExpression in the Epididymal Ducts of AGCR.	168
Figure 4.81	Photomicrographs of S-100 Expression in the Testis of Different Age Groups of AGCR.	169
Figure 4.82	Age-related Changes in Signal Intensity of S-100 Expression in the Testicular Parenchyma in AGCR.	170
Figure 4.83	Photomicrographs of S-100 Expression in the Proximal Initial Segment of Epididymis in AGCR.	171
Figure 4.84	Photomicrographs of S-100 Expression in the Middle Initial Segment of Epididymis in AGCR.	172
Figure 4.85	Photomicrographs of S-100 Expression in the Distal Region of the Initial Segment of Epididymis in AGCR.	173
Figure 4.86	Photomicrographs of S-100 Expression in the Caput Segment of Epididymis in AGCR.	174
Figure 4.87	Photomicrographs of S-100 Expression in the Corpus Epididymal Segment in AGCR.	175
Figure 4.88	Photomicrographs of S-100 Expression in the Caudal Epididymal Segment in AGCR.	176
Figure 4.89	Age-related Changes in Intensity of S-100 Expression in the Epididymal Segments in AGCR.	177
Figure 4.90	Golgi Staining of the Testis of Different Age Groups of the AGCR.	180
Figure 4.91	Age-related Changes in Intensity of Golgi-silverStaining	181

of the Testicular Capsule in AGCR.

Figure 4.92 Photomicrographs of the Testis of Different Age Groups of AGCR. 182

Figure 4.93 Age related Changes In Intensity of Golgi-silver Staining of the Testicular Parenchyma in AGCR 183

Figure 4.94 Golgi Staining of the Proximal Initial Segment (PIS) of the Epididymisin Different Age Groups of AGCR. 184

Figure 4.95 Golgi Staining of the Middle Initial Segment (MIS) of the Epididymis in the Different Age Groups of AGCR 185

Figure 4.96 Golgi Staining of the Distal Initial Segment (DIS) of the Epididymis in the Different Age Groups of AGCR. 186

Figure 4.97 Golgi Staining of the CAPUT Epididymis in the different Age Groups of AGCR. 187

Figure 4.98 Golgi Staining of the CORPUS Epididymis in the Different Age Groups of AGCR . 188

Figure 4.99 Golgi Staining of the CAUDA of the Epididymis in the Different Age Groups of the AGCR . 189

Figure 4.100 Age-related Changes in Intensity of Golgi-silver Impregnation Staining of the Epididymal Segments in AGCR. 190

Figure 4.101 Photomicrographs of Neurofilament Expression in the Testicular Capsule of Different Age Groups of AGCR. 191

Figure 4.102 Age-related Changes in Intensity of Neurofilament Expression in the Testicular Capsule in AGCR. 192

Figure 4.103 Photomicrographs of Neurofilament Expression in the Testis of Different Age Groups of AGCR. 193

Figure 4.104 Age-related Changes in Signal Intensity of Neurofilament Expression in the Testicular Parenchyma in AGCR. 194

Figure 4.105 Photomicrographs of Neurofilament Expression in the Proximal Initial Segment of Epididymis in AGCR. 195

Figure 4.106 Photomicrographs of Neurofilament Expression in the Middle Initial Segment of Epididymis in AGCR. 196

Figure 4.107 Photomicrographs of Neurofilament Expression in the Distal initial Segment of Epididymis in AGCR. 197

Figure 4.108 Photomicrographs of Neurofilament Expression in the Caput segment of epididymis in AGCR. 198

Figure 4.109 Photomicrographs of Neurofilament Expression in the Corpus Epididymal Segment in AGCR. 199

Figure 4.110 Photomicrographs of Neurofilament Expression in the Caudal Epididymal Segment in AGCR. 200

Figure 4.111 Age-related Changes in Intensity of Neurofilament Expression in the Epididymal Segments in AGCR. 201

Figure 4.112 Photomicrographs of Glial Fibrillary Acid Protein (GFAP) Expression in the Testis of Different Age Groups of AGCR. 202

Figure 4.113 Age-related Changes in Intensity of Glial Fibrillary AcidProtein (GFAP) Expression in the Testicular Parenchyma in AGCR. 203

Figure 4.114 Photomicrographs of GFAP Expression in the Proximal Initial Segment of Epididymis in AGCR. 204

Figure 4.115 Photomicrographs of GFAP Expression in the Middle Initial Segment of Epididymis in AGCR. 205

Figure 4.116 205 Photomicrographs of GFAP Expression in the Distal Initial Segment of Epididymis in AGCR. 206

Figure 4.117 Photomicrographs of GFAP Expression in the Caput Segment of Epididymis in AGCR. 207

Figure 4.118 Photomicrographs of GFAP Expression in the Corpus Epididymal Segment in AGCR. 208

Figure 4.119 Photomicrographs of GFAP Expression in the Caudal Epididymal Segment in AGCR. 209

Figure 4.120 Age-related Changes in Intensity of GFAP Expression in the Epididymal Segments in AGCR. 210

Figure 4.121 Age-related Changes in the Testosterone Level in AGCR. 213

Figure 4.122 Age-related Changes in the Luteinising Hormone Level in 214

AGCR.

Figure 4.123 Age-related Changes in the Follicle Stimulating Hormone Level in AGCR. 215

Figure 4.124 Age-related Changes in the Estrogen Level in AGCR. 216

Figure 4.125 Age-related Changes in the Progesterone Level in AGCR 217

LIST OF TABLES

Table 3.1. List of Antibodies Used for Immunohistochemical Labeling. 63

Table 4.1. Age-related Changes in the Biometric Parameters of the Testis and Epididymis of African Greater Cane Rat 70

Table 4.2A. Age-related Changes in Epididymal Ductal Diameter of the African Greater Cane Rat 148

Table 4.2B. Age-related Changes in Epididymal Luminal Diameter of the African Greater Cane Rat. 149

Table 4.2C Age-related Changes in Epididymal Ductal Epithelial Height of the African Greater Cane Rat. 150

Table 4.2D Age-related Changes in Epididymal Stereocilia Height of the African Greater Cane Rat. 151

Table 4.2E Age-related Changes in Epididymal Perimuscular Coat Thickness of the African Greater Cane Rat. 152

Table 4.3 Age-related Changes in Sperm Morphometrics of the African Greater Cane Rat 156

Table 4.4. Age-related Changes in the Testicular And Epididymal Sperm Parameters of the African Greater Cane Rat 157

Table 4.5. Age-related Changes in the Morphological Characteristics of the spermatozoa in the African Greater Cane Rat 158

Table 4.6. Age-related Changes in the Serum Sex Hormone Levels of the African Greater Cane Rat. 218

LIST OF ABBREVIATIONS

ABC	Avidin Biotin Complex
AC	Apical Cell
AGCR	African Greater Cane Rat
AR	Acrosomal Region
BC	Basal Cell
Bl	Basal Lamina
BM	Basement Membrane
BSA	Bovine Serum Albumin
BW	Body Weight
CAW	Caudal Width
CB	Chromatoid Body
CC	Clear Cell
CGRP	Calcitonin Gene-Related Peptide
CNS	Central Nervous System
CP	Connecting Piece
CPW	Corpus Width
CW	Caput Width
DAB	3,3'-diaminobenzidine
DBH	Dopamine Beta Hydroxylase
DD	Ductal Diameter
DEH	Ductal Epididymal Height
DHEA	Dehydroepiandrosterone
DHT	Dihydrotestosterone
DIS	Distal Initial Segment
DLD	Ductal Luminal Diameter
DNA	Deoxyribose Nucleic Acid

DPX	Dibutyl phthalate Xylene
DSH	Ductal Stereocilia Height
EDL	Electron Dense Layer
EL	Epididymal Length
ELISA	Enzyme-Linked Immunosorbent Assay
EM	Electron Microscopy
EP	End Piece
ES	Elongating Spermatid
EW	Epididymal Weight
FS	Fibrous Sheath
FSH	Follicle Stimulating Hormone
GC	Golgi Complex
GFAP	Glial Fibrillary Acid Protein
GnRH	Gonadotropin Releasing Hormone
HC	Halo Cell
hCG	Human Chorionic Gonadotropin
HP	Hypogastric Plexus
IF	Implantation Fossa
ISN	Inferior Spermatic Nerve
IUCN	International Union for Conversation
LH	Luteinising Hormone
LH	Luteinising Hormone
Mi	Mitochondria
MIS	Middle Initial Segment
MP	Mid Piece
MPL	Mid Piece Length
MT	Masson Trichome

MV	Macrovesicle
MVB	Multivesicular Bodies
NF	Neurofilament
NPY	Neuropeptide Y
PAS	Periodic Acid Schiff
PBS	Phosphate Buffer Saline
PC	Principal Cell
PIS	Proximal Initial Segment
PMCT	Periductal Muscle Coat
PP	Principal Piece
PT	Peritubular Tissue
rER	Rough Endoplasmic Reticulum
RP	Renal Plexus
RS	Round Spermatid
RTW	Relative Testicular Weight
S-100	Saturated 100
sER	Smooth Endoplasmic Reticulum
SHBG	Sex Hormone-Binding Globulin
SHD	Sperm Head Diameter
SHL	Sperm Head Length
SP	Substance P
SSN	Superior Spermatic Nerve
ST	Seminiferous Tubule
STL	Sperm Tail Length
SWL	Sperm Whole Length
TA	Tunica Albuginea
TC	Testicular Circumference

TEH	Testicular Epididymal Height
TH	Tyroxine Hydroxylase
TL	Testicular Length
TLD	Testicular Luminal Diameter
TV	Tunica Vaginalis
TW	Testicular Weight
VIP	Vasoactive Intestinal Peptide

CHAPTER ONE

1.0 INTRODUCTION

1.1 Background

The African greater cane rat (*Thryonomys swinderianus* Temminck, 1827) [AGCR] otherwise referred to as grasscutter or marsh cane rat is an hystricomorphic grass-eating rodent found majorly in the several savanna biotic zones of the rainforest of sub-Sahara Africa. (Happold, 1987; Monadjem *et al.*, 2015). It is characterized by a large size, long coarse hairs, massive blunt head, short limbs and a relatively short tail (Happold, 1987). The male cane rat attains sexual maturity at about 8 months of age and can live up to 4 years in captivity (Happold, 1987; Soro *et al*., 2014).

The cane rat is a recognised excellent source of protein with reduced fat per unit weight relative to rabbit and chicken and also contains high calcium and phosphorus (Jori *et al*., 1995; Juste *et al*., 1995; Fayenuwo *et al*., 2003) which accounts for its vigorous exploitation for meat through aggressive hunting and bush burning. It is known to contribute to the domestic and foreign earnings of most contries in the South of the Sahara where its meat is expensively sold and prefentially demanded over other wild rodents (Baptist and Mensah, 1986; Ntiamoa-Baidu, 1998; Asibey and Addo, 2000). Currently, this rodent in Nigeria and other neighboring West Africa countries is being domesticated for increased stocking and intensification of production (Adu *et al*., 2005) to mitigate the existing acute insufficient protein in the face of increasing demand for livestock products (Adekola and Ogunsola, 2009).

The mammalian reproductive biology generally entails knowledge of the structure and function of male reproductive system crucial for suitable management, breeding and reproductive studies (Simões *et al*., 2016). The reproductive system in male mammals is composed of two testes, a paired excurrent duct system consisting of efferent ductules, epididymis and deferent duct and accessory sex glands (Dyce *et al*., 2002). The paired mammalian testes are involved in spermatozoa and sex steroid hormone production, being both exocrine and endocrine in glandular activities (Costa *et al.,* 2006). They are constituted of two compartments: a series of convoluted seminiferous tubules containing Sertoli cells and germ cells and the interstitial compartment housing blood and lymphatic capillaries, myoid, Leydig cells and connective tissue fibres (Costa *et al.,* 2006). Gonadal steroids, androgens and estrogens have been shown to be very important in the male reproductive function (Nilsson and

Gustafsson, 2002; Hess, 2003; Welsh *et al.,* 2009). Unlike the testicular composition, the epididymis remains an essential site for spermatozoa maturation and storage (Cornwall, 2009). It is divided into different segments and zones by connective tissue stroma and has epithelium that houses several cell types with diverse functions (Robaire *et al*., 2006).

The regulation of testicular functions have been found not to be limited to the gonadal steroids and gonadotropins. Recent evidences have associated testicular nerves with the production of growth factors and neurotransmitters mostly cathecolamines and neuropeptides in the control of the gonadal function (Frungieri *et al.,* 2000; Wrobel and Schenk, 2003). These neurotransmitters in the presence or absence of hypophyseal hormones, is validated by numerous studies to be capable of triggering receptors on the Leydig cells, Sertoli cells and smooth muscle cells of the testis (Mayerhofer *et al.,* 1990; Setchell*et al*., 1994; El-Gehani *et al.,* 1998). Several neuronal markers have been utilized to localise testicular nerves around the branches of the testicular artery, interstitial Leydig cells and seminiferous tubules (Kulkarni *et al.,* 1992; Tamura *et al.,* 1996; Lakomy *et al.,* 1997; Wrobel and Moustafa, 2000). Conspicuous evidence of abundant innervations has been reported in the testis of prepubertal pigs in a study that investigated age-related changes in the density, distribution pattern and neurochemical coding of nerve fibers of boars from postnatal period to adulthood (Wrobel and Brandl, 1998).

Similarly, neuronal fibres in the epididymis have been localised within the perimuscular coat, sub-epithelial regions and in the coat of vessels within the interstitium (Kempinas *et al.,* 1998; Ligoury *et al*., 2013). The distribution pattern in the epididymis has been found to be segment- specific with the cauda segment having the highest nerve ramifications owing its thick muscular wall (Kaleczyc *et al*., 1993). The neurotransmitters in the epididymal nerves have been suggested to be important in mediating epididymal epithelial cell function of electrolyte transport and protein processing (Chan *et al*., 1994; Ricker *et al*., 1996).

It is important to know that the morphophysiological changes in the male reproductive system especially the gonads (testes) and epididymis in relation to age differences is becoming popular subject of interest (Haidl *et al*., 1996). Prominent changes in the testis and epididymis of mammals as reported by earlier investigators include;

thickened and plicated seminiferous tubular basal lamina with irregular projections into seminiferous epithelium in advanced senescence, thickened tunica abuginea, germ cell degeneration and decrease tubular diameter, modification in junctional complexes, Leydig cell hyperplasia, numerous lipofuscin accumulation in both testicular and epididymal epithelium and decrease in number and proportion of principal and basal cells with concomitant increase in halo cells in all segments of the epididymis (Andrew, 1971; Johnson and Neaves, 1981; Holstein *et al. ,* 1988; Lowseth *et al.,* 1990; Nipken and Wrobel, 1997; Wang *et al*., 1999; Calvo *et al*., 1999; Pastor *et al*., 2011). The detailed understanding of these age-related changes and their functional implications as it pertains to male grasscutter reproductive biology is highly essential owing to the fact that in cane rat breeding, only one male is used for mating several females (Soro *et al*., 2014).

The existing reports on reproductive biology of African greater cane rats; efferent duct ultrastructure (Aire and Van der Merwe, 2003); morphology of epididymis, accessory sex gland and penis, structural, ultrastructural and immuhistochemical features of seminal vesicle and coagulating gland (Adebayo *et al*., 2009; Adebayo and Olurode, 2010; Adebayo *et al.,* 2014,2015 respectively); sperm morphological characteristics, gonadal and extra gonadal sperm reserves, biometrical observation on the testes and epididymis, testicular and epididymal histomorphometry (Olukole *et al.,* 2009, 2010) focused mainly on the adult group of AGCR. There is paucity of information on the age-related changes in the morphophysiology of the testes and epididymis of AGCR. Hence, this study hopes to fill this gap and possible results emanating from this study will constitute baseline data on age-related changes in the reproductive biology of AGCR. In addition, due to the potential of this animal to become an indigenous laboratory animal for biomedical research in Africa (Opara, 2010) as well as being a rich source of animal protein (Bruntup and Aina, 1999), data to be generated would be beneficial to the rodent researcher, wildlife veterinarian and farmers.

1.2 Justification

Considering the huge economic, nutritional and possible research potentials of African greater cane rats, the ongoing increased intensification of the production practices targeted at actualising the potentials is still being retarded by scanty reports on its reproductive biology most especially as it is influenced by variation in age

(Yeboah and Adamu, 1995; Addo *et al.,* 2002). In addition, there is dearth of information on the age-related changes in the neuronal and glial cell expressions in the testis and epididymis of the African greater cane rat.

1.3 Research Questions

- Specific age-dependent gross morpho-biometrical changes occur in the testis and the epididymis of mammals (Don White *et al*., 2005; Kangawa *et al*., 2016).
  - *i. How do testicular and epididymal morphological characteristics change with age in AGCR?*
- Histological, histochemical and ultra-structural details in the testicular and epididymal architecture change with age (Calvo *et al*., 1999; Morales *et al*., 2004).
  - *ii.* What is the trend of histological, histochemical and ultrastructural changes in testicular and epididymal architecture across the different age-groups of AGCR*?*
- The gonadal and extragonadal sperm reserves are affected by age variation (Robaire *et al*., 2006).
  - ***iii.*** *What is the pattern of sperm reserves in testes and epididymides across different age groups of AGCR?*
- The distribution of Vimentin, S-100,neuronal and glial-like cells in both mammalian testes and epididymis is influenced by age variation (Wrobel and Brandl, 1998; Gong *et al*., 2009; Czykier*et al*., 2010; El–Desouki *et al.,* 2017; Falade *et al*., 2017).
  - *iv. What is the distribution pattern of vimentin, S-100, neuronal and glial-like cells in the testes and epididymides of AGCR of different age groups?*
- Reproductive integrity can be evaluated in the male from the level of follicle stimulating, luteinising, testosterone and estradiol hormones in circulation (Uboh *et al*., 2007).
  - *v. What is the pattern of sex hormone levels in different age groups of AGCR?*

1.4 Aim of the Study

This study is aimed at investigating age-related changes in the morphophysiology of the testis and epididymis of the African greater cane rat.

1.5 Specific Objectives

This study aims at investigating the following in the different age groups of AGCR:

i. To describe the gross morphology and morphometry of the testis and epididymis
ii. To characterize the variation in the histology, histochemistry, histomorphometry and ultrastructure of the testis and epidiymis
iii. To assess the patterns of the gonadal and extra gonadal sperm morphological characteristics and spermiogram
iv. To determine the immunohistochemical expression of structural proteins (Vimentin and S-100), nerves (Neurofilament), glial-like cells (Glial fibrillary acid proteins) as well as histochemical demonstration of nerves using Golgi silver techniques
v. To determine the serum hormonal profiles in AGCR with respect to age variations.

1.6 Significance of Study

i. The changes in the structure and function with advancement in age of this animal will be better understood.
ii. This study will generate data that will be beneficial to cane rat breeders, wild life veterinarians and rodent researchers

CHAPTER TWO

2.0 LITERATURE REVIEW

2.1 Scientific Classification of the African Greater Cane rat

The African greater cane rat (*Thryonomys swinderianus* Temminck, 1827) [AGCR] is a wild herbivorous rodent popularly known as the grasscutter,marsh cane rat and cane cutter in most countries of east, west and southern African continent (Happold, 1987). Based on scientific classification, the taxonomy of AGCR is described as follows;

Kingdom: Animalia

Phylum: Chordata

Class: Mammalia

Order: Rodentia

Sub order: Hystricomorpha

Infraorder: Hystricognathi

Family: Thryonomidae

Genus: *Thryonomys*

Species: *Thryonomys swinderianus* (Greater cane rat) (Temminck, 1827)

2.1.2 Distribution, Physical Features and Habitat

Thryonomis swinderianus is found majorly in the several savanna biotic zones and to a lesser extent in the grassy regrowth areas on the fringes of the rainforest of sub Sahara Africa. (Happold, 1987; Monadjem *et al*., 2015). It is also found in the grassy zones of Southern Africa more specifically in countries like Namibia, Botswana, Zimbabwe, Mozambique and South Africa (van der Merwe, 1999). It is rarely found in the 15°N of the northwestern part of the Africa and in the 5-10°N in the North-eastern Africa (Happold, 1987). In spite of obvious evidence that the population number of AGCR is rapidly declining due to urbanization especially around large urban settlements in sub Sahara Africa as well as decimation through aggressive hunting, AGCR is still being considered by the International Union for Conservation (IUCN) as least concern or threatened animal (Hoffman, 2008). The detailed

description of the physical features of African greater cane rat was documented by Happold (1987). The AGCR is known to be an extremely large rodent characterized by long coarse hairs, massive blunt head with broad flattened muzzle, small eyes, ventrally situated mouth, short and rounded ears, short limbs and a relatively short tail (Happold, 1987). The tail is thick at the base and tapers at the tip. It has a set of broad orange-coloured upper incisor teeth. The AGCR in the wild can be found in the swamps, semi-aquatic habitats, in long grass savanna where grass-cover is dense, in habitats that are subjected to seasonal flooding as well as in fields of sugarcane, maize and guinea corn (Bishop, 1984; Happold, 1987).

Thryonomis swinderianus is the next largest rodent of African origin after the Cape porcupine and has an average body weight of 4.54 kg with a weight range of (3.18-5.22 kg) in adult males and an average weight of 3.58kg with a weight rangeof (3.41-3.8) in adult females (Skinner andSmithers, 1990). The female cane rats give birth at least once a year and more frequently in some areas to litters of two to four fully furred young ones with eyes opened and can follow the mother within an hour of birth (Bishop, 1984).The gestation as well as the weaning periods span between 132-172days and 4-6 weeks respectively (Aluko *et al*., 2014). Sexual maturity in the female is attained at about seven months which could for the first time litter at about one year of age (Asibey, 1974). Similarly, male cane rats attain sexual maturity at about 8 months of age and can live up to 4 years in captivity (Happold, 1987; Soro *et al*., 2014). Generally, the age of AGCR in captive breeding is mostly estimated using birth registration and dental formula (Adjanohoun, 1989). It is important to mention also that in AGCR rearing, the common practice is the use of only one male for mating several females which underscores the crucial need for the male to be healthy reproduction-wise (Soro *et al*., 2014).

2.1.3 Economic, Nutritional and Research Potentials of African Greater Cane Rat

Among the wild rodents of Southern Sahara, cane rat remains the favorites (Asibey and Eyeson, 1973; Clottey, 1981). It is reputed for excellent source of protein even over rabbit and chicken (Fayenuwo *et al*., 2003). It has reduced fat per unit weight relative to rabbit and chicken and also contains high calcium and phosphorus which accounts for its preference (Jori *et al*., 1995; Juste *et al*., 1995; Fayenuwo *et al*., 2003). The AGCR is reputed for impacting on the economic growth of a number of

countries in West Africa where its meat is expensively sold and prefentially demanded over other available wild rodents (Baptist and Mensah, 1986; Ntiamoa-Baidu, 1998; Asibey and Addo, 2000) thereby making it a contributory factor to its vigorous exploitation for meat through aggressive hunting and bush burning (Owen and Dike, 2012). Because of the high demand for AGCR meat, currently, this rodent in Nigeria and several other African countries is being domesticated for increased stocking and intensification of production to mitigate the existing acute shortage of protein in the face of increasing demand for livestock products (Jori *et al*., 1995; Adu *et al*., 2005; Adekola and Ogunsola, 2009).

Figure 2.1: Photograph of the African greater cane rat (*Thryonomys swinderianus*Temminck, 1827). Source: Adoun (1993)

The AGCR is a rodent of African origin that has received impressive interests from many workers who have reported findings on the reproductive system (Aire and Van der Merwe, 2003; Adebayo *et al*., 2009; Adebayo and Olurode, 2010; Adebayo *et al*., 2014a and b, 2015, 2016, 2019; Olukole *et al*., 2009, 2010), circulatory system (Opara *et al*., 2006; Soro *et al*., 2014), nervous system (Dwarika *et al.,* 2008; Spruston, 2008; Byanet *et al*., 2009; Elston and Manger, 2014), digestive system (Byanet *et al*., 2008), endocrine system (Igbokwe, 2010) and skeletal system (Olude *et al*., 2014; Parés-Casanova *et al*., 2015).

2.2 Male Reproductive Biology

The male reproductive system in mammals is composed of the following; the paired testicles and its appendages (rete testes and ductuli efferentes), paired duct system (epididymis and ductus deferens), accessory glands (vesicular, prostate, ampullary and bulbourethral), urethra and penis (Dyce *et al.,* 2002; König and Liebich, 2014). Generally, the full set of accessory glands (vesicular, ampullary, prostate and bulbo-urethral) in mammals release their secretions into the pelvic urethra where they mix with the fluid discharge of both testicular and epididymal origin (Goeritz*et al.,* 2003).

There is marked species variation in the distribution of accessory glands in domestic mammals (König and Liebich, 2014). The full set of accessory glands is present in the bull, stallion and ram. However, the absence of both ampullary and vesicular glands in the cat, ampullary gland in the boar as well as both vesicular and bulbourethral glands in the dog have been documented (König and Liebich, 2014). Male Cane rat just like other mammals bear paired vesicular, prostate and coagulating glands as well (Adebayo *et al.,* 2014a and b, 2015).

2.2.1 Testicular Development

The embryonic development of the testes in mammals especially in the rodent begins with the bipotential gonad, an initial structure, that usually appear as condensation of the ventral side of the mesonephros of the developing embryo at day 10 (Griswold, 2016). Sex specificity is later acquired by the embryo after 2days as a result of primary driving role exerted by the expression of *Sry gene* principally from the cells meant to become the Sertoli cells of the testis (McLaren, 1998). Because of the absence of *Sry* expression in females, the cascade of gene expression events that coordinates the formation of granulosa cells in the developing ovary is then favored.

With regard to male, primordial germ cells (PGCs) which are the precursors of germ cells arise from the endodermal yolk sac and are first seen in the epiblast at day 6 of embryonic development (ED). The PGCs then undergo both passive and active cell migration before their eventual arrival at and infiltration of the developing gonadal ridge at ED day 11 (McLaren, 1998; Dyce *et al.,* 2002).

Sex determination and complete testes formation occur when the PGCs interact with embryonic Sertoli cells, Leydig cells and myoid cells at about ED 12.5 (Cool and Capel, 2009; Cool *et al.,* 2012). Sequel to the interaction, PGCs is seen in close proximity with Sertoli cells and in concert they give rise to seminiferous cords that will end up in becoming the seminiferous tubules. The PGCs of embryonic testis then go through a phase of mitotic proliferation within the cords and are then referred to as pro-spermatogonia or gonocytes (McCarrey, 2013). It is important to mention that the numerous proliferations occur within the medullary aspect of the embryonic testis (gonad) while the cortical aspect thin out to later become tunica albuginea (Dyce *et al.,* 2002). Subsequent to the increased population of PGCs, the pro-spermatogonia progress into a quiescent non-proliferative phase pending the time of birth in the rodent.

The pro-spermatogonia are initially situated near the center of the seminiferous cords but in the end move to the margin where numerous essential changes take place. The changes lead to the appearance of the morphologically distinct spermatogonia in the first few days after birth (McCarrey, 2013). It has been hypothesized that a number of this pool of pro-spermatogonia in mice form the initial differentiating spermatogonia that represent a“first wave” of germ cell development (Nakagawa *et al.,* 2007). Substantial variation exists in the rate of post natal development of the testis in different species. For instance, in the laboratory rat, increase in testicular weight begins shortly after birth and continues until adult size is attained. The weight increase is associated with the onset of spermatogenesis which occurs as early as five days after birth (Dyce *et al.,* 2002).

2.2.2 Testicular Morphology

The paired mammalian testis is an oval structure that is situated in a specialized pouch of skin called scrotum (Banks, 1993). The testis has both exocrine (produce spermatozoa) and endocrine (secrete gonadal hormones) functions (Monteiro *et al*., 2012). In most vertebrate animals, the testis is enveloped by a testicular capsule tissue whose morpho-architecture permits the entrance and exit of blood vessels and nerves into the parenchyma of the organ (Aire and Ozegbe, 2007).

2.2.2.1 Testicular Capsule and Peritubular (Boundary) Tissue

Histologically, from the outside inwards, testicular capsule is made up of three layers; the external (outermost) layer, the tunica serosa, which is detached from the peritoneum, the middle layer, the tunica albuginea, and the innermost which is a less differentiated layer, the tunica vasculosa (Banks, 1993; Singh, 2011). The tunica albuginea remains the massive component of the testicular capsule in most mammals studied so far, and consists of collagen, elastic fibres and abundant fibroblasts (Davis *et al*., 1970; Hodges, 1974). The testicular septa of mammals emanate from the internal aspect of the capsule, and provide channels which extend into the testicular substance for the inward and outward ramification of both the blood vessels and nerves (Davis *et al.*, 1970). The connective tissue of the tunica albuginea in the caudal aspect of the testis expands into a thick fibrous tissue mass (*mediastinum testis*) that project through the middle of the testicular substance containing rete testis (Parsquini *et al*., 1997). Several septa run from the *mediastinum testis* to the *tunica albuginea*, and divide testicular substance into a large number of lobules. Each lobule is nearly conical with the apex of the cone pointing towards the *mediastinum testis* (Banks, 1993; Singh, 2011). Each lobule houses one or more highly convoluted seminiferous tubules (Singh, 2011).

Previous studies by Holstein and Weiss (1967), Davis *et al*. (1970), and Hargrove *et al.* (1977) have reported the presence of smooth muscle cells in the testicular capsule of a number of mammalian species which on contraction may aid in extruding testicular spermatozoa into the excurrent duct system. Also, testicular capsule has been reported to respond by contraction to a variety of chemical and electrical stimulations (Davis *et al*., 1970; Banks *et al*., 2006).

The mammalian testis is structurally constituted into two major compartments: the intertubular or interstistial compartments between seminiferous tubules in a lobule housing blood and lymphatic vessels, nerves, connective tissue cells, besides macrophages, mastocytes, and Leydig cells and tubular compartment which houses the seminiferous tubules (the seat of spermatogenesis) (Costa *et al*., 2006). The individual seminiferous tubule within the testicular parenchyma is enveloped or bounded by peritubular tissue in all mammalian species (Maekawa *et al*., 1996). Although its organisation appears to be specie-specific, the fact that it is widely distributed among different mammalian species implies that boundary tissue is an essential testicular constituent (Maekawa *et al.*, 1996). The peritubular tissue is structurally made up of myoid or smooth muscle-like cells in different species of mammals (Virtanen *et al*., 1986; Maekawa *et al*., 1996) and birds (Rothwell and Tingari, 1973; Aire, 1997). Moniem *et al.* (1980) described the peritubular tissue being constituted of four basic components; a homogenous matrix, collagenous fibres, elongated contractile (myoid) cells and fibroblasts. Functionally, peritubular tissue is assumed to have diverse roles that include; mechanical support, extrusion of spermatozoa and as a physiological barrier controlling material exchange across it (Marettova *et al*., 2010; Rezigalla *et al*., 2012).

2.2.2.2 Testicular Germ Cells

Between the seminiferous peritubular tissue and the tubular lumen, several layers of cells of various sizes and shapes representing stages in the formation of spermatozoa are found and are collectively referred to as germ cells (Singh, 2011). The germ cells are flanked by the sustentacular cells, the Sertoli cells (Young *et al.,* 2006). In mammals at puberty onwards, the germ cells consist of sets of spermatogonia, spermatocytes, spermatids (round and elongating) and spermatozoa (Beguelini *et al*., 2009). Seminiferous epithelium in the newborn of mammals consists of two different cell types; gonocytes and Sertoli cells. The gonocytes are large round cells (approximately 20-24µm in diameter) evident at the centre of the seminiferous cords. They bear spherical nuclei containing homogenous chromatin, and centrally placed filamentous nucleoli as well as low spherical cytoplasmic mitochondria (Bellve *et al.,* 1977).

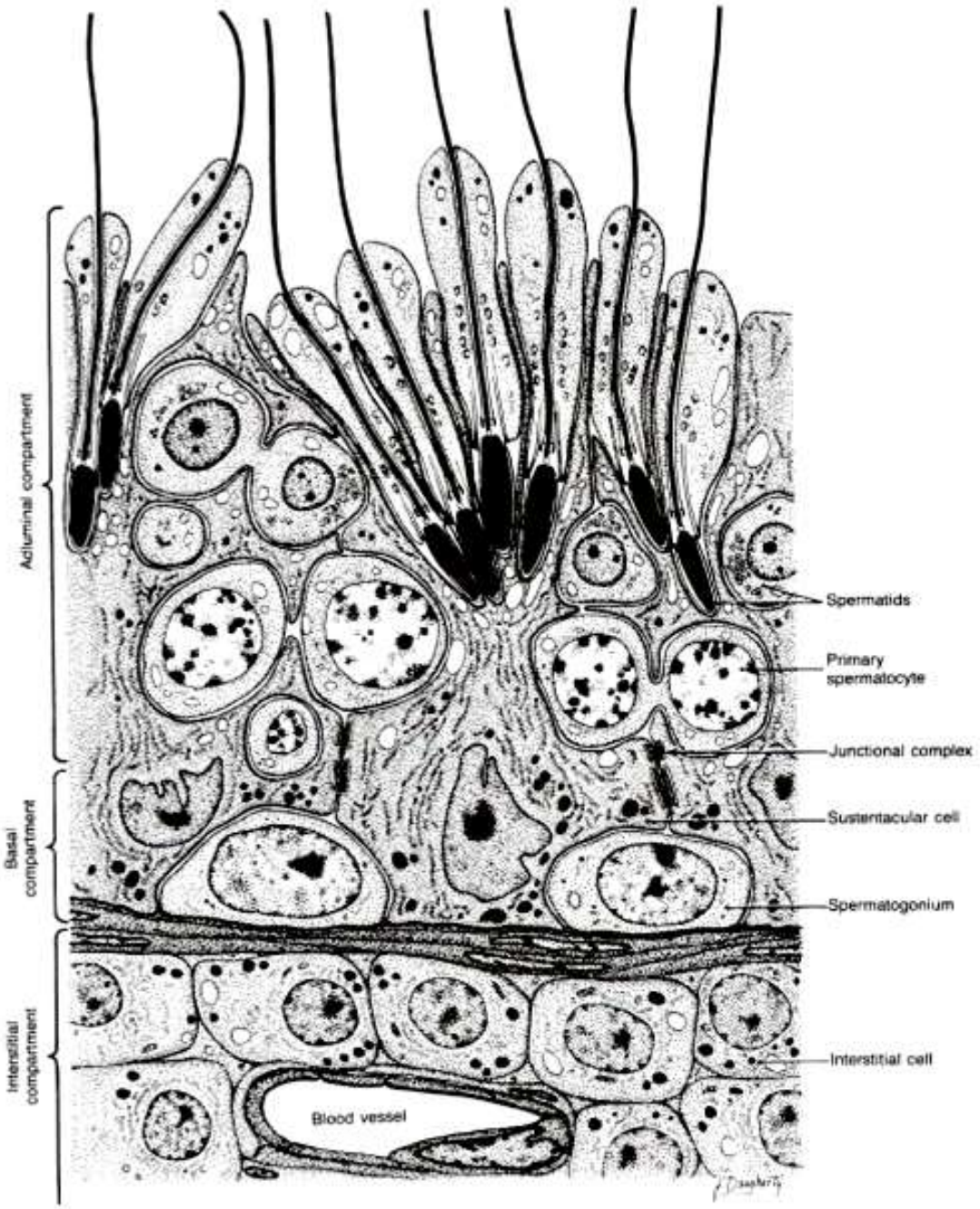

Figure 2.2. Equine seminiferous tubule. Note the relationship in architectural disposition of the Sertoli cells and the developing spermatozoa. Source: Amann (1981).

2.2.2.3 Spermatogonia

Spermatogonia constitute the foundation of spermatogenesis and male fertility (Phillips *et al*., 2010). They are entirely found in the basal compartment along the seminiferous tubular basement membrane and are separated from other developinggerm cells by Sertoli cell tight junctions (Singh, 2011; Beguelini *et al*., 2011). Two forms of spermatogonia are recognised, the stem spermatogonia and the differentiating spermatogonia (Phillips *et al.*, 2010). The former represent only 0.03 percent of the entire germ cells in rodent testes (Tegelenbosch and de Rooij, 1993). The differentiating spermatogonia which are diploid in nature are committed to entering spermatogenesis and undergo a set of mitotic divisions that are species specific, prior to the formation of preleptotene primary spermatocytes (de Rooij, 1983). They can be divided into three major morphological types; A, Intermediate (In) and B, on the basis of their nuclear morphology, chromatin condensation (quantity of heterochromatin within their nuclei) and position within the seminiferous epithelium (Bakst *et al*., 2007; Beguelini *et al*., 2009).

Type A spermatogonia are typically large in nature and bear ovoid nuclei whose long axes lie parallel to the basement membrane of the tubules. The nuclear chromatin of type A is generally described as "homogenous and dust-like" (Setchell, 1978). Contrastly, the intermediate and type B spermatogonia appear to have a somewhat less ovoid to rounded nuclei and increased heterochromasia along their nuclear envelope giving their chromatin a crust-like appearance (Courot *et al*., 1970). Type B spermatogonia have the most pronounced chromatin accumulations compared to others (Setchell, 1978). The basal surfaces of all spermatogonia are generally flattened along the basal lamina, while surfaces in contact with the surrounding Sertoli cells appear rounded (Russell *et al*., 1990b).

2.2.2.4Spermatocytes

Spermatocytes are the next set of germ cells in spermatogenesis that correspondto the meiotic phase, the process in which spermatocytes undergo meiotic divisions that give rise to haploid spermatids (Russell *et al*., 1990a). The meiotic process begins with a single round of DNA replication (Lodish *et al*., 2005) in pre-leptotene spermatocytes. The latter are actually formed by the final spermatogonial division and are the last spermatogenic cell types to go through the S-phase of the cell cycle (Russell *et al*., 1990b). Sequel to the replication of their DNA, primary spermatocytes enter the long prophase of meiosis characterized by genetic recombination to give rise to four

haploid spermatids after two rapid cell divisions. The primary spermatocytes during the duration of the meiotic prophase undergo progressive morphological changes that entail altered cellular and nuclear sizes as well as degree of coiling of the nuclear DNA (Russel and Frank, 1978). These highlighted changes in the spermatocyte nucleus appearance form the basis for partitioning the meiotic prophase into leptotene, zygotene, pachytene and diplotene phases.

2.2.2.4.1 Leptotene

The leptotene phase actually indicates the commencement of the meiotic prophase and begins with the transformation of the crust-like chromatin nature of the preleptotene primary spermatocytes to fine filamentous or thread-like chromatin as a result of spiralization and contraction of the DNA into individual chromosomes (Russell *et al*., 1990a). Morphologically, the cells assume a more rounded form during this phase as they migrate from the basal aspect of the seminiferous tubule (Russell, 1977a; 1978) and then move into the adluminal compartment.

2.2.2.4.2 Zygotene

In zygotene phase, analogous chromosomes form pairs which are attached via synaptonemal complexes, a well conserved structure containing paired lateral material together with a centralized area (Beguelini *et al*., 2011). Thus, the zygotene chromatin threads become visibly thicker than those of the leptotene phase when viewed under light microscopy and also bear conspicuous nucleoli (Setchell, 1978).

2.2.2.4.3Pachytene

Pachytene spermatocyte is typified by fully condensed chromosomes, visible chromatids and crossing over between paired chromosomes that lead to a unique combination of the genetic material, distinct from that of the individual's somatic cells (Setchell, 1978). There is rapid increase in the cellular and nuclear size towards the end of pachytene phase (Russell and Frank, 1978) and hence the chromosomes appear to be more widely distributed within the nucleus (Russel *et al*., 1990b). Also, the synthetic ability of the cells increases (Monesi, 1965) coupled with enlargement of nucleoli as well as appearance of sex vesicle (Solari and Tres, 1967). Of all the spermatocytes, pachytene spermatocytes have the longest life span that range between $1^{1/}_{2}$ - 2 weeks (Courot *et al.,* 1970). On the other hand, pachytene remains thespermocyte most susceptible to damage from testicular heating (Waites and Ortavant, 1968; Setchell, 1978, 1998).

2.2.2.4.4 Diplotene

The Diplotene phase of primary spermatocyte is usually brief and occurs when the nucleus has reached maximum size (Setchell, 1978). There is conspicuous disappearance of synaptonemal complexes between homologus chromosomes. However, the observation of remnants of the synaptonemal complexes can only be seen during diakinesis (Setchell, 1978; Beguelini *et al.,* 2011).

2.2.2.4.5 Secondary Spermatocyte

By the end of first meiosis, one chromosome from each homologus pair is distributed to each of the two secondary spermatocytes formed. Due to the absence of prophase between first meiosis and second meiosis, secondary spermatocyte meiosis II occur within hours of the first, resulting in one chromatid from each chromosome separating into each of the haploid spermatids (Clermont, 1972; Steinberger and Steinberger, 1975). Secondary spermatocytes are difficult to view in sections of testis because their cells transiently remain in interphase for short duration and then progress into the second meiotic division, which is equally fast (Arroyo *et al.,* 2015). By virtue of size, the secondary spermatocytes formed by the first meiotic division, is smaller compared to the primary spermatocytes (specifically diplotene) and bigger relative to the early round spermatids. Both the former and the latter are morphologically identical as a result of the presence of several patches of more deeply stained chromatin and one or two nucleoli (Setchell, 1978; deKrester and Kerr, 1994).

2.2.2.5 Spermatids

Spermatids are spherical cells formed after second meiotic division (Costa *et al.,* 2004). They bear centrally located round nucleus and are about 30% smaller in size than secondary spermatocytes which they resemble morphologically (Russell *et al.,* 1990b). The cytoplasm of a spermatid is characterized by a well developed Golgi complex, a pair of centrioles and numerous mitochondria that are either dispersed throughout the cytoplasm or lie adjacent to the plasmalemma (Russel *et al.,* 1990b; deKrester and Kerr, 1994). The formation of spermatids begins with morphological transformation of round spermatids into highly differentiated, species-specific, spermatozoa via a process known as spermiogenesis. The latter involves concurrent events of a number of morphogenic processes such as the acrosomal development, flagellar development, nuclear condensation and elongation, mitochondrial reorganisation and removal of excess cytoplasm made redundant during the cellular

reshaping process (Courot *et al.,* 1970; Clermont, 1972; Setchell, 1978; Russell, 1993; Sharpe, 1994). Several descriptions of spermiogenesis, at both the light and electron microscopic levels, are available for a range of mammalian species (Leblond and Clermont, 1952;Oakberg, 1956; Clermont, 1963; Ploen, 1971; Holsten, 1976; Russel *et al.*, 1990a; Beguelini *et al.*, 2011; Arroyo *et al.*, 2015).

2.2.2.6Spermiogenesis

Morphological changes in spermiogenesis begin with emanation of the acrosome of the spermatid from the Golgi complex which elaborates a number of small proacrosomal granules that coalesce to form a single acrosomal granule (Olukole *et al*., 2018). The latter together with its vesicle migrate towards the nucleus and become associated with the nuclear envelop and from this, the vesicle spreads over the nuclear surface. The level of coverage of the nucleus by the acrosome generally differ between species ranging between 25% and 60% and in some species extending beyond the nucleus to form an apical segment (Fawcett, 1970; Fawcett, 1975; de Krester and Kerr,1994). Subsequent to the formaton of the acrosome, the Golgi complex begins to migrate caudally and is ultimately included in the residual cytoplasm detached from the spermatozoon during spermiation (Fawcett and Phillips, 1969a; Fawcett *et al*., 1971).

It has been observed that the nuclear position changes from central to eccentric during the formation of the acrosome and the nuclear pole covered by the acrosome become placed closer to the plasmalemma. The repositioning highlighted above is followed by a progressive nuclear chromatin condensation with marked evidence of specie variation in the timing and degree of condensation. For instance nuclear condensation succeed nuclear elongation in the rat and mouse (Meistrich, 1993), but the two processes seem to concurrently occur in the dog (Russell *et al*., 1990b). Another major event is the reshaping of spermatid nuclear and head shape which in rodents dramatically changesfrom spherical to a highly asymmetrical falciform shape. Chromatin structure, DNA constituents, and nuclear proteins within spermatid nucleus has been suggested to contribute to some aspects of nuclear shape by providing resistance to external pressures, albeit, there being no credible evidence to elucidate their major role in the determination of nuclear shape (Meistrich, 1993).

The development of the spermatid tail begins from the centrioles which migrate to a position beneath the cell membrane that is opposite to the acrosomal development

region. The distal centriole is then perpendicularly oriented to the cell membrane leading to the formation of axoneme of the tail and the proximal centriole lies at right angles to it (deKrester, 1969; Fawcett and Phillips, 1969). The development of the tail is advanced by the elongation of the axoneme (nine outer doublet microtubular arrangement surrounding an inner pair of single microtubules) enclosed by the plasmalemma protruding from the spermatid. The distal centriole is then attached to the cell membrane by a ringlike structure, the annulus, situated at the base of the tail so that on distal movement of the spermatid cytoplasm, a canal is formed between the cytoplasmic lobes and the spermatid tail. With continuous elongation of the axoneme, the dense outer fibre complex emanates in continuity with and external to the outer doublet microtubules (Fawcett and Phllips, 1969). Below the level of the annulus, the fibrous sheath, circumferential rib-like structures joined at intervals to two fibrous columns formed from dense fibres three and eight, surround the dense fibres in the principal piece. Caudal to the latter, the mitochondria of the spermatid usually surround the dense fibres in a helical fashion late into spermatogenesis after the degeneration of the manchette to form the middle piece of the tail (Fawcett *et al.,* 1971). Almost around the same time with tail development, the proximal centriole gives rise to a sheet of dense material that in turn develops to form the capitulum or connecting piece that usually links the tail to the nucleus at the implantation fossa precisely on the caudal nuclear surface (Setchell, 1978).

During spermiogenesis, cellular reorganisation within the spermatid results in large quantity of redundant cytoplasm and organelles. It is on record that approximately 75% of all spermatid cytoplasm is eliminated (Sprando and Russell, 1987). The elimination of the excess cytoplasm and organelles in spermatid occurs via three means; by means of water elimination during spermatid elongation (Sprando and Russell, 1987), loss via tubulobulbar complexes (Russell, 1979; Russell and Malone, 1980) and majorly by post caudal displacement within the cell which is possibly facilitated by the manchette (Fawcett *et al.,* 1971).

2.2.2.7 Spermiation

Spermiation encompasses the process involved in the release of matured spermatids by Sertoli cells into the seminiferous tubular lumen before its epididymal transit (O'Donnel *et al.,* 2011). Between the head and tail of the spermatid, residual body (houses many organelles such as Golgi complex, mitochondria and chromatoid bodies

that are not included in the spermatozoa) are formed and then invaginate into the Sertoli cell (Kerr and de Krester, 1974; Beguilini, 2011). The residual body is pinched off from the spermatid at its release from the seminiferous epithelium and then become embedded in the cytoplasm of the Sertoli cell for subsequent phagocytosis (Sapsford *et al.,* 1969; Fawcett and Phillips, 1969a; Kerr and deKrester, 1974). The final minute quantity of excess cytoplasmic remnants attached to the released spermatozoon as a cytoplasmic droplet that migrates from the neck region to a junction between the middle and principal pieces of the tail, from where it is removed during epididymal transport (O'Donnel *et al.,* 2011).

2.2.2.8 Spermatogenesis

Spermatogenesis is a complex process occurring in the seminiferous tubule and involves the transformation of undifferentiated cells of the germ line (spermatogonial stem cells) into a highly specialized haploid cell or spermatozoon (Barratt, 1995; Costa *et al*., 2004). The general arrangement of spermatogenesis is essentially similar in all mammals and can be divided into three phases of which all germ cells must sequentially pass through over time (Hess and Franca, 2008;Santos *et al.,* 2014). They include:

(a) Proliferative phase: in this phase, germ cells undergo fast successive divisions that result in increased cell population size available to enter meiosis. The amount of cell divisions occurring among the spermatogonial stem cell division and meiosis determines the possible number of spermatozoa that can be produced by males and vary between species (Clermont, 1962, 1963; Amman, 1981; Paniagua *et al.*, 1987a). A classical example is found in the laboratory rat in which the pre-meiotic cell population is increased by one thousand fold during the proliferative phase and by a four-fold increase in the germ cell population during subsequent phases of spermatogenesis (Russell *et al*., 1990b).

(b) Meiosis: theoretically, each primary spermatocyte in this phase is expected to produce four haploid spermatids; however, programmed cell death always accompanies the meiotic divisions, thereby reducing the overall cell yield (Roosen-Runge, 1973).

(c) Spermiogenesis (Cytodifferentiation): this phase entails some morphological transformations of the round haploid germ cells to become differentiated to species-specific form of the spermatozoon that is structurally endowed to migrate and fertilize the egg (Arroyo *et al.,* 2015). As previously stated, these

morphological changes are similar in majority of animals and include acrosomal development, nuclear elongation and condensation, development of a flagellum and removal of surplus organelles and cytoplasm as residual bodies (Russell *et al.,* 1990a Chatchavalvanich *et al.,* 2005).

2.2.2.9 Spermatozoa Structure

As viewed by transmission microscope, a normal mammalian spermatozoon is chiefly elongated and structurally divided into four distinct segments namely; head, neck, mid-piece and tail (Toshimori, 2009).

2.2.2.9.1 Spermatozoon Head

The head of sperm cell is flattened bilaterally, mostly oval in appearance and occupied by the nucleus and acrosome together with a minute cytoplasm enveloped within the extent of the plasma membrane (Maree *et al.,* 2010). The acrosome which is vesicular in nature is made up of two membranes (the inner acrosomal membrane overlying the nucleus and the outer acrosomal membrane underlying the plasma membrane) that envelops roughly two thirds of the cranial aspect of the nucleus (Eddy and O'Brien, 2006). Between the acrosomal membranes lies the acrosomal enzyme matrix rich in network of cytoskeletal structures dispersed throughout the sperm head, mostly in the sub-acrosomal layer (between the inner acrosomal membrane and the nuclear envelope) as well as in the post-acrosomal space between the nucleus and the plasma membrane. The two layers of post-acrosomal space form the perinuclear theca, which enclose most of the sperm nucleus apart from the implantation fossa, the narrow region around the attachment of the tail (Eddy and O'Brien, 2006). The dislocation of the spermatozoa nuclear implantation fossa has been implicated in the pathogenesis of flagellar coiling (Ricci *et al.,* 2015). The posterior ring is a structure situated at the junction between the postacrosomal region of the head and the connecting piece (Eddy and O'Brien, 2006).

The nucleus of a mature mammalian spermatozoon is oval and flattened in shape, extremely condensed, much smaller in size compared to that of a somatic cell and bounded by a nuclear envelope consisting of two lipid bilayers, 7-10 nm apart, with a complete absence of nuclear pores (Eddy and O'Brien, 2006). Genetically, the nucleus is haploid in nature, contains a single set of 23 chromosomes due to meiotic divisions during spermatogenesis, and bears inactive nuclear DNA that remains in this state until its protamines are displaced upon entry into an oocyte. Mature sperm cell does

not have the capacity to synthesize RNA due to the absence of organelles like ribosomes and nucleoli (Grunewald *et al.,* 2005).

2.2.2.9.2 Spermatozoon Neck

The spermatozoon neck (connecting piece) defines the border between the sperm head and the middle piece (Teixera *et al.,* 1999). The sperm connecting piece is primarily constituted by two principal structures, the capitulum and the segmented columns (Teixera *et al.,* 1999; Eddy and O'Brien, 2006). The two structures support the spermatozoon head-flagellum attachment. The segmented columns consist of two major and five minor columns extending to the posterior end of the capitulum. At these end, these columns fuse to the nine longitudinal outer dense fibres that extend all through the flagellar length, thus providing the rigidity and structural support known with flagellum (Eddy and O'Brien, 2006; Ricci *et al.,* 2015). Part of the constituents of connecting piece is a pair of centrioles, the proximal and the distal centrioles. The proximal centriole is situated below the basal plate and perpendicular to the long axis of the nucleus; while, the distal counterpart is placed parallel to the spermatozoa long axis beneath the proximal centriole (Sathananthan *et al.,* 1996). The distal centriole is almost degenerated subsequent to the development of the axoneme in a mature spermatozoon, but the proximal centriole persists and participates in the formation of a short microtubular structure known as the microtubule adjunct (Manandhar *et al.,* 2000).

2.2.2.9.3 Spermatozoon Midpiece

The midpiece of the spermatozoon occupies the distance between the caudal end of the connecting piece and the annulus which is a ring-like structure separating the flagellar midpiece from the principal piece (Beguilini *et al.,* 2011). Functionally, the annulus serves as gated diffusion barrier controlling the transport of particles between the two spermatozoa regions and equally seems to stabilize the midpiece by preventing its mitochondria from slipping backwards (Curry and Watson, 1995; Briz and Fabrega, 2013). The midpiece is chiefly made up of mitochondrial sheath of 80 nm thickness and situated directly beneath the plasma membrane (Eddy and O'Brien, 2006). The sheath, reputed as energy source for spermatozoa motility, consists of orderly packs of spirally arranged elongated mitochondria connected from end to end around the underlying axoneme (Briz and Fabrega, 2013). The latter which constitutes the central axis of the midpiece is surrounded by nine keratin-like protein fibres

otherwise referred to as the outer dense fibres. Interestingly, the axoneme together with the dense fibres of the midpiece extends to the caudal tip of the flagellum (Toshimori and Eddy, 2014).

2.2.2.9.4 Spermatozoon Tail

The mammalian spermatozoon tail consists of the principal piece, the longest part of the tail, and end piece (Teixera *et al.,* 1999). Though many authors agree on inclusion of connecting piece and midpiece as part of the tail (Ogwuegbu *et al*., 1985; Meisner *et al*., 2005; Batalha *et al*., 2006; Brito *et al*., 2010). The tail plays significant role in the production of motion force required for sperm movement (Briz and Fabrega, 2013). Flagellar motion force is generated by sliding of the axonemal microtubule doublets against each other resulting in the development of symmetrical propulsive waves that propagate through the tail length for the linear progression (Mortimer, 1997). Specific function of the flagellum is in the provision of cell motility, which facilitate the active transport of spermatozoon through the female reproductive tract to reach and penetrate the oocyte (Briz and Fabrega, 2013). Structurally, the flagellar principal piece has fibrous sheath in addition to the axoneme and the outer dense fibres which replace the mitochondrial sheath of the midpiece. The fibrous sheath is located under the plasma membrane and consists of two longitudinal columns linked by circumferentially oriented ribs and suggested to provide the flagellum with elasticity and support. It is also postulated to modify the beating characteristics of the flagellum, possibly through restriction of the degree of its bending. The fibrous sheath and other cytoskeletal structures are absent in the short end piece of the flagellum but contain only the axoneme surrounded by the plasma membrane (Brito, 2007, Briz and Fabrega, 2013, Curry and Watson, 1995).

2.2.2.9.5 Spermatozoon Axoneme Structure

The axoneme of mammalian spermatozoon consists of highly ordered structure that forms the core of the flagellum (Teixera *et al.,* 1999). It is made up of two central singlet microtubules (doublet) connected to each other by linkages and surrounded by the central fibrous sheath. The doublet microtubules are also surrounded by nine pairs of peripheral placed microtubules (the 9+2 pattern) that extend in almost the entire length of the sperm tail (Toshimori and Eddy, 2014). Each microtubule doublet is composed of two structures reffered to as subunit A and subunit B. The subunit A is a

complete microtubule with circular shape; while the subunit B is incomplete with C-shaped appearance in cross sectional view (Nojima *et al.,* 1995).

The neighboring outer microtubule doublets are linked to each other in a clockwise pattern by two large motor protein projections, dynein arms, projecting from subunit A of one doublet to the subunit B of the adjacent doublet. Dynein arms are multisubunit ATPase complex depicted as inner or outer in accordance to their position relative to the central pair of microtubules (Marchese-Ragona and Johnson, 1990; Neesen *et al.,* 2001). Physiologically, the flagellar dynein arms (outer and inner) are assumed to contribute independently to the regulation of the flagellar waveform and the frequency of beating (Myster *et al*., 1999). The inner dynein arms are postulated to significantly participate in the development and propagation of the flagellar bending motion; while, the outer counterpart tends to maximize the microtubule sliding velocity with consequential acceleration of the flagellar beat frequency (Toshimori and Eddy, 2014). Due to possession of ATPase activities by dyein, there is regular conversion of chemical energy from ATP to the kinetic energy required for sperm motility (Mortimer, 1997).

2.2.2.10 Sertoli Cell

The Sertoli cell, also referred to as Sustentacular cell is an essential component of the seminiferous epithelium aside from the germ cells (Samuelson, 2007). It is columnar in shape and thought to span between the seminiferous tubular basement membrane to the lumen (Russell, 1993; Hess and Franca, 2005). It is referred to as nursing cell because of its ability to extend its cytoplasmic processes to surround the developing germ cells and also by forming specialized junctional complexes (Byers *et al.,* 1986; Cheng *et al.,* 2002). The lateral sides of neighbouring Sertoli cells form numerous infoldings and different types of cell junctional complexes (Cheng *et al.,* 2002). The interactions between the lateral sides of the sustentacular cell have been attributed to the development and functional activities of spermatogenic cells (Weber *et al*., 1983; Samuelson, 2007). Extensive interactions between the Sertoli and germ cell within the seminiferous epithelium has been found to modulate the intermittent events of assembly and disassembly of Sertoli cell -adherens and tight junctions as well as the Sertoli-germ cell adherence junctions that assist in the movement of germ cells across the epithelium (Cheng and Mruk, 2002).

The nucleus of a Sertoli cell is located very close to the basal aspect of the cell in most mammalian species or occasionally could appear resting on the basement membrane (Hess and Franca, 2005). The contrast to the typical Sertoli nuclear location is in the monkey and Spixy yellow toothed cavy rodent testes where it is located at appreciable distance from the basement membrane precisely somewhere in the middle of the seminiferous epithelium (Hess, 1990; Santos *et al.,* 2014). The nuclear size ranges between 250–850 μm^3 and can assume different shapes based on the seminiferous cycle stage and the age of development (Russell *et al*., 1990a). The nucleus is normally elongated in outline and extends toward the lumen from birth to adulthood; but specific changes in nuclear appearance occur with testicular maturity (Heyn *et al.*, 2001). The nuclear envelope of virtually all Sertoli nuclei of adult testis bears deep indentations which confer on it the pyramidal, triangular and the planoconvex shapes (Russell, 1993). The nucleoplasm of Sertoli cell is more euchromatic in nature and contains less amount of scattered heterochromatin along its membrane but the latter is present in remarkable amount in the developing testis (Hess and Franca, 2005).

The cytoplasm of the Sertoli cell contains large quantities of mitochondria, which is an indicator of increased metabolic activity (Russell, 1993). In the body of the cell, mitochondria are abundantly distributed among the other organelles. Smooth endoplasmic reticulum is another major organelle often seen in adult Sertoli cells and is suggestive of the cell capability in lipid metabolism. The smooth endoplasmic reticulum(SER) within Sertoli cell is situated close to the mitochondria and in some species it can be found between the elongated spermatid head in the vicinity of the tubular lumen or surrounding lipid droplets (Russell, 1993). But the rough counterpart is sparsely distributed in the basal aspect of the cell (Hess and Franca, 2005).

Sertoli cell is known for the secretion of several hormones prominent among which is inhibin that acts on the hypothalamus and pituitary glands to exert control on the follicle stimulating hormone (Steinberger and Steinberger, 1976; Lumpkin *et al.*, 1981). Deoxyribose nucleic acid synthesis in the germ cell of rat at the onset of spermatogenesis is usually inhibited by inhibin (Demoulin *et al*., 1979; Setchell, 1980). Testosterone, estrogen and anti-paramesonephric hormones have recently been

found to be secreted by Sertoli cell (Ichihara and Pelleniemi, 2007; Carreau *et al*., 2011).

2.2.2.11 Leydig Cell

The intertubular spaces of the adult mammalian testes are occupied by loose connective tissue with a population of mixed cells including polygonal, fusiform and clear cells as well as complex networks of blood and lymphatic vessels (Burgos *et al*., 1970; Wrobel and Bergmann, 2006). The conspicuously large polygonal cell of the intertubular tissue is the Leydig cell and has been extensively described in variety of mammals (Wrobel and Bergmann, 2006). Two different populations of Leydig cells; fetal and adult are recognised to arise at different times of testicular development in mammals (Lording and de Kretser, 1972; Huhtaniemi and Pelliniemi, 1992). The former corresponds to fetal Leydig cells that appear and function throughout the prenatal masculinization stage of the male urogenital system; while, the latter is the adult Leydig cell that postnatally develops during sexual maturation (Mendis-Handagama and Ariyaratne, 2001; Akhmerova, 2006). Fetal-type Leydig cells are believed to degenerate or de-differentiate almost immediately after the completion of the morphogenesis of the extragonadal tract in male (Byskov *et al*., 1983; Kuopio *et al.,* 1989; Hardy *et al.,* 1991), although fetal Leydig cells can continue into the adult testis where they constitute a tiny minority within the population of adult Leydig cells (Kerr and Knell, 1988). In some mammalian species such as man, the two populations of Leydig cells are recognised easily using the temporal separation, but in the rodents, they are not different from one another due to population overlap (Lording and De Kretser, 1972; Kerr and Knell, 1988). The adult fetal population that appears prior to or during puberty is accountable for spermatogenesis and the preservation of male secondary sex characters (de Kretser and Kerr, 1988).

The Leydig cells produce androgens and this steroidogenic activity is markedly reflected in their cellular ultrastructure (Zirkin *et al.,* 1980; Ewing and Zirkin, 1983). Originally, prospective Leydig cells consist of aggregated undifferentiated mesenchymal cells with oval to irregular dark-staining nuclei and minute cytoplasm. With progressive development, Leydig cells acquire conspicuously increased cytoplasmic volume and appearance of organelles with characteristic features of steroid-producing cells including numerous mitochondria displaying tubular cristae; extensive smooth (agranular) endoplasmic reticulum (SER); some rough (granular)

endoplasmic reticulum (RER); and dark-staining cytoplasm (Byskov, 1986; de Kretser and Kerr, 1988). In addition to this, there is appearance of abundant cytoplasmic lipid in form of distinct electron-dense droplets (Zirkin *et al.*, 1980; Huhtaniemi and Pelliniemi, 1992). In human Leydig cells, specialized crystal (Reinke crystals) and lipofuschin pigment granule are seen within their cytoplasm (Weiss, 1983).

The amount of Leydig cells within the testicular interstitium of aged man is usually reduced (Kaler and Neaves, 1978; Neaves *et al*., 1985), but is not notably altered in the aged rat (Kaler and Neaves, 1981). The Leydig cells of the horse testis are exceptionally different because they display an age-related increase in total volume and quantity from 2 to 20years of age (Johnson and Neaves, 1981). Similarly, there is no marked difference in the Leydig cell ultrastructure of postpubertal, adult and aged horses except for the demonstration of huge accumulation of lipofuschin granules in aged horses (Johnson and Neaves, 1981). Part of the reported age–related changes in the testicular interstital components include hyalinosis of the arterial vasculature, infiltration of lymphocytes into the peritubular space and increase in both collagen and elastic fibres of the lamina propria (Bishop, 1970; Andres*et al*., 1981; Paniagua *et al*., 1987).

The secretory activities of the Leydig cells are regulated by pituitary gonadotrophic hormone, the luteinising hormone otherwise known as interstitial cell stimulating hormone (Wheater *et al.,* 1990). In seasonal breeders, the Leydig cells and other germinal epithelial components are morphologically regressed; while, in non seasonal breeders including man and laboratory rats spermatogenic and Leydig cell activities are continuous throughout the year (Christensen, 1975; Chaves *et al*., 2012).

Apart from the Leydig cells, the other components of the interstitium include very few macrophages which are closely associated with few single or a group of Leydig cells (Bergh, 1987; Gayton *et al.,* 1994). Some blood derived cells such as lymphocytes, plasma and mast cells may also be seen in the interstitium of some species (Christensen and Fawcett, 1977).

2.3 Morphology of the Epididymis

2.3.1 Development of Epididymis

The genital ducts, Wolffian (Mesonephric) and Mullerian (paramesonephric) ducts have common precursor which is intermediate mesoderm. They are simultaneously derived from the latter. Sequel to this, male sexual diffenrentiation commences with the regression of Mullerian duct and further differentiation of mesonephric ducts into the following male organs of reproduction; epididymis, ductus deferens and seminal vesicles (Kobayashi and Behringer, 2003; Hannema and Hughes, 2006). The entire process of sexual differentiation is regulated by genetic influence of sex chromosome (França *et al*., 2005). The triggering mechanism of the latter in Mullerian duct regression is yet to be understood (Arroteia *et al.,* 2012). However, a non steroidal anti-Mullerian hormone produced by Sertoli cell has been implicated (Moore and Persaud, 2003).

Following the regression of Mullerian duct, there is differentiation of Leydig cells under the influence of a placental hormone, human chorionic gonadotropin (hCG), to begin the production of androgens which will in turn exert a positive regulation on the mesonephric duct. The interplayof the earlier stated hormones above induced the cranial aspect of the duct trasnform to tortuous structure and eventually develop to become epididymis (Arroteia *et al*., 2012). The epididymis is predominantly made up of messenchymal tissue at birth (Akbarsha *et al*., 2015). The development of the epididymis during postnatal life is characterized by substantial parenchymal remodeling that involves series of duct elongation and convolution (Hannema and Hughes, 2006). On attainment of puberty, the epididymis become completely differentiated and assumes a well convoluted channel lined by epithelium of diverse component cells (Rodríguez *et al*., 2002).

2.3.2 Gross Anatomy

The Epididymis is a single convoluted duct that is otherwise referred to as ductus epididymis (Akbarsha *et al.*, 2015). It connects the efferent ducts with the vas deferens (Singh, 2011). It is situated subjacent to the testis on each side and adhere to the latter on the medial side via connective tissue. Distally, it is secured by the ligament of the tail of epididymis and the epididymal fat cushion (Dyce *et al*., 2002). In different mammals, the ductus epididymis measure between 3-80 metres. It is a well convoluted duct that is enclosed by a thin capsular covering that ends up forming

the epididymis (Akbarsha *et al*., 2015). The epididymis is in turn divided into many segments by septae that run along its length (Singh, 2011).

2.3.3 Epididymal Histology and Ultrastructure

The epididymis was formerly thought to be histologically divided into three distint regions (segments); the caput which is situated at the testicular cranial pole, the corpus occupies the side of the testes and the cauda segment located at the caudal (posterior) pole (Hermo, 1995). Robaire and Hermo (1988) later discovered an initial (earliest) segment that is situated ahead of caput and an intermediate zone was subsequently between the initial segment and caput especially in rats (Hermo *et al.,* 1991). A number of studies on different mammalian species have identified many other slight histo-architectural differences such as additional zones and segments along the ductus epididymal length (Jones *et al.,* 1979; Oke *et al.,* 1989, Adebayo and Olurode, 2010).

It is important to mention that remarkable differences exist in the ductal diameter, epithelial height (single pseudostratified in nature), parenchymal cell types as well as their distribution in the various segments of the epididymis (Akbarsha *et al.,* 2015). The epididymal epithelial thickness also varies along the tubule being thickest at the proximal caput and thinnest at the caudal region (Arroteia *et al.,* 2012). In most mammals, the proximal to the distal segment of the epididymis usually have progressive increase in luminal diameter and periductal muscle coat thickness (Lasserre *et al.,* 2001). Spermatozoa concentrations are usually scanty in the initial segment, but are largely concentrated in the lumen of cauda epididymal region (Yanagimachi *et al.,* 1985; Cornwall, 2009).

The pseudostriated epithelium of the epididymis is populated by different cell types that include; principal, basal, apical, clear and halo cells which is synonymously called intra-epithelial leucocyte or intraepithelial lymphocyte or macrophages by some authors (Akbarsha *et al.,* 2015). Based on the epithelial cell population, two (principal and basal cells) of these cell types are regarded as main epididymal cells while others are accessory (Agnes and Akbarsha, 2001).

The principal cells constitute the most abundant (roughly 80%) of the epithelial cell type in the cranial segments (initial segment, intermediate zone and caput) of the epididymis and decrease to about 69 and 65 % in corpus and caudal epididymal

segments respectively (Robaire and Hermo 1988). Histologically, the principal cells rest on the basement membrane where they assume high columnar shape and extend through the entire epithelial height (Singh, 2011). Their heights decrease craniocaudally from the initial to caudal epididymal segment (Akbarsha *et al.,* 2015). They bear densely packed stereocilia at their apical border (Karmore *et al.,* 2015). The stereocilia height and distribution decline craniocaudally down the epididymal segments (Calvo *et al.,* 1999). Intercellular communications between neighbouring principalcells are accomplished by series of cell junctions; lateral zonular occludens which form the blood epididymis barrier and the zonular adherens that form tight junctions (Cornwall, 2009; Akbarsha *et al.,* 2015).

The ultrastructural profile of the principal cells in the different segments of the epididymis in most mammals is characterized by spherical to irregular nuclear shape occupying about basal one third of the cell (Akbarsha *et al.,* 2015). The supranuclear region of PC in the initial, intermediate and caput segments of the epididymis is typified by well developed Golgi apparatus which is finely arranged as vertical masses of sacs and discs as well as numerous SER (Dacheux *et al*., 2005). In addition, the apical part of the supranuclear region (luminal border) is characterized by endocytotic apparatus with endososmes, lysosomes, multivesicular bodies, coated and uncoated pits and vesicles (Robaire and Hermo, 1988; Goyal and Williams, 1991; Arroteia *et al.,* 2012). The corpus epididymis has the highest concentration of lysosomes (Robaire and Hermo, 1988). The apical coated pits are physiologically essential in resorption of substances across the lumen via receptor-mediated endocytosis and thus help in controlling luminal microenvironment (Ramos-Ibeas *et al.,* 2013). On the trans-face of the Golgi piles, smooth surface vesicles (secretory vesicles) required for both intra and extracellular movement of secretory material are in abundance. At the perinuclear region, numerous endoplasmic reticulum is evident around the Golgi apparatus and is characteristically granular in nature relative to the supranuclear region (Akbarsha *et al.,* 2015).

The Basal cell is next to the principal cell in term of cell population along the epididymal epithelium (Arrotéia *et al.,* 2012). Histologically, basal cell is located below the principal cells and consists of sets of elongated flattened triangular cells (Yeung *et al.*, 1994). They bear round to somewhat flattened nuclei with cytoplasm characteristically occupied by lysosomes which are filled with lipofuscin pigment

thereby suggesting their roles in scavenging reactive oxygen species from the epididymal interstitial tissues (Robaire *et al.,* 2000; Cornwall, 2009; Akbarsha *et al.,* 2015). In addition, basal cells regulate the role of principal cell in electrolyte and water transport via local production of prostaglandings (Leung *et al.,* 2004). They have also recently been implicated in surveillance of sperm antigens during epididymal sperm movement obstruction which they finally processed to an amorphous structure called dense bodies (Seiler *et al.*, 2000; Aruldhas et al., 2006).

Clear cells are markedly vacoulated cells with very pale cytoplasm. The vacoulations are striking at the apical region of the cell and are also rich in supra nuclear dense granules (Schimming *et al.,* 2012). It also bears some microvilliated structures on its apical surface (Păunescu *et al.,* 2014). In term of distribution, clear cells are confined to the corpus and cauda epididymal segments. Clear cells have variable nuclear positions which are somewhat round in shape and pale staining with conspicuous nucleolus (Schimming *et al.,* 2012). The basal region of the clear cell bears dense bodies in moderate proportion (Akbarsha *et al.,* 2015). Physiologically, they are essential in the removal of sperm cytoplasmic droplet via lysosomal enzymatic action (Akbarsha and Averal, 1999).

The halo cells which are made up of intra-epithelial structures (lymphocytes and macrophages) are located in all the segments of the epididymal epithelium (Akbarsha *et al.,* 2015). They are distinguishably characterized by pale cytoplasm with dense nucleus containing patches of peripherally condensed chromatin (Robaire and Hermo, 1988). Halo cells are typically migratory in nature and are thus found at various heights in clear spaces along the epididymal epithelium (Wang and Holstein 1983; Robaire and Hermo, 1988). They are believed to function in providing immunological barriers to antigenic substances on the epididymal epithelium (Dacheux *et al.,* 2005; Robaire *et al.,* 2006)

2.3.4 Specific Morphological Changes in Testes and Epididymis with Age Advancement

Specific age-related ultrastructural changes in the epithelial cells of corpus and caudal epididymis have been reported to include increase accumulation of secondary lysosomes, residual bodies, lipofuscin pigments, mitochondrial damages and increased cytoplasmic filament bundles in aged hamster (Serre and Robaire, 1998).

Lysosomes are known for housing hydrolytic enzymes that phagocytose aged or damaged cellular organelles, extracellular products and capable of storing lipofuscin, the main cellular undigested material implicated in ageing (Sohal and Brunk, 1990; Brunk *et al.,* 1992; Ivy *et al.,* 1996; Tabatabaie and Floyd, 1996). In addition, epididymis undergoing ageing has been found to demonstrate striking vacoulated principal cells with varying vacuolar sizes depending on species, being smaller in the principal cells of the distal epididymal region of aged rabbit and of giant dimensions in the proximal caudal epididymis of older rats (Cran and Jones, 1980; Serre and Robaire, 1998). The vacuoles usually lack the normal dense lysosomes peculiar to active adults thereby reflecting a clear manifestation of the disruption of regular endosomal maturation (Dunn and Maxfield, 1992). Age-related alterations in the epididymal luminal spermatozoa of aged rats have been observed to be characterized by the presence of spermatozoa debris in small endosomes and giant vacuoles, despite the apparent absence of opening of the endosomal vacuoles into the lumen (Cooper and Hamilton, 1977; Bernard, 1984; Serre and Robaire, 1998). Parts of the progressive structural changes reported in epididymis of mammals is the gradual thickening of the basement membrane with advancement in age and the complementary emission of pseudopods by the basal cells into the thickened membrane which is a morpho-physiological adaptive mechanism to maintain the epithelial homeostasis (Serre and Robaire, 1998).

Epididymal histomorphometric variables such as external ductal diameter, epithelial height, periductal muscular wall width and stereocilia height have been reported to differ in the various epididymal segments and across different age groups in hamster rats (Calvo *et al.,* 1999). External ductal diameter has been found to increase postnatally in all the epididymal segments except in the caudal epididymal tubules of older rat where it is markedly reduced. On the contrary, epithelial height in hamster has been found to progressively decrease cranio-caudally from the proximal to the caudal epididymis during post natal life to adulthood (Calvo *et al.,* 1999). The periductal muscle coat width is similar across different age groups but with marked thickness around the caudal tubules. The profile of the stereocilia height of the principal cells from birth to adulthood is typified by progressive decrease from the proximal caput to the caudal segment of the epididymis (Calvo *et al.,* 1999).

2.3.5 Epididymal Function

The four major functions of the epididymis can be summarized to consist of spermatozoa transportation, sperm motility development, sperm fertilizing ability development and the establishment of specialized luminal environment suitable for spermatozoa maturation process through the absorptive and secretory activities of the epididymal epithelium (Robaire *et al.,* 2006).

The spermatozoa produced in the testes are released into the seminiferous tubular lumen and transported via efferent duct into the epididymal compartment (Singh, 2011). Effort has been directed to determining the transit duration of the sperm within the epididymis and the best approach in the estimation of the total transit through epididymis or transit within each segment is by using the ratio of epididymal sperm reserves and daily testicular sperm production provided there is no difference in inter-segmental transit speed and absence of sperm resorption (Orgebin-Crist, 1962).

2.3.6 Epididymal Sperm Storage

It is important to mention that roughly half of all spermatozoa that leave testicular compartment naturally die, disintegrate and are reabsorbed by the epididymal epithelium (Robaire *et al.,* 2006). With respect to spermatozoa storage, almost 70% of the remaining mature spermatozoa are stored in the cauda epididymis where repetitive fertile ejaculations can easily be favoured (Mortimer, 1994; Sharma and Agarwal, 2011). The cauda epididymis provides the required environment of slightly lower temperature for preserving spermatozoa and bears a volume that is directly proportional to the storage capacity of the male tract (Bedford, 1978). The caudal epididymal storage capacity and the possible frequency of ejaculates vary with species for instance, in stallions and bull, the number of stored spermatozoa in cauda epididymis is adequate for more than ten successive ejaculates while in man, less than three ejaculates capacity are reserved in their poorly developed cauda epididymidis (Sullivan *et al.,* 2005; Frenette, 2006).

Caudal spermatozoa in aged mammals are usually associated with some considerable alterations which have been suggested to arise from prolonged sexual inactivity (Robaire *et al.,* 2006). When these spermatozoa are included in ejaculated sperm cell, there could be impairment of semen quality, unless they are removed from the male reproductive tract at regular interval (Mortimer, 1994).

2.3.7 Sperm Morphology

Sperm morphological evaluation in mammals constitutes an essential part of breeding soundness examination (Oyeyemi and Babalola, 2006). Morphologically, spermatozoa in several species of mammals bear a distinct head compartment that house both the nuclear and the acrosomal materials, a mid-piece and a long tail aspect which is roughly divided into two segments; the principal and the end pieces (Oyeyemi and Babalola, 2006; Oyeyemi *et al.,* 2009). The spermatozoa head houses the dense DNA and in most mammalian species, the shape of the head is flat and oval but the exception is in the rat, golden hamster and volcanomouse (Blandau, 1951; Leblond and Clermont, 1952; Villalpando *et al.,* 2000). Breed (2005) reported that some families of rodents have spermatozoa heads that fold back on to themselves presenting appearances similar to hook shape and thus called the apical hook. Ostriches, galliformes as well as reptiles have filliform type of spermatozoa (Soley, 1992; Jamieson, 2007).

The acrosome, an important structure surrounding the sperm head, bears a thin double layered membraneous sac that seals the anterior two-thirds of the spermatozoon head similar to a crescent cap (Singh, 2011). The sperm head usually acquires acrosome during the last stages of spermiogenesis. The acrosome consists of hydrolytic enzyme, the acrosin (Muller-Esterl and Fritz, 1981) hyalonuronidase (Rowland, 1994; Hunnicult *et al.,* 1996b) esterases (Bradford *et al.,* 1976) and acid hydrolases (NagDas *et al.,* 1996) that are crucial for fertilization.

Morphological abnormalities are also evaluated along with the assessment of morphological integrity because deformed or immature sperm cells have probability of causing a decreased or low chance of oocyte fertilzation (Ayad, 2018). The presence of abnormal shaped spermatozoa in the ejaculate of mammals at a normal acceptable range of up 20% in cat and less than that in rodents is normally encountered (Moss *et al*., 1979; Wildt*et al*., 1999). It might be associated with impairment of fertility when they are present in large numbers (Moss *et al*., 1979). A good knowledge of the types of abnormalities of spermatozoa and their quantities in the ejaculate allows the diagnostician to make fertility prognosis which might specify a treatment course that will aid the recovery of a male with abnormal sperm production (Freneau *et al.,* 2010).

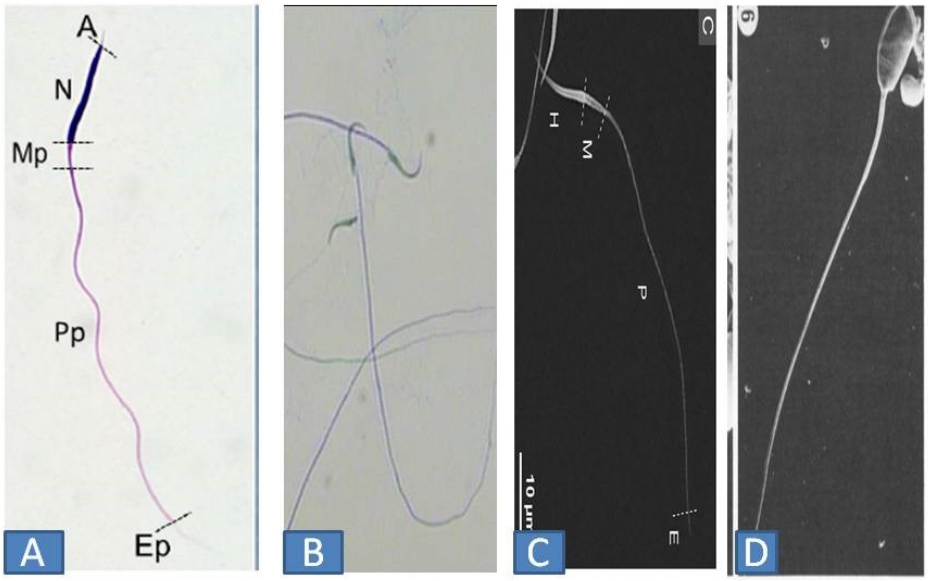

Figure 2.3. Morphological Appearances of Spermatozoa in Different Animals. A. Ostrich B. Rat C. Turtle D. Rabbit. Note the filliform shape of the spermatozoa in A, presence of acrosomal hooks in B and D and ellipsoidal head shape in D. Sources: Hafez and Kanagawa (1973); Soley (1992); Toghyani*et al*. (2013); Zhang *et al*. (2015).A - Acrosome, N - Nucleaus, Mp (M) - Midpiece, Pp (P) - Principal piece, Ep (E) - End piece, H-Head.

The significance of the usage of sperm morphology in determining reproductive success has been documented in many mammalian species; man (Menkveld *et al.,* 1991; Zamboni, 1992) and domesticated animals such as the bull (Barth and Oko, 1989; Freneau *et al.,* 2010), stallion (Brito, 2007), boar (Briz *et al.,* 1996) and dog (Martínez, 2004). It has equally been found that ageing is an important factor in semen quality and is usually impaired in the aged animal due to morphological alteration in the epididymal epithelium most especially in the caudal region of the duct with probable consequential effect of disrupted sperm maturation (Calvo *et al*., 1999).

2.3.7.2 Sperm Morphometry

Sperm morphometry refers to some linear dimensions of the head, mid-piece and the tail of a typical spermatozoon (Banaszewska *et al.,*2011). There is a strong relationship between sperm function and morphometry and has been empirically validated in different mammalian species (Immler *et al.*, 2010). For instance in bulls, spermatozoa head morphometric parameters have been considered as excellent indicators of semen quality (Phillips *et al.,* 2004). Sperm morphology in conjunction with the morphometry are essential reproductive indices to the theriogenologist as spermatozoa ability to fertilize an ovum as well as their motility are all dependent on sperm head and tail parameters respectively. Much interest is geared towards morphology and morphometry in relation to practice as well as theoretical science (Kolodzieyski and Danko, 1995). Also, the age of a male animal has equally been identified as an essential factor in causing difference in spermatozoa morphology and morphometric dimensions (Gregor and Hardge, 1995, Kondracki *et al.,* 2005, Quintero-Moreno *et al.,* 2009).

Spermatozoa morphometric parameters which include head length and width – HL and HW, mid-piece length - MPL, tail length - TL and the entire spermatozoa lengths -SL have been determined in several mammalian species (Cummins, 1983). Morphometric parameters in Maradi goat spermatozoon was reported by Ogwuegbu *et al*. (1985) to be; HL - 8.2 µm, MPL -12.8 µm, TL: 37.2 µm and SL - 58.2 µm respectively. Generally, sperm morphometric analysis determined so far in majority of the mammalian species observed that the tail including the midpiece was the longest segment and on average could represent up to 89% of the total sperm length

(Ogwuegbu *et al*., 1985; Meisner *et al*., 2005; Batalha and Oba, 2006; Brito *et al*., 2010).

2.3.7.3Sperm Motility

Spermatozoa are mostly not motile in the testicular compartment (Dacheux *et al.*, 2003; Ayad, 2018). It undergoes a series of significant maturational changes that culminate in the acquisition and development of motility while it is transiting in the epididymis (Dacheux and Dacheux, 2014). Full motility is induced and exhibited during ejaculation when spermatozoa produced are mixed with secretions from the various accessory glands (Mortimer, 1994).

2.3.7.4 Sperm Concentration

Spermatozoa concentration in the semen is expressed in millions per millilitre and constitutes an essential marker of semen quality as well as a predictive parameter for fertility potential (Guzick *et al.,* 2001; Nallella *et al.,* 2006). Concentration of spermatozoa in an ejaculate varies among mammals (Oyeyemi *et al.,* 2002). In the laboratory sperm concentration is usually estimated by professional observers who are trained to use both macroscopic and microscopic examinations to estimate such (Hafez and Hafez, 2000). Also, the estimation of spermatozoa can be determined using Brown opacity tubes and more objectively the use of absorption meter is more reliable (Laing, 1979). Sperm concentration can be altered by numerous factors that include; drugs, malnutrition, non-use or overuse of the animal in breeding (Oyeyemi *et al.,* 2009; Oloye *et al.,* 2011).

2.4 Testicular and Epididymal Innervations and Astrocyte-like Cell Demonstration

2.4.1 Testicular and Epididymal Innervations

The male gonad neuronal network is formed by the peripheral nerves (the superior and the inferior spermatic nerve (SSN and ISN) fibres that emanate from the autonomic ganglionic system (Motoc *et al.,* 2010). The superior spermatic nerve fibres emanate from the superior mesenteric ganglion coupled with inputs from renal, spermatic and aortic plexuses and descend bilaterally to approach the testes in the company of testicular artery and gain entrance into the testis at the cranial pole (Setchell *et al.,* 1994; Rauchenwald *et al.,* 1995; Sosa *et al.,* 2009). The SSN can also receive afferent and possibly vagal parasympathetic fibres. While the inferior

spermatic nerve fibres carry mostly sympathetic fibers. It originates from the inferior mesenteric ganglion and pelvic plexus accompanied by the vas deferens and then gain access to the caudal pole of the testes through the inferior ligament of the tail of epididymis (Setchell *et al.,* 1994; Rauchenwald *et al.,* 1995).

The morphological closeness between neuronal elements and testicular cells (Leydig cells, boundary tissue and vascular cells) make testicular cells direct targets of catecholamines and neuropeptides and thereby provide strong proof for a functional association (Nistal *et al.,* 1982; Prince, 1992, 1996; Frungieri *et al.,* 2000). These neurotransmitters in the presence or absence of pituitary hormones are capable of intrinsic triggering of receptors on the Leydig cells, Sertoli cells and smooth muscle cells of the testis (El-Gehani *et al.,* 1998, Wrobel and Schenk, 2003).

One of the research paths on the innervations of the reproductive tract in many species of animals studied dealt with distribution and chemical coding of nerve fibres supplying male genital organs (Sienkiewicz et al., 2015). Several workers have optimized neuronal markers: cathecholaminergic (Tyrosine hydroxylase and Dopamine Beta Hydroxylase) and peptidergic (Substance P, Neuropeptide Y and Calcitonin gene-related peptide) to localise testicular nerves around branches of the testicular artery, interstitial Leydig cells and seminiferous tubules in marmoset rat (Wistar), dog, pig and donkey (Kulkarni *et al.,* 1992; Zhu *et al.,* 1995; Tamura *et al.,* 1996; Wrobel and Brandl, 1998; Wrobel and Moustafa, 2000).

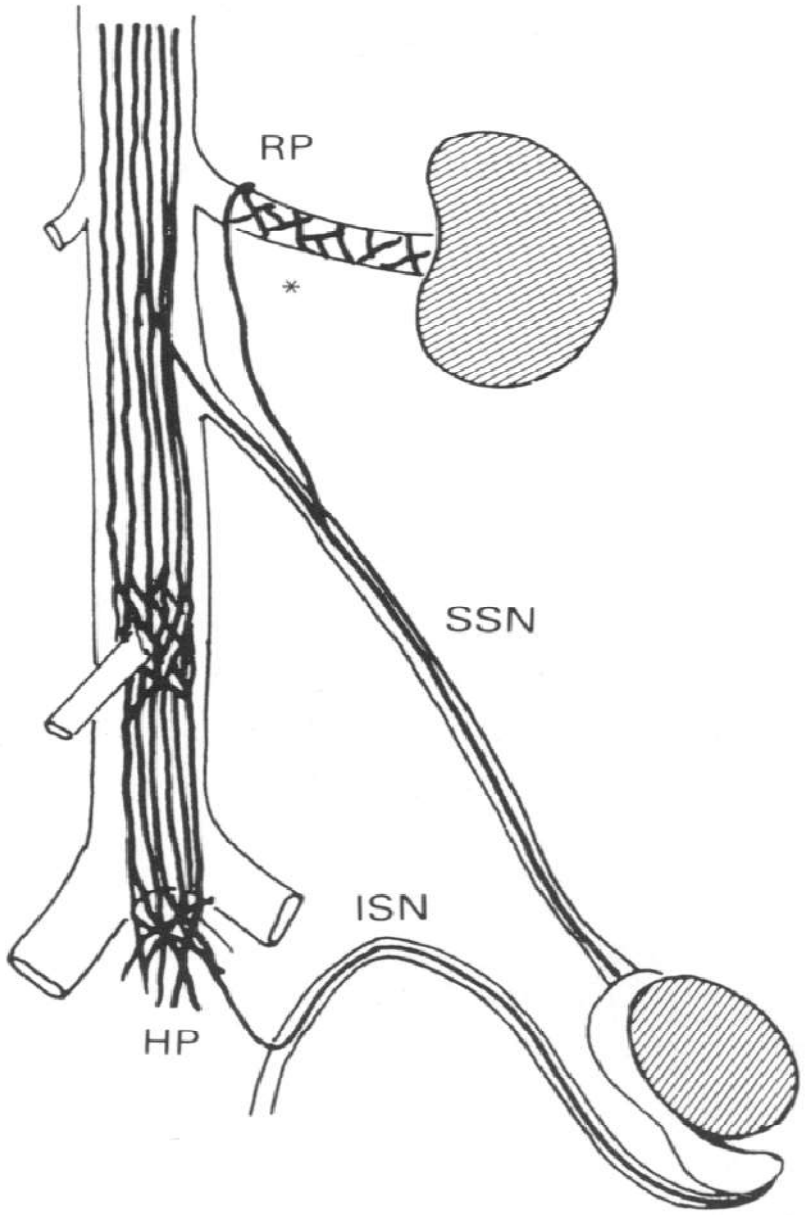

Fig. 2.4. Schematic diagram of the testicular innervation of rat. SSN: superior spermatic nerves; ISN: inferior spermatic nerves; RP: renal plexus; HP: hypogastric plexus [Source: Campos *et al.*, 1990].

Sienkiewicz *et al.* (2015) has described the neuronal architecture of the testes in an adult Chinchilla rabbit. Nerve fibres were found to be very dense in the tunica albuginea portion adjacent to the mesorchial border of the testis. The number of the fibres progressively reduced toward the free border of the testis. In addition, the parts of the tunica albuginea casing both extremities (cranial and caudal) of the testis have higher density of the nerve fibres than those found in the rest of the testicular capsule. Nerve fibres were observed penetrating the parenchyma (interior region of the testis) from the tunica albuginea into septa of the testis to supply neighbouring blood vessels. However, non vascular tissues of the parenchyma are devoid of nerve fibres apart from some intermittently distributed nerve terminals that supply the seminiferous tubules. Nerves fibres running through the testicular septa eventually end in mediastinum of the gonad. Similar testicular innervation has earlier been reported by Wrobel and Abu-Ghali (1997) in bull but with no evidence of dense nerve network terminals within the mediastinum of the gonad.

Age-dependent variance in testicular innervation is assumed to reflect its distinct functions at different age stages (Gong *et al.,* 2009). Age related changes in the distribution of nerves access to the testis and its investment in pigs has been described by Wrobel and Brandl (1998). It was shown that the testes of piglets less than 7-day-old have innervations restricted to the septal and mediastinal regions. While those between 3 to 5 weeks old bear the most intense and steady innervation, which reaches the gonad through three different routes: the funicular, caudal and mesorchial innervations. Their testicular nerve fibers supply the vascular structures of the spermatic cord, the tunica albuginea, almost all the septula testis and the mediastinum. In pigs of 7-10 week-old, varying degree of testicular innervation withdrawal are conspicuous and in the adult boar testes, the funicular nerve supply to the testicular artery and pampiniform plexus are retained but with no evidence of intrinsic nerves.

It has been shown that the intimate anatomical association between peptidergic nerves and Leydig cells enable the numerous neuropeptides released from the nerves to act as modulators for steroidogenesis in Leydig cells (Gong *et al.,* 2009). However, neuropeptide-like substance P has been found to reduce number of luteinising hormone-binding sites in Leydig cells and thus inhibits their testosterone production (Kanchev *et al*., 1995). In addition, the gap junctions between Leydig cells further

facilitates the prompt response of the cells to the physiological effect of neurotransmitters (Pérez-Armendariz *et al*., 1994).

Molenaar *et al*. (1997) has earlier proposed that an inverse functional correlation exist between the nervous and endocrine regulation of mammalian testis more specifically the porcine testis. The porcine endocrine Leydig cell population appears in a wave-like manner during normal postnatal development, and could be divided into four periods of distinct histological characteristics: Fusiform-like Leydig cells become polygonal throughout the period of early postnatal proliferation (from birth to day 14); Leydig cells attain maximal size during the period of prepubertal hypertrophy (3 to 7 weeks) and exhibit all the ultrastructural and histochemical characteristics of steroid production; cellular degeneration and a drastic reduction of the surviving Leydig cells occur during the period of prepubertal regression (7 to 12 weeks) and the period of Leydig cell proliferation in pubertal period (begining at 15 weeks) culminates to the adult phase (Wrobel *et al.*, 1973, 1974; Dierichs *et al.*, 1973). The first period of Leydig cell hypertrophy in adult is accompanied by abundant innervation, while the second period of Leydig cell activity is followed by a complete absence of nerves from the testis proper (Wrobel and Brandl, 1998).

2.4.2 Astrocyte Expression in the Testes

Astrocytes are glial cells that are usually situated close to nerves as support cells in both central and peripheral nervous systems. Functionally, astrocytes have many roles prime of which is the maintenance of blood-brain barrier (Falade *et al.,* 2017). The recognised marker of astrocyte in the CNS remains an intermediate filament, the glial fibrillary acid protein (GFAP) (O'Callaghan and Sririam, 2005; Sofroniew and Vinters, 2010). Recent studies have shown its expression in non CNS tissues with messenchymal stellate cells including the liver, kidney, pancreas, lungs, and testes, which share functional similarity with astrocytes (Bush *et al*., 1998; Zhao and Burt, 2007; Lim *et al*., 2008). Astrocytes have been localised in Leydig cells of the rat and human testes (Holash *et al.,* 1993; Davidoff *et al.,* 2002).

2.5 The Physiology of S-100 and Its Distribution in Mammalian Testis and Epididymis

S-100 protein, a family of calcium binding proteins, bears a low molecular weight ranging between 10 to 12kDa (Heizmann *et al.,* 2002). It was named for its dissolving ability in ammonium sulphate solution saturated at 100% and at pH of 7 (neutral)

(Moore, 1965). S—100 consists of two subunits (S100-α and S100-β) which are expressed selectively by specific cell types that form either homodimers (α – α called S-100 α or β – β referred to as S-100 β) or heterodimers (recognised as S-100a) (Cruzana *et al.,* 2003). Based on phlethora of works, this protein is known for diverse roles ranging from calcium-buffering through intracellular (such as enzymatic activities modulation, energy utilization, movement and secretion) and nuclear (including transcription and apoptosis) roles as well as extracellular activities including secretion, neurite growth and chemotaxis (Heizmann *et al.,* 2002).

Saturated 100 proteins has been demonstrated in physiological conditions in cells and organs like nerve fibers, amnion, trophoblast, decidual cells of fetal membranes, in Sertoli cells, Leydig cells, seminiferous peritubular cells, efferent ductule, thyroid gland parathyroid gland, hair cuticle cells, myeloid cells, lung, kidney, liver, cardiac and skeletal muscle (Schäfer and Heizmann, 1996; Wicki *et al.,* 1996; Boni *et al.,* 1997; Heizmann and Cox, 1998; Vogl *et al.,* 1999; Donato, 1999, 2001; Paulsen *et al.,* 2000; Arcuri *et al.,* 2002; Marinoni *et al.,* 2002). In addition, S100 proteins have recently been used as reliable diagnostic markers for detecting melanoma metastasis (Krähn *et al.,* 2001), brain damage induced by hypoxia, examining the progress of cardiac arrest (Böttiger *et al.,* 2001), squamous-cell carcinomas and breast cancer (Lauriola *et al.,* 2000) and as prognostic indicators for gastric (Yonemura *et al.,* 2000) and esophageal (Ninomiya *et al.,* 2001) cancers.

S-100 proteins have been immuno-localised in the testis and epididymis of different mammalian species including rat and cat (Amselgruber *et al.,* 1994; Cruzana *et al.,* 2000), farm animals (Amselgruber *et al.,* 1992; 1994; Alkafafy, 2005), buffalo (Alkafafy *et al.,* 2011), rabbit and human (Michetti *et al.,* 1985; Haimoto *et al.,* 1987). In these diverse species, S-100 has been suggested to participate in the secretory and absorptive functions and may also play roles in blood-testis barrier formation (Czykier *et al.,* 2000; Cruzana *et al.,* 2000; Cruzana *et al.,* 2003; Abd-Elmaksoud *et al*., 2014).

Generally, S-100 immunostaining of the testicular parenchyma and epididymis have been reported to present varied staining intensity. Strong staining intensity occurred within the vasculature (arteries, veins and capillaries) of testis and epididymis especially in rat, pig, sheep, goat and European bison and man (Amselgruber *et al.,* 1992; 1994; Czykier *et al.,* 1999, 2000 and 2010) as well as in the nuclear and cytoplasmic portions of the Leydig cells of rats, cats, and human (Amselgruber *et al.,* 1994). Also, distinct immunostaining was reported in peritubular cells of the testis of tom, dog and rat (Amselgruber *et al.,* 1994; Cruzana *et al.,* 2000). However, weak S-100 immunostaining was demonstrated in the testicular Leydig cell of pig and stallion (Amselgruber *et al.,* 1994; Czykier *et al.,* 2000). Similarly, the epididymal basal and principal cells nuclear and cytoplasmic parts have been reported to show intense S-100 immunostaing in bovine, donkey, buffalo and camel (Alkafafy, 2005; Alkafafy, 2009; Alkafafy*et al.*, 2011). It is essential to state that in bovine the ciliated cells of the epididymis have been found to be strongly stained by S-100 marker (Alkafafy, 2005).

Age-related changes in the expression of S 100 in the testis and epididymis in mammals is less reported. Czykier *et al.* (2010) observed a weak expression of S-100 in the smooth muscle cells of epididymal arteries and vein of young European Bison relative to their adult counterpart and an equally strong positive expression in the endothelium of the vasculature (arteries, veins and lymphatics) of both young and adult epididymis.

2.6 Role and Distribution of Vimentin in Mammalian Testis and Epididymis

The mammalian tissues are made up of five principal intermediate filaments which include; vimentin (expressed in mesenchymally derived cells), cytokeratins (in epithelial cells), desmin (in muscular precursor cells), glial fibrillary acidic proteins and peripherin (expressed in many components of nervous system) (Kopecky *et al.,* 2005).

Vimentin, a typical intermediate filament, forms component of cytoskeleton in the testicular and epididymal cells and has a molecular weight of 57 kDa (Lydka *et al.,* 2011).Vimentin has been localised in the testicular Sertoli cells, peritubular-myoid and Leydig cells (Steinert *et al*., 1984; Wang *et al*., 1985; Virtanen *et al*., 1986 and

Bilin´ska 1989, 1994) and in sub epithelial myoid cells and interstitial stroma between the epididymal ducts (Sasaki *et al.,* 2010).

In Sertoli cells, vimentin is expressed around the basal and perinuclear regions and progressively radiates towards the cytoplasmic apex to relate with specialized membrane structures existing between the Sertoli cells and adjacent germ cells (Kopecky *et al.,* 2005). Thus, the role of vimentin in this regard has been assumed to be involved in attachement of germ cells to the seminiferous epithelium and in the movement of the elongated spermatid within the epithelium (Show *et al*., 2003; Hejmej *et al*., 2007; Kotula-Balak *et al*., 2007). In addition, their distribution within the Sertoli cells helps in safeguarding spermatogenic process (Lydka *et al.,* 2011). It important to mention that damage to vimentin could result in seminiferous epithelial disintegration and this usually culminates in non favorable restoration of spermatogenesis even after recovery (Kopecky *et al.,* 2005). Vimetin expression in the peritubular myoid cells of mammalian testis has been linked to its crucial role in the contractions of the seminiferous tubules in transporting spermatozoa and testicular fluid (Miyake *et al.,* 1986; Maekawa *et al.,* 1996; Sasaki *et al.,* 2010).

Available data on age-related changes in vimentin expression intensity in testicular cells most especially Sertoli cell was documented by Sasaki *et al.* (2010) in mouse deer. It was observed that despite the existence of variation in Sertoli cell sizes between immature and adult mouse deer, there was no remarkable difference in the localisation and intensity of vimentin positive reaction. Similarly, the sub epithelial myoid cells and the stroma between the epididymal duct interstices positively expressed vimentin in both immature and adult deer (Sasaki *et al.,* 2010).

2.7 Sex Hormone Interplay in Male Mammals

2.7.1 Gonadotropin Releasing Hormone

Gonadotropin releasing hormone neurons of the hypothalamus are the primary driving regulatory factors of the reproductive axis (Gore, 2002a). GnRH neurons secrete pulsatile gonadotropin releasing hormone (GnRH) into the pituitary vascular (hypophyseal portal) system through which it is transported to the anterior pituitary gland. The gonadotrope cells of pituitary bearreceptor sites for GnRH coupling which on binding to the latter stimulates the biosynthesis and secretion of the gonadotropins;

luteinising hormone (LH) and follicle stimulating hormone (FSH) (Ehlers and Halvorson, 2013). The gonadotropins travel through the peripheral circulation to act on the gonads to stimulate gametogenesis (development of sperm) and steroidogenesis (synthesis of estrogen, progesterone and androgens) (Ehlers and Halvorson, 2013). Physiologically, the gonadal steroids exert feedback on the hypothalamus and pituitary to decrease GnRH and gonadotropin secretion (Ehlers and Halvorson, 2013).

The GnRH bears a short half life of about 2-4 min which could be attributed to its rapid cleavage by peptidases. Owing to its fast degradation coupled with its massive dilution, biologically active concentrations of GnRH is not present in the peripheral circulation (Wetsel and Srinivasan, 2002). Thus, the serum levels of LH and FSH are usually employed clinically as substitute markers of pulsatile GnRH secretion (Ehlers and Halvorson, 2013).

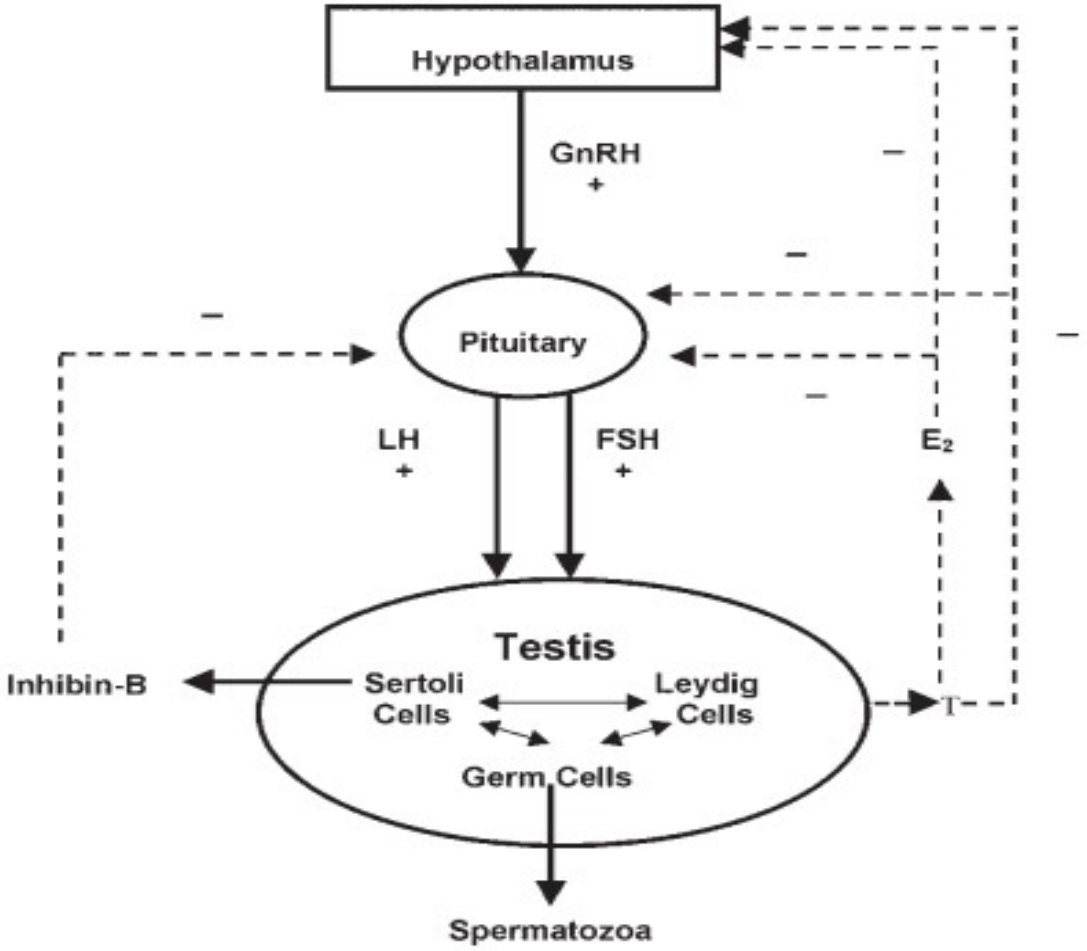

Figure 2.5. Regulation of hypothalamic-pituitary-testis. The solid lines represent stimulating effects and the dashed lines negative feedback actions.

Source: Nadir *et al*. (2016)

2.7.2 Luteinising Hormone

The luteinising hormone (LH) stimulates the secretion of sex steroids from the gonads of both sexes (Banks, 1993). The physiological effect of LH in male subject is usually brought to the fore when it binds to its receptor on testicular Leydig cell membrane to initiate the production of testosterone biosynthetic enzymes which participate in the conversion of cholesterol to testosterone (Speroff and Fritz, 2005; Araujo and Wittert, 2011). Apart from the aforementioned, LH is also needed for the differentiation of Leydig cells and the growth of the testes (Araujo and Wittert, 2011).

2.7.3 Follicle Stimulating Hormone

Follicle stimulating hormone (FSH) regulates spermatogenesis subsequent to its binding to the FSH receptor in the basal aspect of the plasma membrane of Sertoli cells in the testis (Araujo and Wittert, 2011). On its own, FSH is capable of exerting influence and in conjuction with testosterone can initiate Sertoli cell proliferation, maturation and function that will eventually produce regulatory signals and nutrients for the preservation of developing germ cells (Oduwole *et al.,* 2018**).** The production of FSH secretion is under the alteration of two gonadal hormones; activin and inhibin (Kumar, 2009; Peltoketo *et al.,* 2010). Activin is secreted by the Sertoli cell, boundary and Leydig cells (Araujo and Wittert, 2011). In the gonadotroph cells of the pituitary, activin interact by binding to activin receptor type II on it to initiate follicle stimulating hormone secretion (Araujo and Wittert, 2011).

Elevation in the secretion of FSH is postulated to be by the stimulation of hypothalamic GnRH (Kumanov *et al.,* 2005). Similarly, inhibin is largely produced in the Sertoli cells and its release is stimulated by FSH (Araujo and Wittert, 2011). The released inhibin in turn suppresses FSH secretion via a negative feedback mechanism (Meachem*et al.,* 2001; Araujo and Wittert, 2011**).**

2.7.4 Testosterone

Testosterone is a primary male sex hormone that is secreted by Leydig cells of the testis (Banks, 1993). On binding of LH to Leydig cells, there is increased expression of steroidogenic acute regulatory protein (StAR). The latter promotes the transfer of cholesterol (precursor for testosterone synthesis) to the inner mitochondrial membrane and initiates steroidogenesis (Araujo and Wittert, 2011). Scott *et al.* (2009) described the steroidogenetic process on the inner membrane. At the inner mitochondrial membrane, cholesterol is converted to pregnenolone by the action of P450 side chain

cleavage enzyme. Pregnenolone is then converted to dehydroepiandrosterone (DHEA) in a two-step process mediated by 17, 20-lyase (17α-hydroxylase). The DHEA due to high expression levels of 3β-hydroxysteroid dehydrogenase (3β-HSD) and 1 7β-hydroxy steroid dehydrogenase (17β-HSD) in the Leydig cells is rapidly converted to testosterone via the intermediates androstenediol and androstenedione. In target tissues, testosterone is converted to dihydrotestosterone (DHT) by the action of 5α-reductase. The DHT accounts for most of the testosterone's biological action though its concentration is about one-tenth that of testosterone. Plasma testosterone is available as unbound or free testosterone, bound testosterone (i.e with albumin) and testosteronecoupled to sex hormone-binding globulin (SHBG) (Maitsumoto, 2001). The total plasma testosterone assays measure both free testosterone and testosterone coupled to SHBG and albumin (Araujo and Wittert, 2011).

2.7.5 Estrogen

Estrogens, principal female hormones responsible for female sexual characteristics are not entirely found in female only but also synthesized in males (Schulster *et al.,* 2016). Circulating testosterone is first converted to androstenedione which is in turn modified to form estradiol and estrone by the action of aromatase (P450aro) in certain peripheral tissues (Scott *et al.,* 2009). These estrogens (estradiol and estrone) are believed to locally exert their influence and subsequently metabolized in target tissues. It is important to mention that some testicular and brain nuclear receptors modulate estrogenic actions involved in male reproductive function (Schulster *et al.,* 2016; Torran-Allerand *et al*., 2005) and via estrogen –dependent mechanisms through which it can mediate negative feedback exerted by testosterone on GnRH expression (Naftolin *et al.,* 2007).

2.7.6 Progesterone

The importance of progesterone in male endocrine system is less clear before now; however, in recent times its role as modulator of male endocrine system become more obvious (Oettel and Mukhopadhyay, 2004). It is believed to play a role in activating sperm in the female reproductive tract and as a modulator of male sexual response and behaviour (Oettel and Mukhopadhyay, 2004). In steroidogenesis cycle, pregnenolone remains the precursor of progesterone. The latter becomes 17α-OH-Progesterone (P) (main serum metabolites of progesterone) when catalyzed by 17,20-hydroxylase. On further catalysis, the 17α-OH-P yields androstenedione and dehydroepiandrosterone

which are intermediate steroids in the biosynthesis of androgens and estrogens (Shackleton and Malunowicz, 2003).

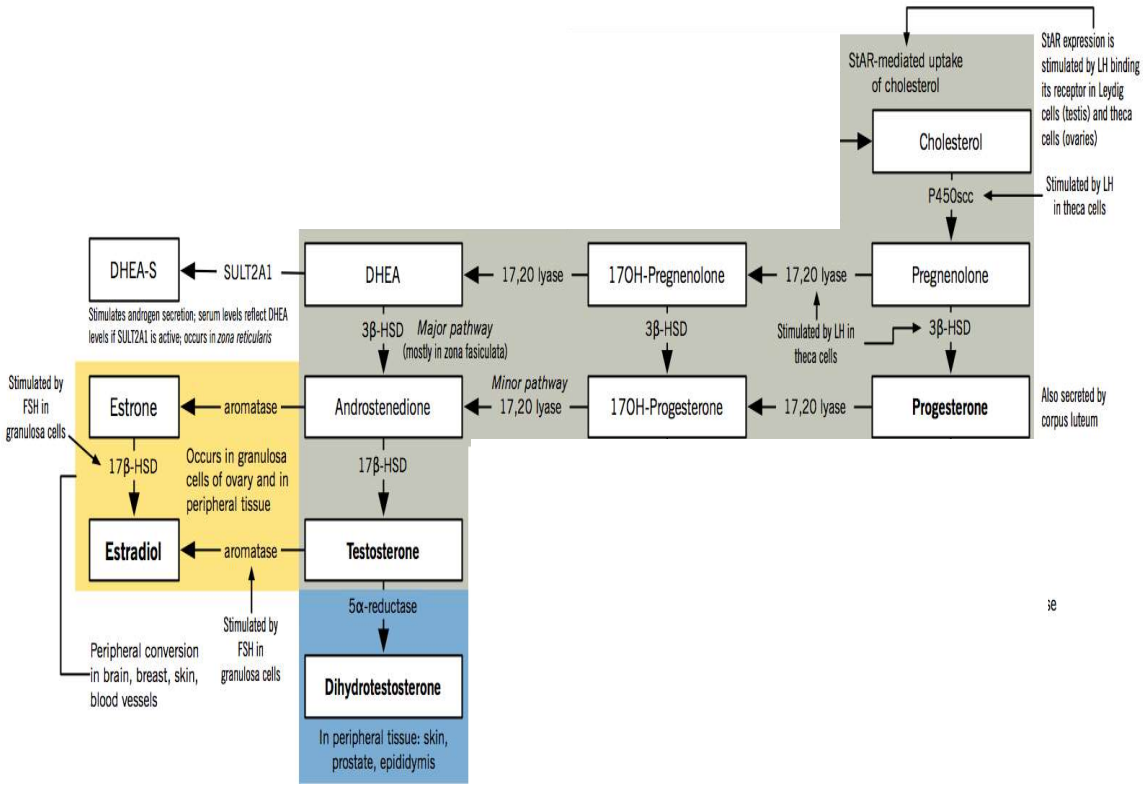

Figure 2.6. Stages involved in steroidogenesis (Source: Mostaghel, 2013)

2.7.7 Age-related Changes in Hormonal Profile

Age-associated alteration in the anterior pituitary gonadotropes'physiology regulating luteinising hormone and follicle stimulating hormone secretions has been associated with reproductive senescence (Hall and Gill, 2001). Available report on the profile of pituitary gonadotropins (LH and FSH) especially in man showed that their levels in the serum increase with age advancement (Feldman *et al.,* 2002). The gonadotropins elevated levels with advancement in age has been found to coincide with the consistent decrease in level of testosterone provided that the feedback pathway is normal to permit suboptimal testosterone level to exert influence on hypothalamic-pituitary axis to permit FSH and LH secretions (Bagatell and Bremnar, 1996). Although study conducted by Woerdeman *et al.* (2010) has shown that a reasonable decrease in the synthesis of testosterone may not be entirely accompanied by elevated LH production even in young male subject which is suggestive of level of moderation within the system to variation in the levels of gonadal steroids.

The climax in the level of testosterone especially at puberty is influenced by a complementary hypertrophy of Leydig cell which has been hypothesized to be involved in inducing proliferation of germ cells and central nervous system differentiation on sexual basis (Choi and Smitz, 2014). Though available data from hormonal profile study in man showed a decline in testosterone level with age, such finding has been found not to be universal as testosterone level may be unchanged or elevated with advancement in age in a number of men and rodents such as hamster rats (Calvo *et al*., 1999; Travison *et al*., 2007).

Serum estrogen level rises with increasing age mainly because of increased body fat as well as increase in aromatase activity (Leder *et al.,* 2004). The elevated level of the latter could result in decline in testosterone level. However, the influence of age variation on the pattern of estrogen levels has been variously reported to either decline or remain steady (Orwoll *et al.,* 2006; Araujo *et al.,* 2008).

CHAPTER THREE

3.0 MATERIALS AND METHODS

3.1 EXPERIMENT ONE

3.1.1 Gross Morphological and Morphometric Studies of the Testis and Epididymis in Different Age Groups of the Cane Rat.

3.1.1.1Experimental Animals

Twenty (20) apparently healthy AGCR were obtained from a commercial farm, Pavemgo grasscutter, Ibereko, Badagry, Lagos state, reputable for keeping birth records. The birth records of the AGCR were taken at the point of purchase. The grossly accessible reproductive organs (testes and penis) were clinically examined for their presence in normal location. Thereafter, they were stabilized for 7days in the Experimental Animal Unit of Department of Veterinary Anatomy, University of Ibadan. During the period, the animals were fed with dry corn feed daily and water *ad libitum*.

3.1.1.2 Experimental Design

The grouping (young: 1-3 months, young adult: 4-7 months and adult:>8 months) reported by Soro *et al*. (2014) for AGCR in a similar age-related study was modified and used for sorting AGCR into four (4) groups of five (5) animals each; prepubertal (1-4 months), pubertal (5-11 months), adult (12- 30 months) and aged (>30 months).

3.1.1.3Anesthesia and Organ Excision

The rats were anaesthetized using intramuscular injection of xylazine and ketamine combinations (20mg/kg: 80mg/kg bdwt; respectively). Thereafter, the abdominal wall of each rat was opened upby a ventral midline incision through the linea alba. Using the approach of Olukole *et al.* (2010), the testes together with their attached epididymis were excised via the opening created by surgical incision on the tunica vaginalis and then placed in petrish dishes containing normal saline to prevent organ dessication.

3.1.1.4Determination of Testicular and Epididymal Gross Morphometric Parameters

Prior to the dissection of the anaesthetized AGCR, bodyweight of each rat was taken using a digital weighing scale (Camry, China). Consistently, the weight of the right

testis and epididymis of the different group of AGCR was determined using digital Microvar weighing balance and biometric parameters were measured using digital vernier caliper (Mitutoyo Company, Japan). The relative weights of each of the organs were calculated with the use of the formular below:

$$\text{Relative Weight (\%)} = \frac{\text{Weight of Organ (g)}}{\text{Weight of animal (g)}} \times 100$$

Gross testicular and epididymal biometric parameters such as length, width and circumference were obtained using the description of Olukole *et al*. (2009). The length was taken as the distance between the anterior to the posterior borders, the width as the distance between the lateral and medial borders and the circumference as the total distance obtained when testis is encircled at its mid-portion with a calibrated nylon tape.

3.1.1.5 Statistical Analysis

Data obtained were expressed as mean ± SE. Using GraphPad Prism Version 4.00 for Windows, GraphPad Software (GraphPad Prism, 2003), one way analysis of variance (ANOVA) was used to evaluate significant difference across groups and the values of $p<0.05$ was considered significant. A Turkey post hoc test was further used to evaluate significant difference between groups.

3.2 EXPERIMENT TWO

3.2.1 Age-related Changes in the Histology, Histochemistry, Histomorphometry and Ultrastructure of the Testis and Epididymis of the African Greater Cane Rat

3.2.2 Experimental Animals

A total of thirty (32) AGCR were obtained from the same commercial farm and stabilized as stated in section 3.1.1

3.2.3 Experimental Design

This is similar to the design in section 3.1.1.2. However, testes and epididymaltissues from twenty (20)out of the 32 animals were used for histological, histochemical and microsterological analysis. While, the remaining twelve (12) were used for ultrastructural study.

3.2.4 Preparation of Secondary Fixative (10% buffered formalin solution) for Light Microscopy

The secondary fixative was prepared by adding 100 ml of formalin (37-40% stock solution) into 900 ml of distilled water. Phosphate buffer salts (6.5 g/L of sodium phosphate dibasic, Na_2 HPO_4i.e disodium hydrogen orthophosphate, anhydrous) and 4g/L sodium phosphate monobasic, NaH_2PO_4 (i.e sodium dihydrogen phosphate) were added to the solution to neutralise the pH of the fixative.

3.2.5 Preparation of Karnovsky Glutaraldehyde Fixative for Electron Microscopy

The fixative was prepared by mixing paraformaldehyde powder (2 g) with distilled water (25 ml) in a beaker. The mixture was then heated to 60°C on a magnetic stirrer plate (78-1 Magnetic hot plate, China). Once moisture started appearing on the sides of the flask, 2-4 drops of (1M) sodium hydroxide was added and stirred until the solution became clear and thereafter allowed to cool. The solution was then filtered and to the filtrate 10ml of 25% glutaraldehyde was added as well as 20 ml of 0.2M cacodylate buffer maintained at pH range of 7.2 to 7.4.

3.2.6 Anaesthesia

The same protocol described in section 3.1.1.3 was used.

3.2.7 Dissection and Perfusion

The abdominal wall of each rat was dissected open through a ventral midline incision and the thoracic cage opened to expose the heart. This was then followed by the perfusion of 0.5 L of pre-perfusion (primary) solution [0.9% sodium chloride (Aventra, Fidson, Nigeria) and 25, 000 IU of heparin (2IU\ML) (Heparinum; Polfa). The pre-perfusion fluid was introduced with an 18G x ¾ butterfly needle via the left ventricle. A complementary slit was made into the right atrium to minimize pressure build-up within cardiac chambers. The heparin in the pre-perfusion solution helped to prevent blood clotting in the smaller capillaries during perfusion so that a clean perfusion can be achieved. The primary solution was followed with secondary perfusion of either 10% buffered formalin for tissues meant for light microscopy or Karnovsky glutaraldehyde fluid perfusion for tissues needed for ultrastructural investigation. The perfusion persisted till satisfactory change was observed in the testes colour.

3.2.8 Organ Excision

The testes and epididymides were carefully excised from the anaesthetized rats using the description in section 3. 1. 1. 3 and trimmed for further processing. For those tissues required for electron-microscopy, further trimming into tiny pieces using sharp razor blade into a rice grain size for thorough permeation of the fixative into the tissue during post fixation in sample bottle was carried out. In case of epididymal ultrastructure, tissues were carefully taken from three segments (caput, corpus and cauda) of the epididymis.

3.2.9 Tissue Processing for Histology, Histochemistry and Histomorphometry

Trimmed right testicular and epididymal tissues were processed for histology using the protocol of Olukole *et al.* (2010). Briefly, trimmed tissues were dehydrated in graded concentrations of alcohol; 70% for 1 hour, 90% thrice for 1hour and two times in absolute alcohol (100%) for 1 hour each. This was then followed by clearing of dehydrated tissues in xylene for 2 hours each and in turn embedded in paraffin wax at 60°C. The waxed tissue blocks were then sectioned at 5µm thickness using rotary microtome (Leica, USA). Sections obtained were mounted on clear albuminized slides subsequent to floating on a warm water bath and then dried in an oven and stained with haematoxylin and eosin (H & E). The stained tissues were then examined

under light microscope (Olympus BX3-CBH, USA) for variation in histoarchitecture in relation to age differences.

Masson trichome staining:This was carried out in accordance with the method of Kumari (2013). Briefly, sections from tissue blocks were dewaxed in xylene for 5 minutes. The dewaxed tissues were later rinsed in 100%, 96% and 70% alcohol each for 1minute. This was followed by rinsing in distilled water for 5 minutes and subsequently stained in filtered Celestine blue solution for 15 minutes. This was succeeded by rinsing the tissue thrice in distilled water and followed with staining in Lily-Mayer haematoxylin for 1minute. Bluing was then done under tap water for 10 minutes, followed by staining with the Biebrich Scarlet Fuchsin solution for 15 mins and rinsed again in distilled water. The tissues were then subjected to mordanting in Phosphotunstic-phosphomolybdic acid for 5 mins, counter-stained in aniline blue for 5 minutes and in turn rinsed in distilled water. Rinsed tissues were then differentiated for 3mins in 1% glacial acetic acid, dehydrated in 96% and 100% alcohol, cleared in xylene and mounted on Entellan slide. On viewing, parts of the tissues that were positive for collagen fibres stained bluish while the nuclei appeared black and cytoplasm, keratin, muscle fibre and intercellular fibres stained reddish

Periodic Acid Schiff's staining: This was carried out as earlier described by Rajani *et al*. (2008). Briefly, waxed sections of testis and epididymis from the different AGCR groups were dewaxed in xylene for 5 minutes and rinsed consecutively in 100%, 96% and 70% alcohol for 1minute each. This was followed by placing rinsed tissues in distilled water and subsequently treating with undiluted periodic acid for 10 minutes. The treated tissues were washed in eight changes of distilled water, exposed to Schiff's solution for 1hour and washed in running tap water for 10 minutes. The nuclei were distinctly stained with Lilly Mayer's heamatoxylin for 1 min and further differentiation was avoided. Bluing of the tissues was done under tap water for 10 minutes. This was followed by tissue dehydration in 96% and 100% alcohol, cleared in xylene and mounted in Entellan. When viewed under microscope, parts of the tissue that were positive for glycogen stained magenta while the nuclei stained bluish.

Photomicrographs of the captured slides of the testis and epididymis of different age groups of AGCR were evaluated for variations in testicular (seminiferous tubular diameter, luminal diameter and epithelial height) and epididymal (ductal diameter,

ductal height, luminal diameter, stereocilia height and peritubular muscle coat thickness) parameters using GIMP2 Software.

3.2.10 Processing of Cane Rat Tissues for Electron Microscopy

Post-fixed tissues were transferred from fixative to sample bottle containing Millonig's buffer two times and centrifuged at 3000 revolution per minute (rpm) on a rotator for 10 minutes each during the changes. Thereafter, the tissues were taken through two (2) changes of Osmium tetraoxide in Millonigs buffer for 1 hour. Then, they were rinsed twice in distilled water for a duration of 10 minutes each. They were subsequently passed through increasing grades of alcohol; 50%, 70%, 80%, 96% for 10 minutes duration in each of them and in two changes of 100% ethanol (with molecular sieve) for 10 minutes each. This was followed by; changes in propylene oxide (PO) two times at 10 minutes each, 2:1 ratio of PO to epoxy resin (ER) for 30 minutes to 1 hour, 1:2 ratio of PO to ER for 24 hours. The tissues were then embedded in labeled moulds containing 100% epoxy resin with aid of a stereo microscope (Zeiss Stemi DV4, USA) for 36 hours under vacuum. Afterwards, tissues were further embedded in fresh ER and cured in oven at 65°C for 48 hours for microtomy. Semi-thin sections were stained with toluidine blue and viewed under the light microscope (Olympus BX63 with a DP72 camera). Thereafter, ultra-thin sections (70–80 nm) were cut using a diamond knife on an ultramicrotome (Leica EM UC7, USA). The sections were placed on copper grid screen, stained for five minutes in uranyl acetate (2% in distilled water) and ten minutes in lead citrate (0.5% in distilled water) respectively. The copper grids were viewed under a transmission electron microscope (Philips CM 10 TEM, USA) functioning at 80 kv. Micrographs of different stages of spermiogenesis were captured using a Gatan 785 Erlangshen digital camera (Gatan Inc., Warrendale PA)

3.2.11 Statistical Analysis

Data obtained from histomorphometry and image J quantification of PAS and Masson trichrome staining intensities were statistically analysed using GraphPad Prism Version 4.00 for Windows, GraphPad Software (San Diego, CA, USA). The differences between the four groups of AGCR were compared using one-way analysis of variance (ANOVA) and Turkey test was used for multiple comparisons *post hoc*. The results were expressed as group mean ± standard error of mean (SEM), with level of significance at $p<0.05$.

3.3 EXPERIMENT THREE

3.3.1 Age-related Changes in the Sperm Parameters of the Testis and Epididymis in the African Greater Cane Rat

3.3.2 Experimental Animals

The same animals used in experiment 3.1.1.

3.3.3 Experimental Design

This is as described in 3.1.2.

3.3.4 Anaesthesia and Organ Excision

These were carried out as described in 3.1.3. The left testis of each of the group of AGCR was milked out of the incision site and exposed by incising the tunica vaginalis.

3.3.5 Sperm Morphological Characteristics

Morphological defects in the spermatozoa architecture were observed from a total of 400 sperm cells using the method of Wells and Awa (1970). Briefly, a drop each of Wells and Awa stain (0.2g of Eosin and 0.6g of Fast green dissolved in distilled water and ethanol in ratio 2:1) and semen were placed on a warm slide, mixed and a smear was made with another slide. The stained smear was then air dried and viewed under the light microscope. Normal spermatozoa and site of defects in the abnormal spermatozoa (head, neck/midpiece, tail) were recorded and classified according to Bloom (1973) and Parkinson (2001) description. The following classical abnormalities; head (tailless head and headless tail), mid piece (curved mid-pece and bent mid-piece) and tail (rudimentary tail, bent tail, curved tail and looped tail) abnormalities were carefully look out for in the smear.

3.3.6 Determination of Sperm Morphometrics

Spermatozoa morphometry was performed as earlier reported by Sousa *et al.* (2013). Parameters measured were; sperm head length - SHL (the vertical distance between the tip of the acrosome and the boundary with the neck of spermatozoa), sperm head diameter (width) - SHD (longest horizontal distance between the two edges of sperm head), Sperm mid-piece length - SML (distance between the commencement and the end of the mid-piece), STL (distance between the anterior end of the neck and the tip of the tail), SWL (the distance between anterior tip of the sperm head and the tip of

the spermatozoa tail). Sperm morphometric analysis of sections captured for morphological study was performed using GIMP2 Software. For each of the five (5) animals per group, 10 spermatozoa devoid of any morphological defects were selected totalling 50 spermatozoa per group of AGCR.

3.3.7 Determination of Sperm Motility

The percentage of spermatozoa displaying a unidirectional progressive movement over a field on a microscope slide was observed with a camera mounted light microscope using the method described by Zemjanis (1970). Briefly, the excised testis and epididymal segments (caput, corpus and cauda) from each of the different groups of AGCR were incised on the surface and a small drop of semen was taken and mixed with 2.9% warm sodium citrate buffer on a clean slide. The percentage of motile spermatozoa moving in a straight forward unidirectional rectilinear motion were counted by quick observation at x10 low power microscope objective;while, spermatozoa in circular movement, in reverse backward directions or those showing pendulous pattern of movements were ignored.

3.3.8 Determination of the Testicular and Epididymal Sperm Counts

The method of testicular and epididymal sperm count assessments described by Olukole *et al.* (2010) was used. Briefly, testicular and epididymal sections (caput, corpus and cauda) were crushed separately using scissors, washed out with 10 ml of saline and homogenized at 6000 rev/min for 2 mins. Eosin was then added for staining the spermatozoa heads in the obtained homogenate. The testicular and epididymal sperm counts were then estimated as the total number of late spermatids and spermatozoa in the sperm samples obtained from the testes and the various segments of epididymis. All samples were finally made up to 1:20 before counting on the improved Neubauer hemocytometer counter.

3.3.9 Assessment of Live-Dead (Liveability) Ratio

From each of the incised testicular and epididymal tissues, a drop of semen was placed on a well labelled warm slide, mixed with a drop of warm Eosin-Nigrosin stain and then observed under the microscope at X40 objective. It was performed immediately to avoid wrong results. Live sperm cells fail to pick up the stain and

appeared as clear cells while, dead sperm cells picked up the stain and are seen to be purplish in colour. The live and the dead sperm cells were separately counted from a total of 600 spermatozoa in smears stained with Eosin-Nigrosin and the ratio was determined according to the method of Zemjanis (1970).

3.3.10 Statistical Analysis

Data obtained were expressed as mean ± SE. One way analysis of variance (ANOVA) was used to evaluate significant difference between groups and the values of $p<0.05$ were considered significant. A Turkey post ad-hoc test was used to evaluate significant difference between groups using GraphPad Prism 4.0 (GraphPad software Inc., California, USA.) statistical package.

3.4 EXPERIMENT FOUR

3.4.1 Age-Related Changes in the Immunohistochemical Expression of Structural Proteins (Vimentin and S-100), Nerves (Neurofilament) and Glial-like cells (Glial Fibrillary Acid Protein) as well as Histochemical Demonstration of Nerves and Glial Cells Using Golgi Silver Techniques

3.4.2 Experimental Animals

The same animals in 3.2.1 were used for this experiment.

3.4.3 Experimental Design

The left testis and epididymis of the twenty (20) animals used for histological, histochemical and microsterological analysis in section 3.2.2 was used for Golgi silver nerve demonstration technique. Also, the waxed tissue blocks prepared in section 3.2.8 were further processed for all the immunohistochemical protocols.

3.4.4 Anaesthesia and Perfusion

Same as described in 3.2.5 and 3.2.6

3.4.5 Tissue Processing for Golgi-silver Staining Procedure

For the histochemical demonstration of nerves and glial cells, the method described by Olude *et al*. (2015) was adopted. Briefly, trimmed testicular and epididymal tissues (1 mm thick) were immersed in sample bottles of 10-30 mL capacity containing 3% potassium dichromate solution for 5 days. During these days, the bottles were wrapped externally with foil paper to prevent light penetration into the solution.Stale solutions of dichromate were discarded and fresh one added on daily basis within the five days. On the 6th day, the tissue blocks were moved into 2% silver nitrate solution for impregnation in the next 3 days at room temperature. On day 9, the impregnated tissues were removed from silver nitrate into a clean filter paper to remove excess silver precipitates on the tissues. The clean tissues were processed histologically by dehydration through increasing grades of alcohol; 70%, 90%, 100% alcohol and xylene for 5 minutes duration each. Dehydrated tissues were then infiltrated in molten wax at 56°C for 30 minutes. Sections (60 µm thick) were made from the tissue block using microtome (Microm – HM 330, Germany) and then air-dried for 10 minutes and cover-slipped using DPX.Slides were viewed with light microscope for the presence of glial and neuronal structures.

3.4.6 Tissue Processing for Immunohistochemical Localisation of Structural Protein, Nerve Fibres and Astrocyte-like Cells in the Testes and Epididymis of the African Greater Cane Rat

Sections cut from the testicular and epididymal blocks used in experiment 3.2 were processed for immunolocalisation of structural proteins (Vimentin and S-100), nerve structures (Neurofilament) and glial (GFAP) using the Avidin Biotin Complex method (ABC) described by Alkafafy (2009). Briefly, prepared slides were labeled with pencil, dewaxed in oven operated at 60°C and deparaffiinized in 2 changes of xylene. Sections were then hydrated in ascending grades of alcohol to water. This was followed by rinsing in distilled water and antigen retrieval was subsequently carried out on the sections to unmask antigenic sites using 10mM citrate buffer at pH of 6.0 for 25 minutes. Non specific antibody binding and endogenous peroxidase activities were inhibited by subjecting the testicular and epididymal tissue sections to 3% H_2O_2 /methanol for 15 minutes. The sections were then wash in Phosphate Buffered Saline (PBS) and later encircled withPAP pen to create a hydrophobic barrier. This was succeded by blocking in phosphate buffered saline (2% PBS) containing 5% bovine serum albumin for an hour. Each section was then immunolabeled using the following primary antibodies; anti-S-100 (cytoskeleton),anti-Vimentin (cytoskeleton), anti-Neurofilament (neuronal fibres) and anti-GFAP antibodies (astrocyte-like cells). Thereafter, each section was diluted in 1% PBS milk and 0.1% Triton X detergent (for rapid penetration of antibody) and then incubated overnight for 18hrs at 4°C. At this stage, HRP-conjugated secondary antibodies were consequently used by strictly adhering to the manufacturer protocol to detect the bound antibody. The end-product of the reaction was enhanced with 3, 3'-diaminobenzidine (DAB; Vectastain ABC kit) chromogen at 1:25 dilution ratio for 5 minutes. The sections were later dehydrated in grades of alcohol concentrations, de-alcoholized in xylene, mounted with DPX permanent mounting media, coverslipped and allowed to dry. The prepared slides were then viewed and photographed with the light microscope.

3.4.7 Statistical Analysis

Data obtained from the image J quantification of staining intensities of the different immunolabellings were analysed using GraphPad Prism Version 4.00 for Window (GraphPad software Inc., California, USA.) statistical package. The variations in the staining intensity of each immunolabelings were compared using one-way analysis of

variance (ANOVA) and Turkey test was used for multiple comparisons *post hoc*. Results were expressed as group mean ± standard error of mean (SEM) and level of significance at $p<0.05$.

Table 3.1. List of Antibodies Used for Immunohistochemical Labeling.

Primary Antibody & Manufacturer	**Concentration**	**Pre-incubation serum**	**Secondary Antibody**
Polyclonal rabbit anti-S 100 (Dako)	1:400	Normal horse serum	Horse anti-rabbit
Monoclonal mouse anti-vimentin (Dako)	1: 200	Normal bovine serum	Bovine anti-mouse
Monoclonal mouse anti-human neurofilament (Dako)	1:100	Normal horse serum	Horse anti-mouse
Polyclonal rabbit anti-glial fibrillary acid protein (Dako)	1:500	Normal horse serum	Horse anti-rabbit

3.5 EXPERIMENT FIVE

3.5.1 Age-Related Changes in the Serum Hormonal Profile of African Greater Cane Rat

3.5.2 Experimental Animals

Fifty two animals were used for this study and were mainly from those used for experiments 3.1, 3.2 and 3.5.

3.5.3 Experimental Design

The design is as described in section 3.1.2

3.5.4 Anaesthesia

This is as described in 3.1.3.

3.5.5 Blood Collection

The linea alba was incised and extended cranially to the xyphoid cartilage to expose the heart. The left ventricle of the exposed heart was punctured using an 18G x ¾ butterfly needle. Two (2) millilitres of blood was drawn from each of the rat's heart into 5 ml gauge syringe (Agary-ject, China) and released into a plain test tube (Micropoint Diagonistica, China). The blood samples were centrifuged at 3500 revolutions per minute (rpm) for 5 minutes using centrifuge (Gallenkamp, England). Subsequent to the centrifugation, blood was separated into two layers (serum and aggregated blood cell portions). The tube was gently tilted and 1ml insulin syringe was inclined into it to draw the serum into ependorf tubes (Micropoint Diagonistica, China). The tubes were stored at -20°C prior to subsequent hormonal (testosterone, estrogen, progesterone, luteinising and follicle stimulating hormones) assays which were conducted within 48 hours using commercial kits; Dialab, Germany - for FSH, LH, Progesterone and testosterone determinations and Rapid Lab Ltd., UK - kit was used to determine estrogen level.

3.5.6 Hormonal Assay Procedure

The method described by Uboh *et al*. (2007) was adopted for the determination of serum hormonal levels. Briefly, serum levels of testosterone, estrogen, progesterone, follicle stimulating and luteinising hormone were assayed for each of the animals in the different age groups of AGCR using the microplate immunoenzymometric assay kits specifically produced for each of the hormone. The test procedure for the five kits was almost similar for the five hormones and was carried out in accordance to the

manufacturer's description. Twenty five (25µl) microlitre of each of the calibrators, control and serum samples of each of the thirteen cane rats from each of the different age groups of AGCR were pipetted carefully into well labeled microtitre wells in duplicate. One hundred (100 µl) microlitre of the conjugate was added to each well and then swirled for 20-30 seconds to mix. The latter was later covered and incubated for 60 minutes at room temperature after which the contents of the microplate were decanted and blot-dried with absorbent tissue paper. Three hundred (300 µl) microlitre of reconstituted washing solution (prepared by mixing the concentrated washing solution and distilled water at ratio 1:25 in a separate jar) was then added into each well. The latter was then decanted and blot-dried. This washing was repeated for four consecutive times, after which 100 µl of TMB-substrate was pipetted into each well at timed intervals and subsequently incubated for 15-20minutes at room temperature in a dark cupboard. The reaction was then stopped by the inclusion of 150 µl of the stopping reagent into each well at timed intervals and the microtitre wells eventually read on an ELISA reader (Robonik 11-2000, England). A calibration curve was plotted with the optic densities/absorbance on the Y-axis and calibrator concentration on the X axis for five hormonal parameters. The serum concentration of the hormone in each sample was estimated by locating the point of intersection of the average absorbance of the sample duplicates on the vertical axis of the graph to its complementary concentration on the horizontal axis of the graph. The test validity criteria for each of the assay were met in accordance with the kit manufacturer's instructions.

3.5.7 Statistical Analysis

Data obtained were expressed as mean ± SE. One way analysis of variance (ANOVA) was used to evaluate significant difference between groups and the value of $p<0.05$ was considered significant. A Turkey post ad-hoc test was used to evaluate significant difference between groups using GraphPad Prism 4.0 (GraphPad software Inc., California, USA.) statistical package.

CHAPTER FOUR

4.0 RESULTS

4.1 EXPERIMENT ONE

4.1.1 Age-related Changes in the Morphology and Morphometrics of the Testis andEpididymis ofthe African Greater Cane Rat

4.1.1.1 Testicular and Epididymal Gross Appearances in Different Age Groups of the African Greater Cane Rat

The paired testes were suspended in the scrotal sac situated caudo-ventral to the penis. The colouration and shape of the testes were characteristically cream to milky-white and ellipsoidal respectively. The testes were secured at the cranial pole by the mesofurniculus fold (an homologue of the visceral lamina of the vaginal layer enveloping the spermatic cord). The testeswere adhered loosely to the epididymis at the epididymal border by ligament. The testes across all age groups were grossly covered by a transparent capsule, the tunica albuginea (Fig 4.1A&B).

Unlike the testes, the epididymis of all AGCR hadinverted S-shaped outline and was loosely attached to the testis (T). Grossly, epididymis was less distinctly divided into caput (a), corpus (b) and cauda (c) segments. The caput and corpus segments showed visible convolutions relative to the caudal segment (Fig. 4.2A&B).

4.1.1.2 Age-related Changes in the Gross Biometric Parameters of the Testis and Epididymis of theAfrican Greater Cane Rat

The details of the testicular and epididymal biometric parameters were summarized in Table 4.1. The body weights (BW) of the AGCR used for this study increasedsignificantly ($p<0.05$) as age advances with the extremes of BW (0.75 ± 0.14; 4.63 ± 0.24kg) observed in the pre-pubertal and aged respectively. Testicular weight was significantly reduced ($p<0.05$) in the pre-pubertal rat compared to other groups. Also, testicular weights markedly increased ($p<0.05$) in both the adult and aged testes when compared to others. The testicular weight appeared to increase with the age of the animal.

Regarding the relative testicular weight (RTW) or testiculosomatic index, significant decrease ($p<0.05$) was observed in the pre-pubertal rat when compared to others. There was no significant difference ($p>0.05$) in the RTW from pubertal to aged.An insignificant increase ($p>0.05$) was seen in the adult AGCR when compared to others. Similarly, testicular length (TL) and testicular width (TW) weresignificantly reduced

($p<0.05$)in the pre-pubertal rat relative to others. However, significantly increased ($p<0.05$) TL and TW values were seen in both adult and aged AGCR when compared to others. For testicular circumference (TC), significantly decreased ($p<0.05$) values were observed in the prepubertal rat compared to others. There was no significant difference ($p>0.05$) in the TC of pubertal AGCR onwards, though, an insignificant increase ($p>0.05$) existed in the value of TC in adult AGCR relative to others.

Epididymal weight (EW), epididymal length (EL), caput (CW), corpus (CPW) and cauda (CAW) widths presented similar trends of significantly decreased values in the pre-pubertal rat compared to other groups. There was no significant difference ($p>0.05$) in the values of these parameters from pubertal to aged,although, an insignificant increase ($p>0.05$) in their values occurs in the aged AGCR. In addition, there was no significant difference ($p>0.05$) in the relative epididymal weights in all the AGCR groups.

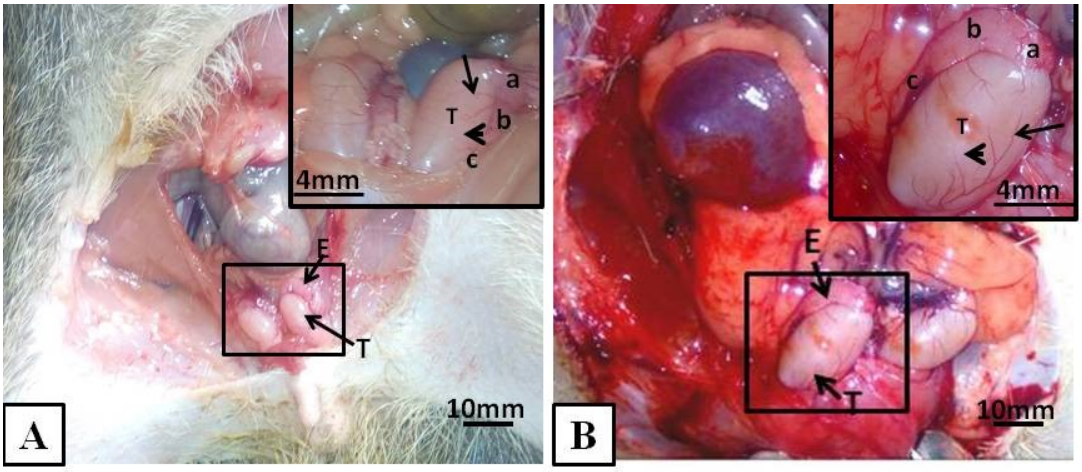

Figure 4.1. Photographs of the male reproductive organs in the cane rat in-situ. A. Pre-pubertal B. Adult. Note the creamy white ellipsoidal testes (T), the inverted S-shaped epididymis (E) and its caput (a), corpus (b) and cauda (c) segments. Also observe the conspicuous albuginea vessels (arrow) and transparent tunica albuginea (arrow-head).

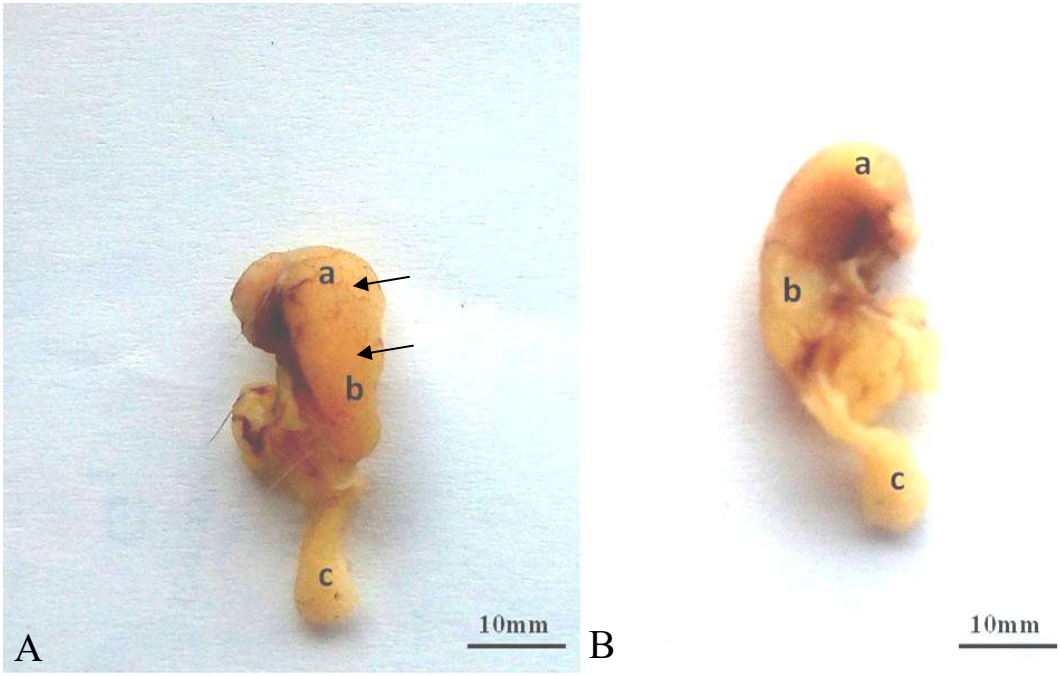

Figure 4.2. Photographs of the epididymis of the African greater cane rat . A. Lateral view B. medial view. Note the inverted S-shaped epididymis and its caput (a), corpus (b) and cauda (c) segments. Also, observe the visible convolutions (arrows) within caput and corpus segments.

Table 4.1. Age-related Changes in the Biometric Parameters of the Testis and Epididymis of African Greater Cane Rat

	PRE	PUB	ADULT	AGED
Body Weight (kg)	0.75 ± 0.14^{a}	1.95 ± 0.08^{b}	3.08 ± 0.15^{c}	4.63 ± 0.24^{d}
Testi. Weight (g)	0.13 ± 0.04^{a}	0.83 ± 0.09^{b}	1.55 ± 0.13^{c}	1.73 ± 0.05^{c}
Rel. Testi. Wt. (%)	0.02 ± 0.00^{a}	0.04 ± 0.00^{b}	0.05 ± 0.00^{b}	0.04 ± 0.00^{b}
Testi. Length (mm)	12.50 ± 0.80^{a}	20.00 ± 0.31^{b}	28.00 ± 0.18^{c}	30.03 ± 0.20^{c}
Testi. Width (mm)	5.70 ± 0.70^{a}	9.00 ± 0.10^{b}	14.00 ± 0.60^{c}	11.30 ± 0.88^{c}
Testi. Circum (mm)	15.00 ± 0.12^{a}	30.30 ± 0.18^{b}	38.00 ± 0.15^{b}	36.80 ± 0.12^{b}
Epid. Weight (g)	0.06 ± 0.00^{a}	0.28 ± 0.00^{b}	0.35 ± 0.00^{b}	0.50 ± 0.00^{c}
Rel. Epid. Wt. (%)	0.01 ± 0.00	0.01 ± 0.00	0.01 ± 0.00	0.01 ± 0.00
Epi. Length (mm)	13.30 ± 0.14^{a}	20.55 ± 0.27^{a}	34.30 ± 0.49^{b}	40.25 ± 0.36^{b}
Cap. Width (mm)	3.25 ± 0.75^{a}	8.00 ± 0.18^{b}	11.00 ± 0.13^{c}	12.25 ± 0.63^{c}
Cor. Width (mm)	1.75 ± 0.48^{a}	6.75 ± 0.85^{b}	9.00 ± 0.13^{b}	10.00 ± 0.71^{b}
Cau. Width (mm)	1.43 ± 0.37^{a}	5.50 ± 0.910^{b}	7.88 ± 0.89^{b}	9.25 ± 0.32^{b}

Values with different alphabet superscripts in the row are significantly different

PRE- Pre-pubertal, PUB – Pubertal, Testi –Testicular, Rel – Relative, Wt - Weight, Cap – Caput, Cor – Corpus, Cau –Cauda

4.2 EXPERIMENT TWO

4.2.1 Age-related Changes in the Histology, Histochemistry, Histomorphometry and Ultrastructure of the Testes and Epididymis of African Greater Cane Rat

4.2.1.1 Histological Changes in the Testes of Different Age Groups of the African Greater CaneRat

The testis in all the groups was enveloped by a capsular covering which was made up of two distinct divisions; tunica albuginea and tunica vaginalis (Fig. 4.3). The tunica albuginea was the closest division to the testicular parenchyma and was composed of dense connective tissue rich in blood vessels, fibrocytes and collagens. Tunica vaginalis was the outermost layer of thin mesothelium. The thickness of testicular coverings seen in this study increased with age. On the difference in the seminiferous tubular architecture (Fig. 4.10), pre-pubertal AGCR (1-3months) lacked a patent lumen within its tubule and instead, the tubule is filled with cords of immature cells (spermatogonia, Sertoli cells and spermatocytes) (Fig. 4.10A). Evidence of patent seminiferous tubular lumen specifically begins in pre-pubertal 4 month old rat (Figure 4.11). Complete spermatogenetic and sustentacular cells (spermatogonia, spermatocytes, spermatids (round and elongated), spermatozoa and Sertoli cell) are visible only in the seminiferous tubules of pubertal to aged AGCR (Fig. 4.10B-D). In addition, the intertubular space (interstitium) in the pre-pubertal rat contains wide non- cellular areas i.e scanty interstitial components (Fig. 4.17A) as opposed to the high Leydig cell presence in the interstitium of pubertal to aged AGCR (Fig 4.17B-D). The cellularity of the interstitum in this study seems to increase with age.

4.2.2 Masson's Trichrome and Periodic Acid Schiff Stainings of the Testes of Different African Greater Cane Rat Groups

With the use of Masson's trichrome, portions of testes positive for collagen fibres were demonstrated in the capsule, peritubular tissue and in the interstices of seminiferous tubules in all the AGCR groups (Figs. 4.6 and 4.13). The PAS positive stained areas for glycogen presence in the testes of different age groups of AGCR include the following; the testicular capsule, seminiferous tubular basement membrane and interstitum (Figs. 4.8 and 4.19). The quantification of the intensity of expression of the stains shows that the trend of both MT and PAS intensities were

similar in the testicular capsule and they increase significantly ($p<0.05$) with the advancement in age of AGCR (Figures 4.7 and 4.9 respectively). For the testicular parenchyma, the intensity of PAS stain was significantly higher ($p<0.05$) in the pubertal ACGR compared to others (Fig. 4.16B). However, there was no significant difference ($p>0.05$) in the MT intensity of all AGCR groups (Fig. 4.14) though; an insignificantly increased MT intensity values were observed in both the adult and aged AGCR.

4.2.3 Age-related Changes in Testicular Histomorphometry

4.2.3.1 Testicular Capsule Thickness and Percentage Capsular Tunic Thickness

Testicular capsule thickness as shown in Fig. 4.4 was significantly reduced in the pre-pubertal AGCR relative to others. In addition, there was no significant difference between the testicular capsule thickness of the adult and aged AGCR though the values were insignificantlyhigher in aged. The pattern of testicular capsule thickness displayed in this study seems to increase with age advancement.

On the percentage capsular tunic thickness (Fig. 4.5), the contribution of the tunica albuginea (TA) to capsular thickness was significantly higher relative to the tunica vaginalis counterpart. With the exception of the significant increase ($p<0.05$) in TA thickness in pre-pubertal, TA thickness was not significantly different from pubertal onwards. Similarly, there was no significant difference in the TV thickness from the pubertal to aged AGCR.

4.2.3.2Seminiferous Epithelial Height, Luminal Diameter and Tubular Diameter

Due to the absence of patent lumen whose boundary is essential in determining the extent of seminiferous epithelial height (SEH), it was difficult to correctly determine the epithelial height as well as seminiferous luminal diameter (SLD) in prepubertal AGCR. In other AGCR groups, SEH trend displayed a decrease with increasing age of AGCR, with the pubertal showing significantly higher levels ($p<0.05$) while the adult and aged demonstrated no significant ($p>0.05$) difference.

For the seminiferous luminal diameter (Fig. 4.12B), significant increase ($p<0.05$) was noticed in both adult and aged relative to the pubertal AGCR, though insignificantlyhigher ($p>0.05$) values occur in the adult when compared to the aged AGCR (Fig. 4.12B). In this study, SLD trend seems to increase with age increment.

On the profile of Seminiferous Tubular Diameter (STD) (Fig. 4.12C), significant increase ($p<0.05$) values was seen from pubertal to aged groups relative to prepubertal AGCR (Fig. 4.12C). Although, increase STD value was noticed in pubertal AGCR, this was not significant ($p>0.05$) enough to establish difference between the three groups (Fig. 4.12C). Thus, with exception of the prepubertal, the trend of STD with age advancement observed in this study appears to be constant.

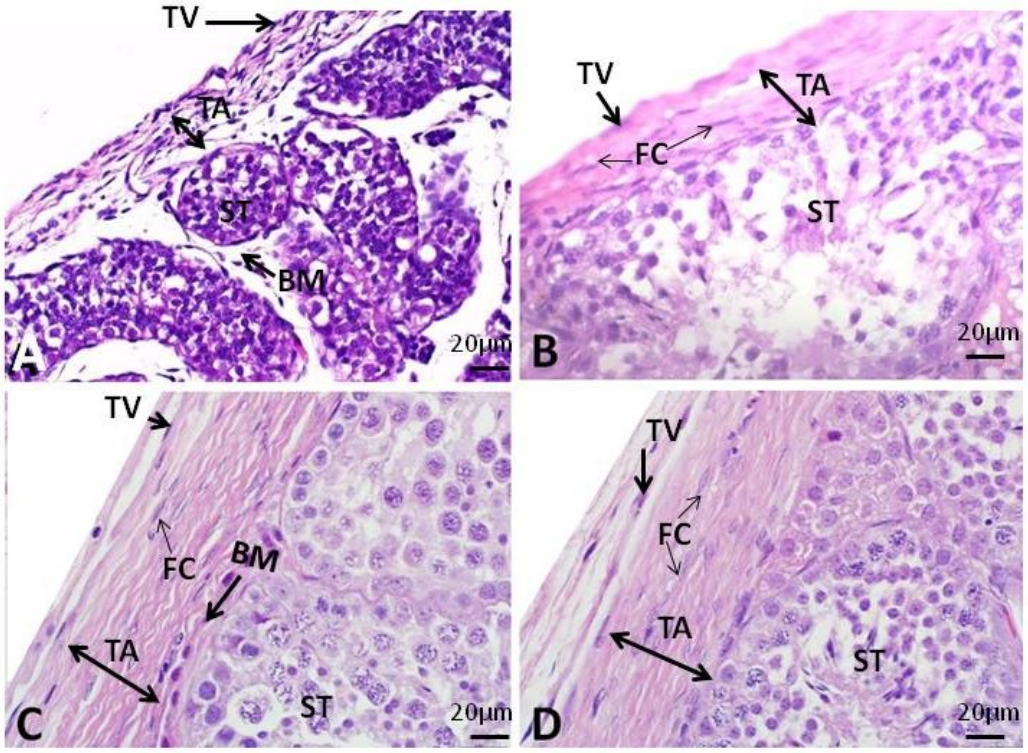

Figure 4.3. Photomicrographs of the Testes of Different Age Groups of AGCR with Their Capsular Coverings. A. Prepubertal: B. Pubertal: C. Adult: D. Aged: Note the tunica vaginalis (TV) with conspicuous elongated nuclei. TA: Tunica albuginea, FC: Fibrocytes, BM: Basement membrane, ST: Seminiferous tubule. Stain: H&E.

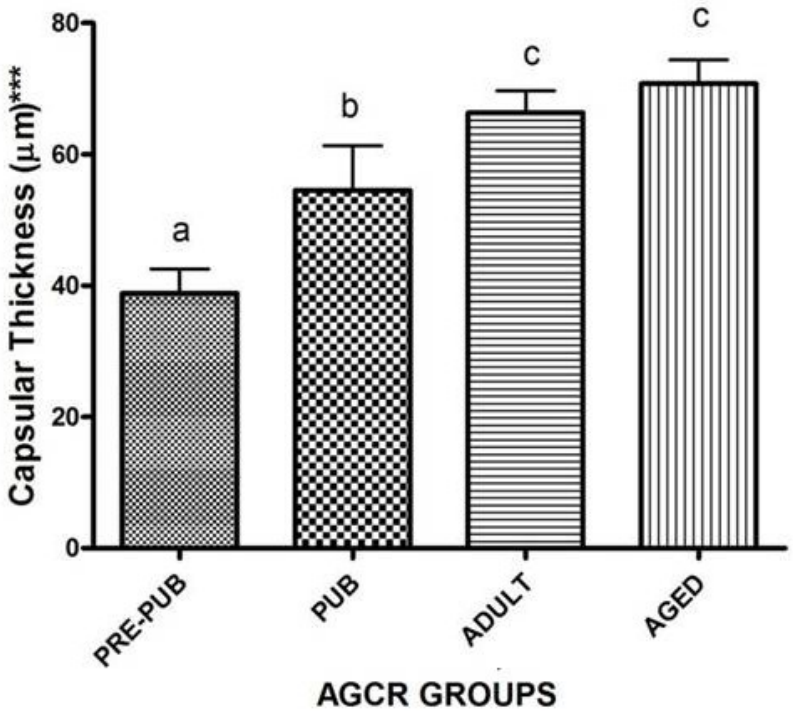

Figure 4.4. Age-related Changes in the Testicular Capsule Thickness of Different Age Groups of AGCR. Bars with different alphabet superscripts (a,b,c) are significantly different.

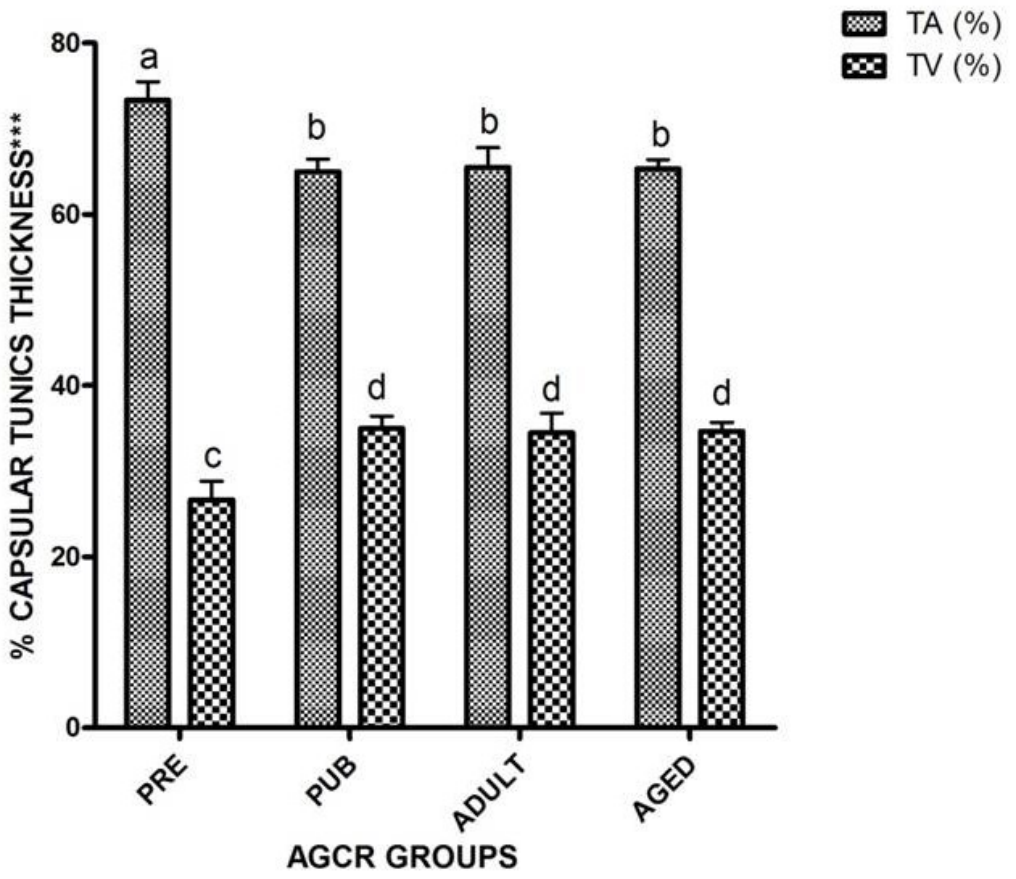

Figure 4.5. Age-related Changes in the Percentage Capsular Tunic Thickness of the Testes of Different Age Groups of AGCR. Bars bearing dissimilar superscripts (a,b,c,d) are significantly different. TA- Tunica albuginea, TV- Tunica vaginalis

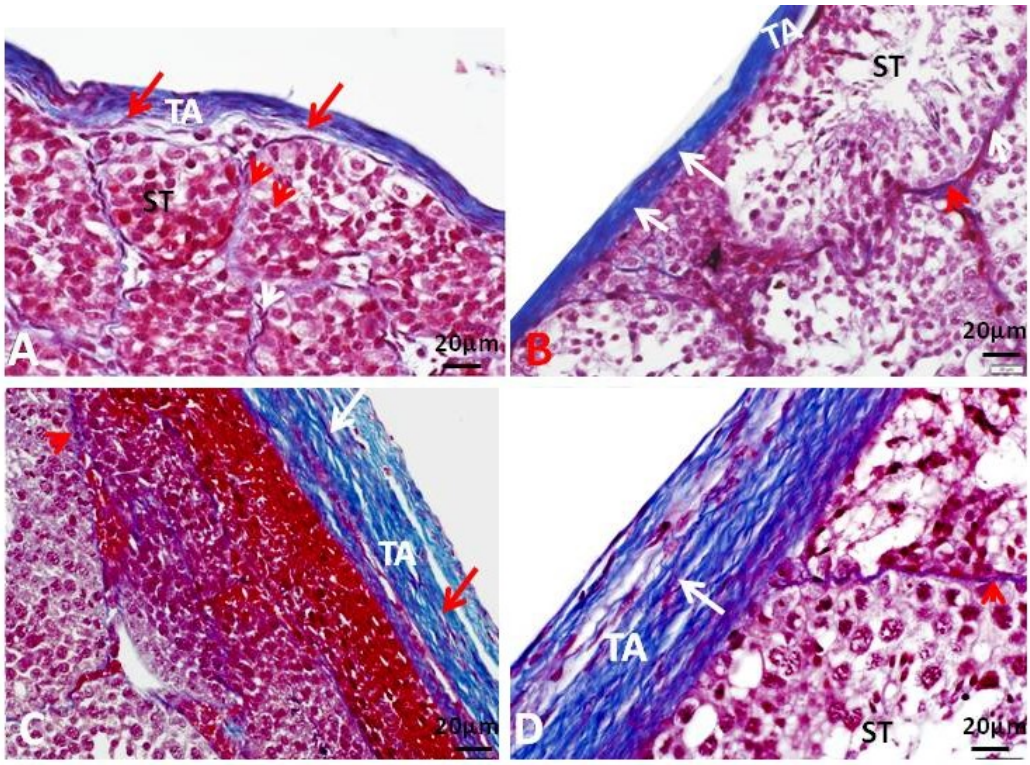

Figure 4.6. Photomicrographs of the Testicular Capsule of Different Age Groups of AGCR with their Capsular Coverings. A. Prepubertal B. Pubertal C. Adult D. Aged. Note that the capsules are showing pink-staining smooth muscles (arrow) within the blue staining collagen fibres of tunica albuginea (TA); the collagen fibres surround the seminiferous tubules (ST). Stain: Masson Trichome; Scale bar: 20µm

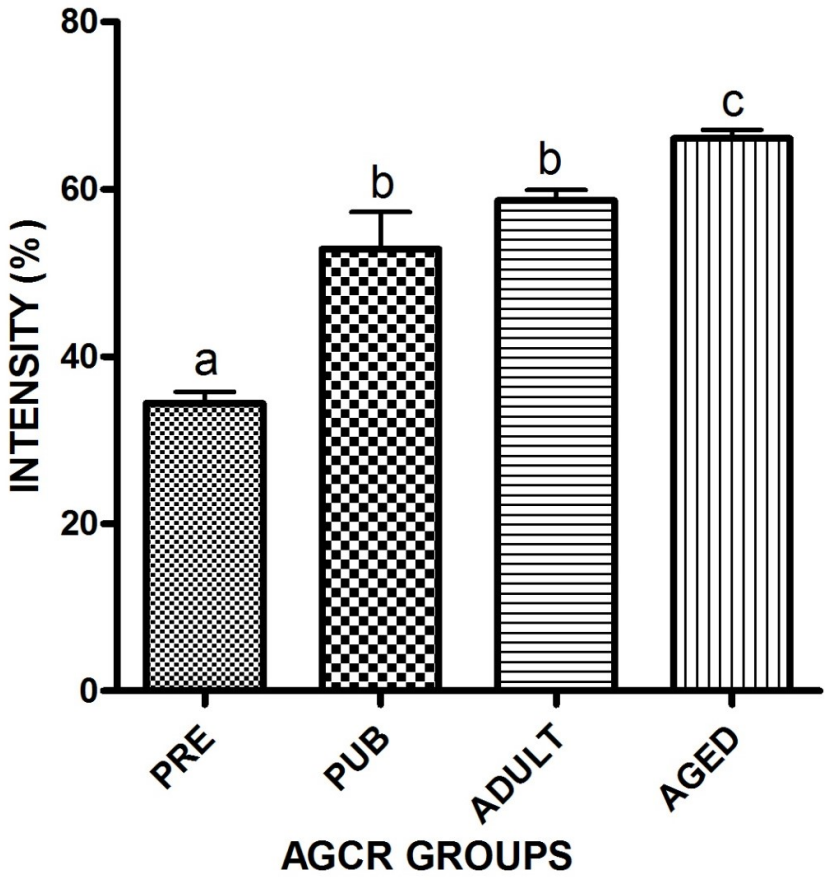

Figure 4.7. Age-related Changes in the Intensity of Masson Trichome Staining of the Testicular Capsule in AGCR. Bars with different alphabet superscripts (a,b,c) are significantly different.

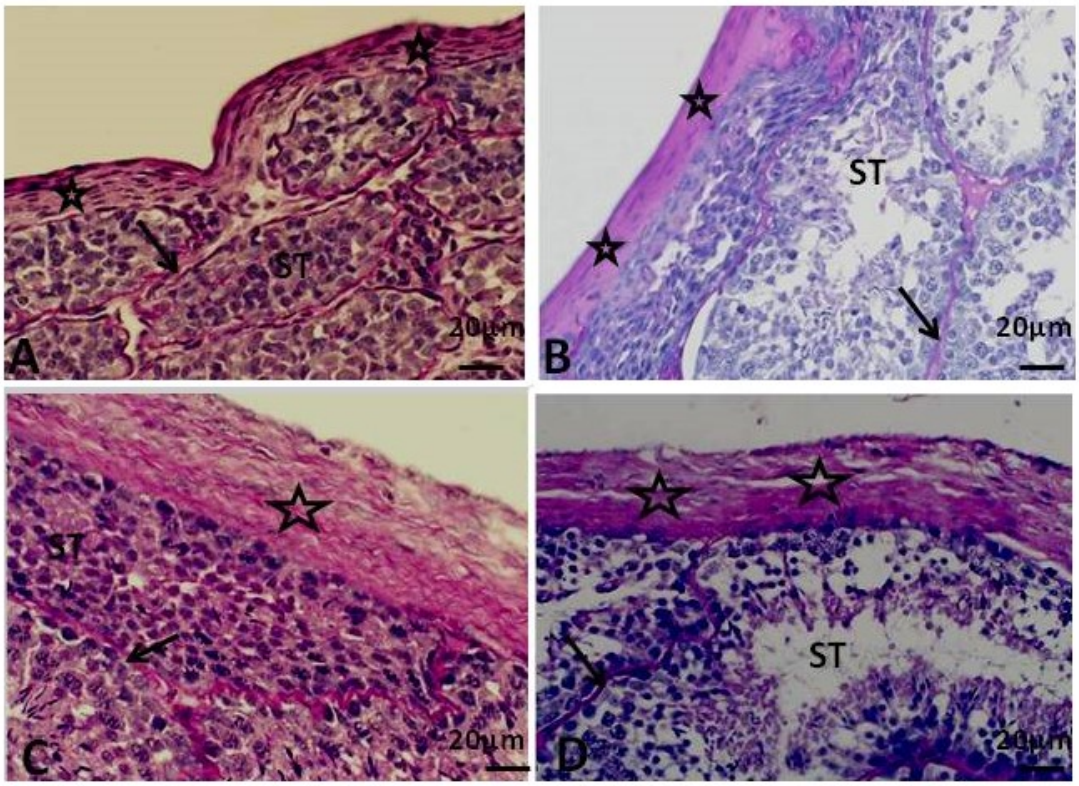

Figure 4.8. Photomicrographs of the Testicular Capsule of Different Age Groups of AGCR with their Capsular Coverings. A. Prepubertal B. Pubertal C. Adult D. Aged. Note the demonstration of PAS positive glycogen content in the capsules (star) as well as in the seminiferous tubular surroundings (arrow) Stain: PAS; Scale bar: 20µm

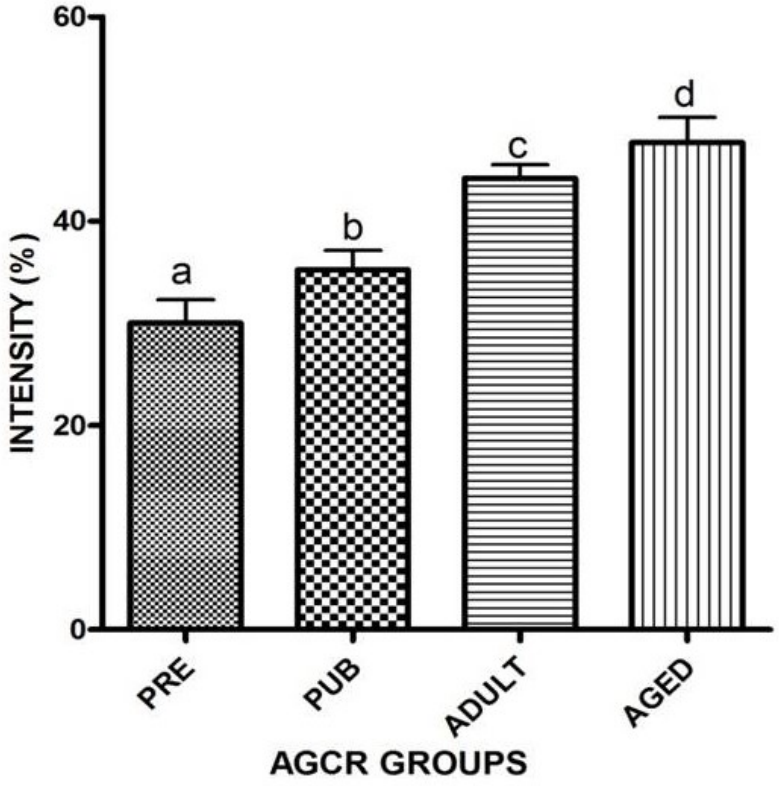

Figure 4.9. Age-related Changes in Intensity of PAS Staining of the Testicular Capsule in AGCR. Bars bearing dissimilar alphabet superscripts (a,b,c) are significantly different.

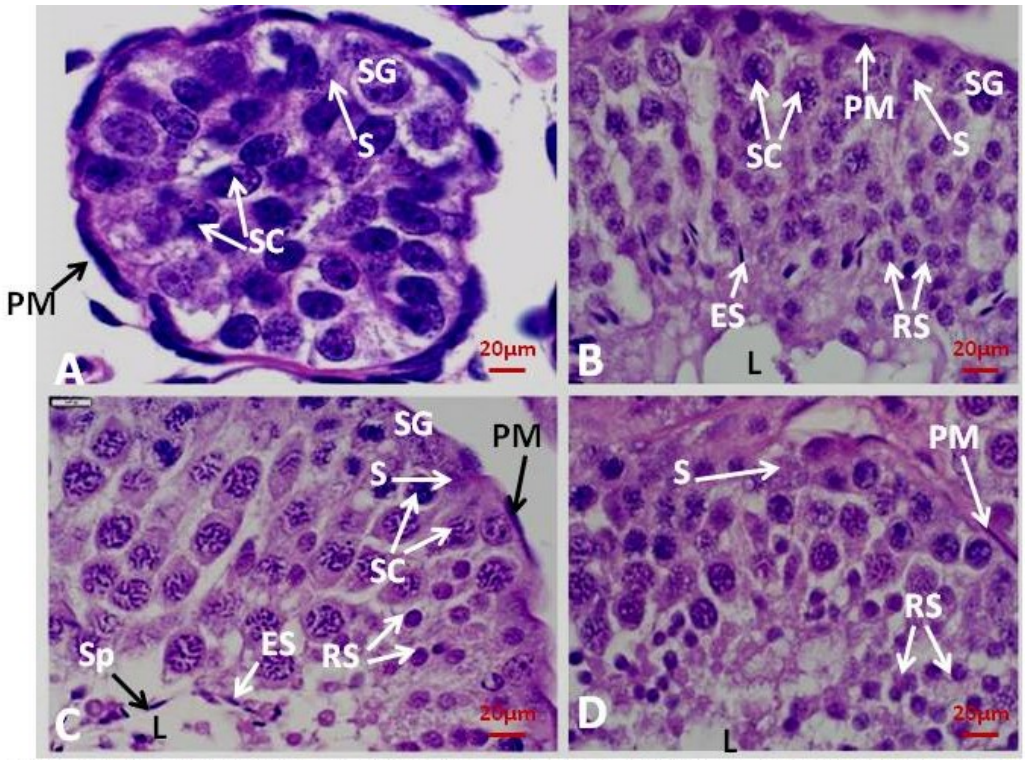

Figure 4.10. Photomicrographs of the Testis of Different Age Groups of AGCR. A. Prepubertal: B. Pubertal: C. Adult: D. Aged: Note the absence of patent lumen (L) as well as the different types of spermatids in A. PM - Peritubular myoid cell, SG- Spermatogonia, S- Sertoli, SC- Spermatocyte, ES- Elongating spermatids, RS- Round spermatids, L- Lumen. Stain: H&E; Scale bar: 20µm

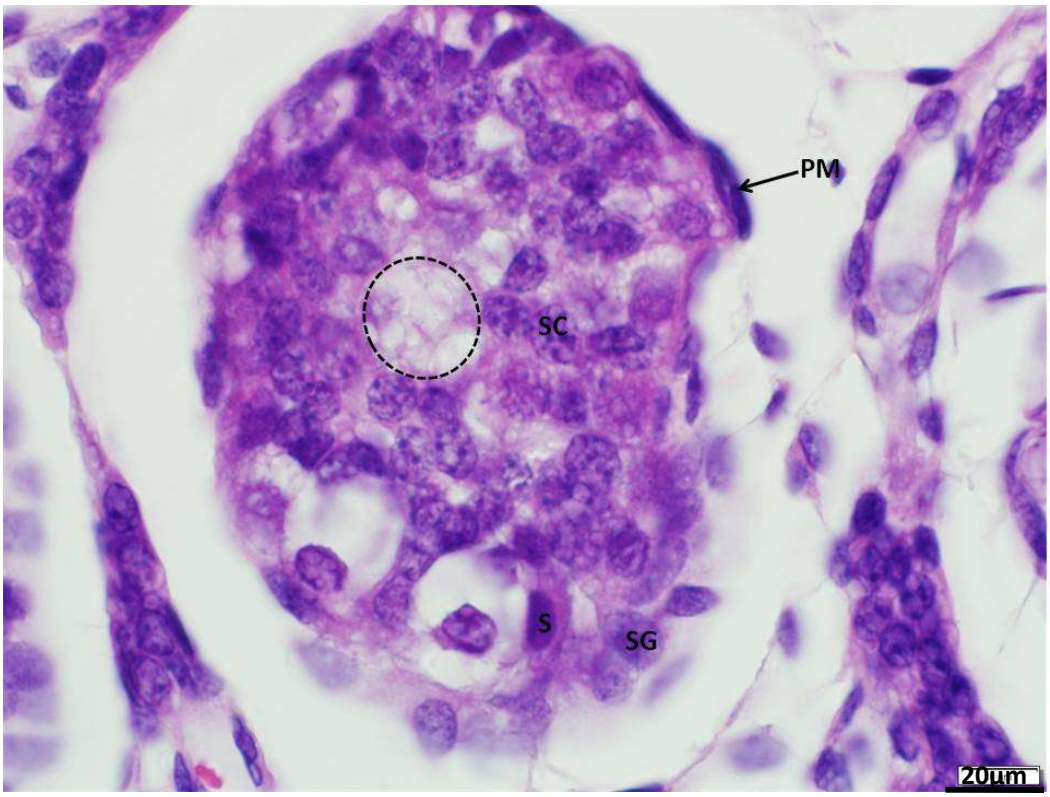

Figure 4.11. Photomicrograph of the Testis of Pre-pubertal (4-month) Cane Rat. Note the appearace of patent lumen (circle outline) within the seminiferous tubule. PM - Peritubular myoid cell, SG- Spermatogonia, S- Sertoli, SC- Spermatocyte. Stain: H&E; Scale bar: 20µm

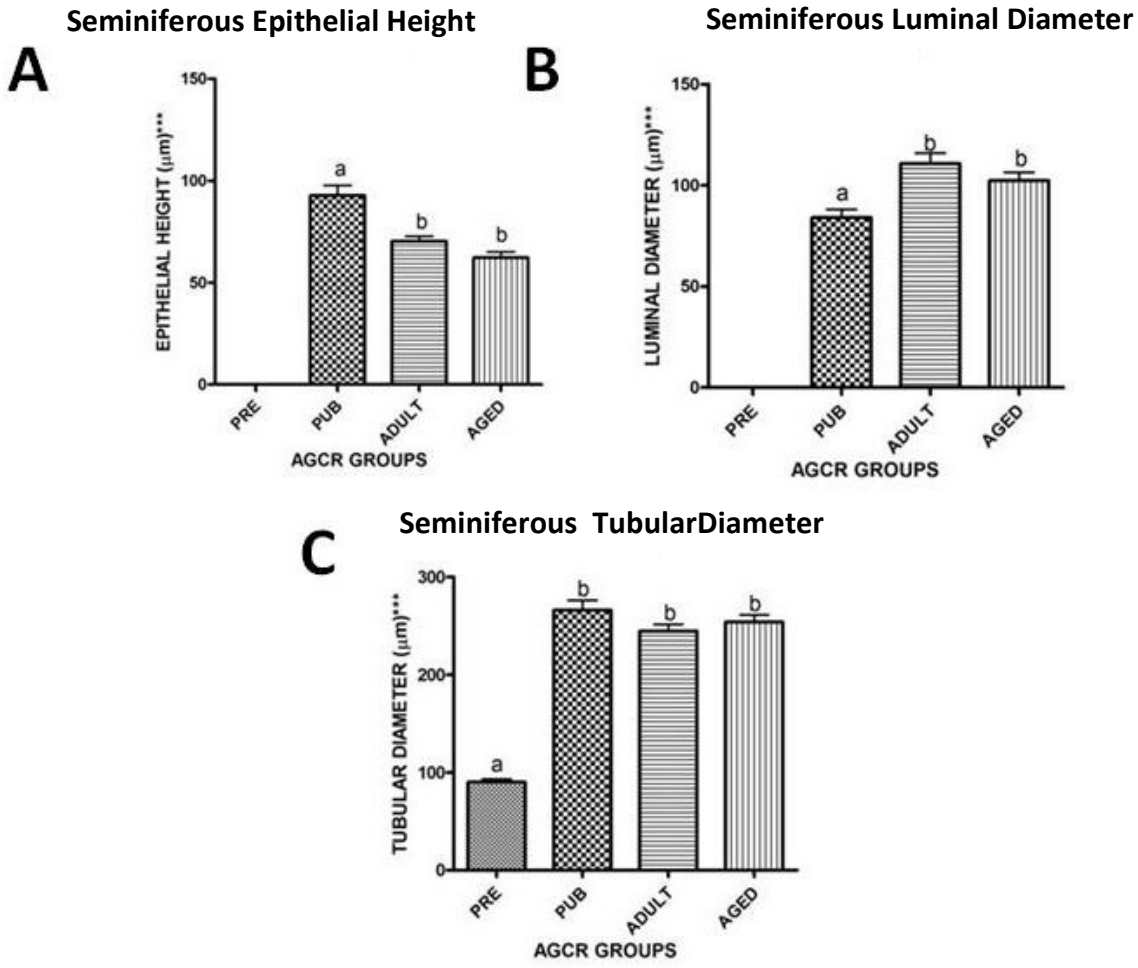

Figure 4.12 A-C. Age-related Changes in the Testicular Parameters of AGCR. A. Epithelial height B. Luminal diameter C. Tubular diameter. Bars with different alphabet superscripts (a,b,c,d) are significantly different

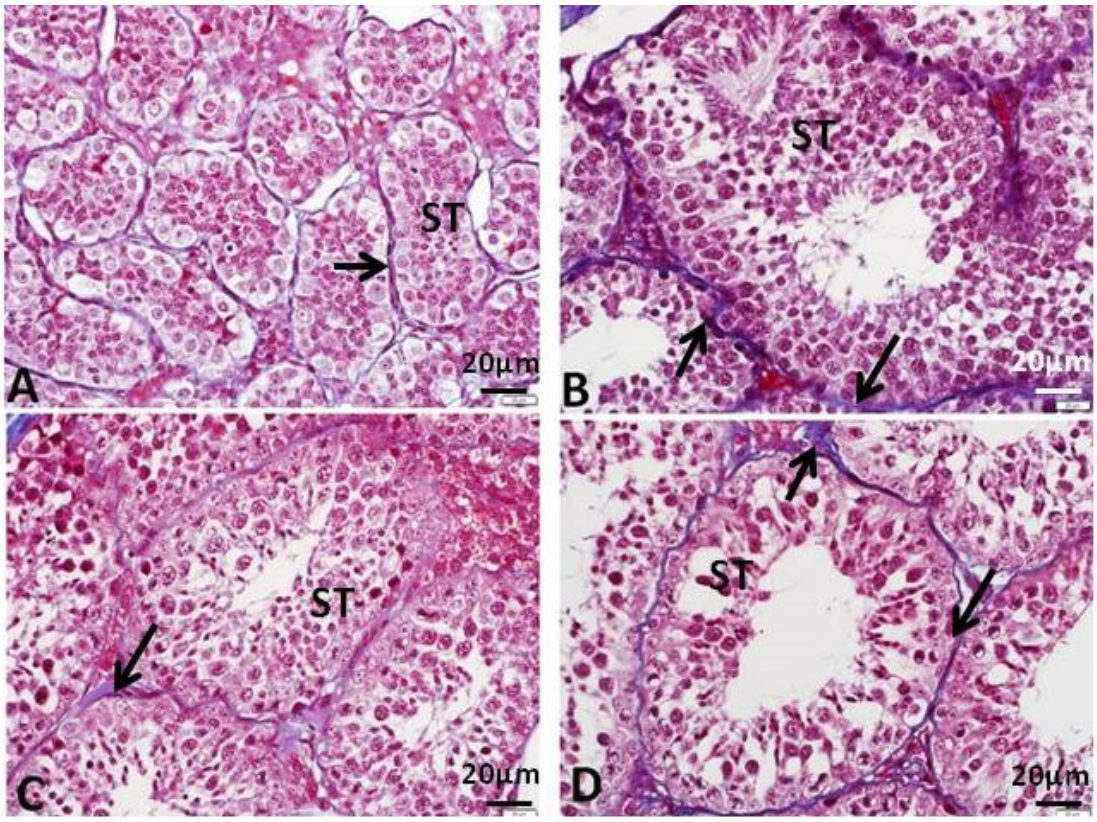

Figure 4.13. Masson's Trichome Staining of the Testis of Different Age Groups of AGCR. A. Prepubertal: B. Pubertal: C. Adult: D. Aged. Note the less bluish staining collagen fibres (blackarrows) surrounding the seminiferous tubules (ST) in the different age-groups. Scale bar: 20µm

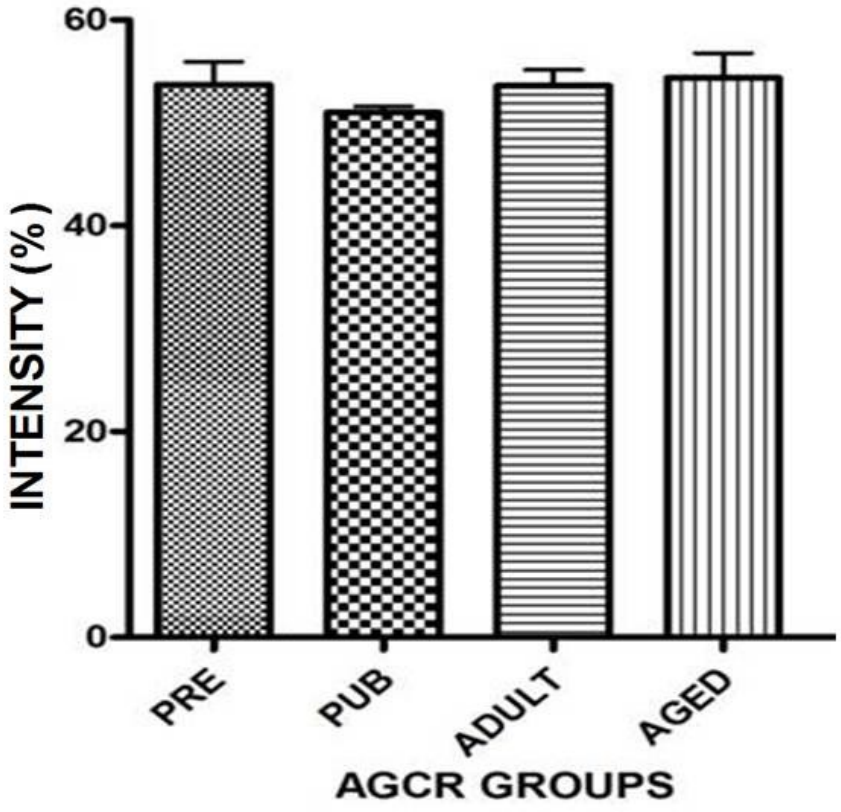

Figure 4.14. Age-related Changes in Intensity of Masson's Trichome Staining of the Testicular Parenchyma in AGCR.

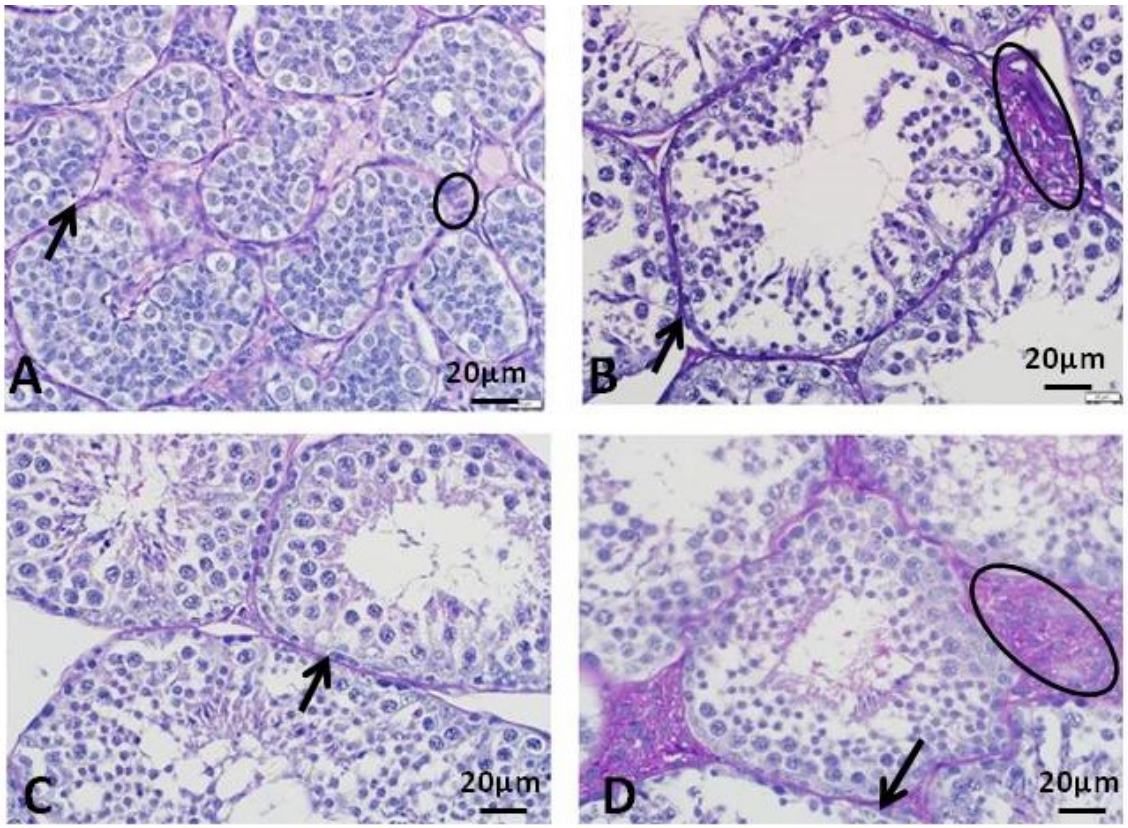

Figure 4.15. PAS Stainings of the Testis of Different Age Groups of AGCR. A. Prepubertal: B. Pubertal: C. Adult: D. Aged. Note the demonstration of PAS positive areas in the interstitium (oval) as well as in the seminiferous tubular sorrounding (arrow). Scale bar: 20µm

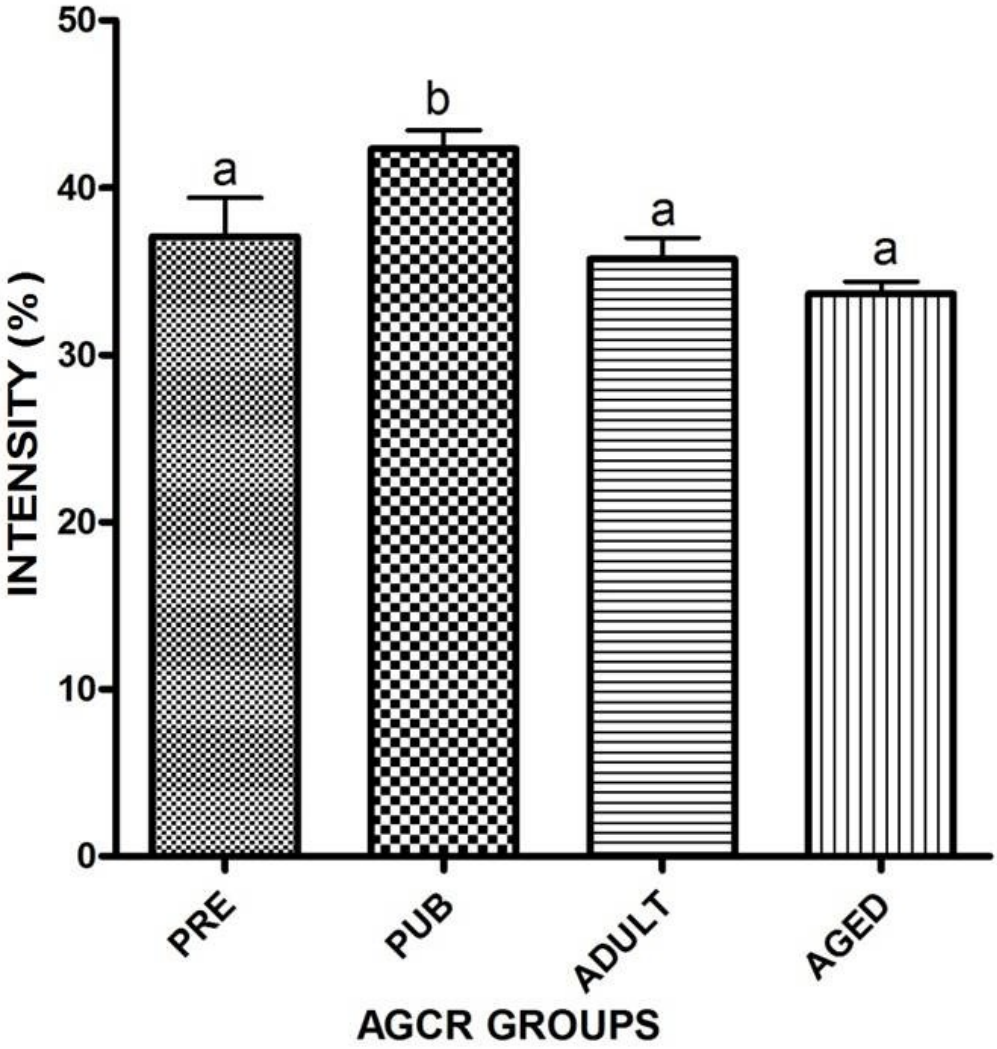

Figure 4.16. Age-related Changes in Intensity of PAS Staining of The Testicular Parenchyma in AGCR. Bars bearing dissimilar alphabet superscripts (a,b,c) are significantly different.

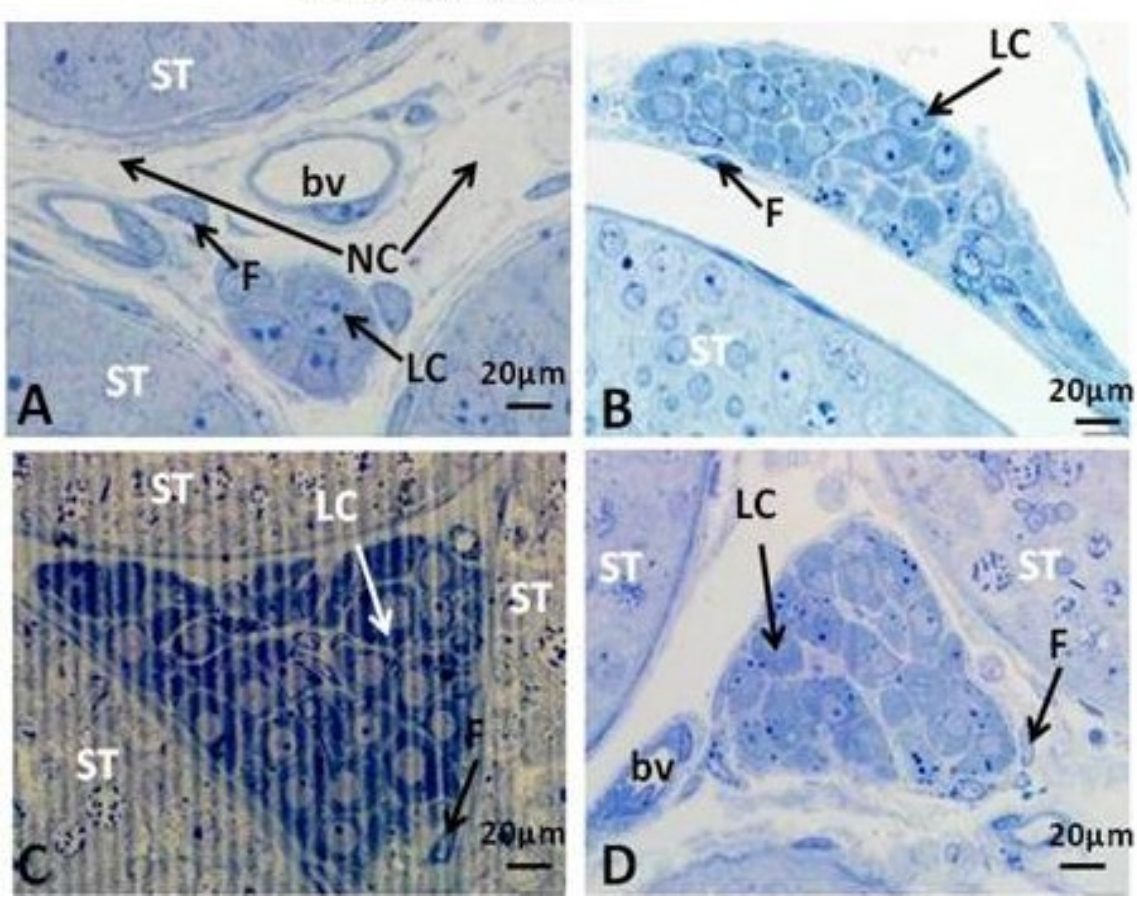

Figure 4.17. Photomicrographs of the Testicular Interstitum of Different Age Groups of AGCR. A. Prepubertal: B. Pubertal: C. Adult: D. Aged. Note the presence of wide non cellular (NC) area within theinterstitium of A. LC- Leydig cell, F-Fibroblast, bv-blood vessel. Stain: Toludine blue; Scale bar: 20µm

4.2.4 Changes in the Testicular Ultrastructure with Age Advancement

Age-related changes were sequentially observed from the wall of the seminiferous tubule to the core of the parenchyma as follows:

4.2.4.1 Peritubular Tissue (Boundary Tissue)

Testicular boundary tissue component was observed to be similar across the different age groups of AGCR investigated (Fig. 4.19). It was made up of the basal lamina, additional 4 basal lamina-like structures separated by single layer of myoid cell, collagen fibres and microfilament substances.

4.2.4.2 Sertoli Cell

The Sertoli cells of the different AGCR groups were seen close to the basement membrane and extended towards the tubular lumen (Fig. 4.18). It visibly formed junctional complexes around germ cells (Figures. 4.20 and 4.21). Sertoli cell contained roundish nucleus in pre-pubertal rat (Fig. 4.21A) while in pubertal onwards it was more triangular in shape with conspicuous nuclear cleft evident in the adult Sertoli cell (Fig. 4.21C).

4.2.4.3 Spermatogonia

Three (3) distinct spermatogonia types; Type A, Intermediate and Type B were identified close to the basal lamina from pre-pubertal rat onwards (Fig. 4.22-4.24). The nuclear chromatin nature, the presence as well as the location of nucleoli within spermatogonia were used to morphologically identify the spermatogonia types. Type A spermatogonia in all AGCR groups (Fig. 4.22) was characterized by oval nuclei that is devoid of nucleoli, the presence of mitochondria and interdigitations with basal lamina in all the groups. However, the nucleus in pre-pubertal was more euchromatic than others (Fig. 4.22A). Type B spermatogonia contain centrally positioned nucleoli with some degree of nuclear chromatin condensation (Fig. 4.23). Numerous mitochondria were seen in the cytoplasm of type B spermatogonia in pre-pubertal rat as well as increased nuclear euchromasia when compared to others (Fig. 4.23A). Intermediate spermatogonia were identified by the presence of some degree of chromatin condensation and with the presence of nucleoli that were almost approaching the centre of the nuclei (Fig. 4.24).

4.2.4.4 Spermatocyte

Ultrastucturally, five types of spermatocyte (pre-leptotene, leptotene, zygotene, pachytene and diplotene) were recognised within the seminiferous epithelium of the different age groups of AGCR (Figs. 4.25-4.29). The spermatocyte types were characterized by progressive increase in nuclear size, synaptonema formation and chromatin condensation. Preleptotene in all AGCR was characterized by spherical nucleus with granular chromatin and reduced cytoplasmic organelles except for prepubertal rat with intense euchromasia and conspicuous presence of many mitochondria (Fig. 4.25). Leptotene spermatocyte was observed to have spherical nucleus with well defined nuclear membrane and less chromatin condensation in all groups except for pre-pubertal rat with a somewhat ellipsoidal nuclear shape, intense nuclear euchromasia and numerous tubular mitochondria (Fig. 4.26). Zygotene spermatocytes in the different age groups of AGCR was observed to have reduced cytoplasm, less prominent synaptonemal complexes, more nuclear heterochromasia from pubertal onwards relative to the pre-pubertal rat (Fig. 4.27). There was also increased mitochondrial presence in the cytoplasm of zygotene in the pre-pubertal rat compared to others (Fig. 4.27A). The pachytene spermatocyte of all AGCR has prominent nucleolus, synaptonemal complex and extensive cytoplasm (Fig. 4.28A). The pre-pubertal rats have numerous mitochondria in their cytoplasm when compared to others (Fig. 4.28A). Diplotene spermatocyte in all AGCR was characterized by deep nuclear chromatins which were aggregated to one side of the nucleus and the presence of nucleoli (Fig. 4.29). The numerous mitochondria and higher degree of nuclear euchromasia consistently seen in the earlier listed spermatocytes of pre-pubertal were also observed in this spermatocyte (Fig. 4.29A).

4.2.4.5 Leydig Cell

With the exception of the scanty nature of the Leydig cells in the interstitium of pre-pubertal rat, the interstitial spaces in pubertal onwards were filled with Leydig cells (Fig. 4.17). It was observed that the Leydig cell was ovoid in outline and showed a roundish nucleus which in pre-pubertal contains greater amount of heterochromatin relative to other groups (Fig. 4.30A). Also, Leydig cell cytoplasm in pubertal rat contained numerous mitochondria, lipid droplets as well as smooth endoplasmic reticulum when compared to others (Fig. 4.30B). Numerous stacks of concentric

rough endoplasmic reticulum and smooth endoplasmic reticulum were seen in the cytoplasm of Leydig cell in adult and aged AGCR (Fig. 4.30Cand D).

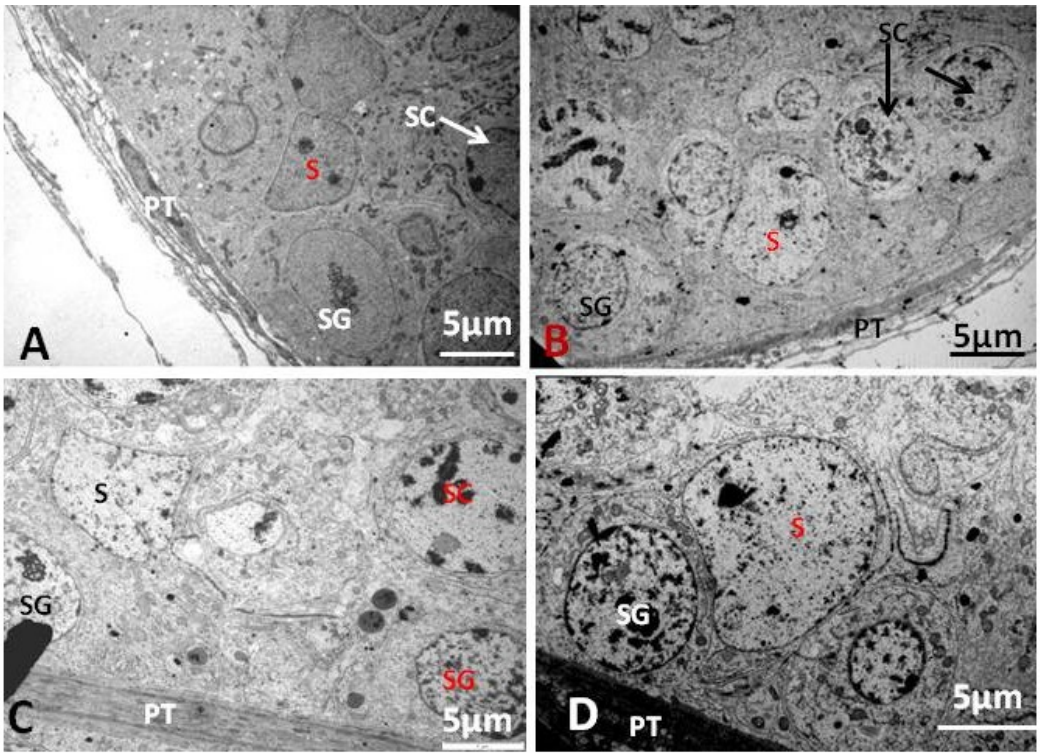

Figure 4.18. Transmission Electron Micrographs of the Seminiferous Epithelium in the Testes of Different Age Groups of African Greater Cane Rat. A. Prepubertal B. Pubertal C. Adult D. Aged. Note the closeness of the Sertoli cell nucleus to the semiiferous tubular wall in the different AGCR. SG-Spermatogonia, S-Sertoli cell, SC- Spermatocyte, PT- Peritubular tissue.

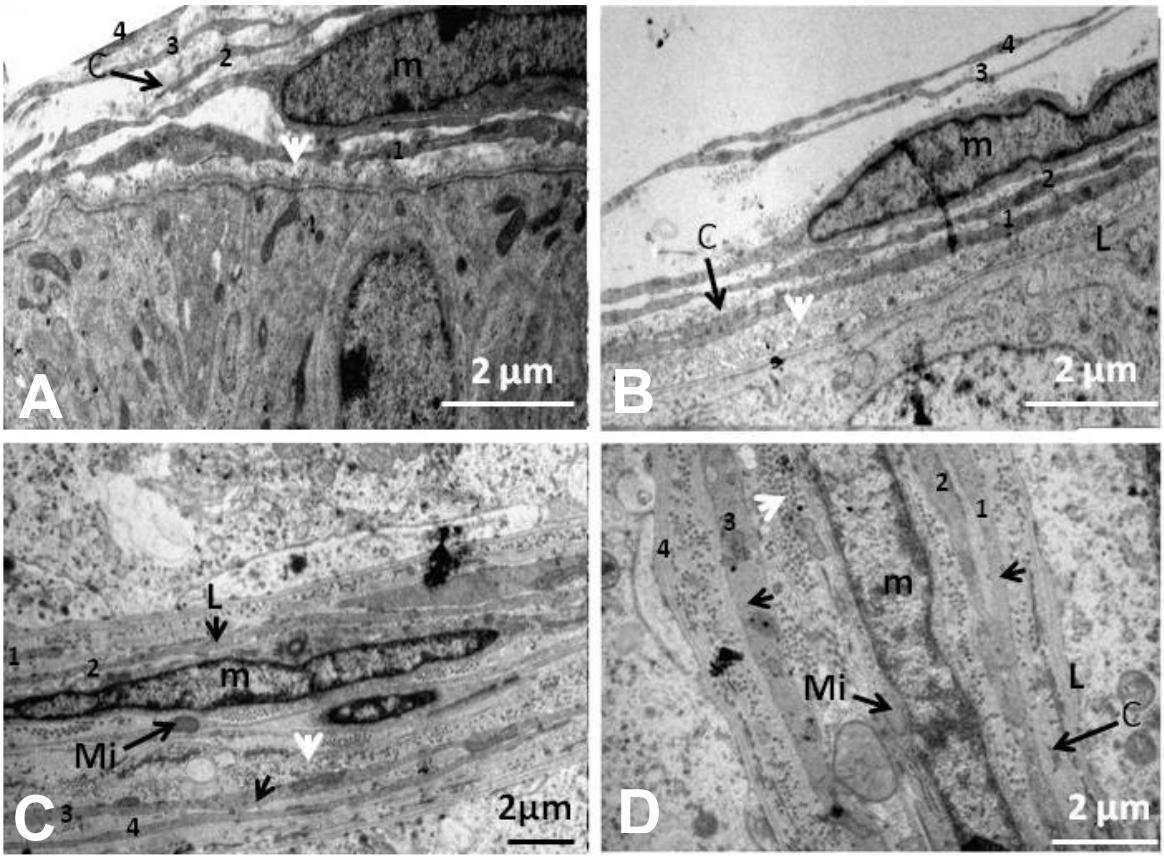

Figure 4.19. Transmission Electron Micrographs of the Testicular Boundary Tissue of the African Greater Cane Rat. A. Prepubertal B. Pubertal C. Adult D. Aged. Note the basal lamina (L) as well as the several layers (1-4) of basal lamina-like structures (arrow heads) separated by myoid cells (m), collagen fibrils – C and Microfilament (White arrow-head). Mi – Mitochondria.

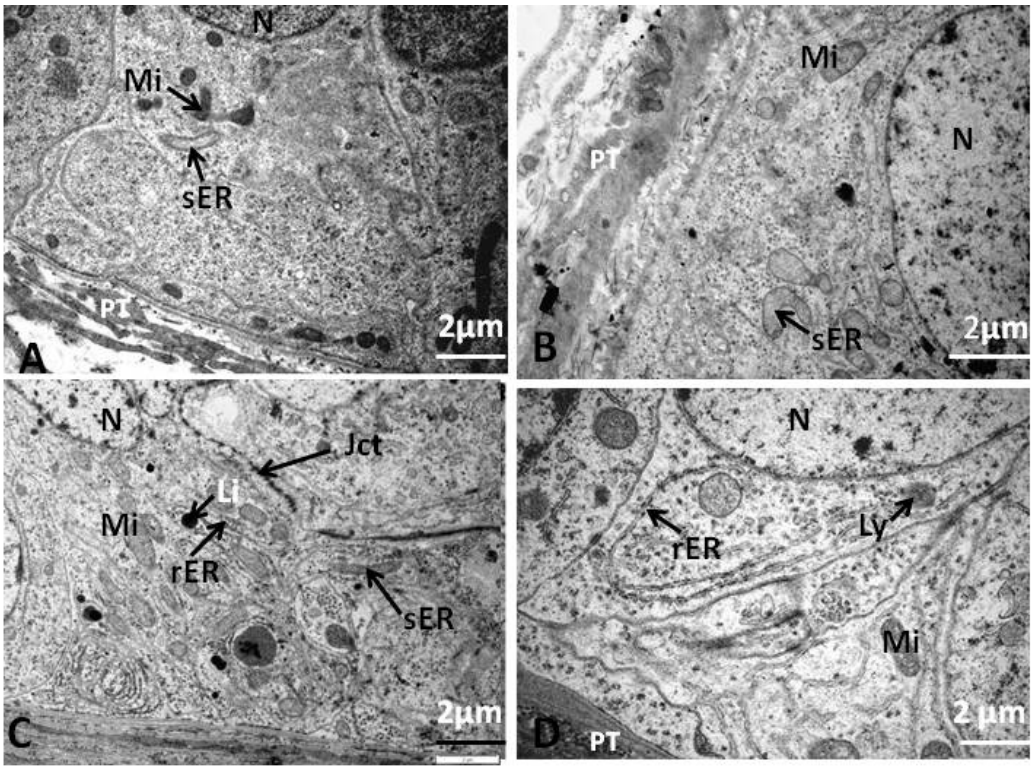

Figure 4.20. Transmission Electron Micrographs of the Basal Aspect of Sertoli Cell of the African Greater Cane Rat. A. Prepubertal B. Pubertal C. Adult D. Aged. rER- Rough endoplasmic reticulum, sER- Smooth endoplasmic reticulum, N-Sertoli cell nucleaus, Mi- Mitochodria, Ly- Lysosome, Li- Lipid droplet, Jct- Sertoli cell junction, m- Myoid cell, PT- Peritubular tissue

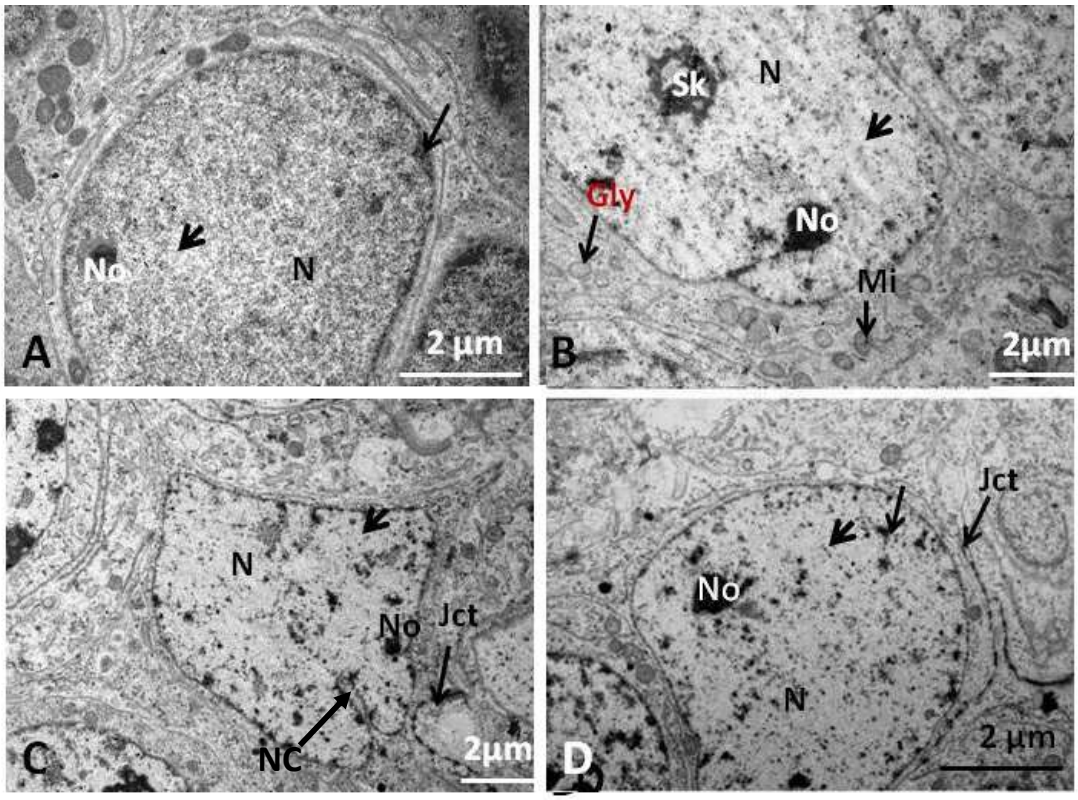

Figure 4.21. Transmission Electron Micrographs of the Perinuclear Area of Sertoli Cell of the African Greater Cane Rat. A. Prepubertal B. Pubertal C. Adult D. Aged. Note the intense nuclear heterochromatin (arrow) in the Sertoli cell nucleus (N) of A. No- Nucleolus, Sk- Satellite karyosomes, N-Nucleus, NC-Nuclear cleft, Jct- Sertoli cell junction, arrow head- euchromatin

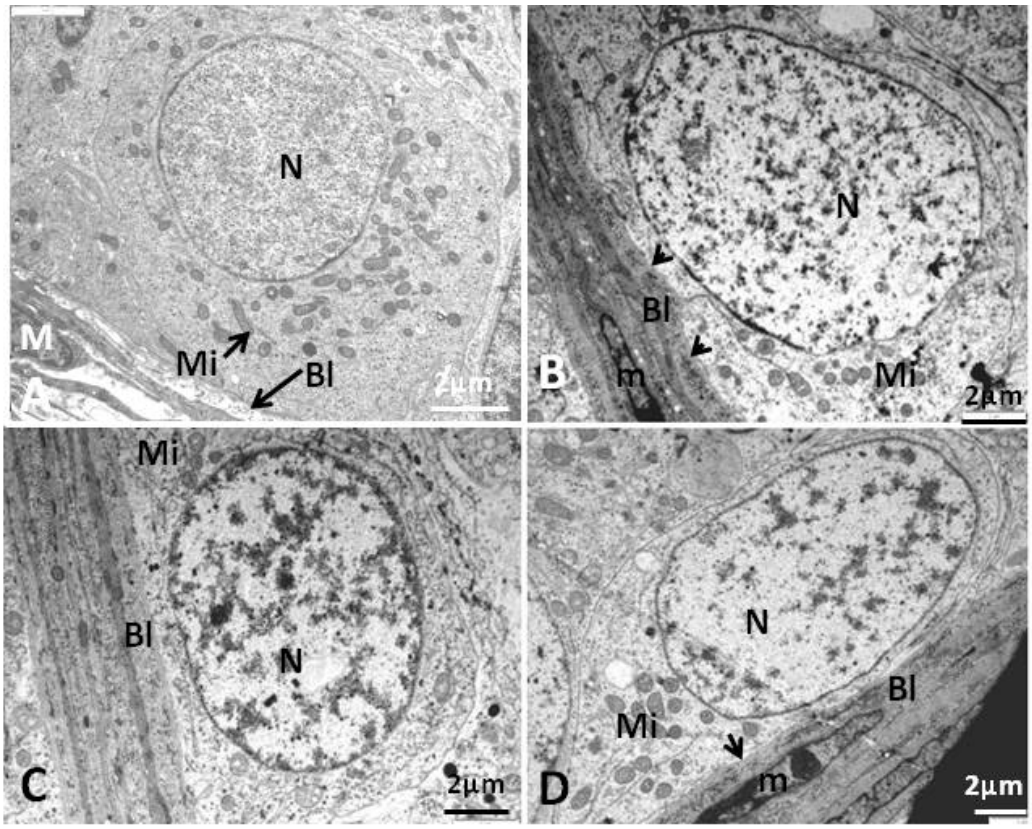

Figure 4.22. Transmission Electron Micrographs of the Type A Spermatogonium in the Testis of the African Greater Cane Rat. A. Prepubertal B. Pubertal C. Adult D. Aged. Note the oval nuclei (N) devoid of nucleoli, the presence of mitochondria (Mi) and interdigitations (arrow head) with basal lamina (Bl) in all the groups. Also, note that the nucleus in A is more euchromatic and numerous mitochondria in the cytoplasm. m: Myoid cell.

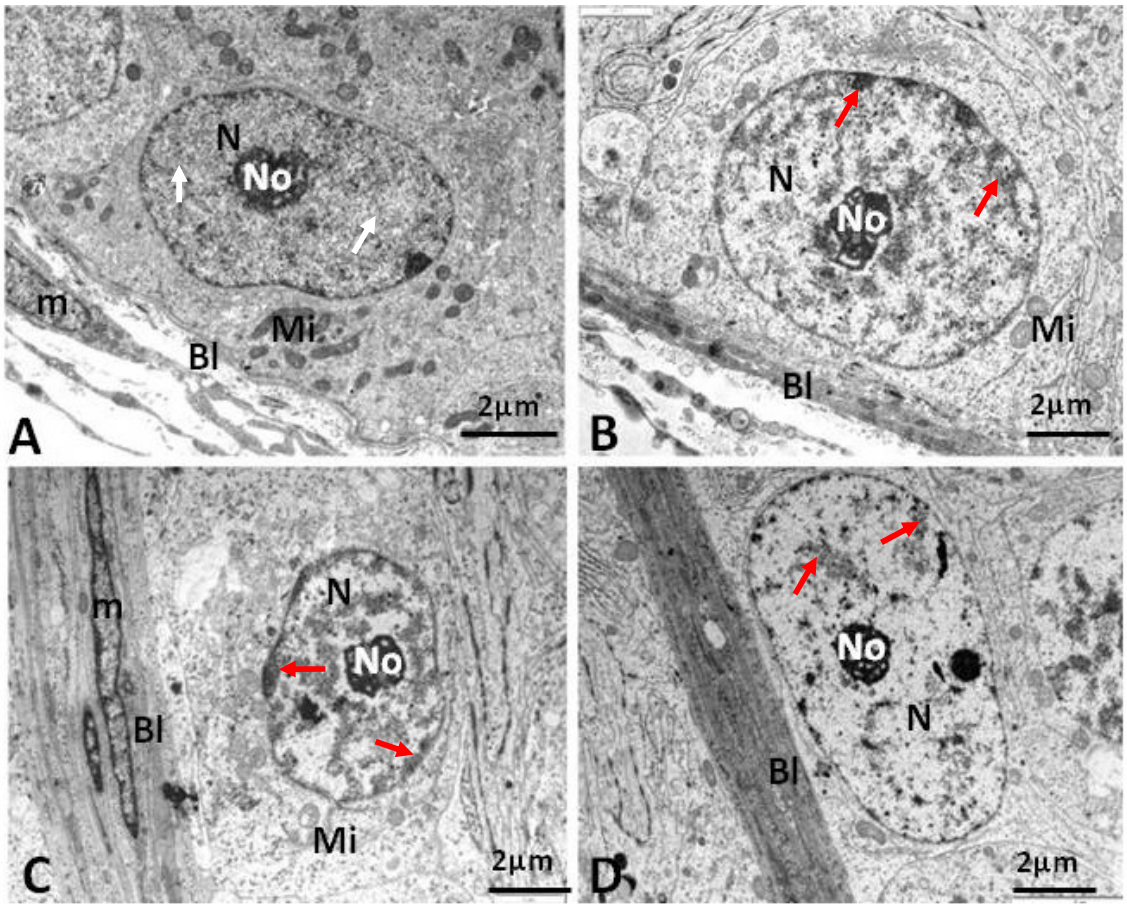

Figure 4.23. Transmission Electron Micrographs of the Type B Spermatogonium in the Testis of the African Greater Cane Rat. A. Prepubertal B. Pubertal C. Adult D. Aged. Note the centrally positioned nucleoli (No), marked euchromatic nucleus (white arrow) in A as well as conspicous nuclear heteromasia in B-D (red arrow). m - Myoid cell.

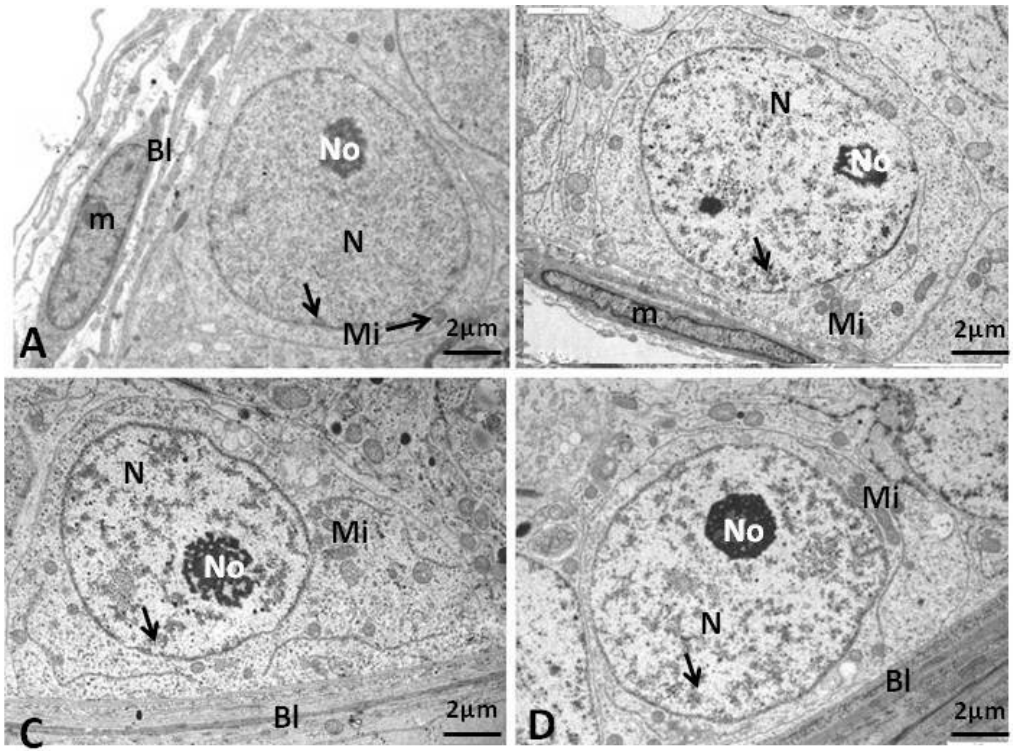

Figure 4.24. Transmission Electron Micrographs of the Intermediate Spermatogonium Type in the Testis of the African Greater Cane Rat. A. Prepubertal B. Pubertal C. Adult D. Aged. Note condensed nuclear chromatin (arrow) and nucleoli (No) approaching the centre of the nuclei (N). Bl: Basal lamina, m: myoid cell, Mi: Mitochondria. Scale bar: 2µm

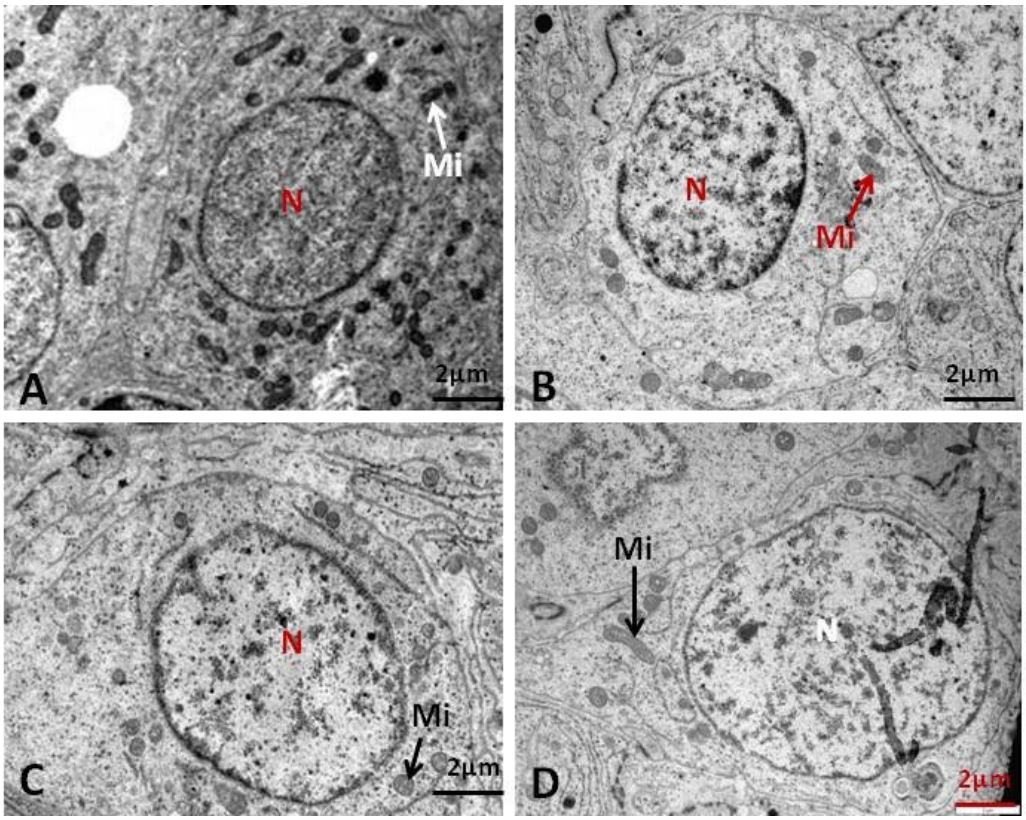

Figure 4.25. Transmission Electron Micrographs of the Preleptotene Spermatocytes of the African Greater Cane Rat. A. Prepubertal B. Pubertal C. Adult D. Aged. Note the presence fine granular chromatin in the nucleus (N) and clear cytoplasm (Cy) across all age groups.

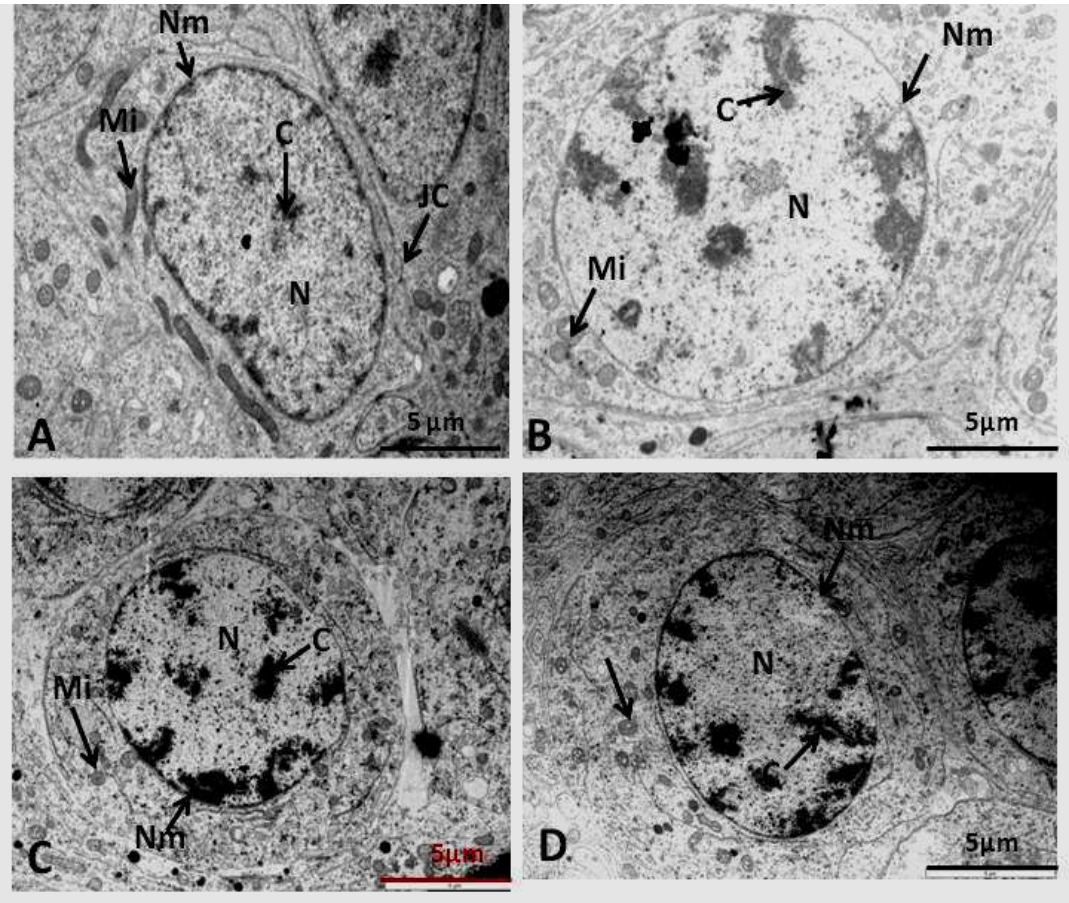

Figure 4.26. Transmission Electron Micrographs of the Leptotene Spermatocytes of the African Greater Cane Rat. A. Prepubertal B. Pubertal C. Adult D. Aged. Note the presence of spherical nucleus (N) with well defined nuclear membrane (Nm) and less chromatin (C) condensation in all groups except for the somewhat ellipsoidal nuclear (N) shape of pre-pubertal. Also note the numerous tubular mitochondria in A. JC-Junctional complex.

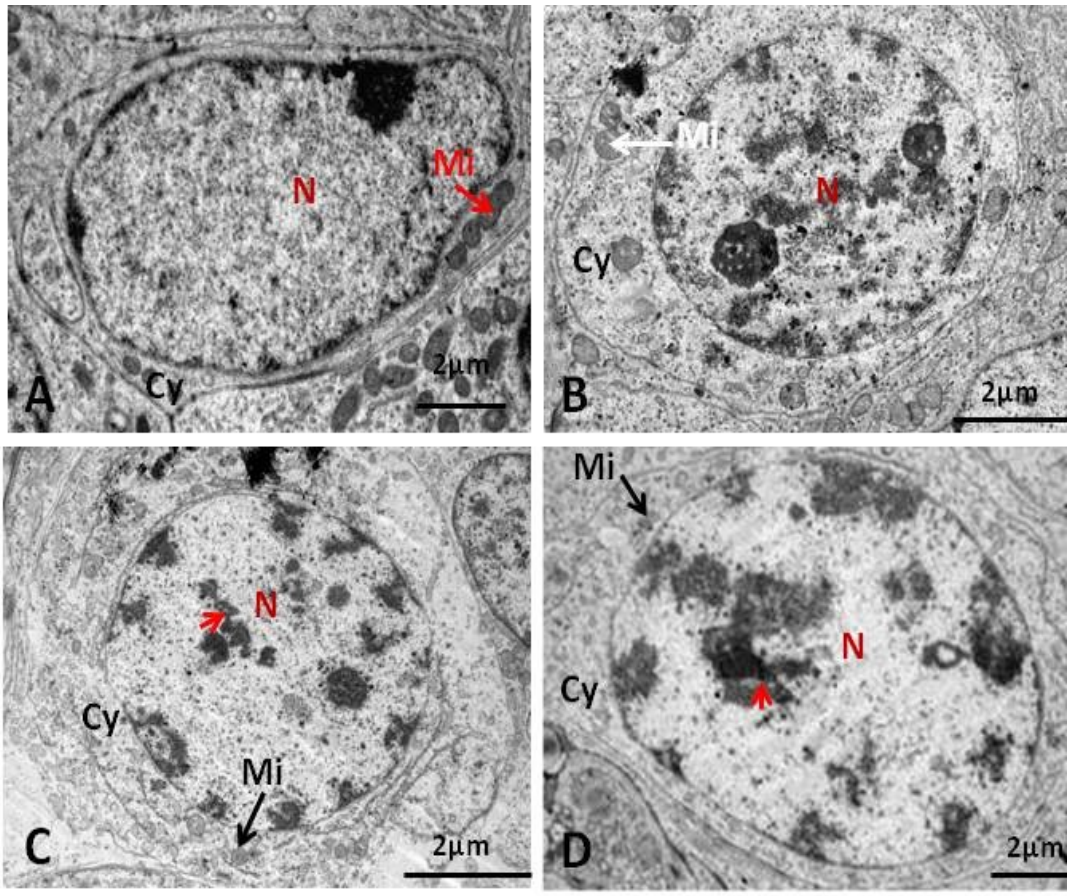

Figure 4.27. Transmission Electron Micrographs of the Zygotene Spermatocytes of the African Greater Cane Rat. A. Prepubertal B. Pubertal C. Adult D. Aged. Note the reduced cytoplasm (Cy) across groups as well as less prominent synaptonemal complexes (arrow head). Also, observe the somewhat ellipsoidal nuclear (N) shape of pre-pubertal zygotene ccompared to others.

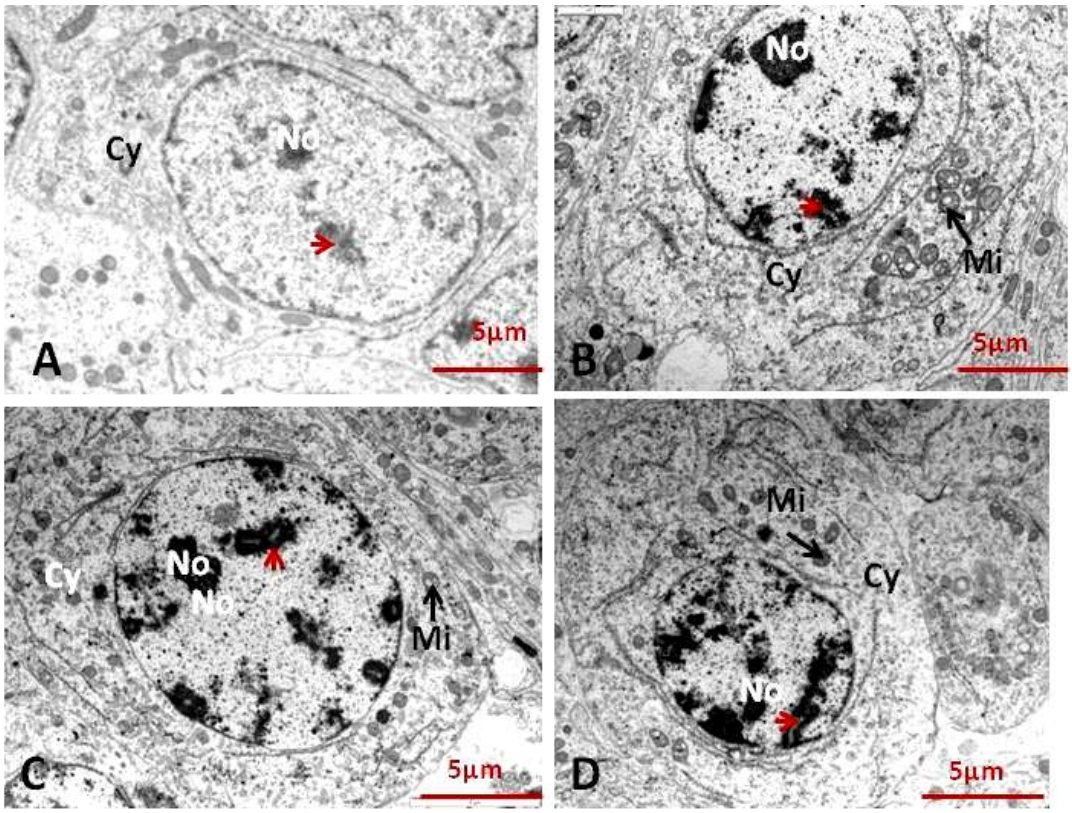

Figure 4.28. Transmission Electron Micrographs of the Pachytene Spermatocytes of the African Greater Cane Rat. A. Prepubertal B. Pubertal C. Adult D. Aged. Note the prominent nucleolus (No), synaptonemal complex (arrow head) and extensive cytoplasm (Cy).

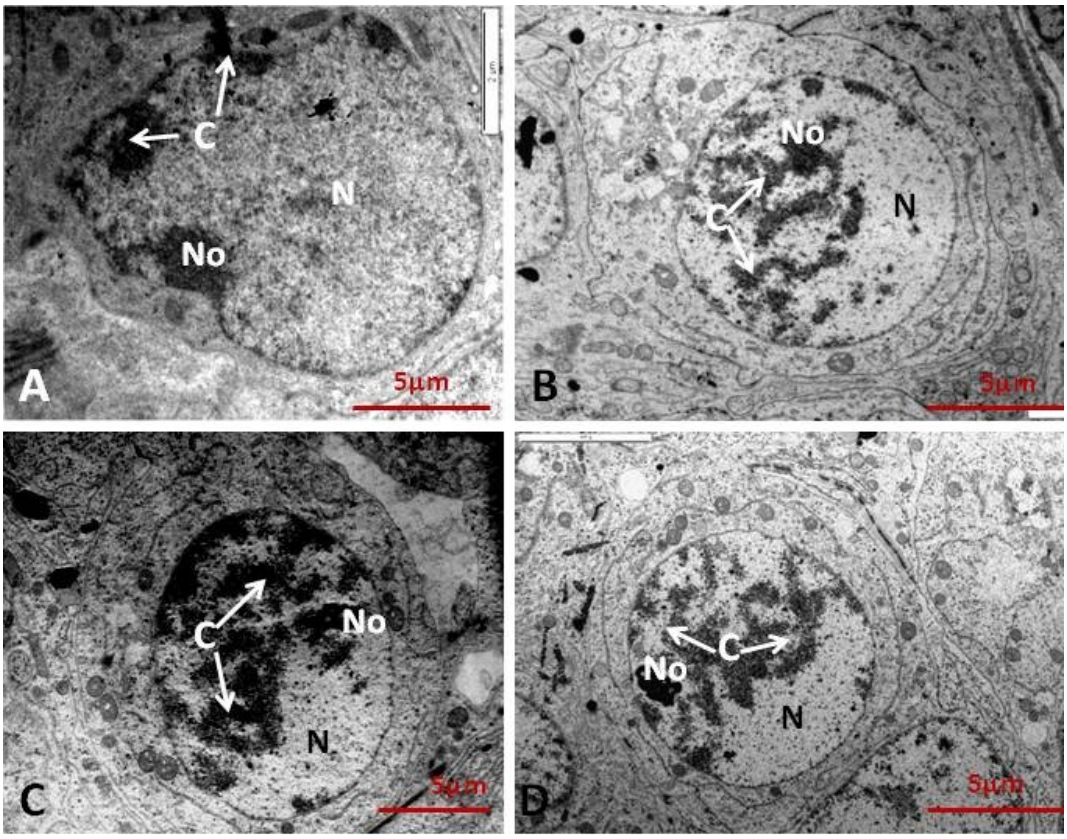

Figure 4.29. Transmission Electron Micrographs of the Diplotene Spermatocytes of the African Greater Cane Rat. A. Prepubertal B. Pubertal C. Adult D. Aged. Note the aggregation of the deep chromatin (C) towards one side of the nucleus and prominence of nucleoli (No). Also, observe the irregular shape of the nucleus (N) in A as well as high nuclear heterochromatin.

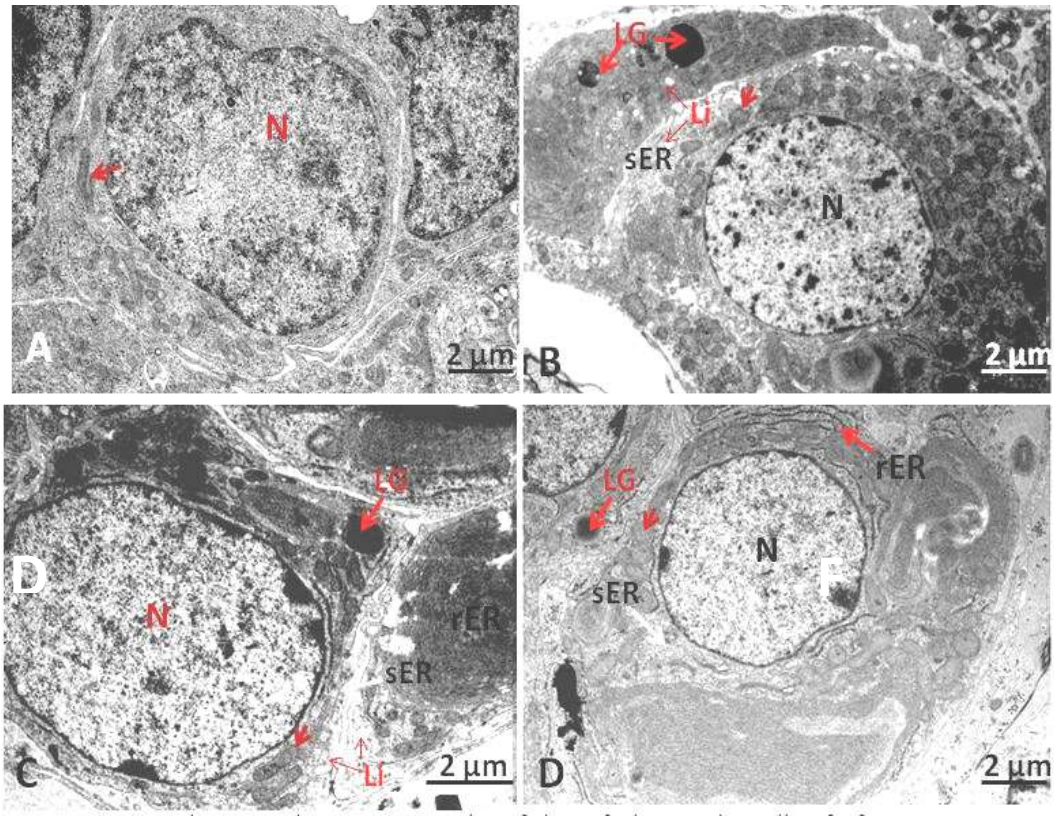

Figure 4.30. Transmission Electron Micrographs of the Leydig Cells of the AGCR. A. Prepubertal: B. Pubertal: C. Adult: D. Aged. Note the great amount of mitochondria (arrowhead), lipid droplets (Li), smooth endoplasmic reticulum (sER) in Leydig cell (LC) cytoplasm of pubertal AGCR relative to others. Also, observe the reduced organelles in A compared to others and the numerous stacks of concentric rough endoplasmic reticulum (rER) in the cytoplasm of the adult and aged AGCR LC. LG- Lipofuschin granule.

4.2.5 Histological Changes in the Epididymis of Different Age Groups of the African Greater Cane Rat

Based on some histological characteristics such as connective tissue stroma partitioning, luminal diameter and shape as well as the nature of the epithelial lining cells, the epididymis in all AGCR groups was made up of four segments of six distinct zones; zone I, zone II, zone III (initial segment), zone IV (caput), zone V (corpus) and zone VI (cauda) (Figs. 4.31, 4.32 and 4.33). The first (initial) segment unlike others is further partitioned by connective tissue septae into three (3) histologically distinct sub-segments or regions or zones namely; proximal (zone I), middle (zone II) and caudal (zone III) initial segments (Fig. 4.32). The shape of the lumen of all the epididymal segments in the pre-pubertal rat was roundish (Figs. 4.34, 4.39, 4.44, 4.49, 4.55 and 4.64). However, in the pubertal to aged AGCR, the proximal to the distal sub-segments of initial epididymal segment had stellate-shaped lumens (Figs. 4.34, 4.39 and 4.44), while their caput segment downwards bear characteristic round luminal shape (Figs. 4.49, 4.55 and 4.64). With respect to age-related differences in the nature of the epithelial lining of the epididymal segments, pre-pubertal epididymal duct was lined by predominantly simple cuboidal to columnar cells (Figs. 4.34A, 4.39A, 4.44A, 4.49A, 4.55A and 4.64A). The epithelial lining of the epididymal duct in pubertal onwards was the typical pseudostratified ciliated columnar epithelium (Figs. 4.34B-D, 4.39B-D, 4.44B-D, 4.49B-D, 4.55B-D and4.64B-D).

4.2.6 Age-related Changes in theContent of Glycogen and Collagen Fibres in the Epididymis of the African Greater Cane Rat

Positive Masson's Trichrome-stained areas within the segments of the epididymal duct of all AGCR groups were observed as bluish collagen substances in the ductal interstices and in the peritubular muscle coats (Figs. 4.35, 4.40, 4.45, 4.50, 4.56 and 4.65). With respect to PAS staining of the epididymis, positive areas appeared as magenta colour in the epididymal interstitium, lamina propria, peritubular muscle coat, perinuclear region of epididymal epithelial cells, ductal stereocilia and luminal content especially in the caput, corpus and cauda segments (Figs. 4.37, 4.42, 4.47, 4.52, 4.58 and 4.67). On the intensity of MT (Figs. 4.36, 4.41, 4.46, 4.51, 4.57 and 4.66) and PAS (Figs. 4.38, 4.43, 4.48, 4.53, 4.59 and 4.68) expressions in the segments of epididymal duct, significant age-related increase ($p<0.05$) in values were

consistently observed for both stains. Interestingly, strong PAS and MT intensities were displayed in virtually all the segments of pubertal and adult epididymis relative to other AGCR groups.

4.2.7 Age-Related Ultrastructural Changes in the Epididymal Architecture of the African Greater Cane Rat

The principal cell of the caput epididymis (Fig. 4.54A) in the prepubertal rat was characterized by the presence of numerous mitochondria in the basal and perinuclear portions of its cytoplasm when compared to other age groups (Fig. 4.54B-D). However, the cytoplasm of principal cells of the adult and aged (Fig. 4.54 C, D) were riched in numerous long rough endoplasmic reticulum.

Regarding the age-related differences in corpus epididymal ultrastructure, the nucleus of the principal cell in the corpus epididymis of all AGCR is irregular in shape and bears some degree of indentations that appeared to increase with the advancing age of AGCR (Figs. 4.60B-D; 4.61B-D and 4.62B-D). In addition, numerous lysosomal granules were more evident in the basal and perinuclear aspect of the principal cell of aged corpus epididymis (Figs. 4.61D and 4.62D). Prominent apical vacoulations were observed in the principal cell of pubertal rats (Figs. 4.63B).

With respect to age-related changes in caudal epididymal ultrastructure, the principal cell in the aged AGCR was observed to bear numerous lysosomal granules as well as degenerating mitochondria (Fig 4.69D inset and 4.70D). In addition, prominent principal cell nuclear indentation was noticed in pubertal rat onwards (Figs. 4.69B-D).

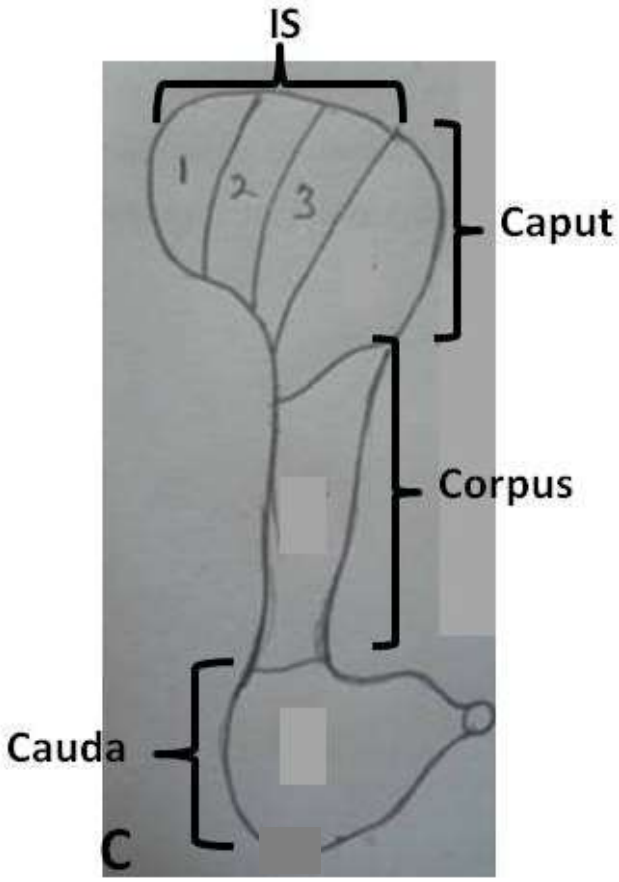

Figure 4.31. Schematic Representation of the African Greater Cane Rat Epididymis Illustrating its Partitioning by Connective Tissue Septae.IS - Initial Segment.

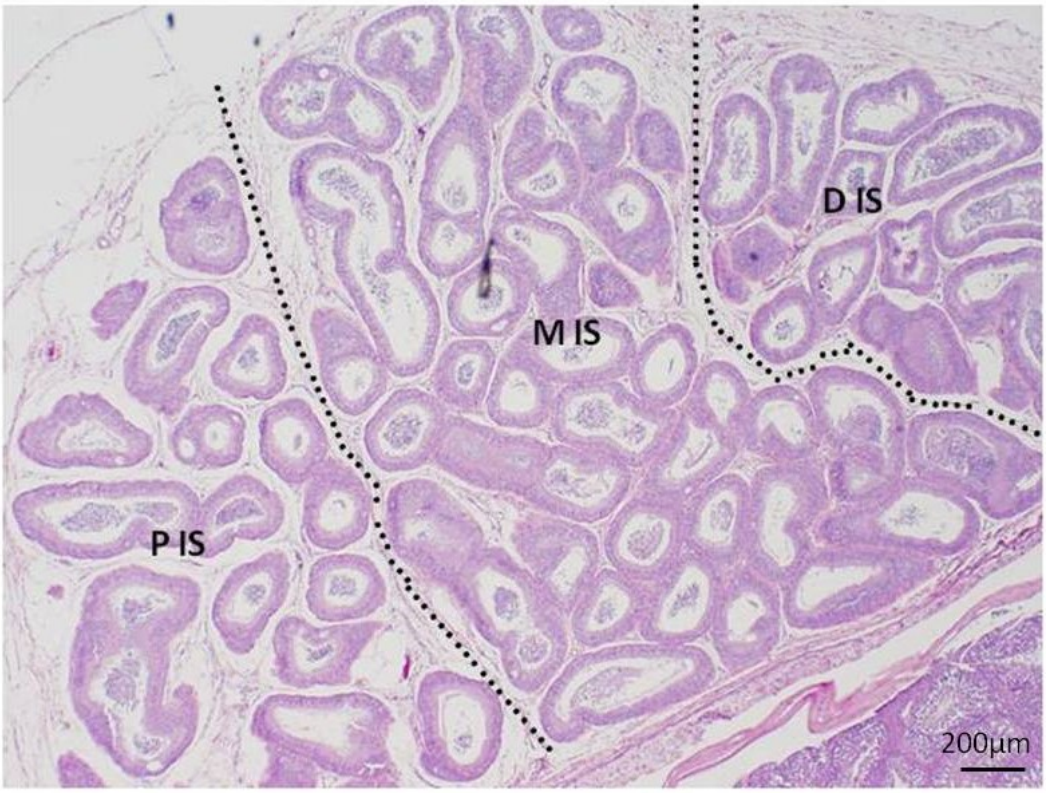

Figure 4.32. Photomicrograph of the Subdivisions of the Initial Segment (IS) of the Epididymis in Pubertal AGCR. Note that IS is partitioned by connective tissues stroma (dashed lines). PIS – Proximal initial segment, MIS – Middle initial segment, DIS – Distal initial segment. Stain: H&E.

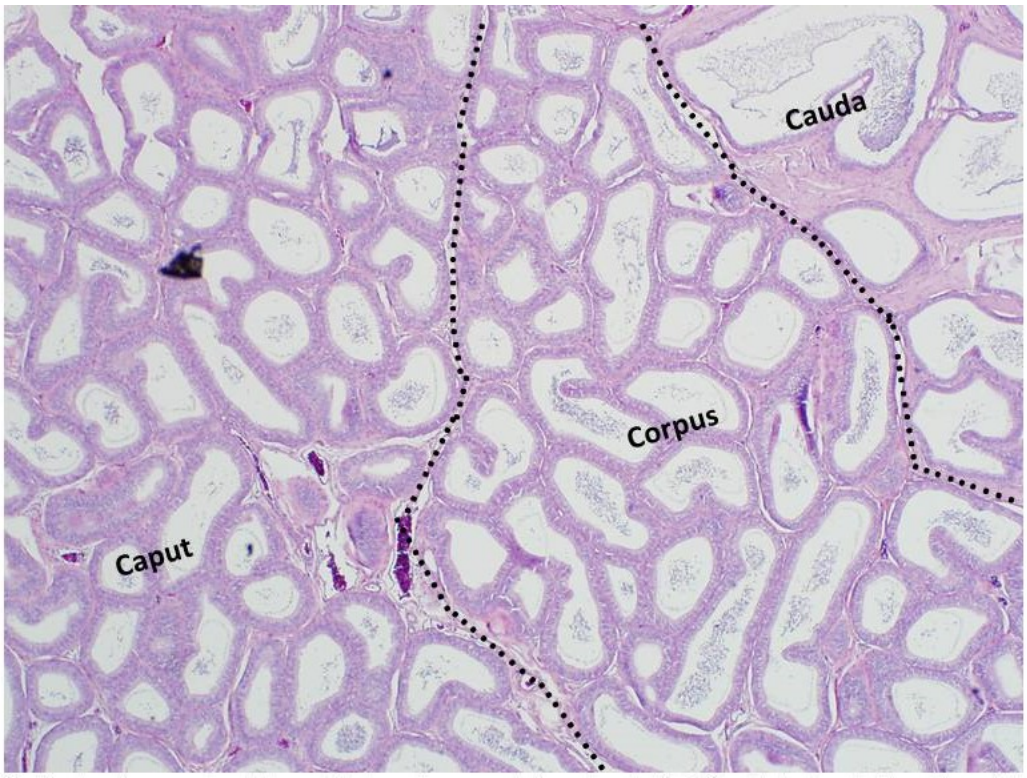

Figure 4.33. Photomicrograph of the Epididymal Segments in Pubertal AGCR. Note the delineation of the caput, corpus and cauda by connective tissues stroma (dashed lines). Stain: H&E; Scale bar: 200µm

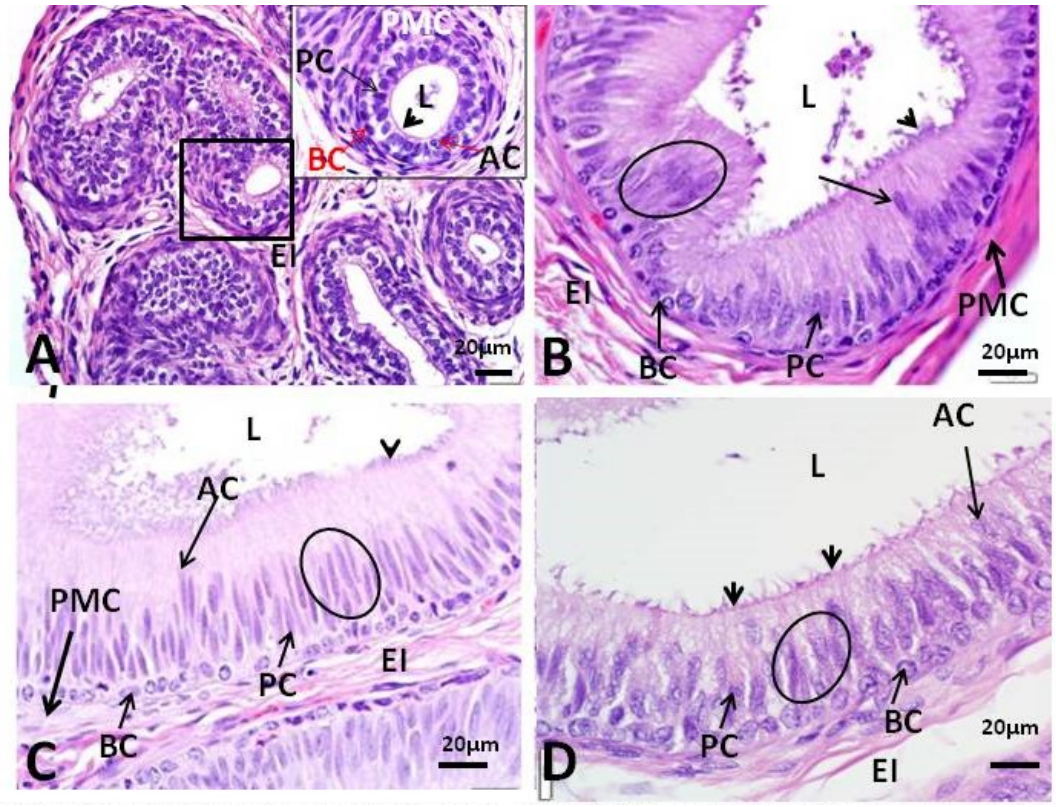

Figure 4.34. Photomicrographs of the Proximal Initial Segment of the Epididymis in Different Age Groups of the AGCR. A. **Prepubertal**: shows conspicuously reduced but almost absent stereocilia height (arrow head), round ductal lumen (L) lined by simple columnar epithelial cells and more cellular epididymal interstitium (EI) B. **Pubertal,** C. **Adult** and D. **Aged**: display stellate-shaped ductal lumen prominently lined by pseudostratified columnar epithelium (oval) with prominent stereocilia (arrow head) as well as component cell types; basal cells (BC), Principal cells (PC) and apical (AC). Stain: H&E; Scale bar: 20µm

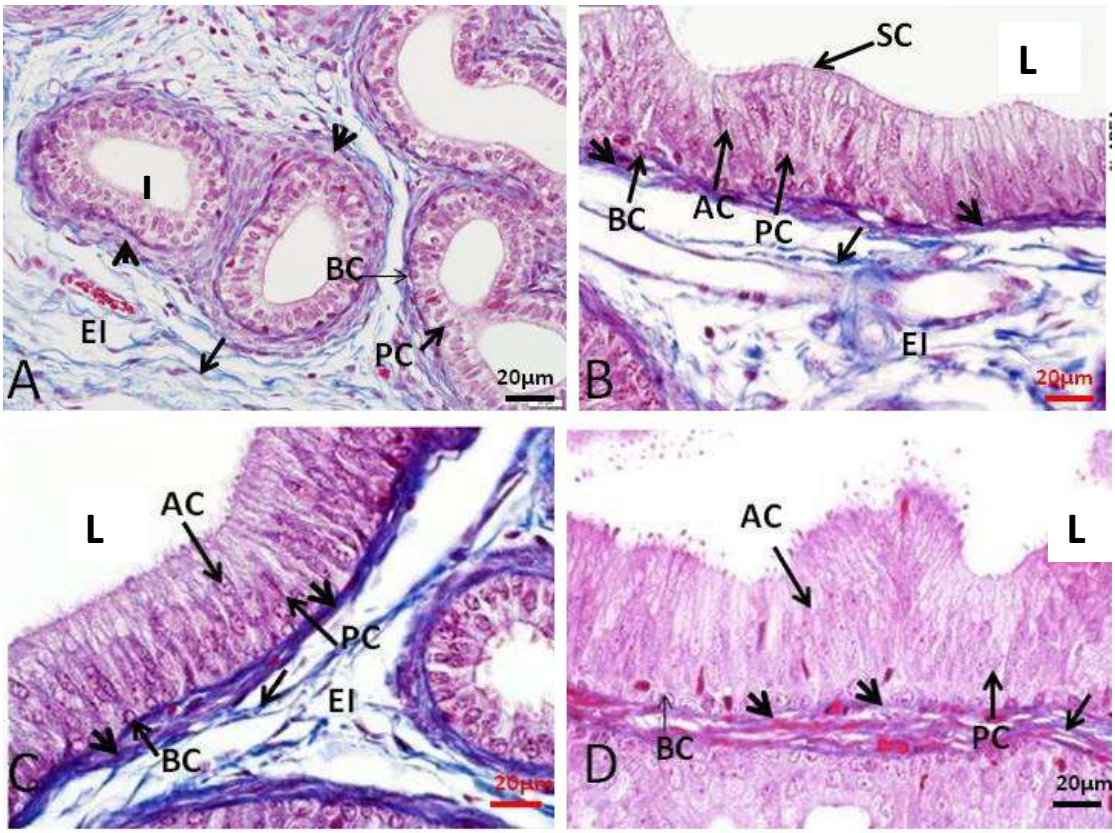

Figure 4.35. Masson's Trichrome Staining of the Proximal Region of the Initial Segment of Epididymis in the Different Age Groups of AGCR. A. Prepubertal: B. Pubertal: C. Adult: D. Aged. BC- Basal cells, PC- Principal cells, AC- Apical cells, SC- Stereocilia, L-Lumen. Note the blue staining collagen fibres (arrow) in the epididymal ductal interstices (EI) together with pink-staining smooth muscles (arrow heads) surrounding the epididymal ducts Scale bar: 20µm

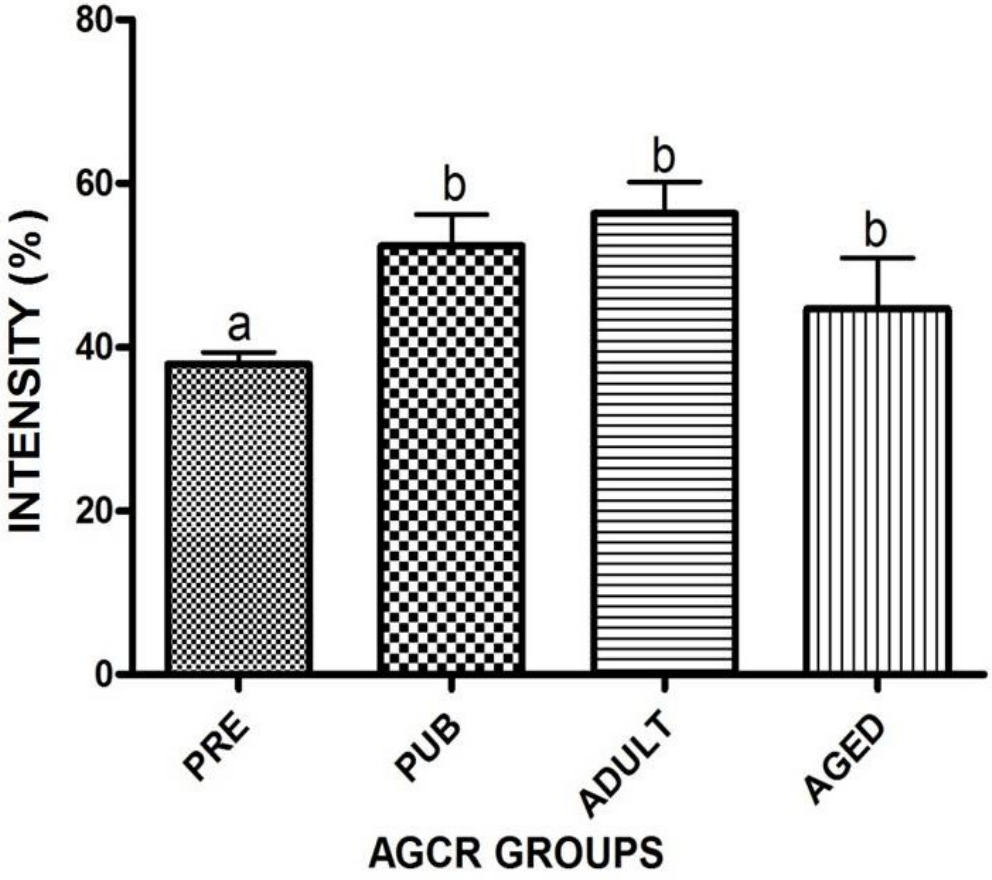

Figure 4.36. Age-Related Changes in the Intensity of Masson'sTrichrome Staining of the Proximal Initial Segment in the AGCR.

Bars with different alphabets are significantly different ($p<0.05$)

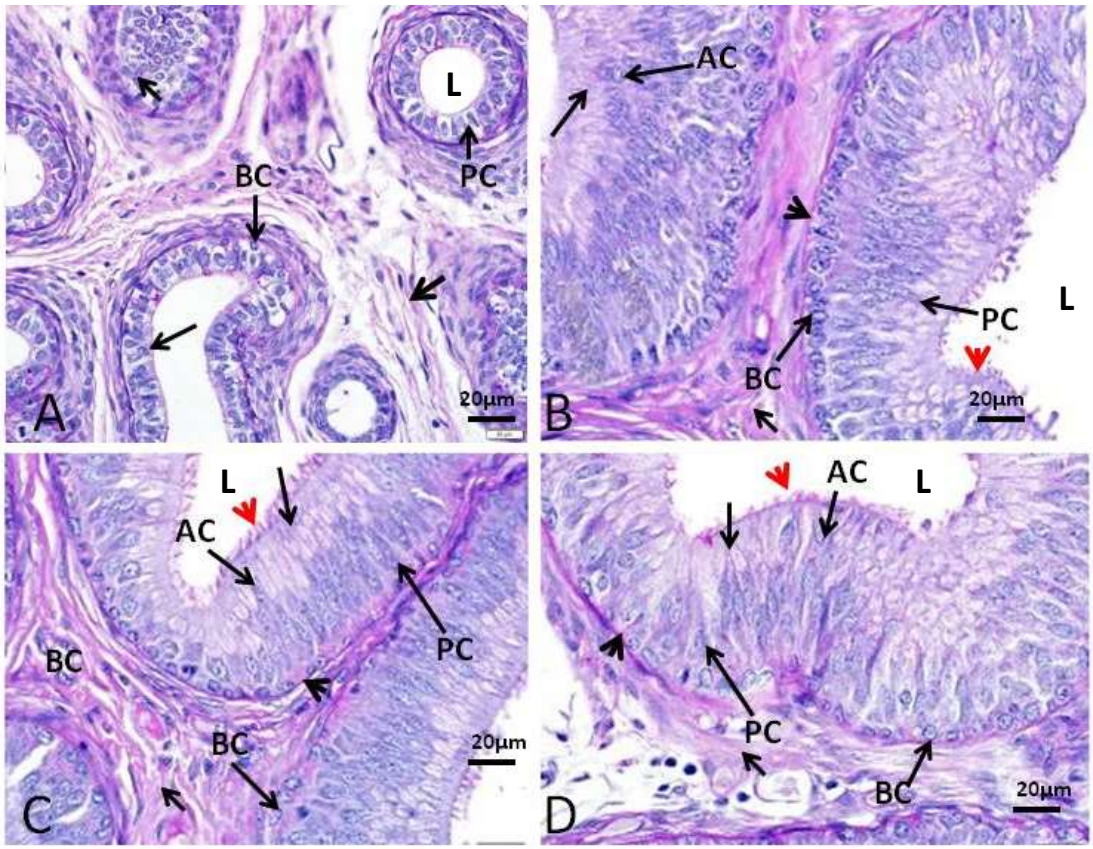

Figure 4.37. PAS Staining of the Proximal Initial Segment of Epididymis in Different Age Groups of AGCR. A. Prepubertal: B. Pubertal: C. Adult: D. Aged. BC- Basal cells, PC- Principal cells, AC- Apical cells, SC- Stereocilia, L-Lumen. Note the PAS-positive areas in the interstitium (short arrow), lamina propria (arrow head), ductal stereocilia (red arrowhead), supranuclear region (long arrow) of the epididymal epithelium. Scale bar: 20µm

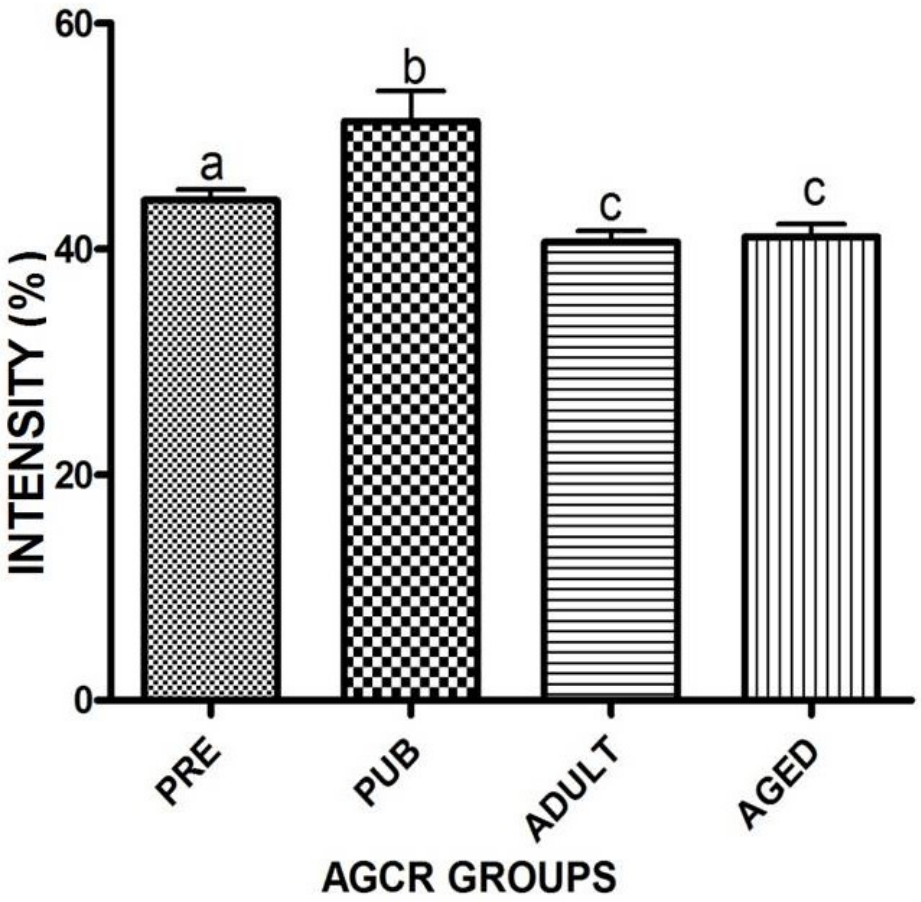

Figure 4.38. Age- related Changes in the Intensity of PAS Staining of the Proximal Initial Segment in AGCR.

Bars with different alphabets are significantly different ($p<0.05$)

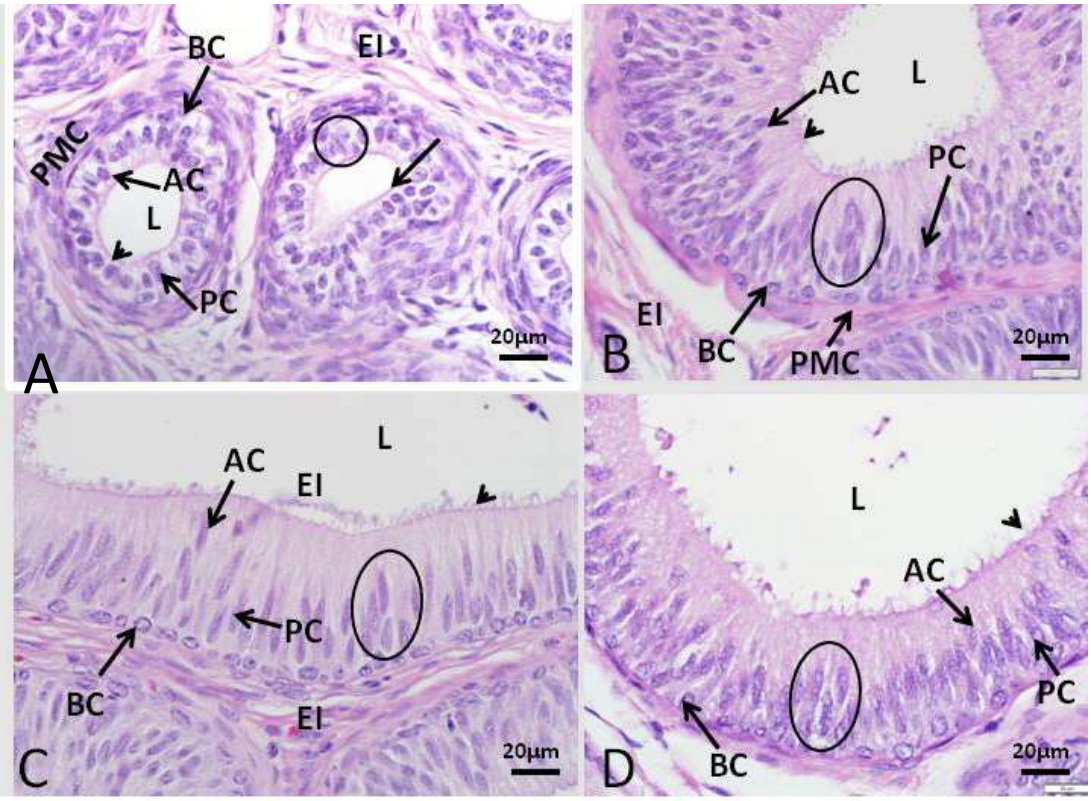

Figure 4.39. Photomicrographs of the Middle Region of the Initial Segment of Epididymis in Different Age Groups of AGCR. A. **Prepubertal**: shows markedly reduced stereocilia height (arrow head), round ductal lumen (L) lined by simple columnar epithelium and more cellular epididymal interstitium (EI) B. **Pubertal,** C. **Adult** and D. **Aged**: bear stellate-like lumen, duct lined by pseudostratified columnar epithelium (oval) with prominent stereocilia (arrow head) as well as the presence of basal cells (BC), Principal cells (PC) and moderate increase in apical cells (AC). Stain: H&E

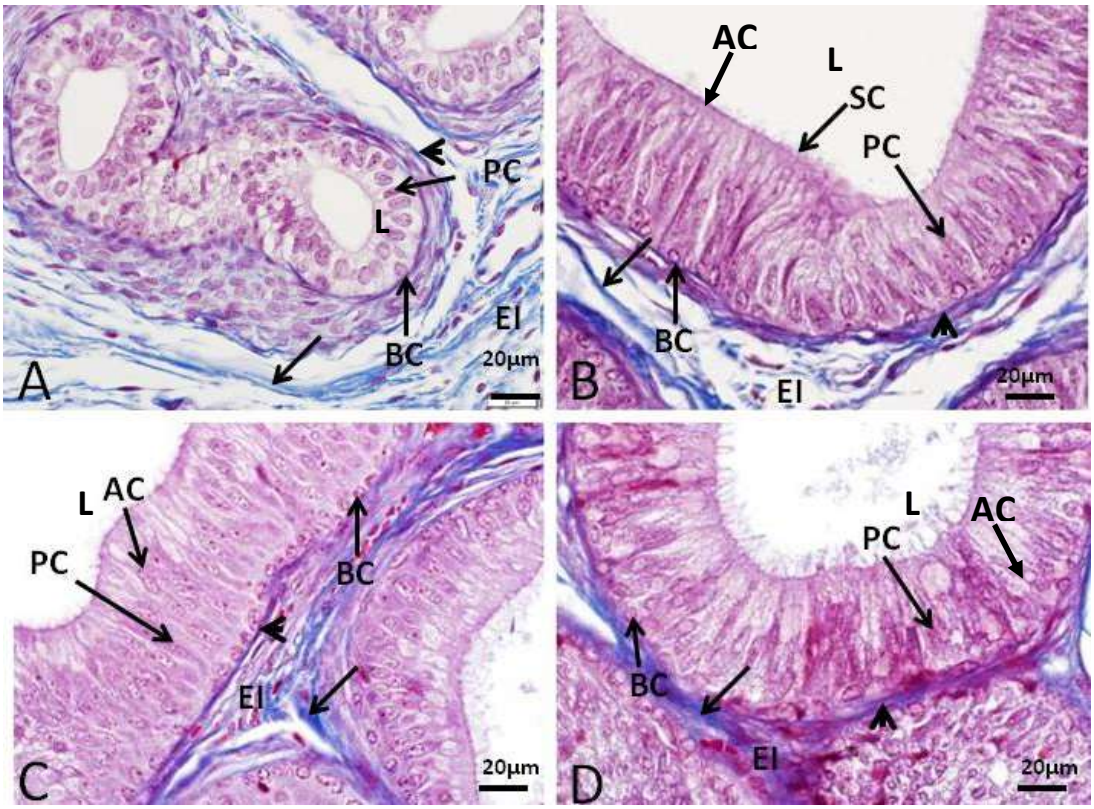

Figure 4.40. Masson's Trichrome Staining of the Middle Initial Segment of Epididymis in Different Age Groups of AGCR. A. Prepubertal: B. Pubertal: C. Adult: D. Aged. BC- Basal cells, PC- Principal cells, AC- Apical cells, SC- Stereocilia, L- Lumen. Note the blue staining collagen fibres (arrow) in the epididymal ductal interstices (EI) together with pink-staining smooth muscles (arrow heads) surrounding the epididymal ducts. Scale bar: 20µm.

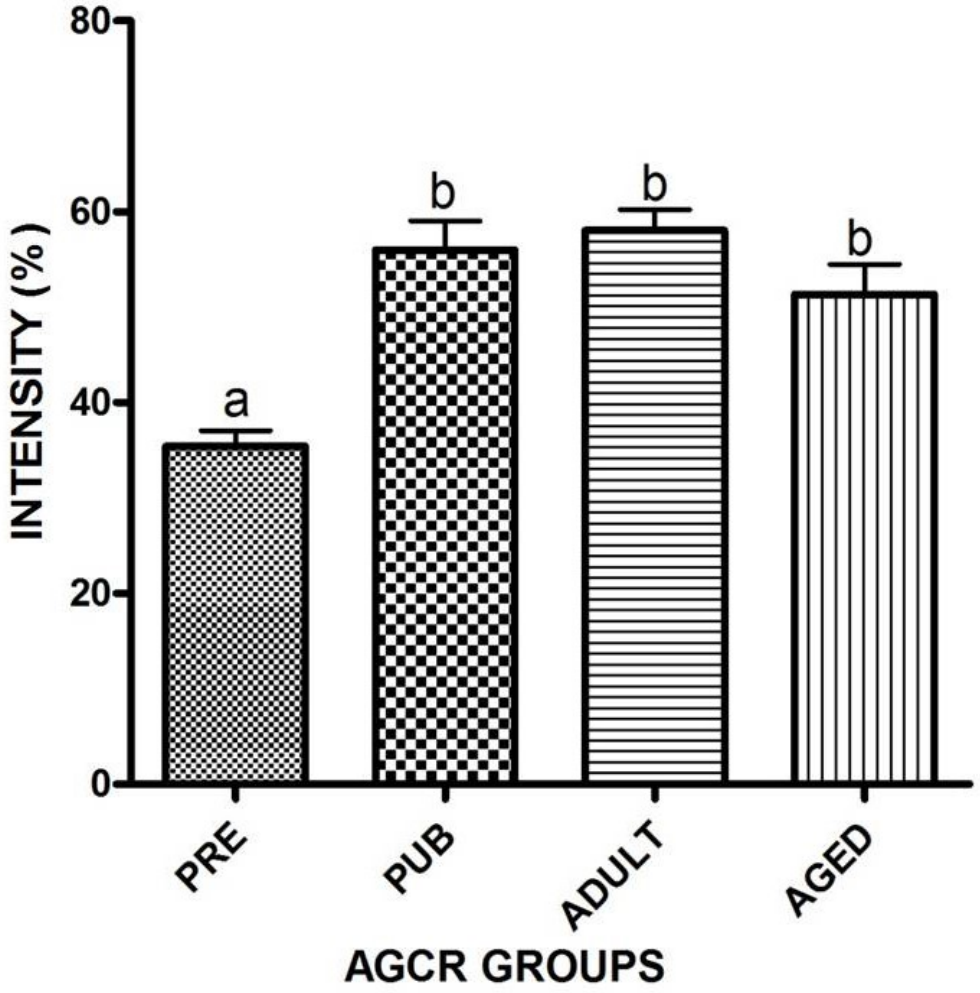

Figure 4.41. Age-Related Changes in Intensity of Masson'sTrichrome Staining of the Middle Initial Segment in AGCR.

Bars with different alphabets are significantly different ($p<0.05$)

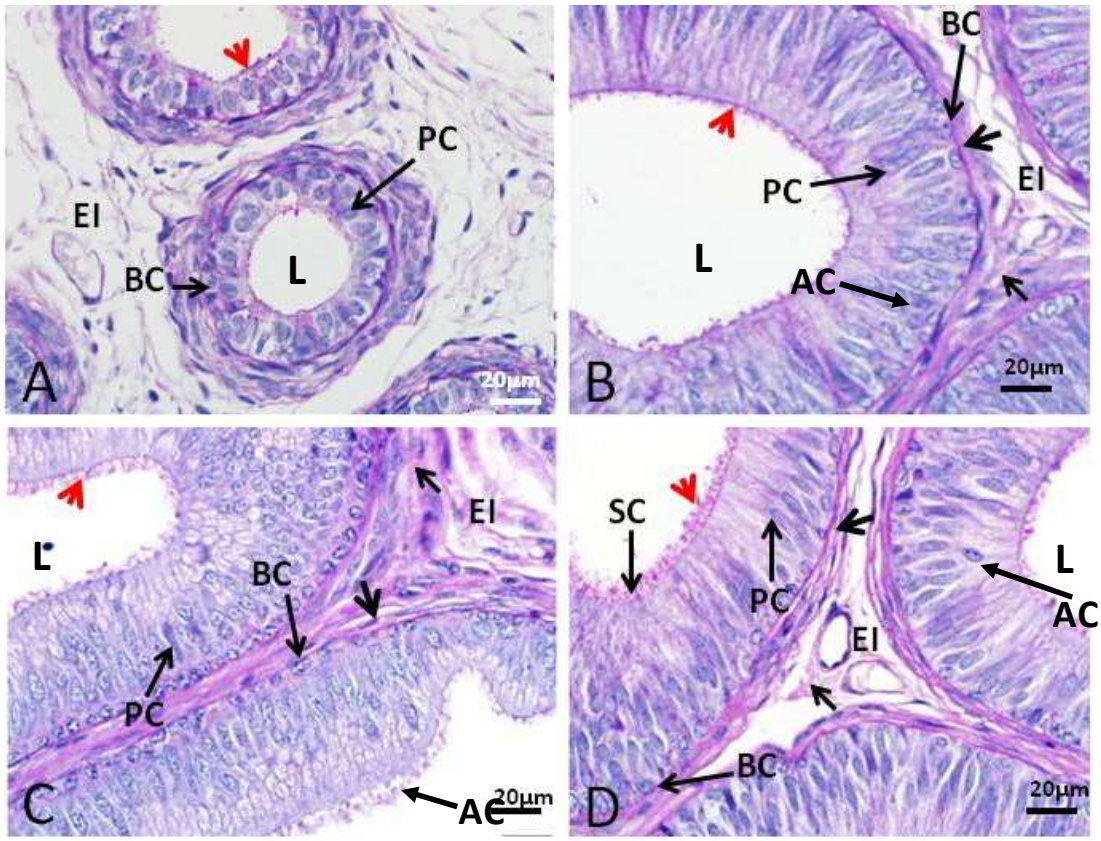

Figure 4.42. PAS Staining of the Middle Region of the Initial Segment of Epididymis in Different Age Groups of AGCR. A. Prepubertal: B. Pubertal: C. Adult: D. Aged. BC- Basal cells, PC- Principal cells, AC- Apical cells, EI- Epididymal interstitium, SC- Stereocilia, L-Lumen. Note the PAS positive areas in the interstitium (short arrow), lamina propria (arrow head) and supranuclear region (long arrow) of the epididymal epithelium. Scale bar: 20µm

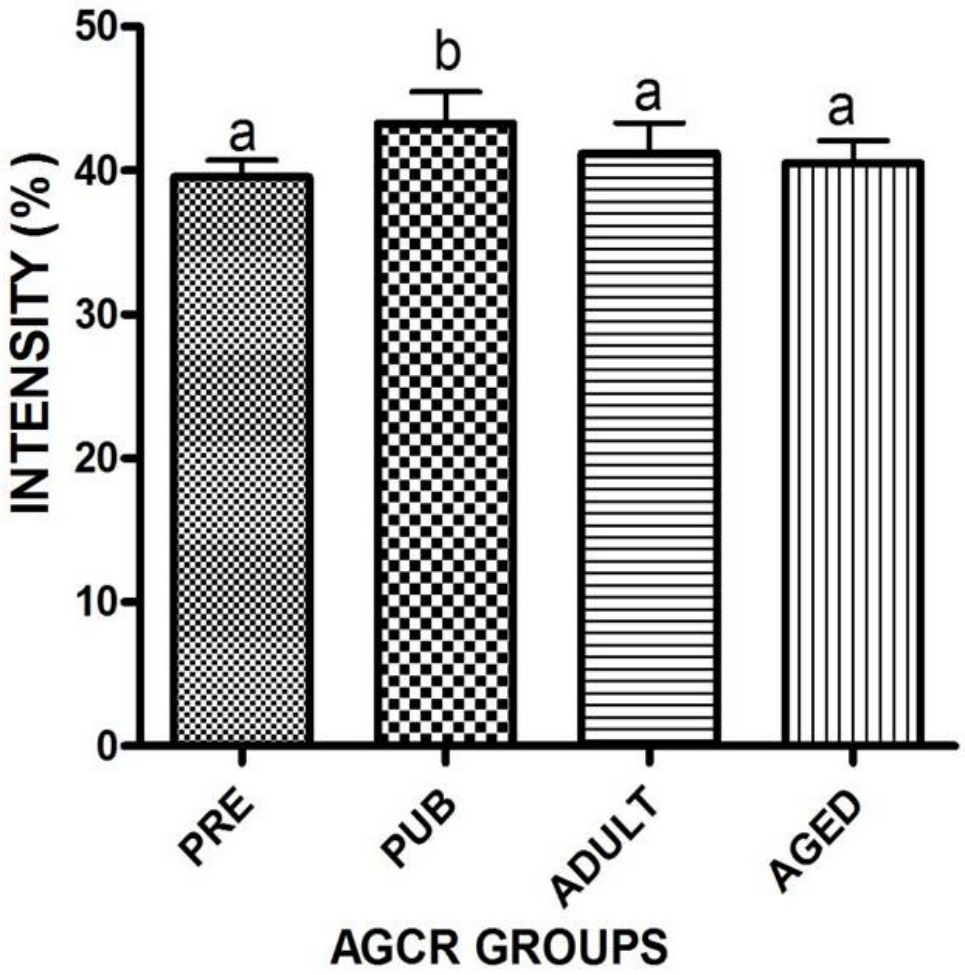

Figure 4.43. Age-related Changes in theIntensity of Periodic Acid Schiff'sStaining of the Middle Initial Segment in AGCR.

Bars with different alphabets are significantly different ($p<0.05$)

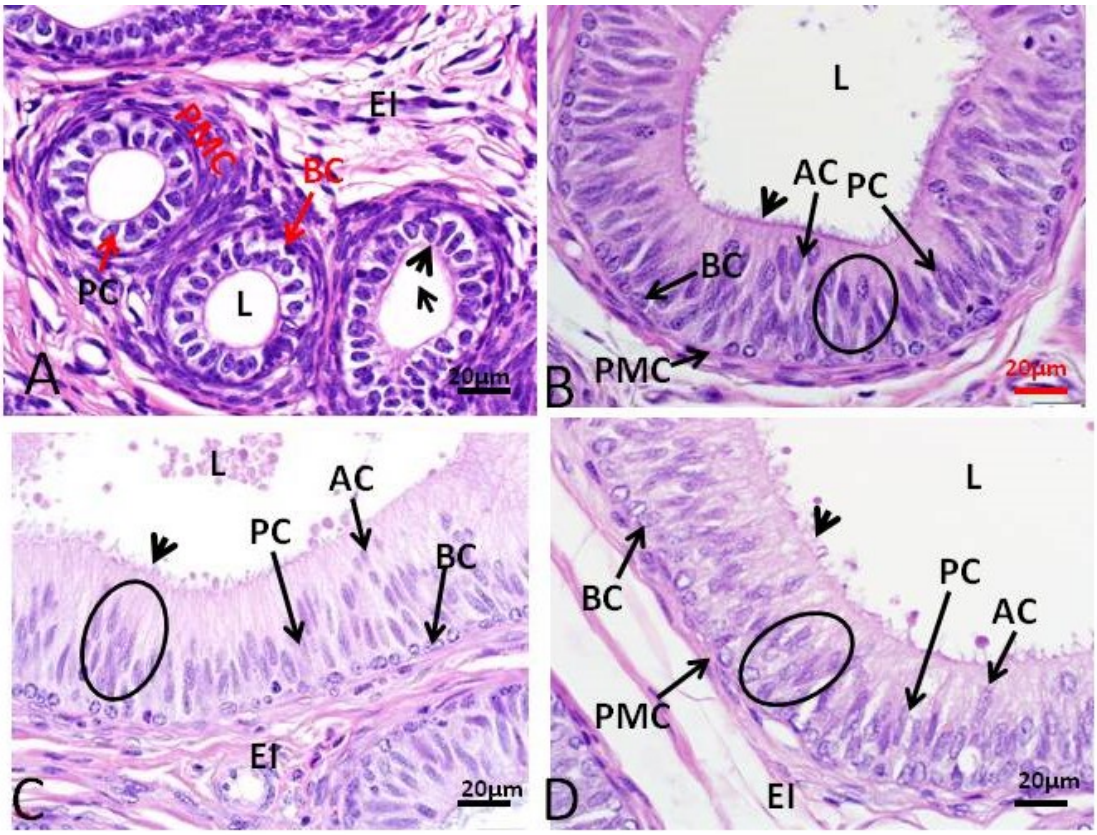

Figure 4.44. Photomicrographs of the Distal Initial Segment of Epididymis in the Different Age Groups of AGCR. A. **Prepubertal**: shows thickened peritubular muscular coat (PMC), reduced stereocilia height (arrow head), round ductal lumen (L) lined by simple columnar epithelium and more cellular interstitium B. **Pubertal,** C. **Adult** and D. **Aged**: bear stellate-like luminal shape, ducts lined by pseudostratified columnar epithelium (oval) with prominent stereocilia (arrow head) as well as the presence of basal cells (BC), Principal cells (PC) and markedly increase in apical cells (AC). Stain: H&E; Scale bar: 20µm

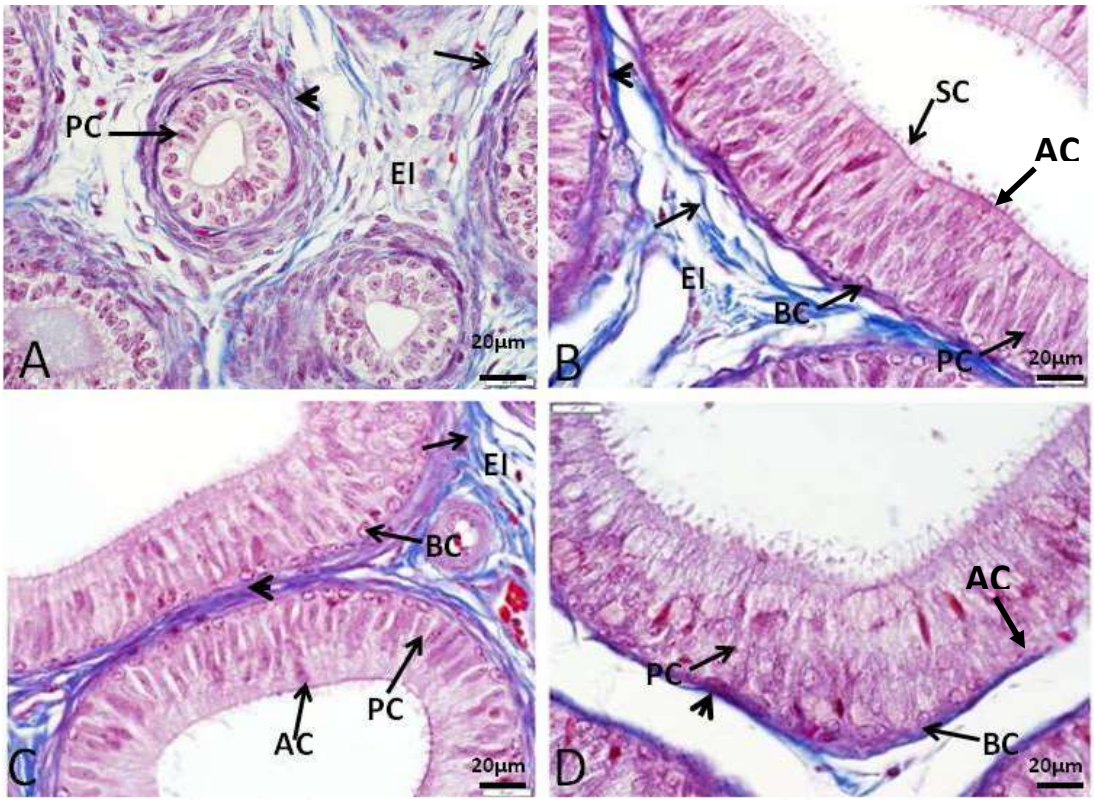

Figure 4.45. Masson's Trichrome Staining of the Distal Region of the Initial Segment of Epididymis in Different Age Groups of AGCR. A. Prepubertal: B. Pubertal: C. Adult: D. Aged. BC- Basal cells, PC- Principal cells, AC- Apical cellsTI- Tubular interstitium, SC- Stereocilia, L-Lumen. Note the blue staining collagen fibres (arrow) in the epididymal ductal interstices (EI) together with pink-staining smooth muscles (arrow heads) surrounding the epididymal ducts. Scale bar: 20µm

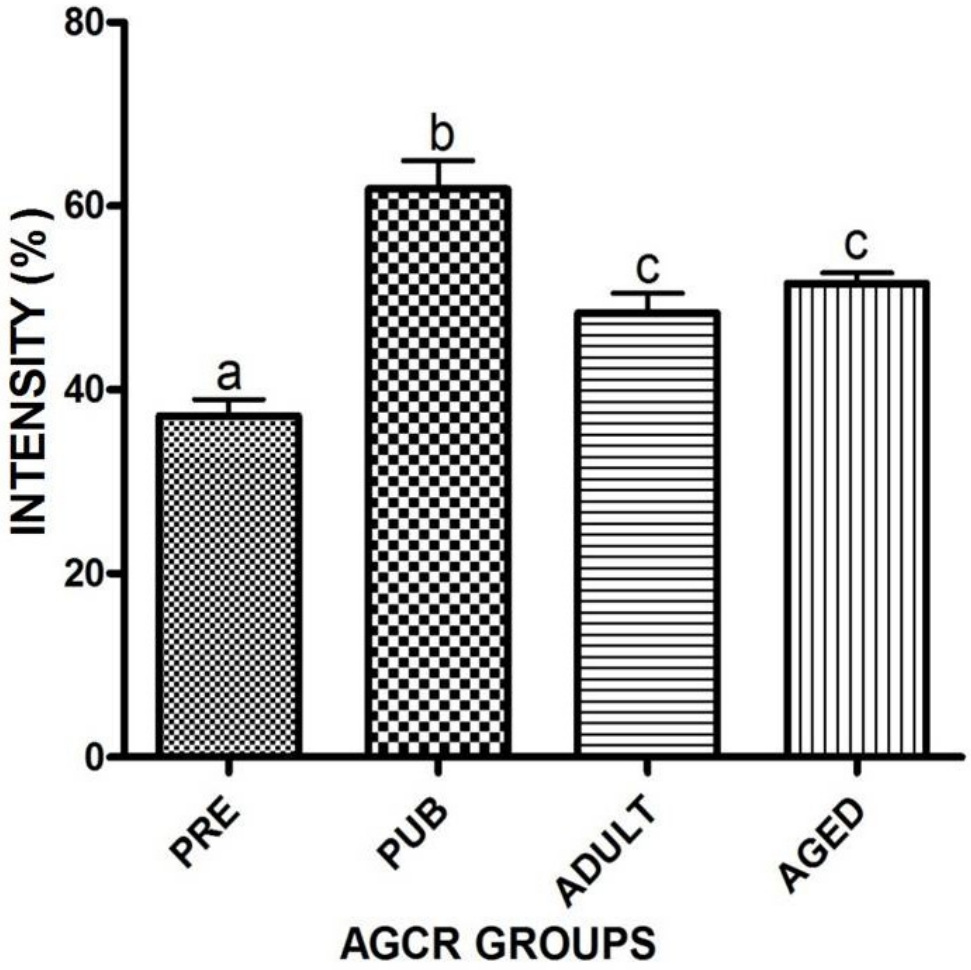

Figure 4.46. Age-related Changes in the Intensity of Masson'sTrichrome Staining of the Distal Initial Segment in AGCR.

Bars with different alphabets are significantly different ($p<0.05$)

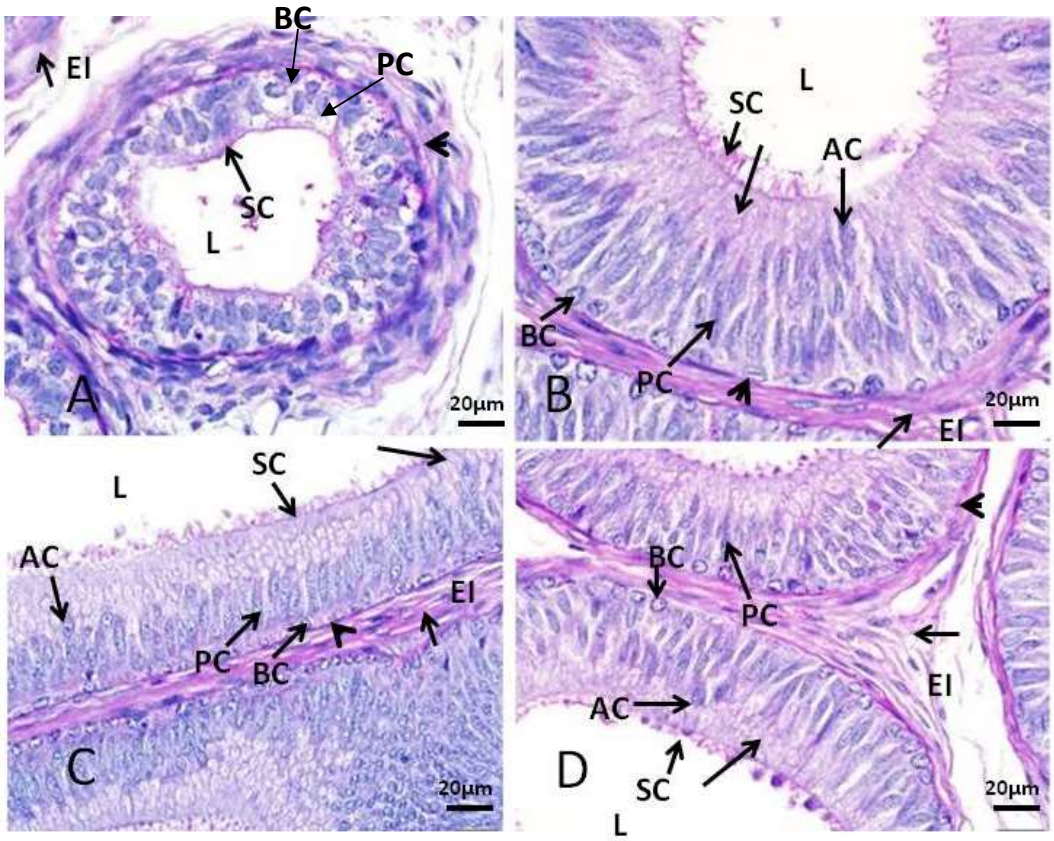

Figure 4.47. PAS Staining of the Distal Initial Segment of the Epididymis in the Different Age Groups of AGCR. A. Prepubertal: B. Pubertal: C. Adult: D. Aged. BC- Basal cells, PC- Principal cells, AC- Apical cells, SC- Stereocilia, EI – Epididymal duct interstices and L- Lumen. Note the PAS positive areas in the interstitium (short arrow), lamina propria (arrow head) and supranuclear region (long arrow) of the epididymal epithelium. Scale bar: 20µm

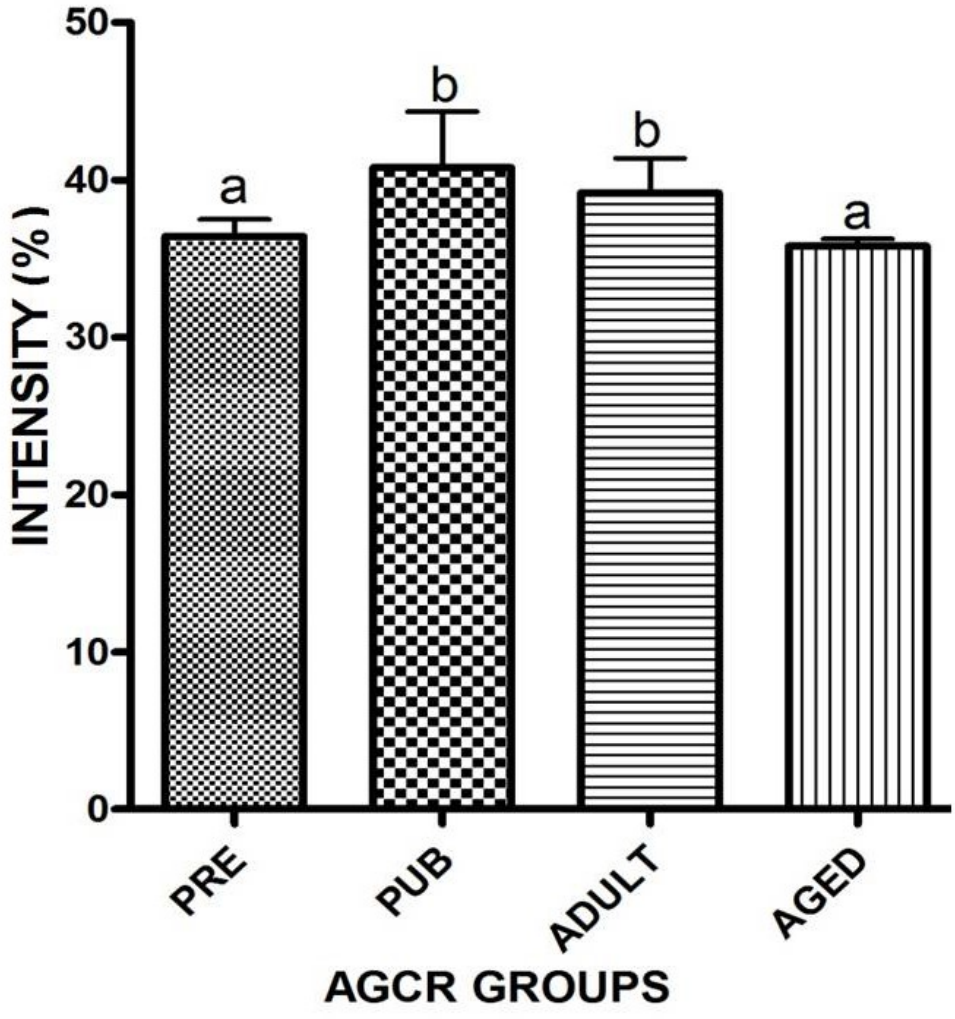

Figure 4.48. Age-related Changes in the Intensity of PAS Staining of the Distal Initial Segment in AGCR.

Bars with different alphabets are significantly different ($p<0.05$)

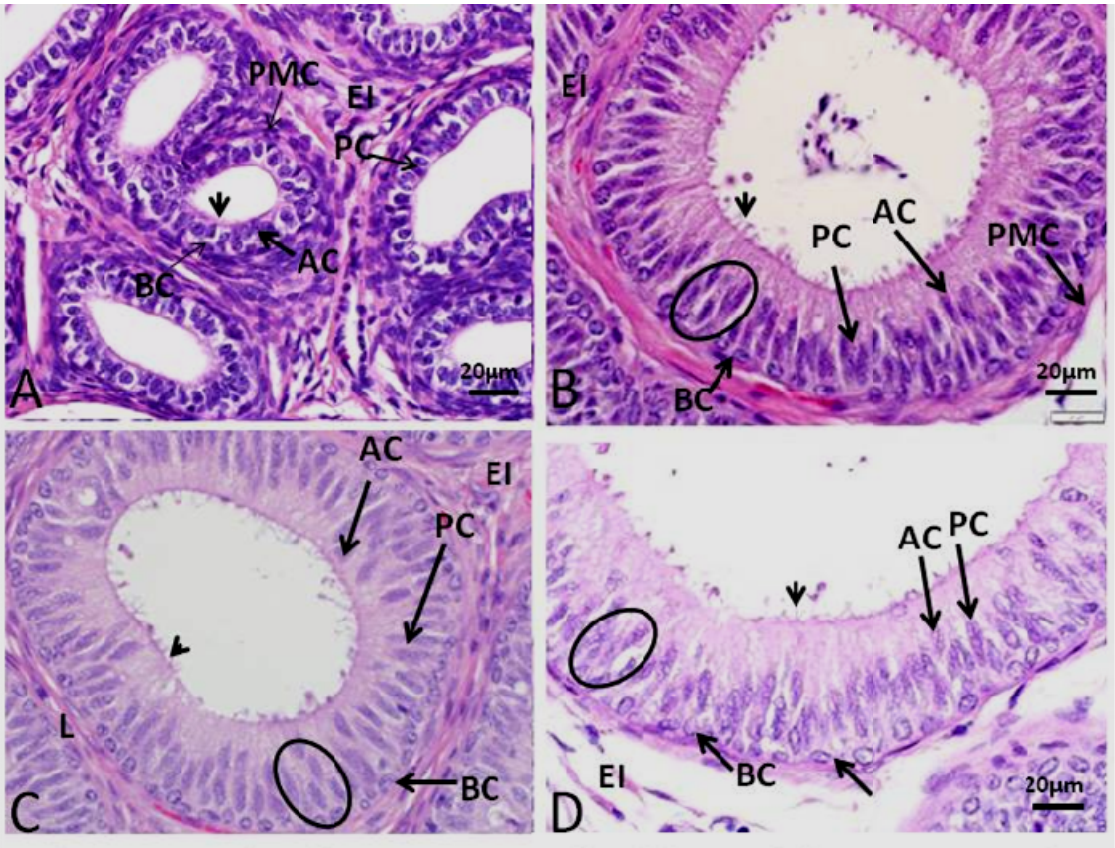

Figure 4.49. Photomicrographs of the Caput Segment of Epididymis in the Different Age Groups of AGCR. A. **Prepubertal**: displays markedly thickened peritubular muscular coat (PMC), reduced stereocilia height (arrow head), roundish ductal luminal (L) shape lined by simple cuboidal to columnar epithelial lining. B. **Pubertal,** C. **Adult** and D. **Aged**: bear stellate to roundish like luminal shape, ducts lined by pseudostratified columnar epithelium (oval) with prominent stereocilia (arrow head) as well as the presence of basal cells (BC), Principal cells (PC) and more apical cells (AC). Stain: H&E; Scale bar: 20µm

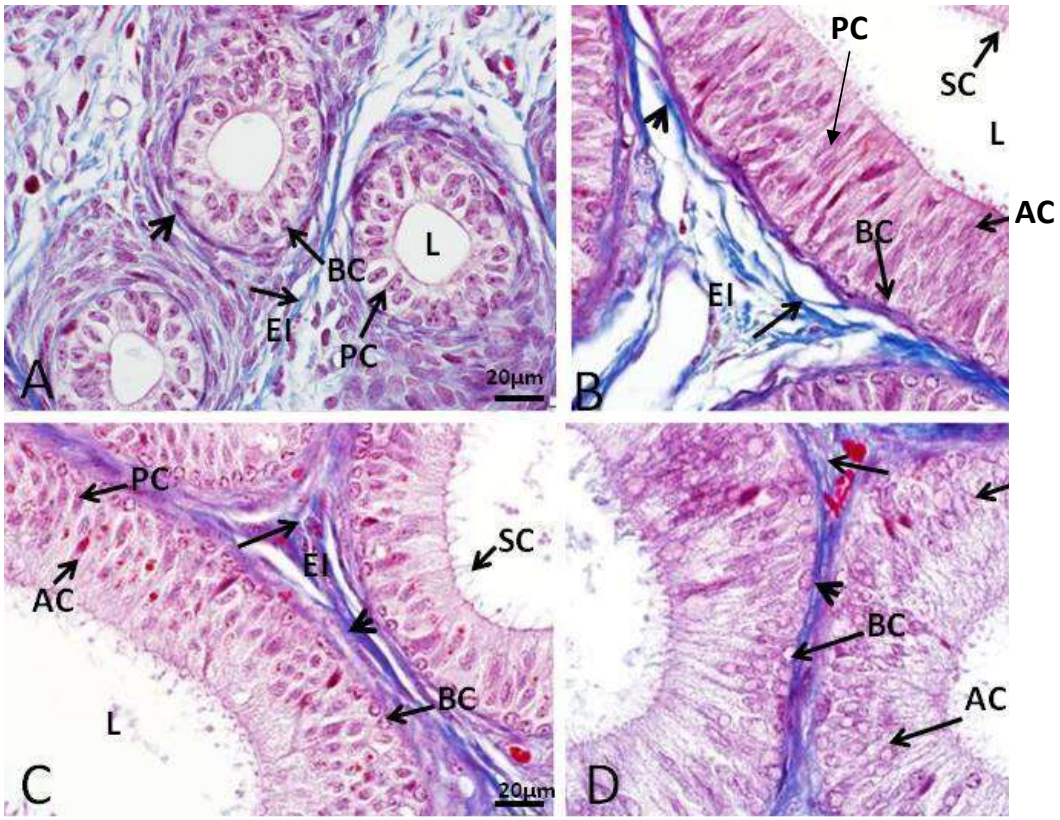

Figure 4.50. Masson's Trichome Stainingof the Caput Segment of Epididymis in Different Age Groups of AGCR . A. Prepubertal: B. Pubertal: C. Adult: D. Aged. BC-Basal cells, PC- Principal cells, AC- Apical cells EI- Epididymal interstitium, SC-Stereocilia, L-Lumen. Note the blue staining collagen fibres (arrow) in the epididymal ductal interstices (EI) together with pink-staining smooth muscles (arrow heads) surrounding the epididymal ducts. Scale bar: 20µm

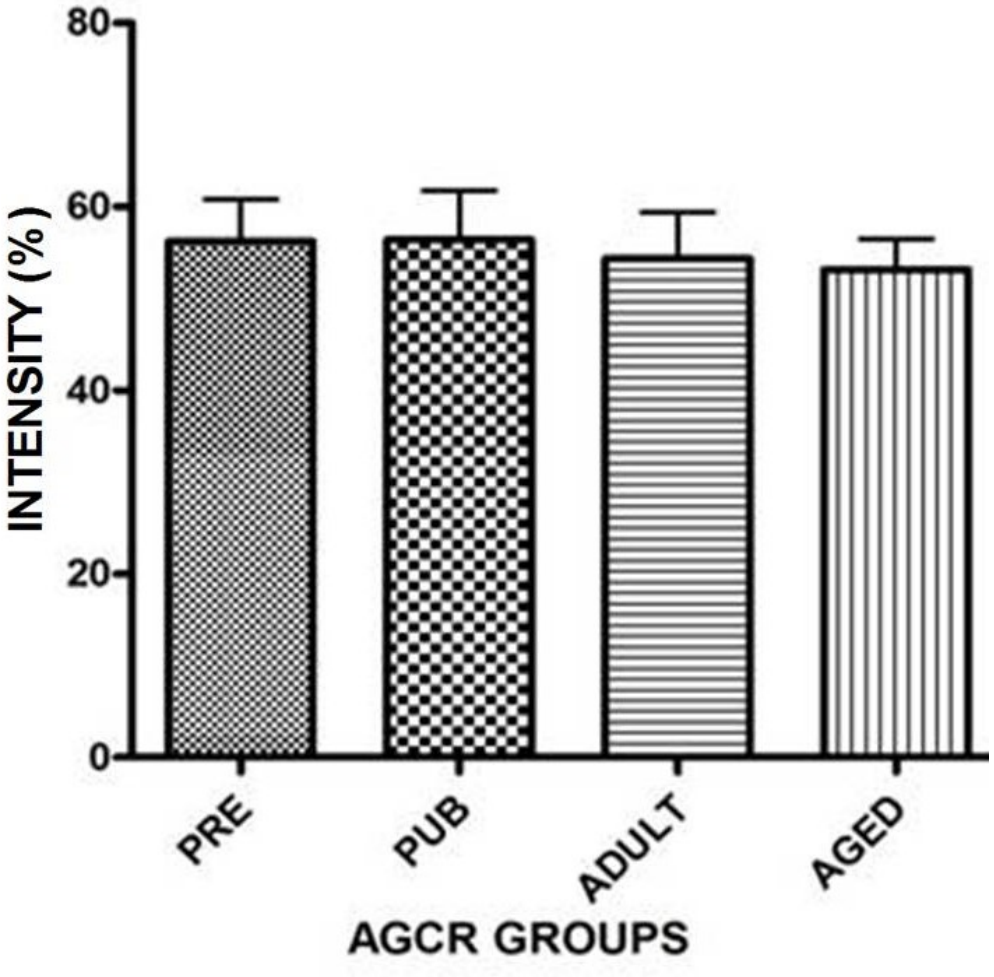

Figure 4.51. Age-related Changes in the Intensity of Masson'sTrichrome Staining of the Caput Segment in AGCR.

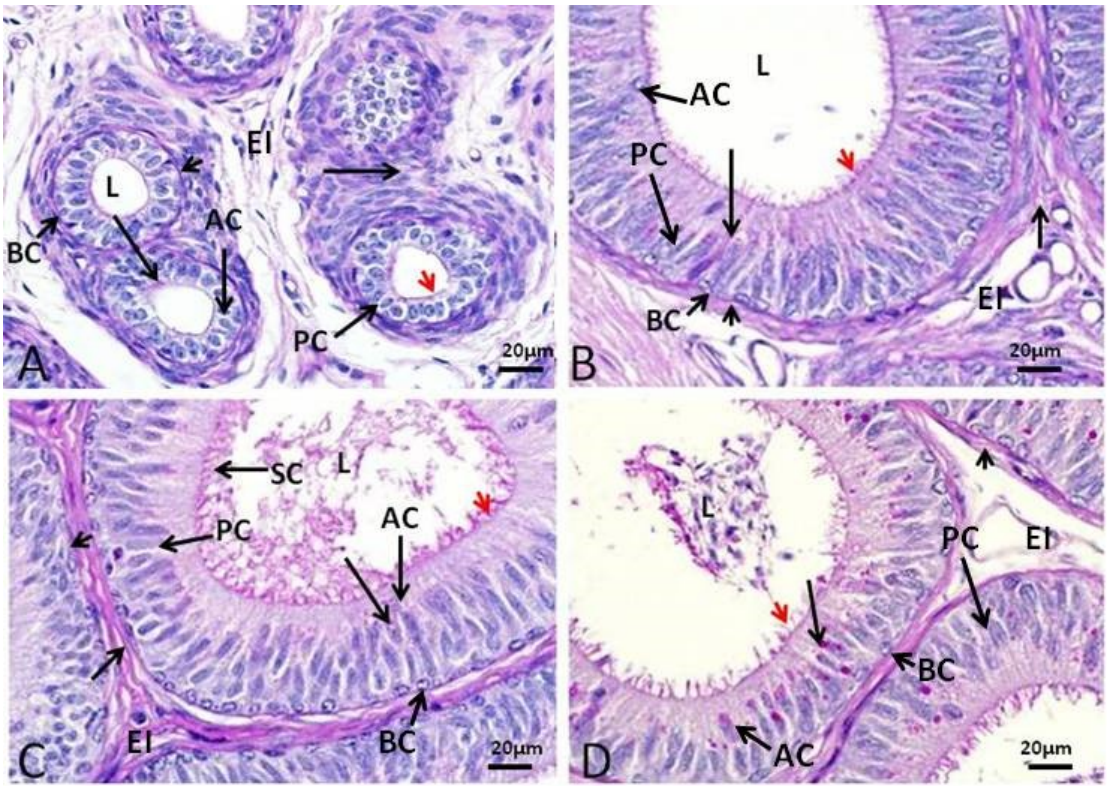

Figure 4.52. PAS Staining of the Caput Segment of Epididymis in the Different Age-Groups of AGCR. A. Prepubertal: B. Pubertal: C. Adult: D. Aged. BC- Basal cells, PC- Principal cells, AC- Apical cells, EI- Epididymal interstitium, SC- Stereocilia, L-Lumen. Note the PAS positive areas in the interstitium (short arrow), lamina propria (arrow head), ductal stereocilia (red arrow head) epithelial perinuclear region (long arrow) and luminal spermatozoa. Scale bar: 20µm

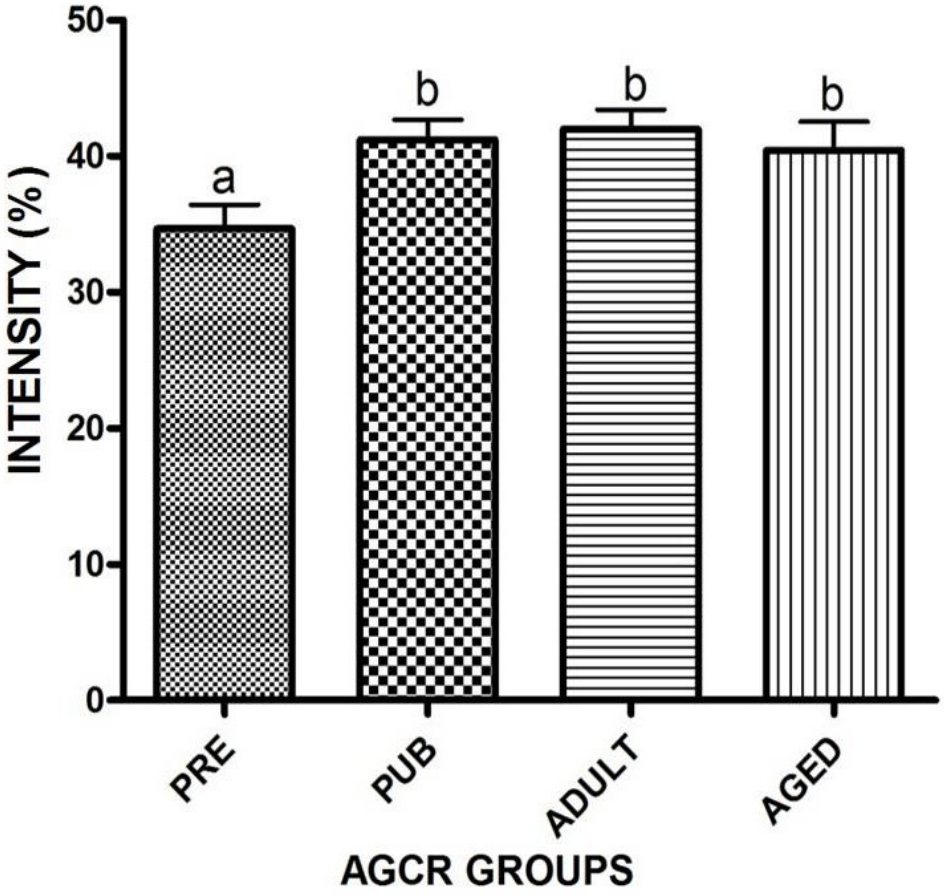

Figure 4.53. Age-related Changes in the Intensity of PAS Staining of the Caput Segment in AGCR.

Bars with different alphabets are significantly different ($p<0.05$)

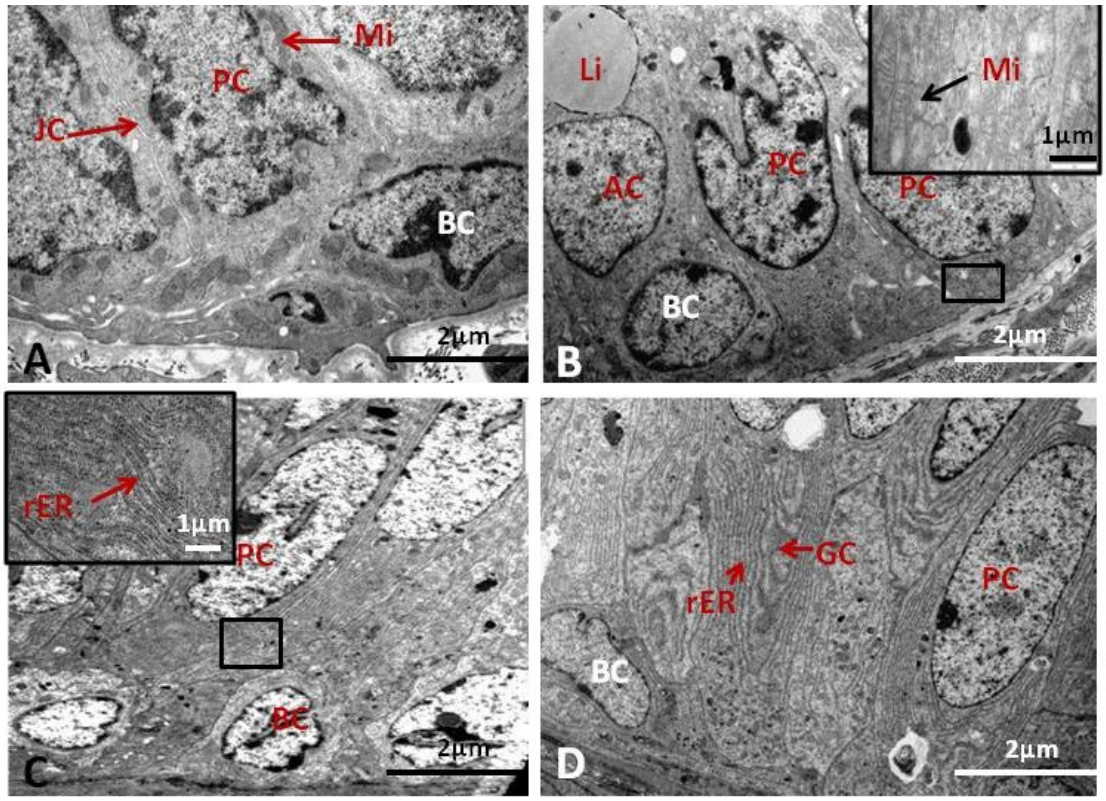

Figure 4.54. Transmission Electron Micrographs of the Basal Aspect of Caput Epididymis of the African Greater Cane Rat. A. Prepubertal: B. Pubertal: C. Adult: D. Aged. Note the presence of numerous mitochondria (Mi) in the basal part of A and B as well as abundant long rough endoplasmic reticulum (rER) in C and D. BC- Basal cell, PC- Principal cell, CC- Clear cell, AC- Apical cell, JC- Junctional complex, Li- Lipid, GC-Golgi complex. Scale bar: main (2µm), inset (1µm).

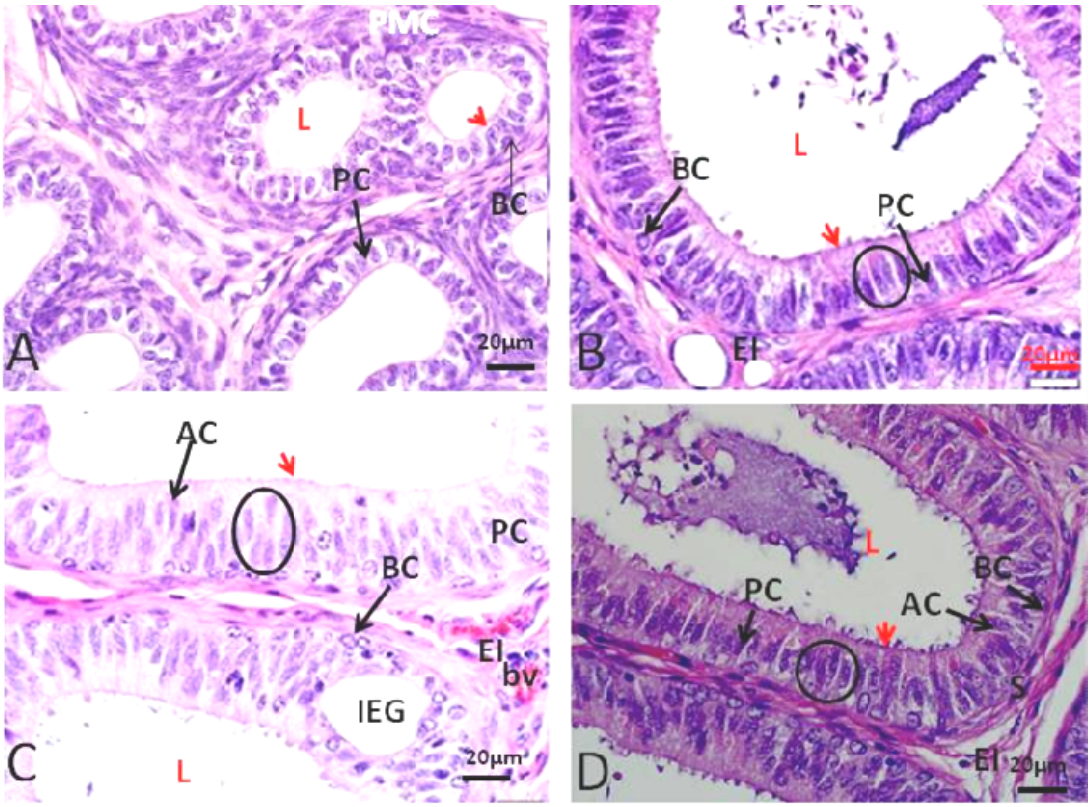

Figure 4.55. Photomicrographs of the Corpus Segment of Epididymis in the Different Age-groups of AGCR. A. **Prepubertal**: displays reduced stereocilia height (arrow head) and roundish ductal luminal (L) shape lined by simple cuboidal to columnar epithelial cells. B. **Pubertal,** C. **Adult** and D. **Aged**: bear numerous intraepithelial glands, round ductal lumen shape containing spermatozoa, ducts lined by pseudostratified columnar epithelium (oval) with prominent stereocilia (arrow head) as well as the presence of basal cells (BC), Principal cells (PC) and reduced apical cells (AC). EI- Epididymal interstitium, bv- blood vessel. Stain: H&E; Scale bar: 20µm

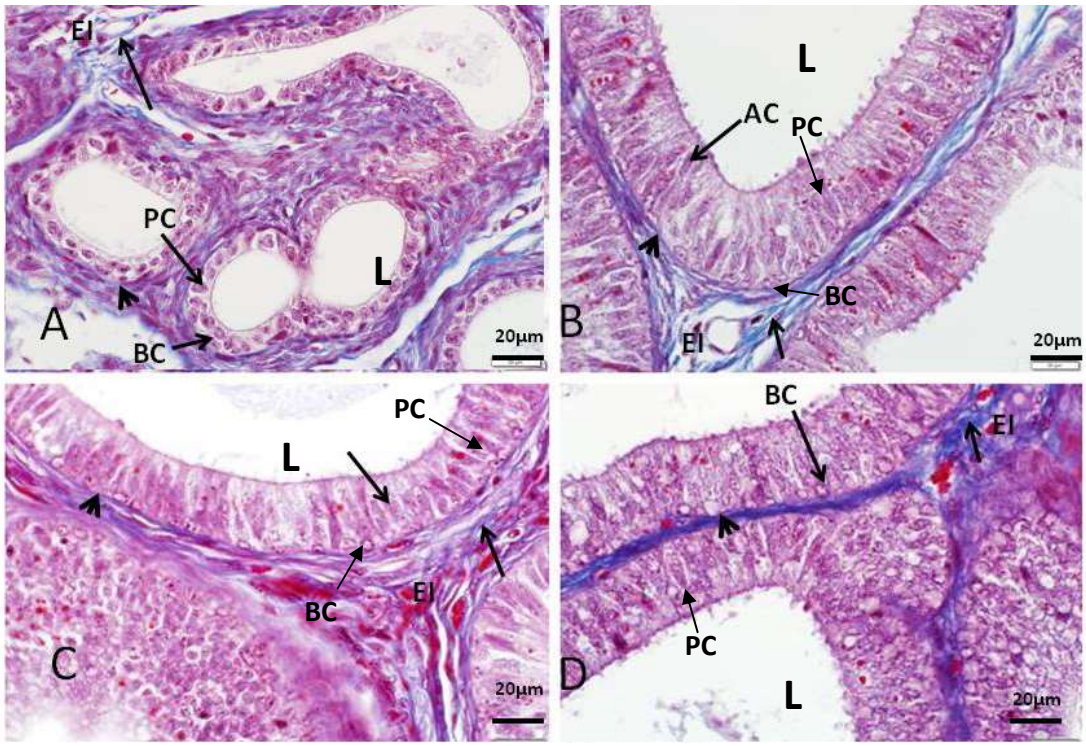

Figure 4.56. Masson's Trichrome Staining of the Corpus Segment of Epididymis in the Different Age Groups of AGCR. A. Prepubertal: B. Pubertal: C. Adult: D. Aged. BC- Basal cells, PC- Principal cells, AC- Apical cells EI- Epididymal interstitium, SC- Stereocilia, L-Lumen. Note the blue staining collagen fibres (arrow) in the epididymal ductal interstices (EI) together with pink-staining smooth muscles (arrow heads) surrounding the epididymal ducts. Scale bar: 20µm

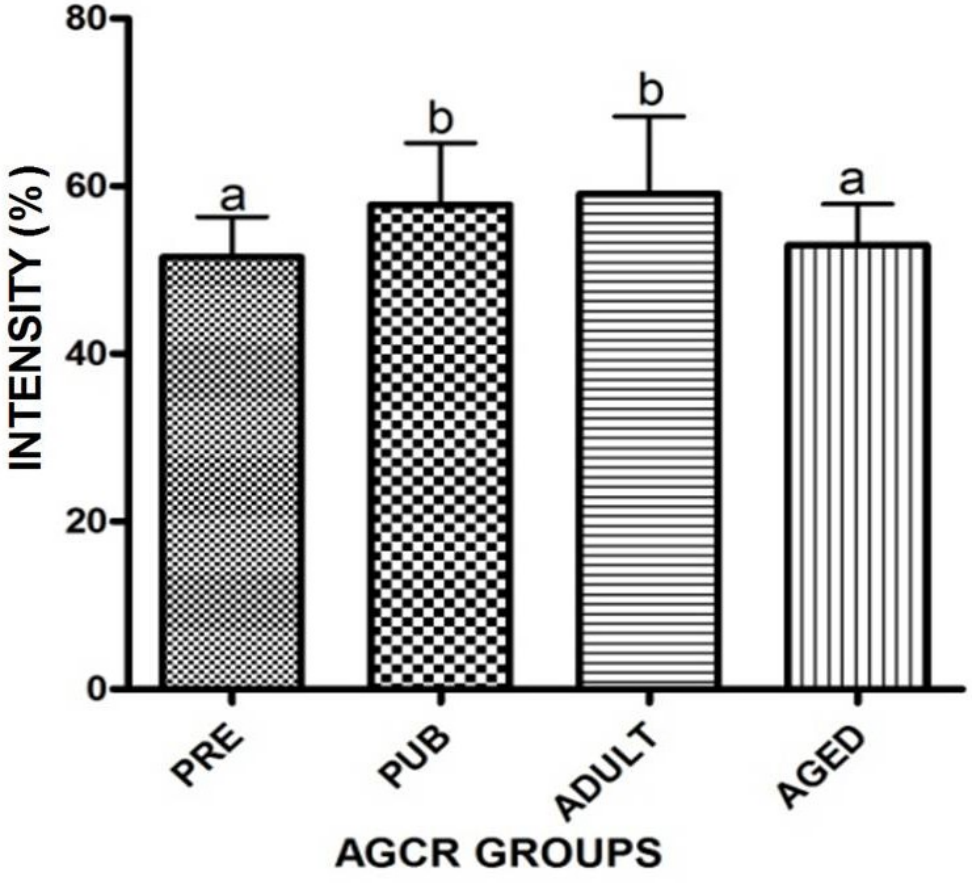

Figure 4.57. Age-related Changes in the Intensity of Masson's Trichrome Staining of the Corpus Segment in AGCR.

Bars with different alphabets are significantly different ($p<0.05$)

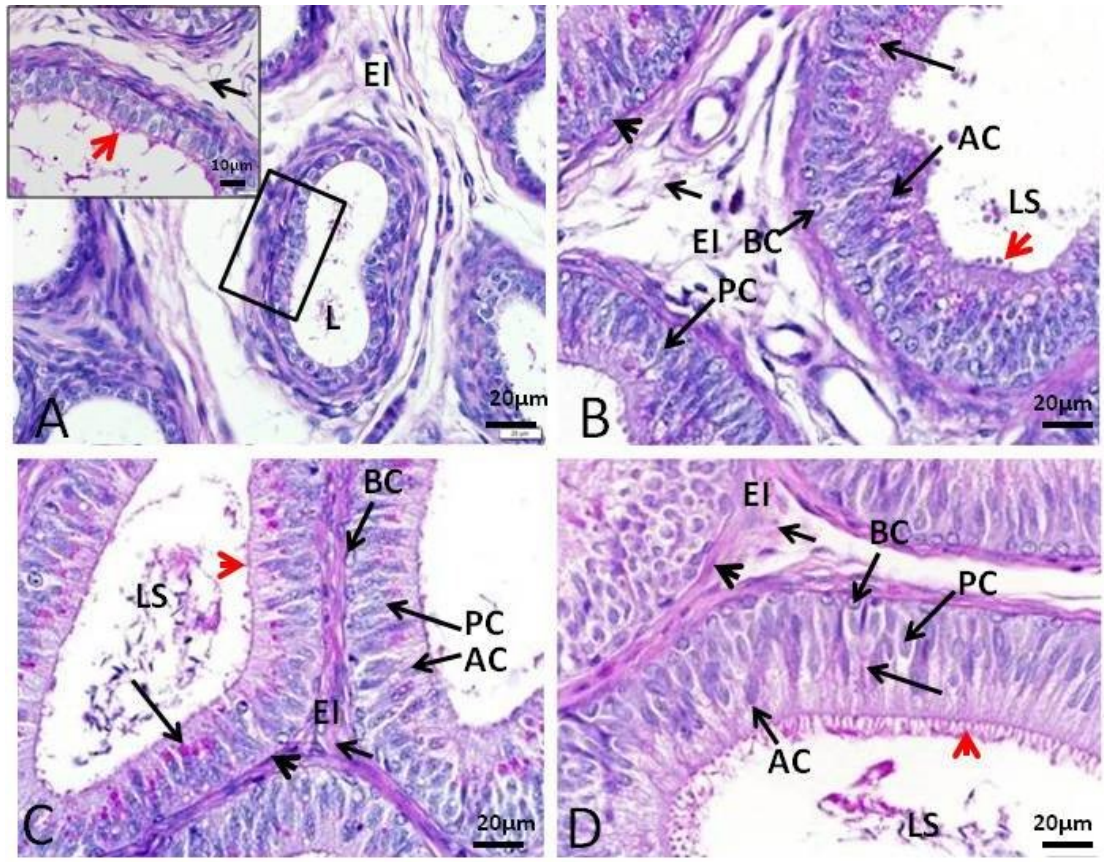

Figure 4.58. PAS Staining of the Corpus Segment of Epididymis in the Different Age Groups of the AGCR. A. Prepubertal: B. Pubertal: C. Adult: D. Aged. Note the PAS positive areas in the interstitium (short arrow), lamina propria (arrow head), epithelial perinuclear region (long arrow), ductal stereocilia (red arrow head) and luminal spermatozoa (LS) in B, C and D. Also observed the PAS positive areas within prepubertal epididymal duct [stereocilia (red arrow head)] as revealed by the insert from the black rectangular area. BC- Basal cells, PC- Principal cells, AC- Apical cells, EI- Epididymal interstitium, L-Lumen. Scale bar: 20µm

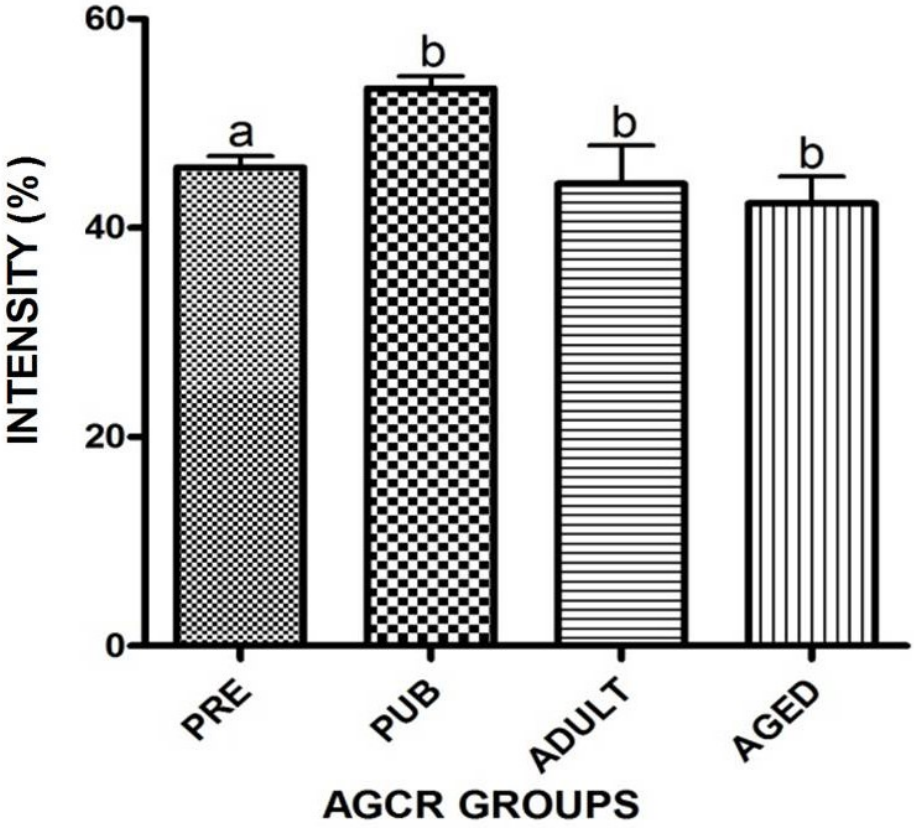

Figure 4.59. Age-related Changes in the Intensity of PAS Staining of the Corpus Segment in AGCR.

Bars with different alphabets are significantly different ($p<0.05$)

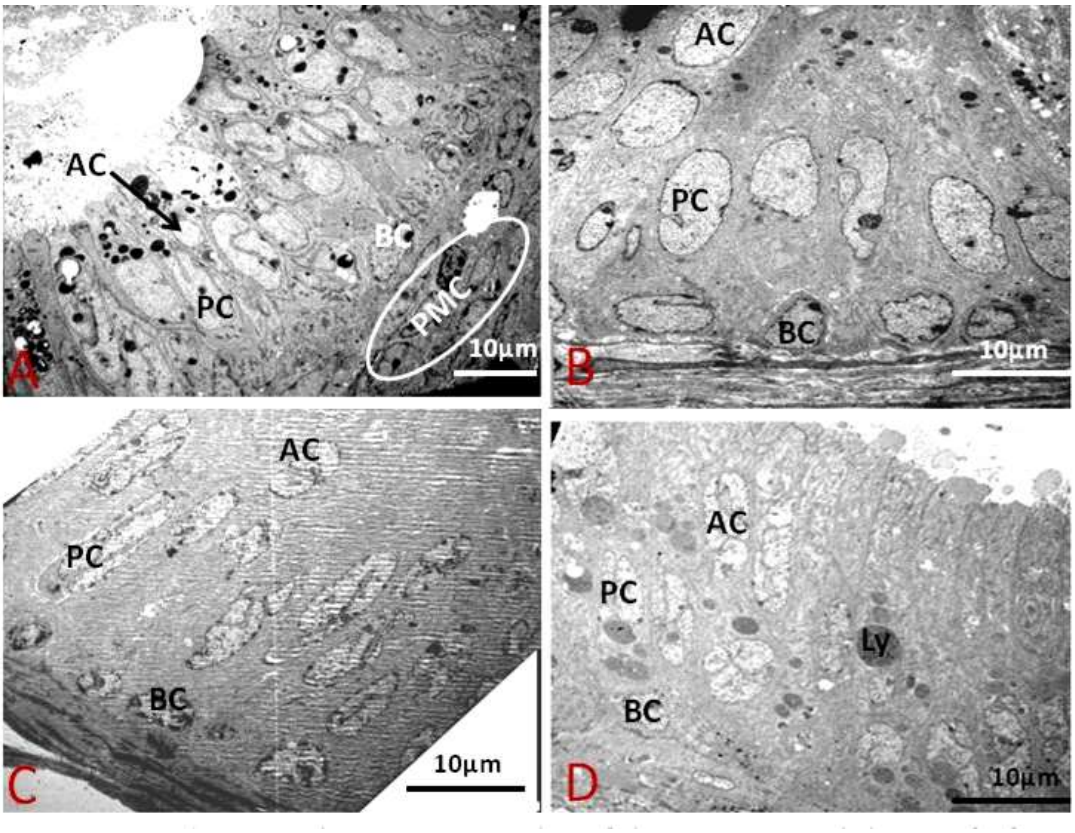

Figure 4.60. Transmission Electron Micrographs of the Corpus Epididymis of African Greater Cane Rat. A. Prepubertal: B. Pubertal: C. Adult: D. Aged. Note the irregularly shaped nucleus bearing some indentations in the principal cell (PC). BC-Basal cell, AC- Apical cell, PMC-Peritubular muscle coat, Ly -Lysosome. Scale bar: 10µm**.**

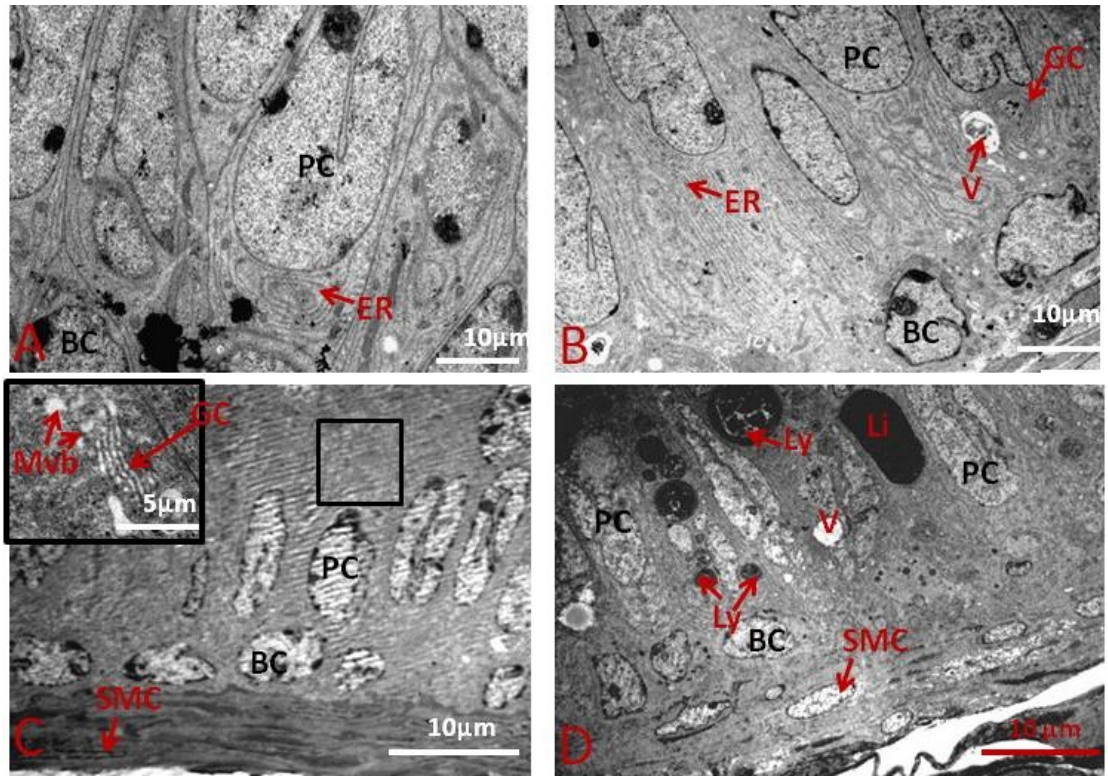

Figure 4.61. Transmission Electron Micrographs of the Basal Aspect of the Corpus Epididymis of African Greater Cane Rat. A. Prepubertal: B. Pubertal: C. Adult: D. Aged. Note numerous lysosomal granules (Ly) in the aged corpus epididymis. The irregular shaped nuclei bearing some indentations that appear to increase with advancing age. BC-Basal cell, PC- Principal cell, SMC- Smooth muscle cell, Li-Lipofuschin granules, GC-Golgi complex, Mvb –Multi-vesicular bodies, ER-Endoplasmic reticulum, V-Vacoules.

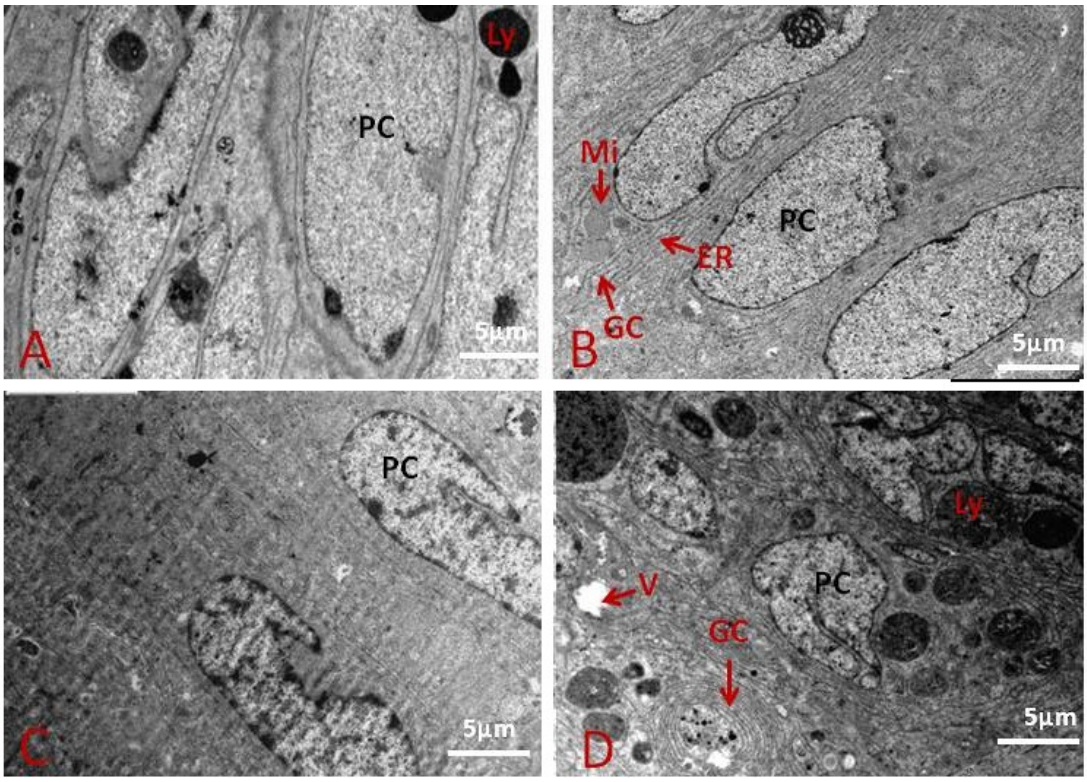

Figure 4.62. Transmission Electron Micrographs of Perinuclear Aspect of the Corpus Epididymis Principal Cell of African Greater Cane Rat. A. Prepubertal: B. Pubertal: C. Adult: D. Aged. Note the irregularly shaped nuclei and their indentations that appear to increase with age as well as the prominent increase in lysosomal granules in the principal cell cytoplasm of D. PC- Principal cell, Ly- Lysosome, GC-Golgi complex, Mvb –Multi-vesicular bodies, ER-Endoplasmic reticulum, V-Vacoules. Scale bar: **5µm**

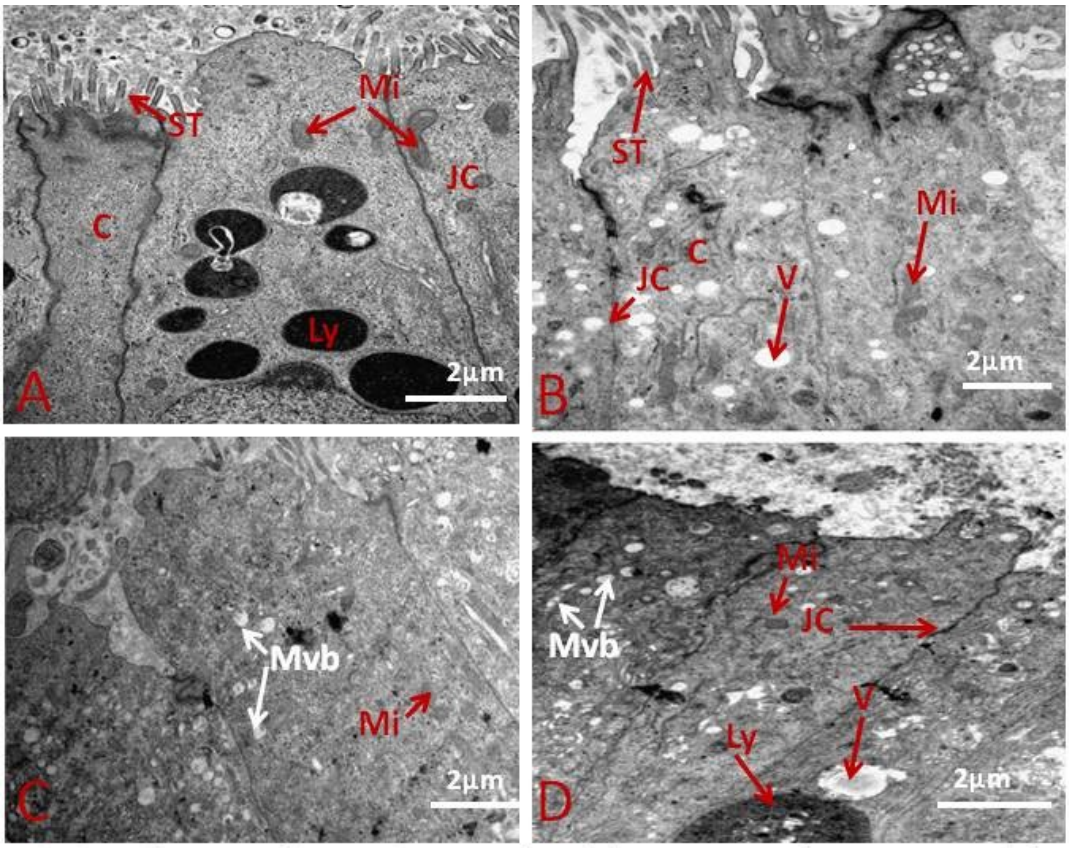

Figure 4.63. Transmission Electron Micrographs of the Supranuclear Aspect of the Corpus Epididymis Principal Cell in the African Greater Cane Rat. A. Prepubertal: B. Pubertal: C. Adult: D. Aged. Note the conspicuous apical vacoulations (V) especially in the pubertal rats. Also observe the numerous lysosomal granules in the apical region of A. Ly- Lysosomal granules, JC-Junctional complex, Mvb –Multi-vesicular bodies, V-Vacoules, ST-Stereocilia, C-Ciliated cell.

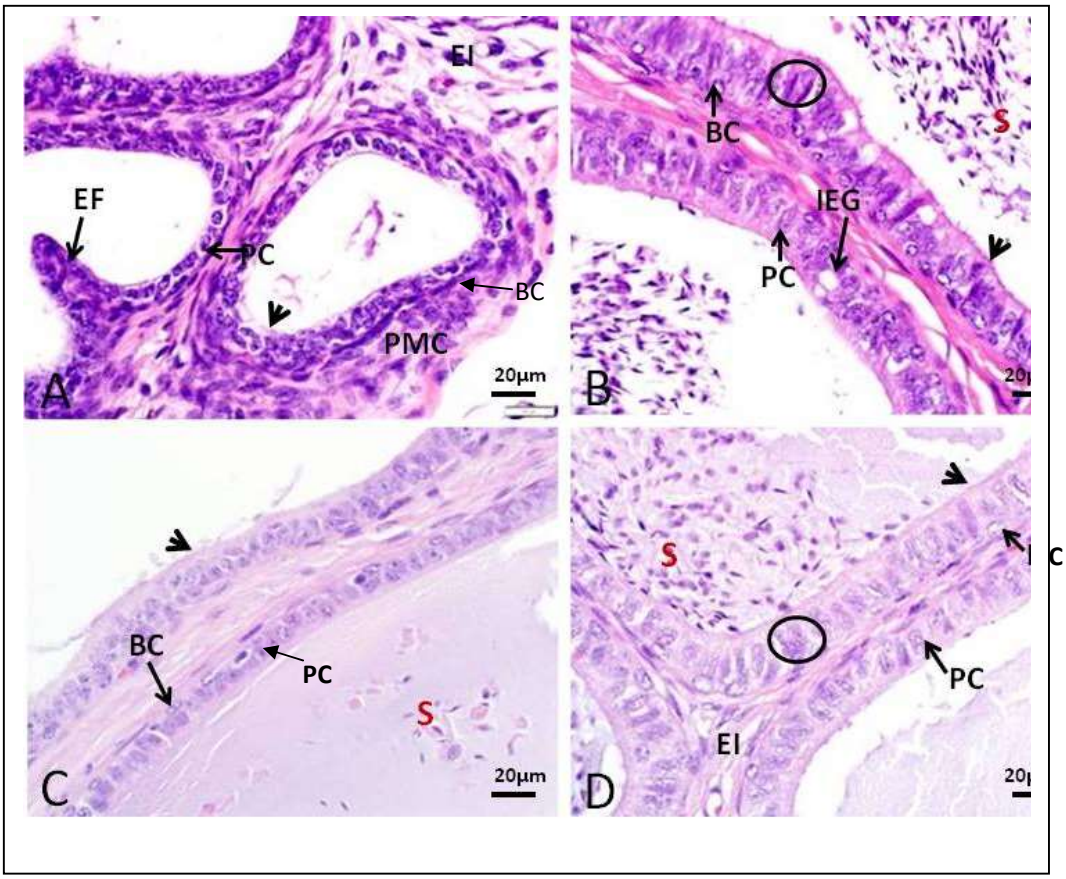

Figure 4.64. Photomicrographs of the Cauda Segment of Epididymis in Different Age Groups of AGCR. A. **Prepubertal**: displays markedly thickened peritubular muscular coat (PMC), reduced stereocilia height (arrow head), almost roundish ductal luminal (L) shape and copius epithelial fold (EF). B. **Pubertal,** C. **Adult** and D. **Aged**: bear numerous intraepithelial glands, large roughly round ductal lumen shape containing spermatozoa (S), ductal lining bears a markedly reduced pseudostratified columnar epithelium (oval) with prominent stereocilia (arrow head) as well as the dominating population of basal cells (BC) and Principal cells (PC). EI- Epididymal interstitium, bv- blood vessel. Stain: H&E; Scale bar: 20µm.

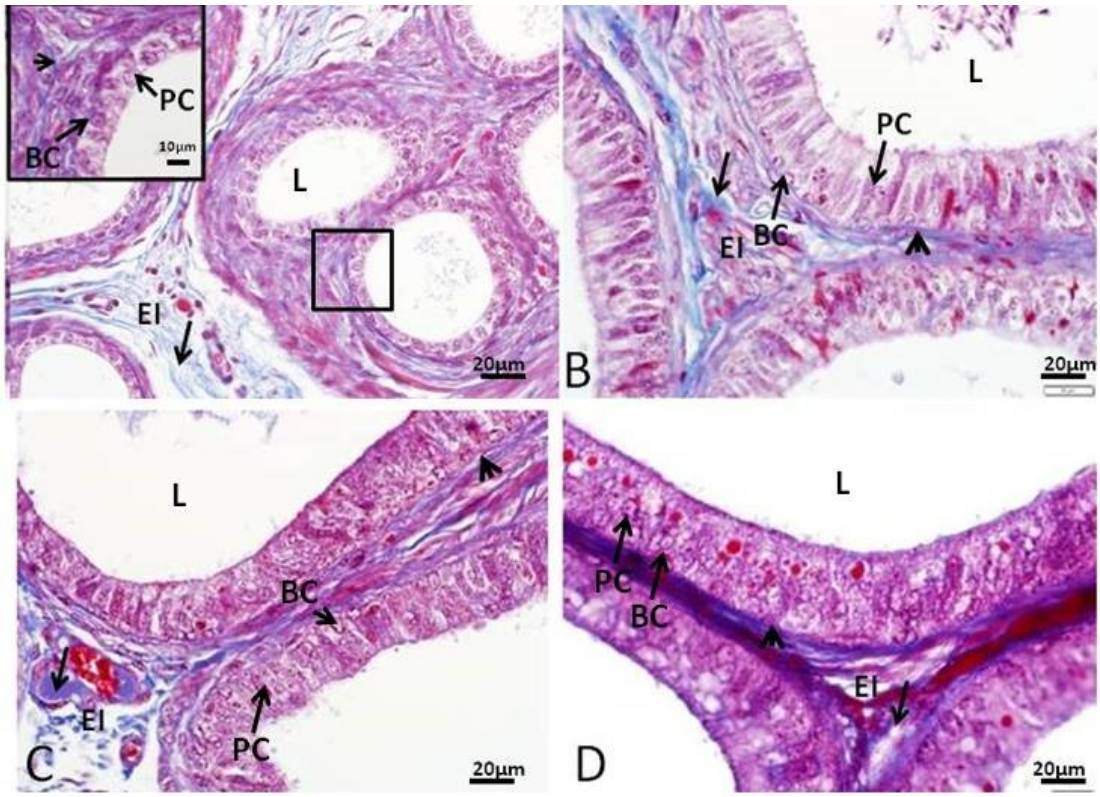

Figure 4.65. Masson's Trichrome Staining of the Caudal Segment of Epididymis in the Different Age Groups of AGCR. A. Prepubertal: B. Pubertal: C. Adult: D. Aged. BC- Basal cells, PC- Principal cells, AC- Apical cells EI- Epididymal interstitium, SC- Stereocilia, L-Lumen. Note the blue staining collagen fibres (arrow) in the epididymal ductal interstices (EI) together with pink-staining smooth muscles (arrow heads) surrounding the epididymal ducts in inset A and in other groups.Scale bar: Main 20 µm; inset 10µm

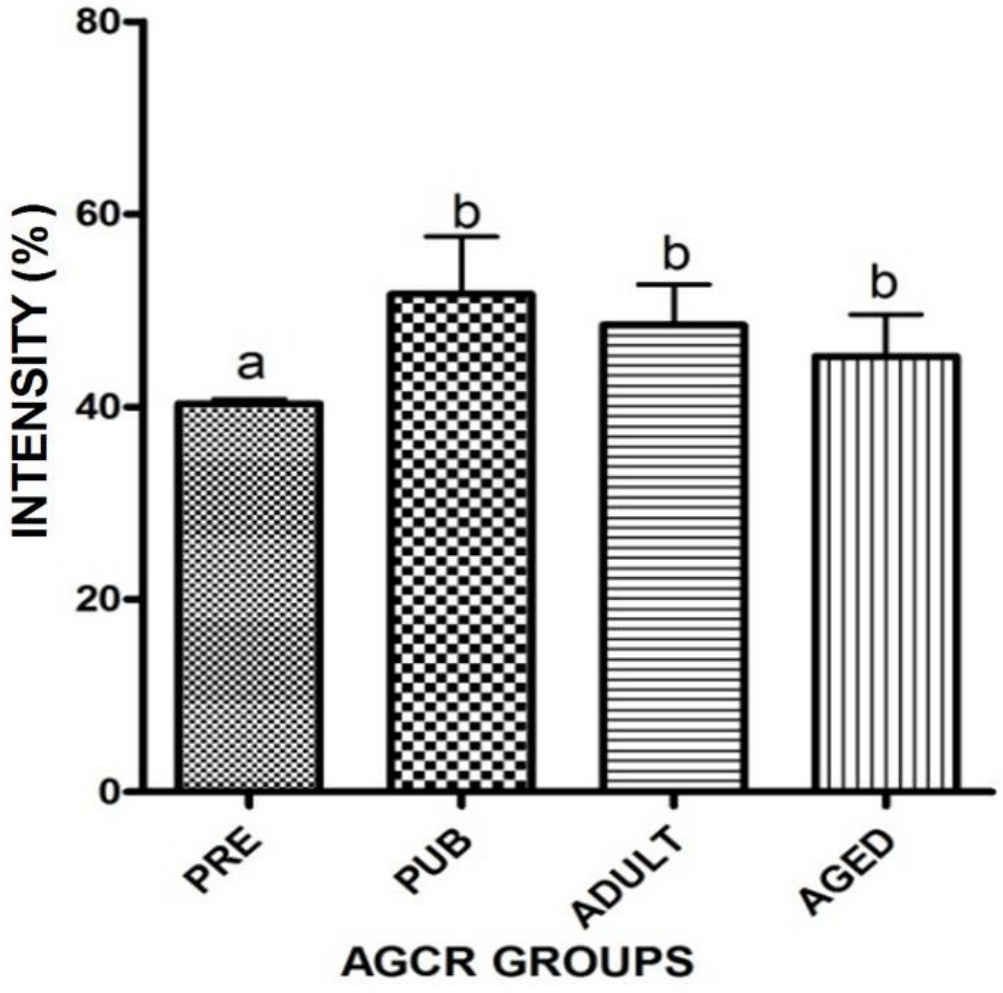

Figure 4.66. Age-related Changes in the Intensity of Masson'sTrichrome Staining in the Cauda Segment of the AGCR.

Bars with different alphabets are significantly different ($p<0.05$)

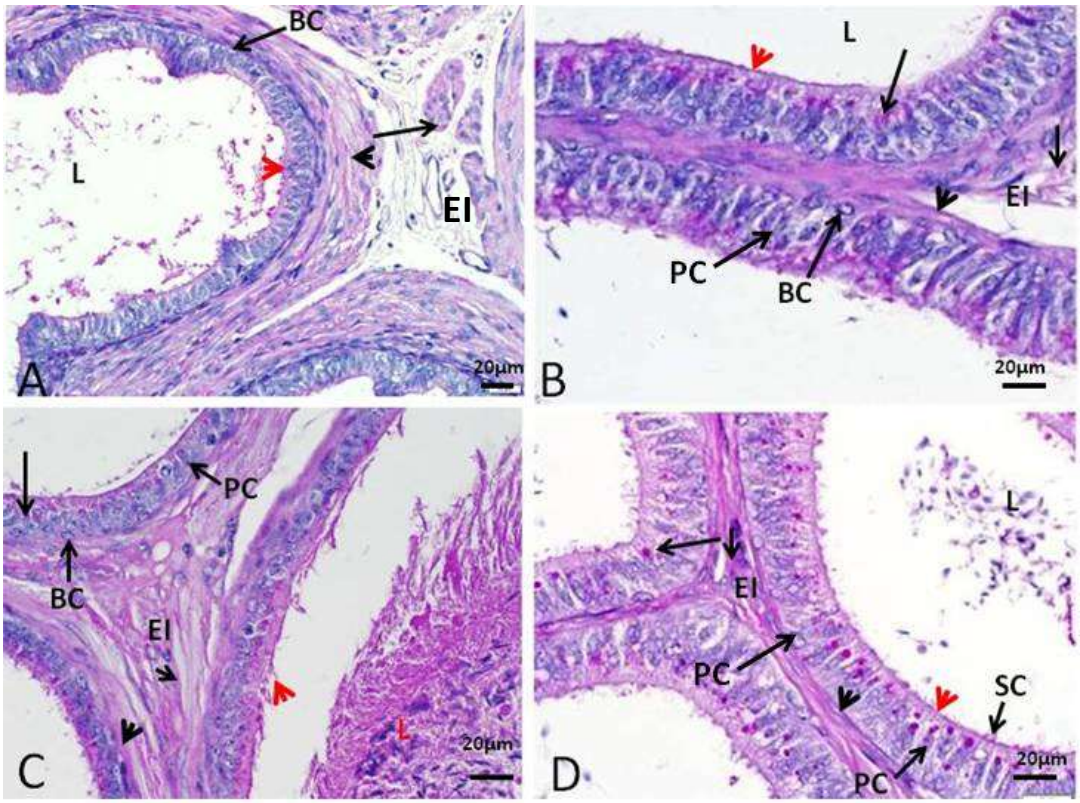

Figure 4.67. PAS Staining of the Caudal Segment of Epididymis in the Different Age-Groups of the AGCR. A. Prepubertal: B. Pubertal: C. Adult: D. Aged. BC- Basal cells, PC- Principal cells, AC- Apical cells, EI- Epididymal interstitium, SC- Stereocilia, L-Lumen. Note the PAS positive areas in the interstitium (short arrow), lamina propria (arrow head), epithelial supranuclear region (long arrow) and lumina (L) spermatozoa. Scale bar: 20µm

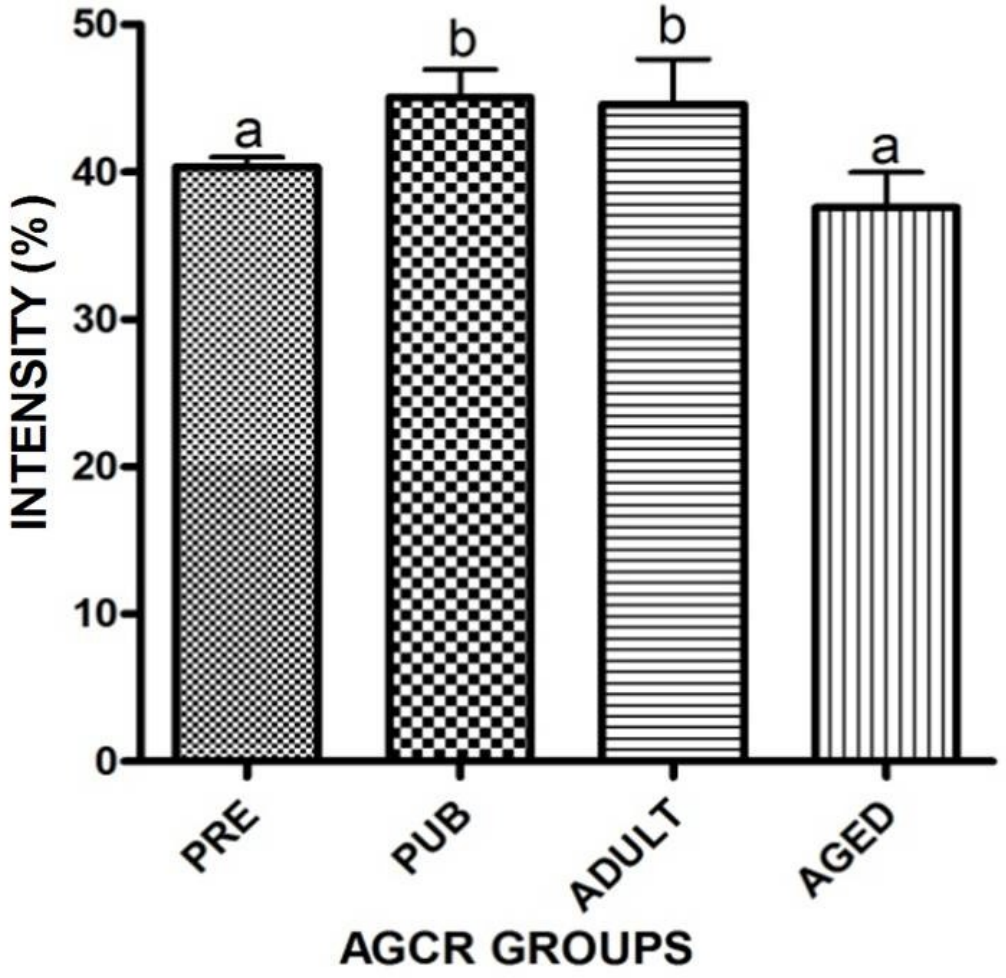

Figure 4.68. Age-related Changes in the Intensity of PAS Staining in the Cauda Epididymal Segment of AGCR.

Bars with different alphabets are significantly different ($p<0.05$)

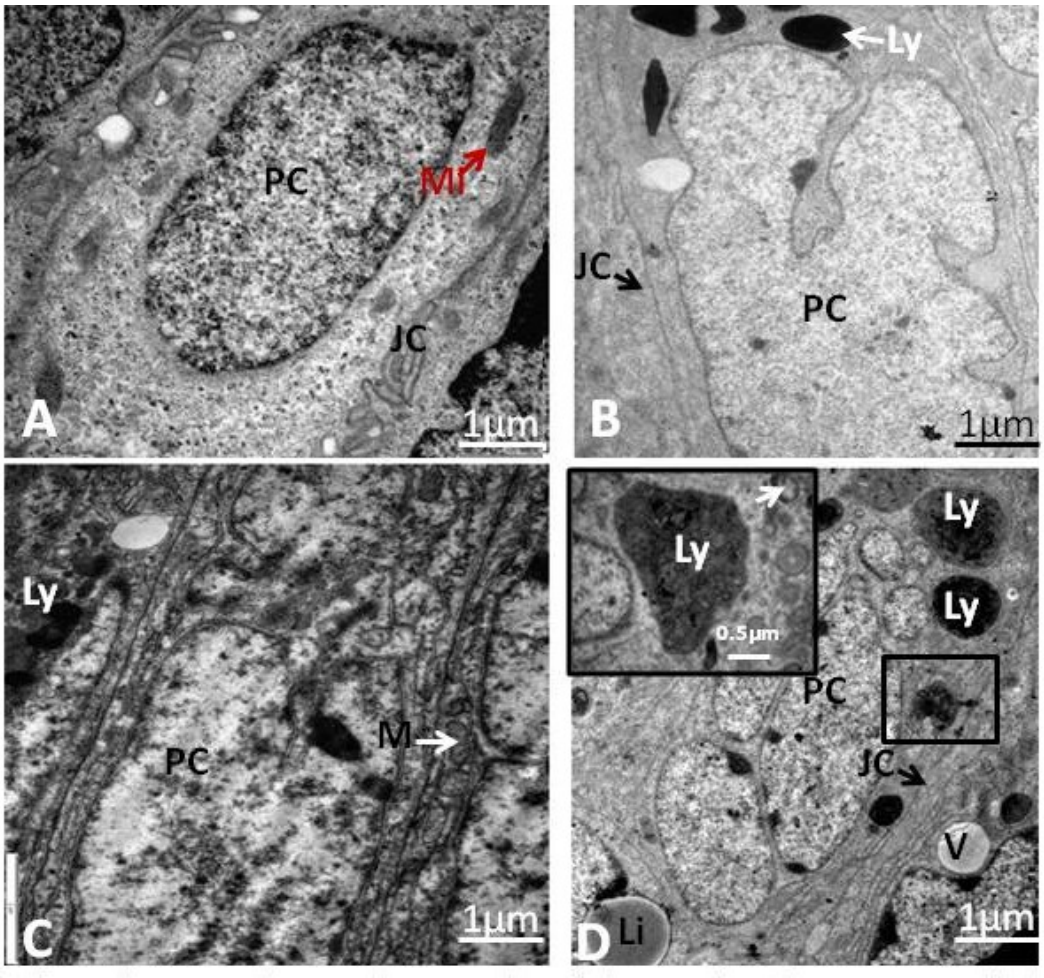

Figure 4.69. Transmission Electron Micrographs of the Perinuclear Aspect of the Cauda Epididymis Principal Cells in the African Greater Cane Rat. A. Prepubertal: B. Pubertal: C. Adult: D. Aged. Note the conspicuous interdigitation of junctional complex (JC) between principal cells (PC) in A, numerous lysosomal granules and degenerating mitochondria (inset arrow) especially in aged AGCR and prominent nuclear lobulations of PC in B, C and D. Ly- Lysosome, Li- Lipid, V- Vacoules, JC- Junctional complex, Mi- Mitochondria. Scale bar; Main (1µm) and Inset (0.5 µm).

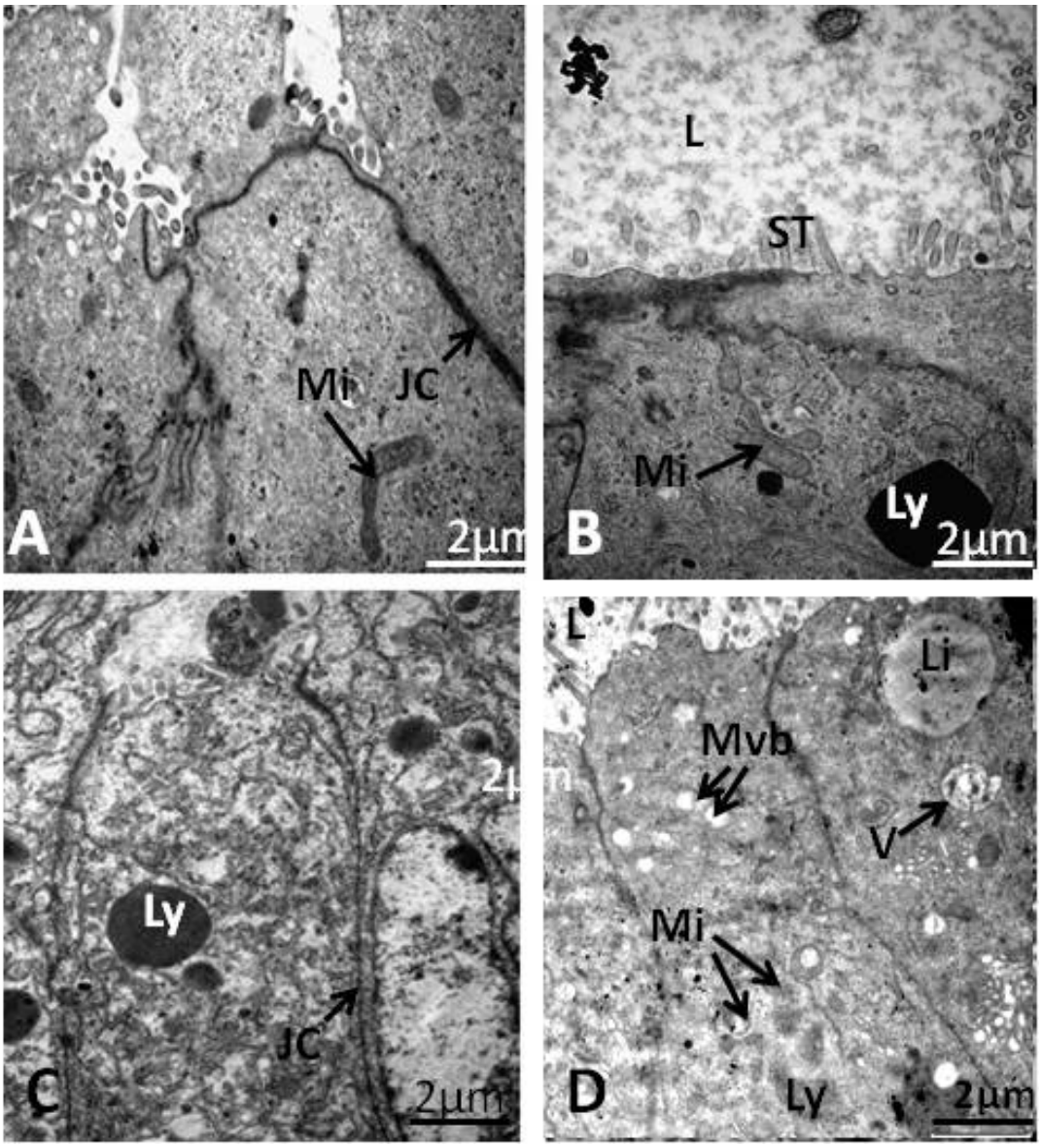

Figure 4.70. Transmission Electron Micrographs of the Supranuclear Aspect of the Cauda Epididymal Principal Cell of Cane Rat. Note the degenerating mitochondria(Mi) within the apical PC of aged AGCR. Ly- Lysosomal granules, JC-Junctional complex, Mvb –Multi-vesicular bodies, V-Vacoules, ST-Stereocilia, L-Lumen.

4.2.8 Age- related Changes in the Histomorphometric Parameters of the Epididymis of the African Greater Cane Rat

4.2.8.1 Ductal Diameter (DD)

The DD was smallest in all the segments of epididymis in the prepubertal AGCR relative to others. The various segments of the epididymal duct show a significant increase in DD from prepubertal to aged AGCR. The comparison along the rest of the epididymal duct of each AGCR group showed a significant ($p<0.05$) cranio-caudal increase in the DD with the highest in the caudal segments (Table 4.2A).

4.2.8.2 Ductal Luminal Diameter (DLD)

The ductal luminal diameter was significantly low ($p<0.05$) in the prepubertal relative to other AGCR groups. Also, the DLD of the entire epididymal segment was significantly higher ($p<0.05$) in the aged AGCR compared to others. The DLD of the epididymal duct in all age groups shows a significant increase ($p<0.05$) with advancing age. On the difference along the epididymal duct within each group, a significant cranio-caudal increase ($p<0.05$) in luminal diameter more particularly in the caudal segment of all groups was observed (Table 4.2B).

4.2.8.3 Ductal Epithelial Height (DEH)

The ductal epithelial height of the prepubertal AGCR was significantly low($p<0.05$) when compared to other groups. The DEH in nearly all the epididymal segments(initial, middle and distal segments) were not significantly different ($p>0.05$) from pubertal to aged, though a markedly reduced DEH was noticed in the caudal segment of the aged AGCR. On comparison along epididymal duct, a progressive significant cranio-caudal decrease in DEH was seen in this study (Table 4.2C).

4.2.8.4 Ductal Stereocilia Height (DSH)

The ductal stereocilia height of the prepubertal epididymis was significantly low ($p<0.05$) relative to other groups. The DSH values from the pubertal to aged AGCR were not significantly different ($p>0.05$), though; an insignificant decrease DSH was exclusively found in the epididymal segments of aged AGCR. With respect to variation along the segments of epididymal duct of each AGCR group, a cranio-caudal decrease in the trend of DSH values was noted. Also, the initial segments of each group bear significantly higher ($p<0.05$) stereocilia and a simultaneous

significantly lower ($p<0.05$) DSH values in the caudal segment of the epididymis (Table 4.2D).

4.2.8.5 Periductal Muscle Coat Thickness (PMCT)

The periductal muscle coat thickness was significantly increased ($p<0.05$) in the adult AGCR compared to other groups. The PMCT appear to increase significantly ($p<0.05$) with age. Regarding the differences along the epididymal duct, a fairly progressive increase PMCT was noticed with a consistently significant higher ($p<0.05$) values obtained in the caudal epididymal segment of all AGCR groups (Table 4.2E).

Table 4.2A. Age-related Changes in the Epididymal Ductal Diameter of the African Greater Cane Rat

Parameter	AGCR group	Pro. Ini. Seg	Middle Ini. Seg	Distal Ini. Seg	Caput	Corpus
Ductal	**Prepub.**	166.9 ± 8.89^{a}	151.2 ± 6.98^{a}	168.4 ± 15.51^{a}	$106.5 \pm 5.47^{a\#\#}$	167.6 ± 1
Diameter (µm)	**Pub.**	$329.5 \pm 16.42^{b\#\#}$	250.5 ± 6.65^{b}	257.5 ± 8.58^{b}	282.1 ± 11.06^{b}	$252.3 \pm 7.$
	Adult	$309.0 \pm 18.50^{b\#\#}$	274.8 ± 7.64^{b}	289.7 ± 16.86^{b}	270.5 ± 13.70^{b}	272.2 ± 1
	Age	329.0 ± 8.78^{b}	295.8 ± 9.87^{b}	305.7 ± 12.13^{b}	370.8 ± 10.49^{b}	308.8 ± 1

- Values with the different alphabet superscripts (a,b,c,d) within the column are significantly different

- Values with different number of harsh tag (#) in the same row are significantly different

Pro. Ini. Seg - Proximal initial segment, Prepub - Prepubertal, Pub - Pubertal

Table 4.2B. Age-related Changes in the Epididymal Luminal Diameter of the African Greater Cane Rat.

Parameter	AGCR group	Pro. Ini. Seg	Middle Ini. Seg	Distal Ini. Seg	Caput	Corpus
Luminal Diameter (µm)	**Prepub.**	$75.27 \pm 6.73^{a\#\#\#}$	60.14 ± 3.99^{a}	53.32 ± 3.08^{a}	49.95 ± 4.39^{a}	$112.3 \pm 8.$
	Pub.	$133.5 \pm 10.57^{b\#\#\#}$	118.6 ± 5.38^{b}	110.4 ± 6.35^{b}	$171.8 \pm 9.36^{b\#\#}$	$158.9 \pm 9.$
	Adult	$187.8 \pm 12.77^{c\#\#}$	117.4 ± 7.15^{b}	107.5 ± 8.25^{b}	$161.9 \pm 10.64^{b\#\#}$	$183.2 \pm 7.$
	Age	213.7 ± 9.53^{c}	190.6 ± 13.89^{c}	190.2 ± 8.82^{c}	219.9 ± 16.20^{c}	208.8 ± 1

- Values with the different alphabet superscripts (a,b,c,d) within the column are significantly different
- Values with different number of harsh tag (#) in the same row are significantly different

Pro. Ini. Seg - Proximal initial segment, Prepub - Prepubertal, Pub - Pubertal

Table 4.2C. Age-related Changes in the Epididymal Ductal Epithelial Height of the African Greater Cane Rat.

Parameter	AGCR group	Pro. Ini. Seg	Middle Ini. Seg	Distal Ini. Seg	Caput	Corpus
Epithelial Height (µm)	**Prepub.**	$41.74 \pm 1.90^{a\#}$	$47.32 \pm 2.21^{a\#}$	$47.80 \pm 0.95^{a\#}$	$33.33 \pm 1.65^{a\#\#}$	39.23 ± 2.4
	Pub.	$65.43 \pm 2.41^{b\#\#}$	$76.54 \pm 2.35^{b\#}$	$73.41 \pm 4.11^{b\#}$	$61.58 \pm 2.37^{b\#\#}$	55.95 ± 2.5
	Adult	$85.75 \pm 3.39^{c\#}$	$86.43 \pm 4.37^{b\#}$	$77.86 \pm 2.55^{b\#}$	$66.61 \pm 3.09^{b\#\#}$	$51.10 \pm 1.$
	Age	$90.77 \pm 4.06^{c\#}$	$64.50 \pm 1.75^{c\#\#}$	$72.47 \pm 5.01^{b\#\#}$	$70.24 \pm 2.93^{b\#\#}$	$50.61 \pm 2.$

- Values with the different alphabet superscripts (a,b,c,d) within the column are significantly different

- Values with different number of harsh tag (#) in the same row are significantly different

Pro. Ini. Seg - Proximal initial segment, Prepub - Prepubertal, Pub - Pubertal

Table 4.2D. Age-related Changes in the Epididymal Stereocilia Height of the African Greater Cane Rat.

Parameter	AGCR group	Pro. Ini. Seg	Middle Ini. Seg	Distal Ini. Seg	Caput	Corpus
Stereocilia Height (µm)	**Prepub.**	$3.96 \pm 0.24^{a\#}$	2.76 ± 0.09^{a}	2.59 ± 0.12^{a}	2.44 ± 0.10^{a}	2.53 ± 0.2
	Pub.	$8.51 \pm 0.45^{c\#\#}$	$10.51 \pm 0.47^{c\#}$	$8.71 \pm 0.24^{b\#\#}$	$7.62 \pm 0.30^{b\#\#}$	7.94 ± 0.3
	Adult	$8.73 \pm 0.49^{c\#}$	$7.74 \pm 0.19^{b\#\#}$	$7.62 \pm 0.24^{b\#\#}$	$6.47 \pm 0.14^{b\#\#}$	7.24 ± 0.1
	Aged	$6.95 \pm 0.25^{b\#}$	$7.45 \pm 0.38^{b\#}$	$6.99 \pm 0.36^{b\#}$	$6.21 \pm 0.29^{b\#}$	5.79 ± 0.3

- Values with the different alphabet superscripts (a,b,c,d) within the column are significantly different

- Values with different number of harsh tag (#) in the same row are significantly different

Pro. Ini. Seg - Proximal initial segment, Prepub - Prepubertal, Pub - Pubertal

Table 4.2E.Age-related Changes in the Epididymal Perimuscular Coat Thickness of the African Greater Cane Rat.

Parameter	AGCR group	Pro. Ini. Seg	Middle Ini. Seg	Distal Ini. Seg	Caput	Corpus
Perimuscular Coat Thickness (µm)	**Prepub.**	$13.25 \pm 0.90^{a\#\#\#\#}$	$16.17 \pm 1.21^{b\#\#\#}$	$10.54 \pm 0.65^{a\#\#\#\#}$	$23.3 \pm 2.40^{d\#\#}$	$21.12 \pm 1.$
	Pub.	14.74 ± 0.80^{a}	17.93 ± 1.01^{b}	13.2 ± 0.75^{b}	11.36 ± 0.91^{b}	$16.87 \pm 1.$
	Adult	20.00 ± 0.90^{c}	21.03 ± 1.90^{c}	17.1 ± 1.40^{c}	14.28 ± 1.30^{c}	15.9 ± 1.4
	Aged	$17.22 \pm 1.70^{b\#\#}$	$12.4 \pm 0.91^{a\#\#}$	$16.1 \pm 1.90^{c\#\#}$	$8.97 \pm 0.44^{a\#\#\#}$	$14.17 \pm 0.$

- Values with the different alphabet superscripts (a,b,c,d) within the column are significantly different

- Values with different number of harsh tag (#) in the same row are significantly different

Pro. Ini. Seg - Proximal initial segment, Prepub - Prepubertal, Pub - Pubertal

4.3 EXPERIMENT THREE

4.3.1 Age-related Changes in the Sperm Parameters of the Testis and Epididymis of the African Greater Cane Rat

4.3.2 Spermatozoa Morphological Characteristics

The spermatozoa heads of the African greater cane rat were typically flat and ovoid in shape with indistinct neck (Figure 4.71B-D). The acrosomal head of sperms in all AGCR bear no evidence of hook (Figure 4.71B-D). There was no age-related difference in the division of the spermatozoa tail of AGCR which was characteristically made up of three distinct segments, namely; the midpiece, principal piece and endpiece. The base of the head continued with the midpiece, the first segment of the tail (Figure 4.71B-D insets).

In addition, the percentage of the different types of abnormal sperm cells in both testis and epididymis were not significantly different ($p>0.05$) in pubertal to aged AGCR (Table 4.5). Across all age groups, curved and bent midpieces as well as curved and bent tail defects appeared to be present in greater amount relative to other types of abnormalities. It was also evident that roughly 85% of the spermatozoa of the pubertal, adult and aged AGCR displayed the normal morphology outlined in the inserts of Figure 4.71B-D.

4.3.3 Sperm Morphometrics

There was no significant difference ($p>0.05$) in the morphometric parameters in all the different age groups of AGCR (Table 4.3), although, the parameters tended to increase with advancement in age. The mean lengths of the spermatozoa in the different age groups of AGCR were 55.92 ± 1.39 µm, 57.06 ± 0.95 µm, and 58.41 ± 0.67 µm respectively for pubertal, adult and aged. The tail lengths were 45.22 ± 1.14 µm, 46.16 ± 0.84 µm and 48.47 ± 1.08 µm respectively for pubertal, adult and aged. The mean sperm head lengths were 9.52 ± 0.44 µm,10.26 ± 0.45 µm and 10.46 ± 0.50 µm respectively for pubertal, adult and aged, while; the mean sperm widths or diameters include 5.04 ± 0.23 µm, 5.18 ± 0.18 µm and 5.63 ± 0.19 µm in pubertal, adult and aged accordingly. Both the spermatozoa mean length and width linear measurements were comparatively shorter when compared to their tail counterpart and also increased insignificantly with age.

4.3.4 Sperm Motility

Testicular spermatozoa were observed to be immotile in all the age group of AGCR. There was consistent significant increase ($p<0.05$) in the epididymal sperm motility of the pubertal and adult AGCR relative to the aged (Table 4.4). The sperm motility profile displayed in the epididymis appeared to increase with age increment. Motility values in the caudal epididymal segment of all age groups were markedly higher relative to other segments and were more remarkably elevated in the cauda epididymis of adult cane rats.

4.3.5 Testicular and Epididymal Sperm Count

Similarly, sperm count as shown in Table 4.4 followed similar pattern described for motility. Though, testicular sperm count (TSC) was significantly reduced ($p<0.05$) in the aged AGCR relative to other groups, the TSC values were not significantly different ($p>0.05$) in adult and pubertal AGCR. In the caput and corpus epididymal segments, sperm count values were not significantly different ($p>0.05$) in pubertal to aged AGCR, while in the caudal segment, spermatozoa counts of aged cane rats were significantly lowered ($p<0.05$) relative to the spermatozoa counts in pubertal and adult rats.

4.3.6 Sperm Livability (Live-Dead) Ratio

With respect to sperm livability, there was no significant difference ($p>0.05$) among the age groups (Table 4.4).

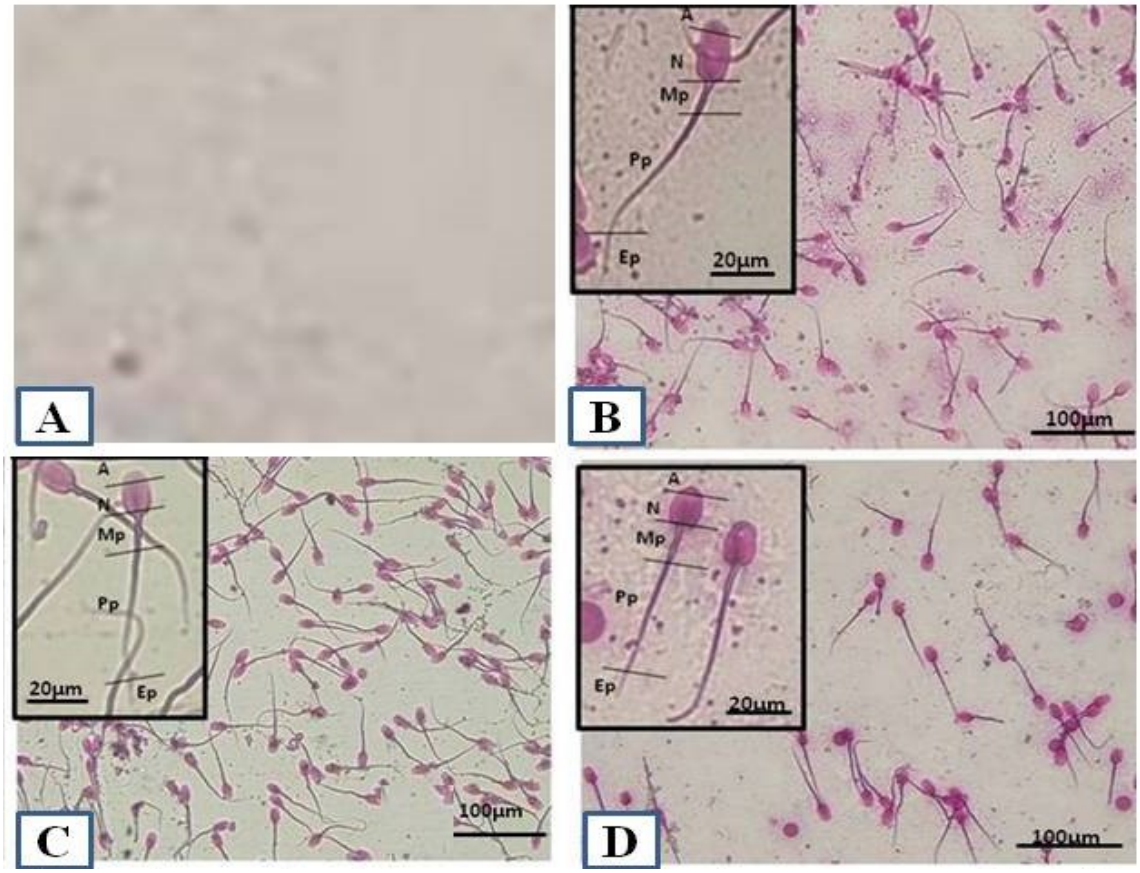

Figure 4.71. Photomicrographs of the Caudal Epididymal Spermatozoa of the African Greater Cane Rat. A. Pre-pubertal B. Pubertal C. Adult D. Aged. Note the absence of spermatozoa in A as well as absence of hook in the spermatozoa head of B-D. A-Acrosome, N- Nucleus, Mp-Mid piece, Pp- Principal piece, Ep-End piece. Stain: Nigrosin-eosin.

Table 4.3. Age-related Changes in Sperm Morphometrics of The African Greater Cane Rat.

	SPERM MORPHOMETRICS (µm)				
	SHL	**SHD**	**MPL**	**STL**	**SWL**
Pre-pubertal	-	-	-	-	-
Pubertal	9.52 ± 0.40	5.04 ± 0.23	12.82 ± 0.33	45.22 ± 1.14	55.92 ± 1.39
Adult	10.26 ±0.45	5.18 ± 0.18	13.21 ± 0.27	46.16 ± 0.84	57.06 ± 0.95
Aged	10.46 ± 0.50	5.63 ± 0.19	13.86 ± 0.35	48.47 ± 1.08	58.41 ± 0.67
P-values	0.5020	0.0580	0.6180	0.2530	0.4070

SHL- Sperm head length, SHD- Sperm head diameter, MPL- Mid-piece length, STL-Sperm tail length, SWL-Sperm whole length

Table 4.4. Age-related Changes in the Testicular and Epididymal Sperm Parameters of the African Greater Cane Rat.

SPERM MOTILITY (%)				
ORGAN	**PRE-PUBERTAL**	**PUBERTAL**	**ADULT**	**AGED**
TESTES	-	Nm	Nm	Nm
CAPUT	-	55.00 ± 5.00[a]	65.00 ± 0.89[a]	37.50 ± 2.50[b]
CORPUS	-	60.00 ± 7.07[a]	65.00 ± 2.89[a]	37.50 ± 4.79[b]
CAUDA	-	62.50 ± 4.79[a]	80.00 ± 4.08[b]	55.00 ± 5.00[a]
SPERM COUNT (X10^6 ml)				
TESTES	-	37.25 ± 2.49[a]	37.75 ± 2.02[a]	28.50 ± 1.04[b]
CAPUT	-	43.25 ± 0.85	44.25 ± 1.11	42.50 ± 1.04
CORPUS	-	48.00 ± 1.08	50.00 ± 0.71	46.50 ± 0.96
CAUDA	-	101.5 ± 7.96[a]	135.3 ± 6.42[b]	91.25 ± 2.56[c]
LIVE DEAD RATIO				
TESTES	-	92.75 ± 1.03	94.25 ± 0.85	96.75 ± 0.75
CAPUT	-	97.25 ± 0.75	98.00 ± 0.25	96.25 ± 063
CORPUS	-	97.25 ± 0.75	98.00 ± 0.00	96.00 ± 0.71
CAUDA	-	97.50 ± 0.50	97.25 ± 0.75	97.30 ± 0.7500

Values with different superscript are significantly different ($p<0.05$). Nm- Not motile

Table 4.5. Age-related changes in the morphological characteristics of the spermatozoa African greater cane rat

		PERCENTAGE ABNORMAL CELL								
		HEAD		MID-PIECE		TAIL				
ORG	**GRP**	**% TH**	**%HT**	**%CMP**	**%BMP**	**%CT**	**%RT**	**%BT**	**% LT**	**% TAC**
	Pre	-	-	-	-	-	-	-	-	-
TES	Pub	1.35 ± 0.11	1.03± 0.09	3.21 ± 0.16	2.55 ± 0.14	2.54 ± 0.06	0.43 ± 0.13	2.71 ± 0.24	0.41±0.13	14.42± 0.
	Adult	1.43 ± 0.06	1.12± 0.12	2.74 ± 0.10	2.49 ± 0.14	2.68 ± 0.06	0.50 ± 0.10	2.68 ± 0.16	0.38± 0.07	14.02 ±0.
	Aged	1.48 ± 0.17	1.07± 0.16	2.97 ± 0.24	2.84 ± 0.23	2.75 ± 0.15	0.67 ± 0.08	3.00 ± 0.14	0.33±0.05	15.11±0.9
p value		0.7673	0.8877	0.2318	0.3765	0.3753	0.3054	0.3054	0.8368	0.60
	Pre	-	-	-	-	-	-	-	-	-
CAP	Pub	1.48± 0.10	1.30± 0.08	3.06 ± 0.20	2.62 ± 0.13	2.38 ± 0.47	0.79 ± 0.03	2.79 ± 0.03	0.70 ± 0.08	15.86±0.3
	Adult	1.35± 0.12	1.23 ± 0.19	2.85 ± 0.24	2.46 ± 0.15	2.58 ± 0.19	0.53 ± 0.12	2.45 ± 0.16	0.57± 0.06	14.03± 1.
	Aged	1.41±0.06	1.08 ± 0.06	2.57 ± 0.06	2.30 ± 0.04	2.39 ± 0.12	0.68 ± 0.06	2.86 ± 0.06	1.40 ± 0.87	13.60± 0.
p value		0.6627	0.4935	0.2372	0.2041	0.5786	0.1286	0.347	0.4894	0.07
	Pre	-	-	-	-	-	-	-	-	-
COR	Pub	1.15± 0.08	1.49 ± 0.10	2.45 ± 0.04	2.56 ± 0.11	3.21 ± 0.19	0.53 ± 0.02	2.65 ± 0.08	0.45 ± 0.07	14.21 ±0.
	Adult	1.12± 0.13	1.09 ± 0.18	2.43 ± 0.08	2.49 ± 0.05	2.75 ± 0.21	0.64 ± 0.07	2.75 ± 0.14	0.51 ± 0.14	13.69 ±0.
	Aged	1.47± 0.04	1.15 ± 0.09	2.73 ± 0.10	2.45 ± 0.06	2.65 ± 0.13	0.68 ± 0.06	2.89 ± 0.29	0.53 ± 0.12	14.55± 0
p value		0.1101	0.1197	0.0682	0.5857	0.1135	0.2055	0.6849	0.8840	0.28
	Pre	-	-	-	-	-	-	-	-	-
CAU	Pub	1.25±0.10	1.05 ± 0.12	2.48 ± 0.17	2.88 ± 0.15	2.29 ± 0.25	0.64 ± 0.06	2.46 ± 0.26	0.58 ± 0.11	13.90 ±0.
	Adult	1.32±0.06	1.14 ± 0.18	2.52 ± 0.07	2.39 ± 0.18	2.52 ± 0.14	0.82 ± 0.06	2.39 ± 0.11	0.32 ± 0.07	13.41 ± 0
	Aged	1.09±0.11	1.23 ± 0.07	2.16 ± 0.16	2.62 ± 0.13	2.37 ± 0.12	0.81 ± 0.11	2.68 ± 0.35	0.58 ± 0.16	13.53 ± 0
p value		0.0733	0.6878	0.1913	0.1406	0.6695	0.2732	0.7212	0.2564	0.90

Values with different superscript are significantly different

TH – Tailless head, HT- Headless tail, RT- Rudimentary tail, BT- Bent tail, CT- Curved tail, CMP- Curved midpiece, BMP- Bent midpiece, LT- Looped tail, TAC- Total abnormal cell, TNC- Total normal cell, TES- Testis, CAP- Caput, COR- Corpus, CAU- Cauda, Pre- Prepubertal, Pub- Pubertal

4.4 EXPERIMENT FOUR

4.4.1 Age-related Changes in the Immunohistochemical Expressions of Structural Protein (Vimentin), Nerves (Neurofilament) and Glial Cells (Glial fibrillary acid protein) in the Testis and Epididymis as well as Histochemical Demonstrations of Nerves and Glial Cells Using Golgi-silver Technique

4.4.1.1 Immunohistochemical Expressions of Structural Proteins (Vimentin) in the Testis and Epididymis

Vimentin-positive areas in the testes of all AGCR groups as shown in Fig. 4.72 include the Sertoli cell especially the perinuclear region with intense staining situated along the base with strands of vimentin projecting to the tips of elongated spermatids as well as the testicular interstitium. However, in the various segments of the epididymal duct (Figs. 4.74-4.79), vimentin positive areas consisted of peritubular coat and interstitium (stroma and perivascular components). With respect to testicular vimentin staining intensity across the different groups of AGCR, significantly higher ($p<0.05$) intensity was displayed by the adult group relative to others and the intensity appeared to increase with age (Fig. 4.73). Conversely, vimentin expression intensities along the epididymal duct (initial segments, caput, corpus and cauda segments) in the different age-groups of the AGCR decreased with age with consistently strong intensity observed in the prepubertal AGCR when compared to others (Fig. 4.80 A-F).

With the exception of the negative reaction observed in the prepubertal testis as well as in the seminiferous interstitium of all age group of AGCR, Sertoli cell nuclei and cytoplasm of pubertal onwards were positive to S-100 staining (Fig. 4.81). In addition, conspicuous S-100 positive areas were exclusively evident in the perimuscular coats and perivascular tissue of the interstitium of the proximal and distal initial segments, corpus and cauda segments of the epididymal duct in the different age groups of AGCR (Figs. 4.83, 4.85, 4.87 and 4.88). On the intensity of S-100 in the testicular parenchyma of different ACGR, significantly higher ($p<0.05$) intensity was seen in the aged AGCR relative to others and the intensity increases with age (Fig. 87). S-100 intensity in the proximal initial segment was significantly higher in the aged AGCR compared to the adult rat (Fig. 4.89A). Also, the intensities of the positive areas within the distal initial segment, corpus and cauda showed consistently significant increased values in pubertal rat when compared to others (Fig. 4.89 C, E and F).

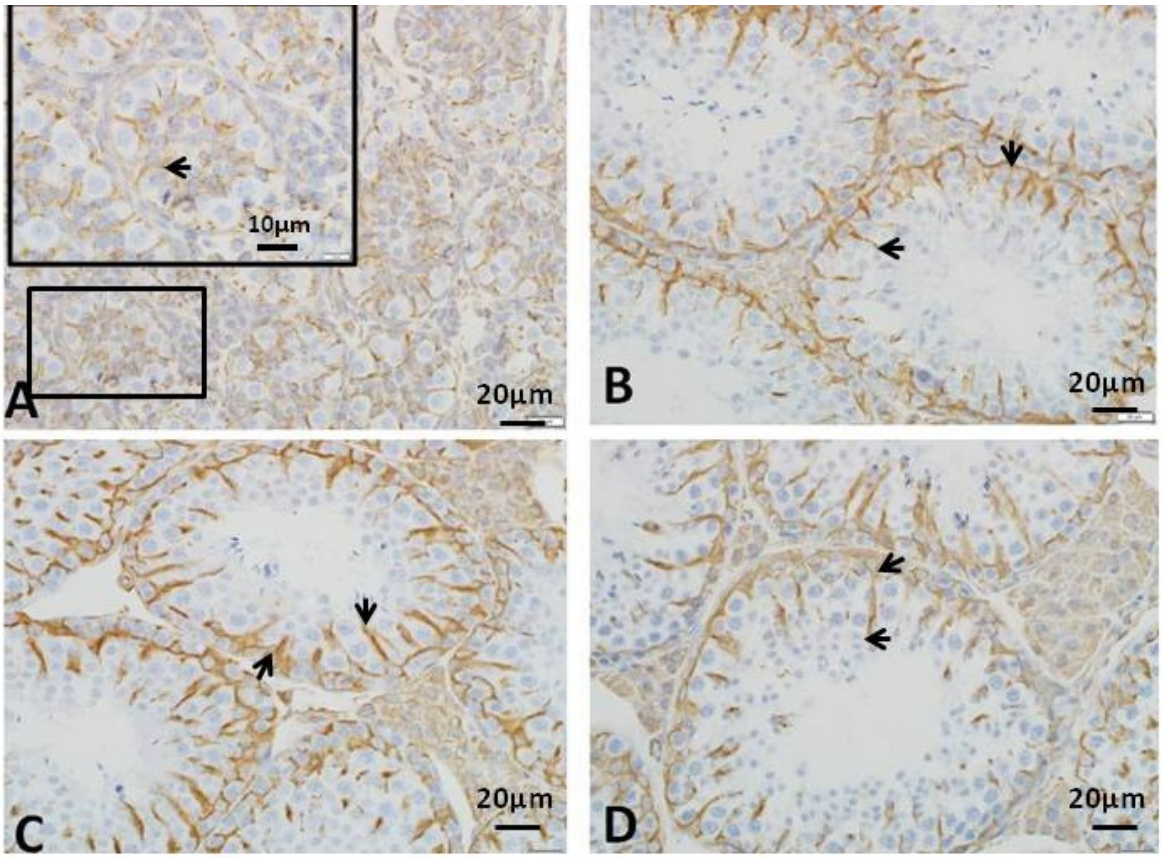

Figure 4.72. Photomicrographs of Vimentin Expression in the Testis of Different Age Groups of the AGCR. A. Prepubertal B. Pubertal C. Adult D. Aged. Note that the vimentin staining (arrows) is expressed in the Sertoli cell with intense staining locatedin perinuclear areas of Sertoli cell and along the base with strands of vimentin reaching out to the tips of elongated spermatids in B, C and D. Scale bar: 20µm

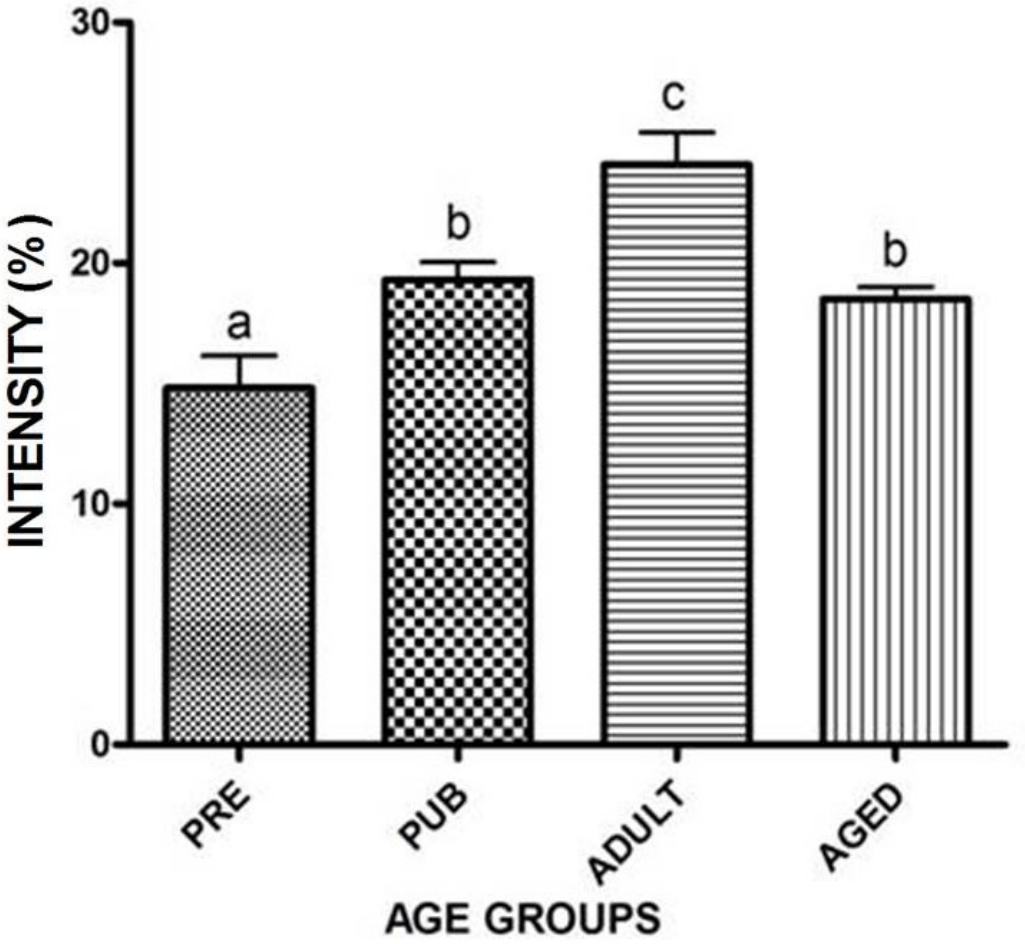

Figure 4.73. Age-related Changes in the Intensity of Vimentin Expression in the Testicular Parenchyma of the AGCR. Bars bearing dissimilar alphabet superscripts (a,b, c) are significantly different.

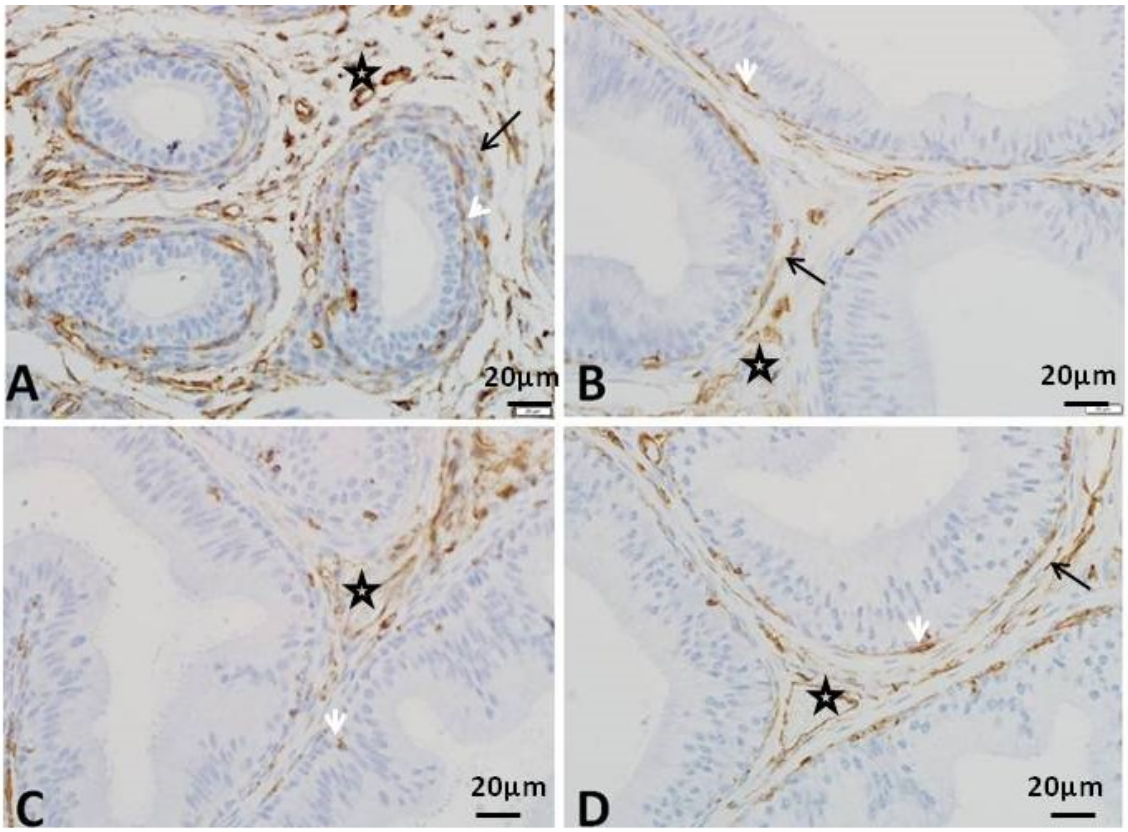

Figure 4.74. Photomicrographs of Vimentin Expression in the Proximal Initial Segment (PIS) of the Epididymis in the AGCR. A. Prepubertal: B. Pubertal: C. Adult: D. Aged: Note that the Vimentin staining (arrows) is expressed in the epididymal perimuscular coat (black arrow), peribasal cell region (arrow head) and interstitial vasculature(star). Intensity appears more in the pre-pubertal group.

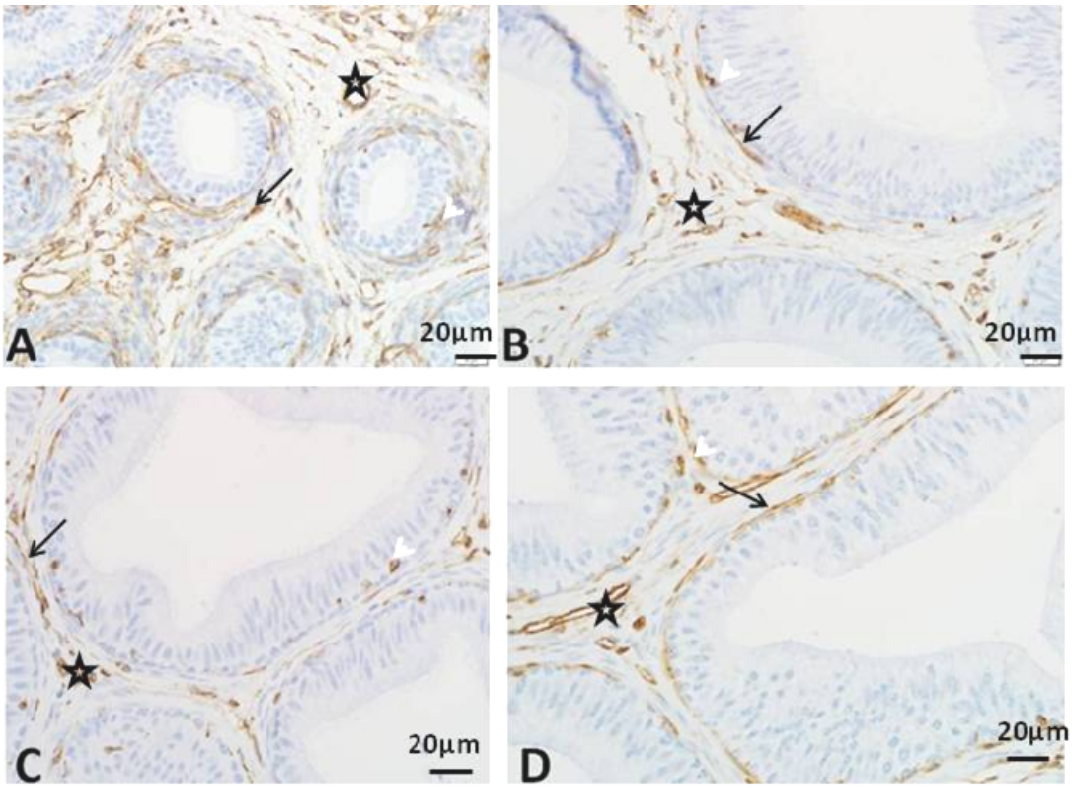

Figure 4.75. Photomicrographs of Vimentin Expression in the Middle Initial Segment(MIS) of the Epididymis in AGCR. A. Prepubertal: B. Pubertal: C. Adult: D. Aged. Note that the Vimentin staining is expressed in the epididymal perimuscular coat (black arrow), peribasal cell region (arrow head) and interstitial vasculature (star). Intensity appears more in the pre-pubertal group.

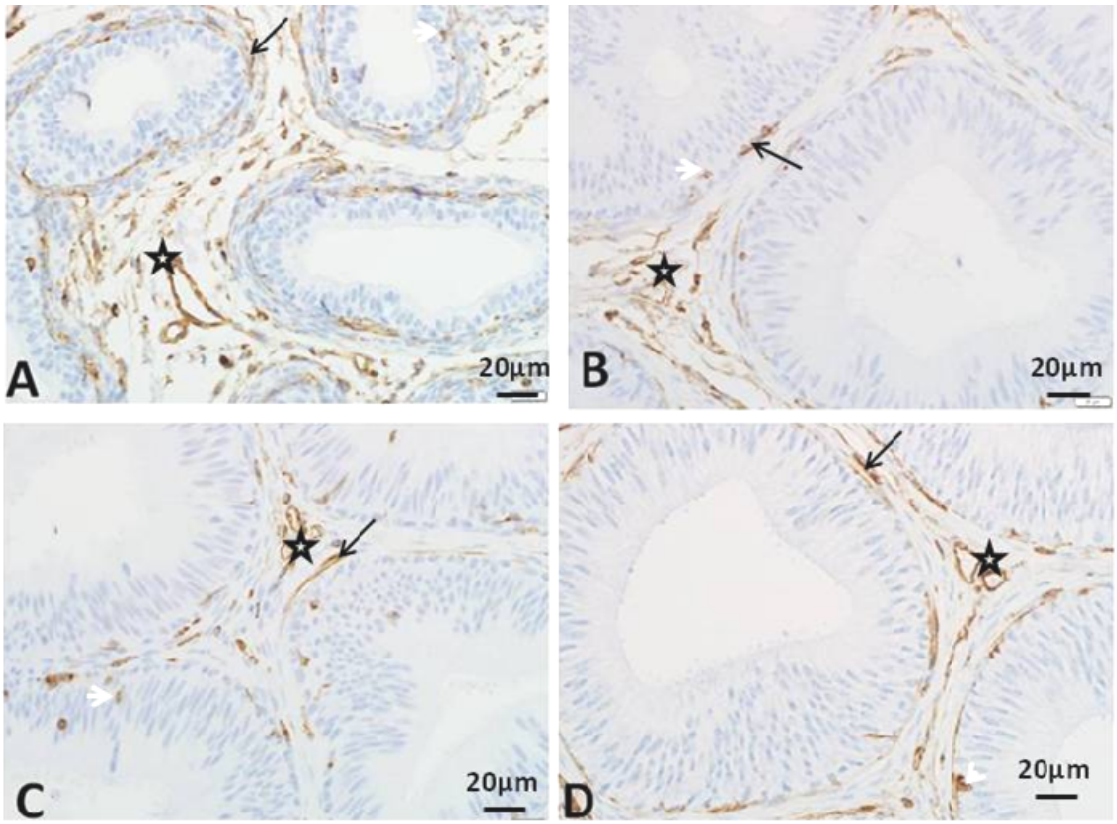

Figure 4.76. Photomicrographs of Vimentin Expression in the Distal Initial Segment (DIS) of the Epididymis in AGCR. A. Prepubertal: B. Pubertal: C. Adult: D. Aged: Note that the Vimentin staining is expressed in the epididymal perimuscular coat (black arrow), peribasal cell region (arrow head) and interstitial vasculature (star). Intensity appears more in the pre-pubertal group.

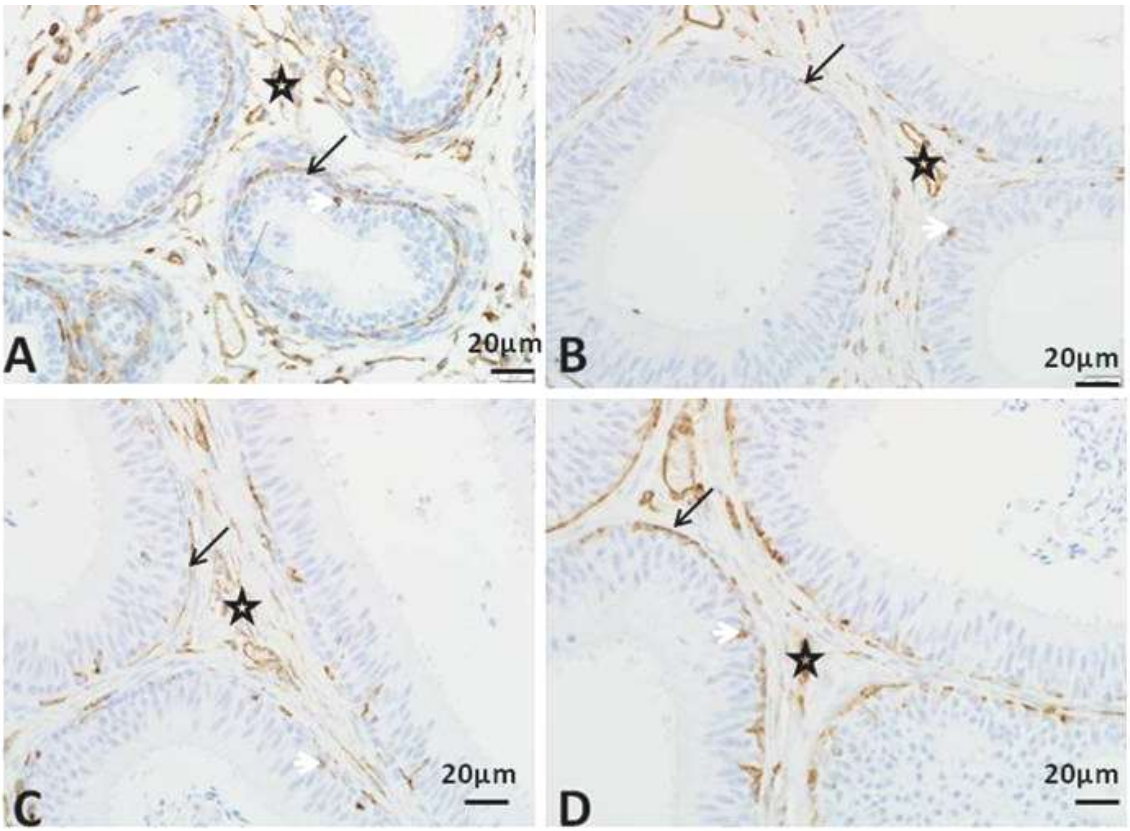

Figure 4.77. Photomicrographs of Vimentin Expression in the CAPUT Segment of the Epididymis in AGCR. A. Prepubertal: B. Pubertal: C. Adult: D. Aged. Note that the staining is expressed in the epididymal perimuscular coat (black arrow), peribasal cell region (arrow head) and interstitial vasculature (star). Intensity appears more in the pre-pubertal group.

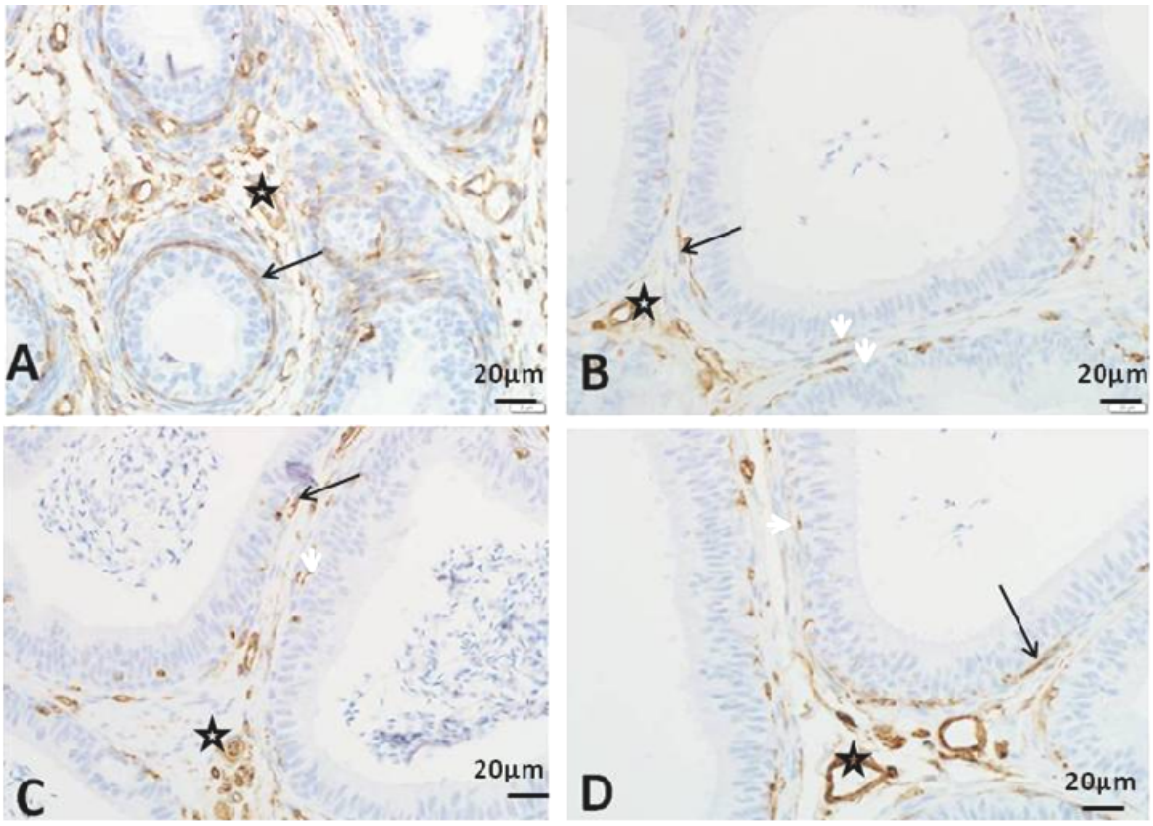

Figure 4.78. Photomicrographs of Vimentin Expression in the CORPUS Segment of Epididymis in AGCR. A. Prepubertal: B. Pubertal: C. Adult: D. Aged. Note that the Vimentin staining is expressed in the epididymal perimuscular coat (black arrow), peribasal cell region (arrow head) and interstitial vasculature (star). Higher intensity occurs in the pre-pubertal group.

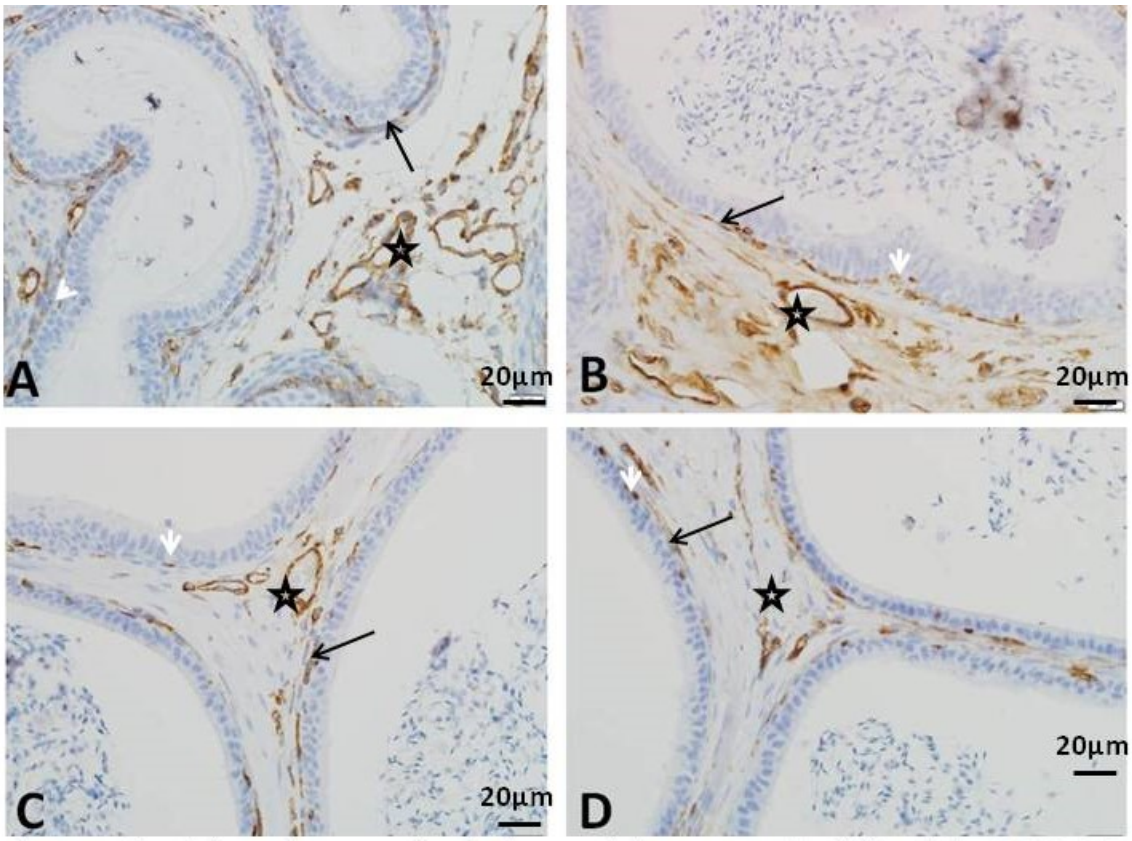

Figure 4.79. Photomicrographs of Vimentin Expression in the CAUDA Segment of the Epididymis in AGCR. A. Prepubertal B. Pubertal C. Adult D. Aged. Note that the Vimentin staining is expressed in the epididymal perimuscular coat (black arrow), peribasal cell region (arrow head) and interstitial vasculature (star). Highest intensity occurs in the pre-pubertal group.

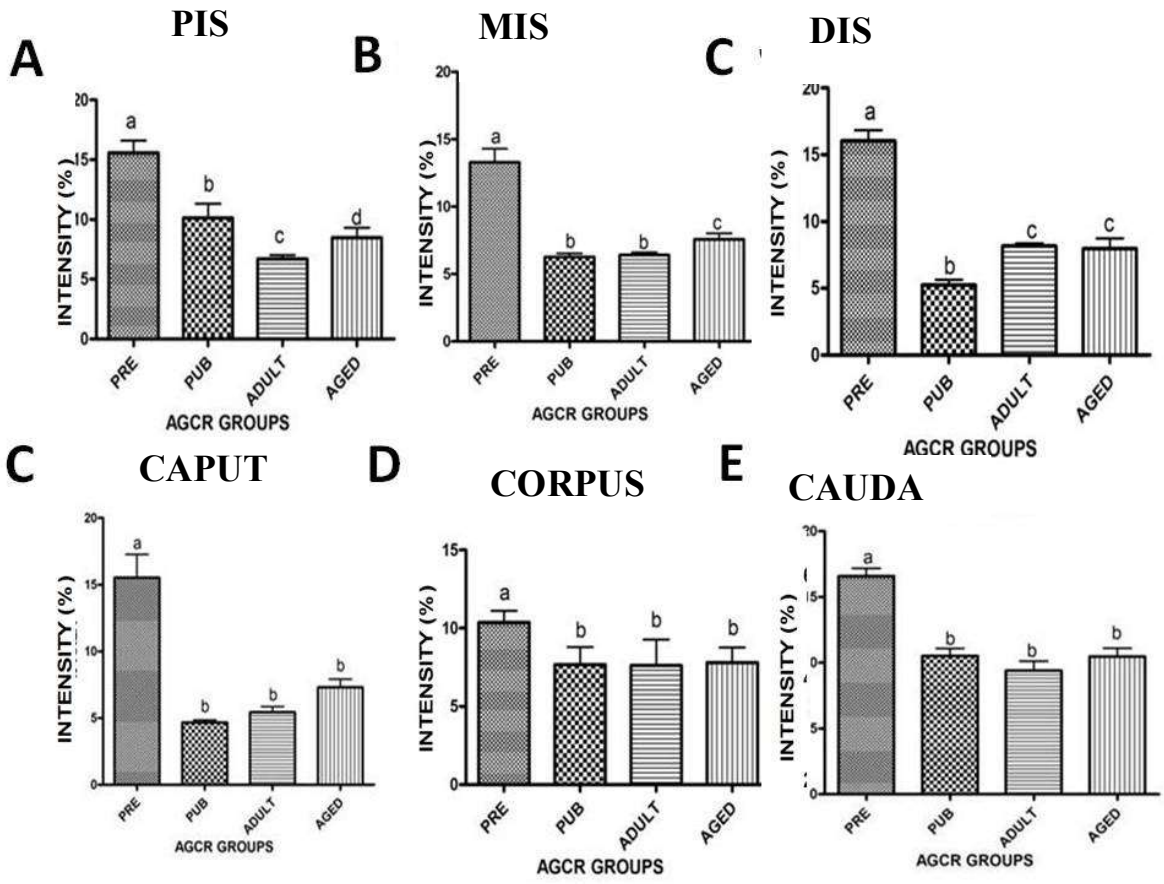

Figure 4.80 A-F. Age-related Changes in Intensity of Vimentin Expression in the Epididymal Ducts of AGCR. A Proximal initial segment (PIS); B Middle initial segment (MIS); C Distal initial segment (DIS); D. Caput; E. Corpus; F Cauda. Bars bearing dissimilar alphabet superscripts (a,b, c) are significantly different.

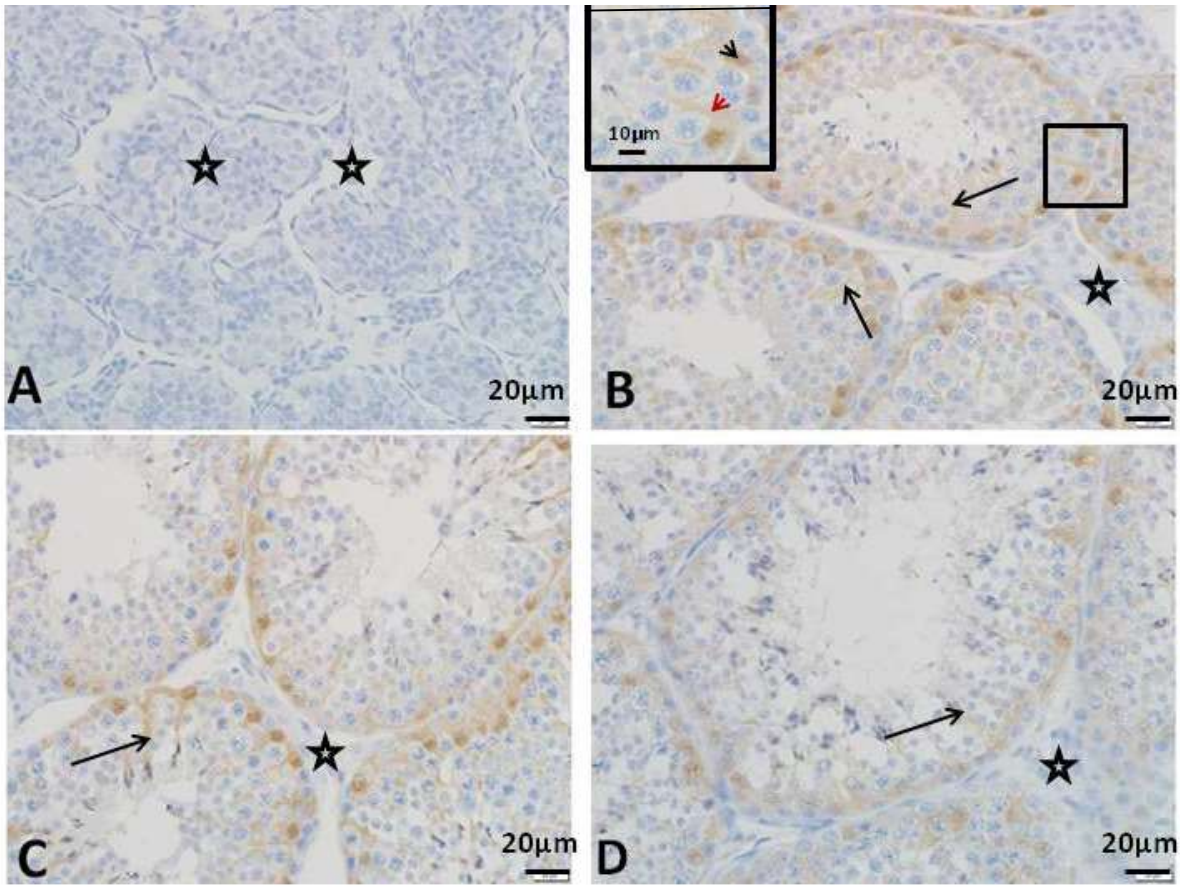

Figure 4.81. Photomicrographs of S-100 Expression in the Testis of Different Age Groups of AGCR. A. Prepubertal: B. Pubertal: C. Adult: D. Aged: Note the positive S-100 staining in the Sertoli cells (**inset;** nuclei [black arrow head] and cytoplasm [red arrow head] (arrows), negative staining in the interstitial tissue (star) and slide A. Scale bar: 20µm (main) and 10µm (inset)

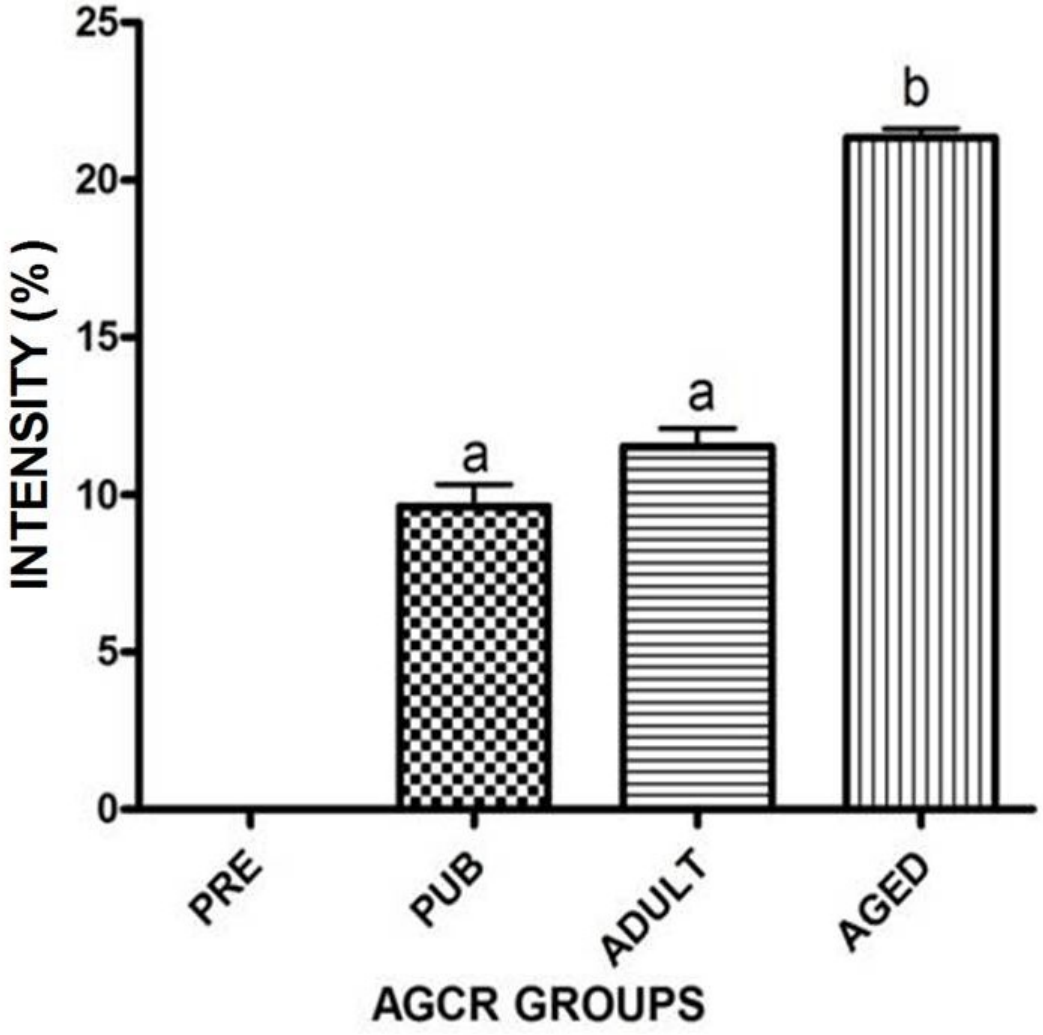

Figure 4.82. Age-related Changes in the Signal Intensity of S-100 Expression in the Testicular Parenchyma in AGCR. Bars bearing dissimilar alphabet superscripts (a,b, c) are significantly different.

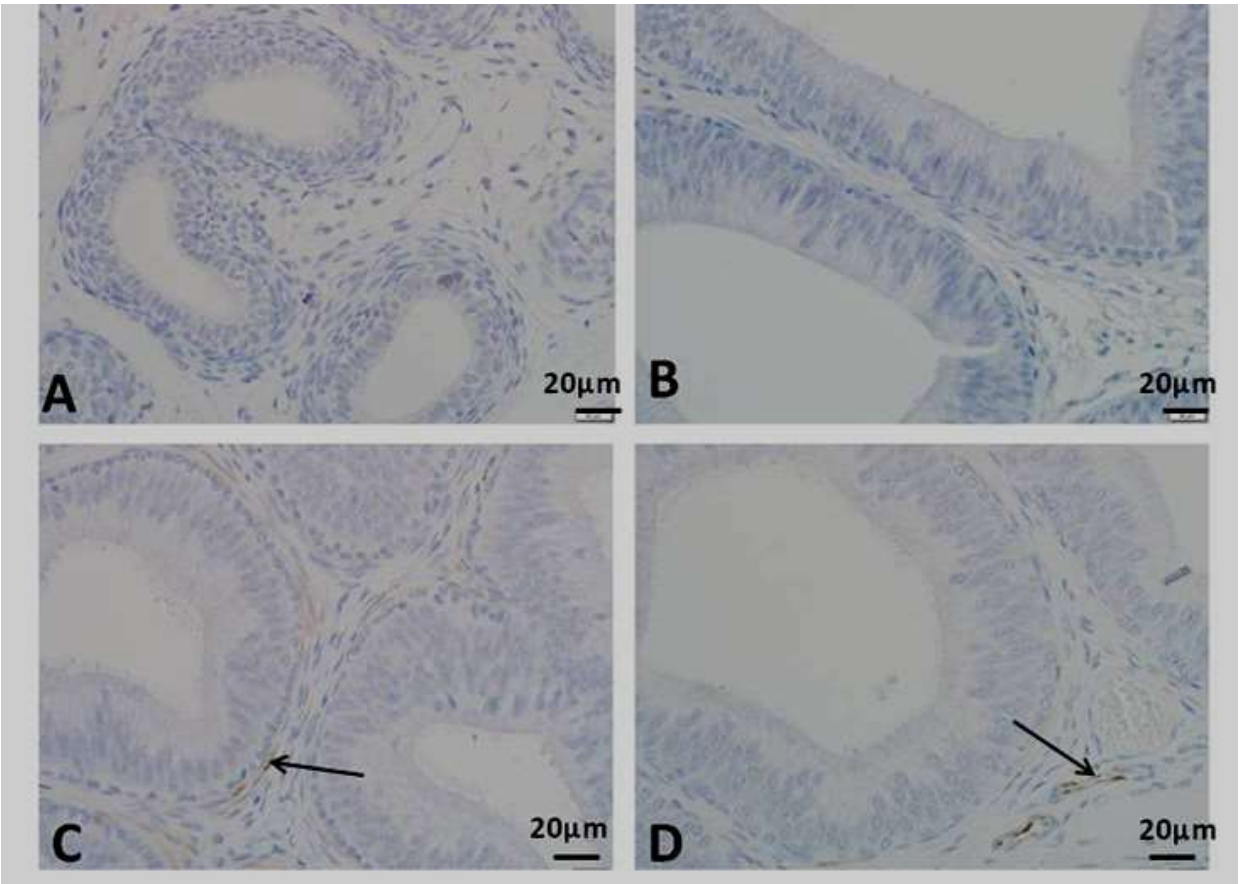

Figure 4.83. Photomicrographs of S-100 Expression in the Proximal Initial Segment (PIS) of the Epididymis in AGCR. A. Prepubertal B. Pubertal C. Adult D. Aged. Note the positive S-100 staining in the perimuscular coat (arrow) of C and D. Scale bar: 20µm

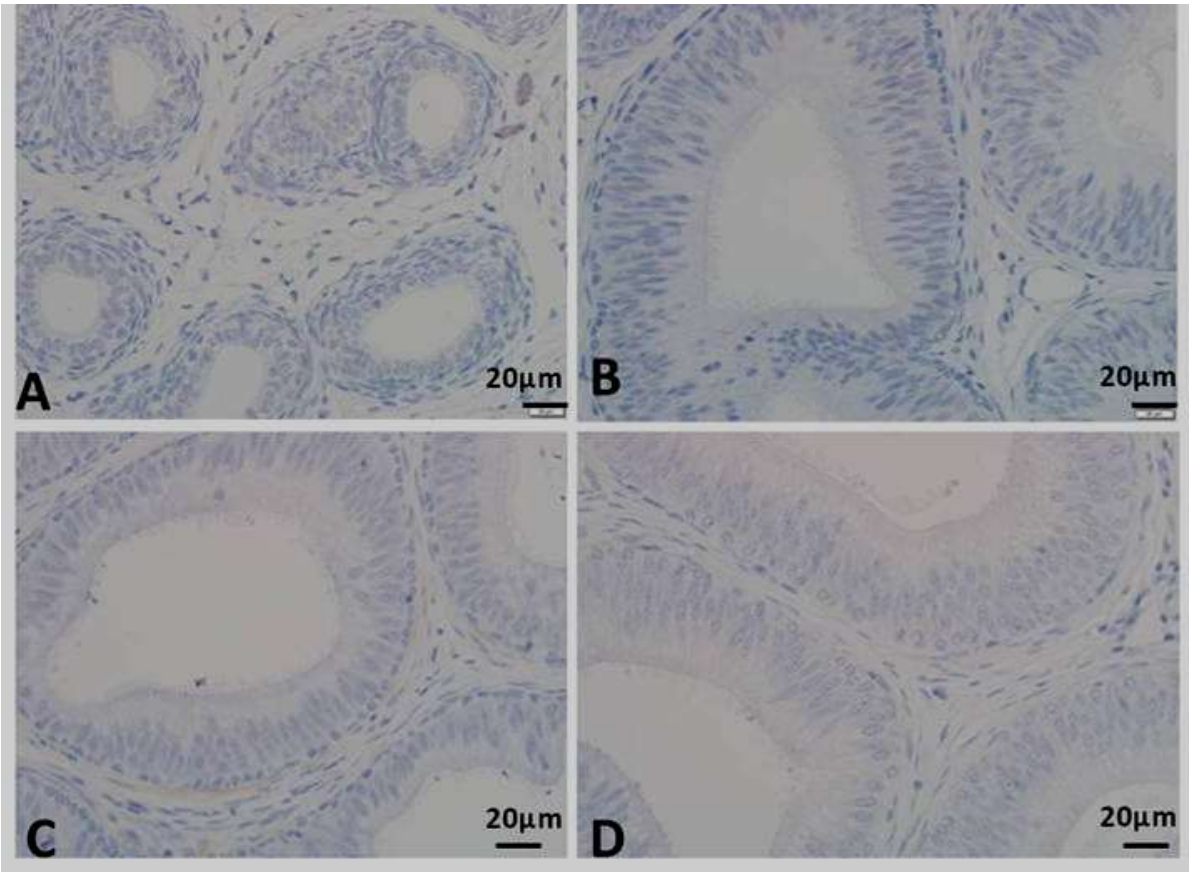

Figure 4.84. Photomicrographs of S-100 Expression in the Middle Initial Segment(MIS) of the Epididymis in AGCR. A. Prepubertal B. Pubertal C. Adult D. Aged. Note the positive S-100 staining in the perimuscular coat (arrow) as well as negative staining in A, B and D Scale bar: 20µm

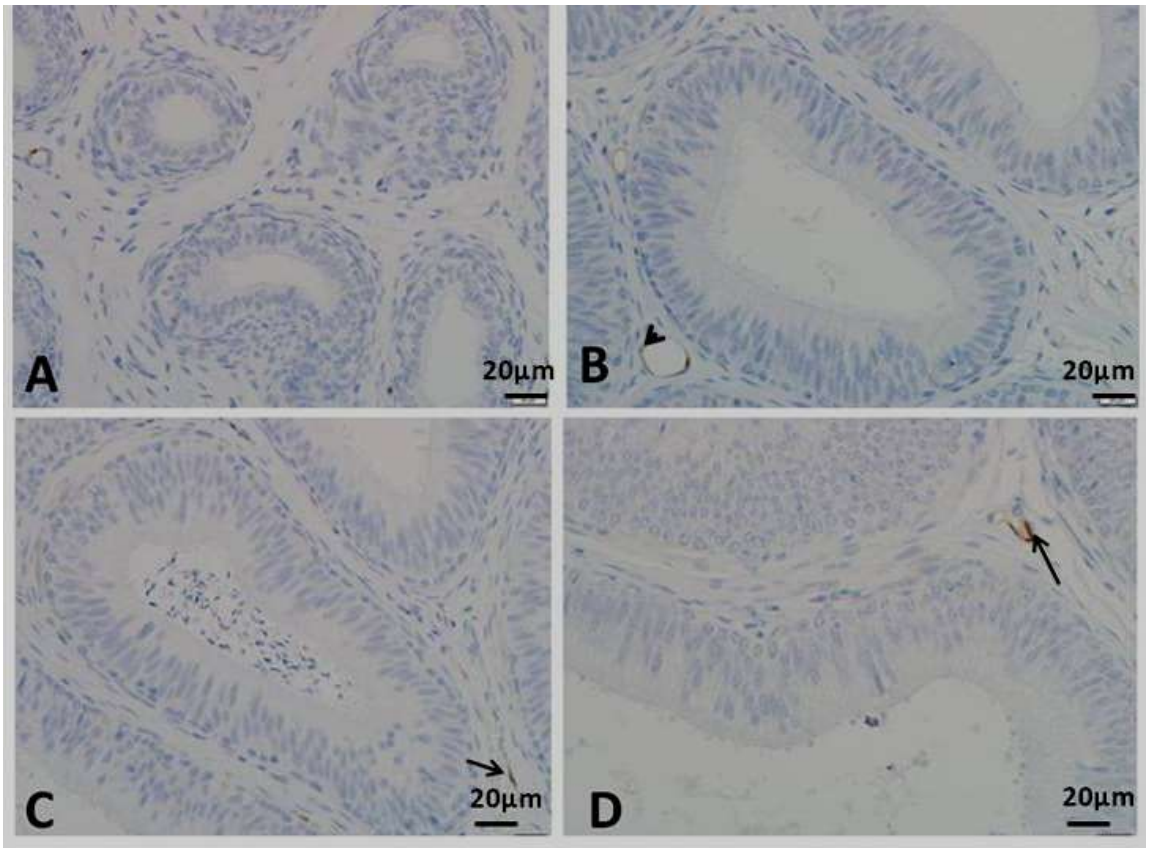

Figure 4.85. Photomicrographs of S-100 Expression in the Distal Initial Segment(DIS) of the Epididymis in AGCR. A. Prepubertal B. Pubertal C. Adult D. Aged Note the positive S-100 staining in the perimuscular coat (arrow) and interstitial vessel (arrow head). Scale bar: 20µm

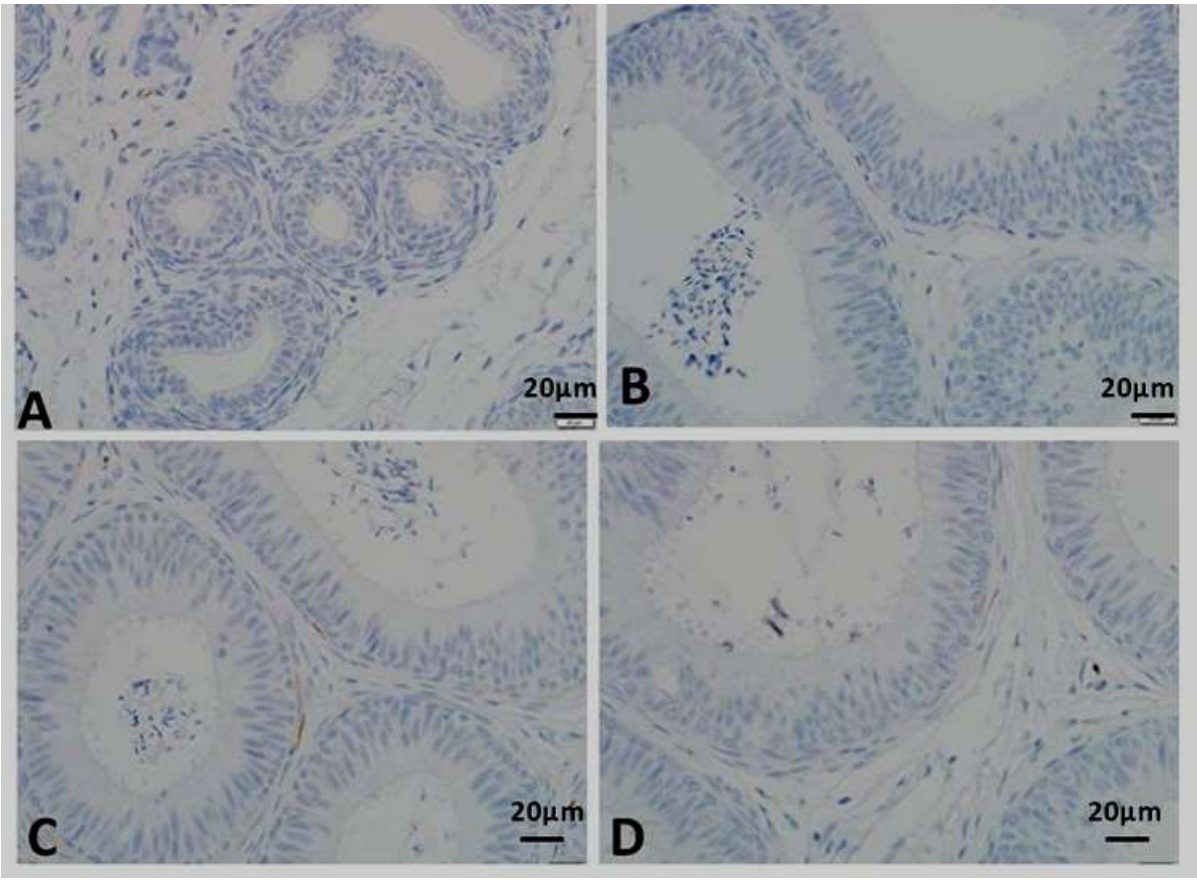

Figure 4.86. Photomicrographs of S-100 Expression in the CAPUT Segment of Epididymis in AGCR. A. Prepubertal B. Pubertal C. Adult D. Aged Note the positive S-100 staining in the perimuscular coat (arrow) as well as negative staining in A, B and D. Scale bar: 20µm

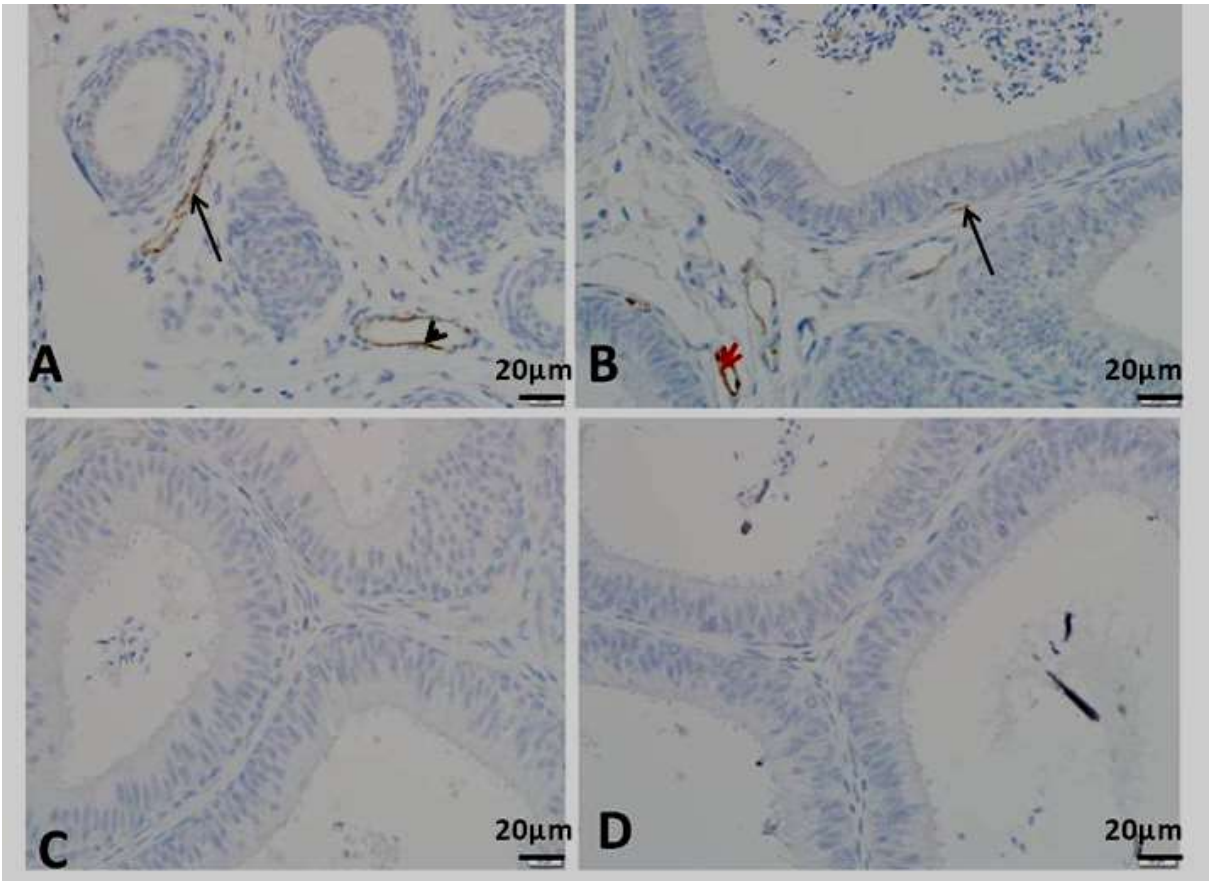

Figure 4.87. Photomicrographs of S-100 Expression in the CORPUS Epididymal Segment in AGCR. A. Prepubertal: B. Pubertal: C. Adult: D. Aged: Note the positive S-100 staining in the perimuscular coats (arrows) and interstitial vessels (arrow heads) as well as negative staining in C and D. Scale bar: 20µm

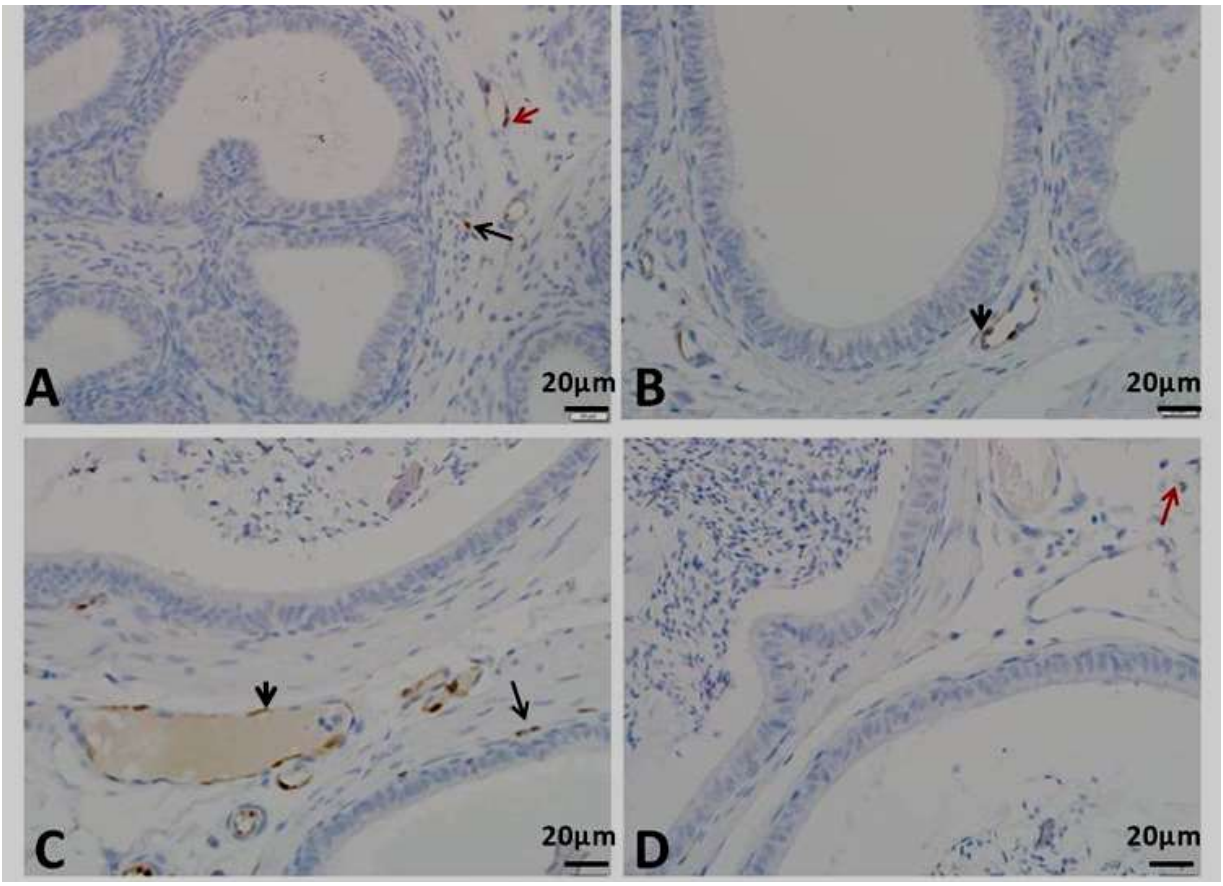

Figure 4.88. Photomicrographs of S-100 Expression in the CAUDASegment of Epididymis in AGCR. A. Prepubertal: B. Pubertal: C. Adult: D. Aged: Note the positive S-100 staining in the perimuscular coats (arrows), interstitium proper (red arrow) and interstitial vessels (arrow heads) . Scale bar: 20µm

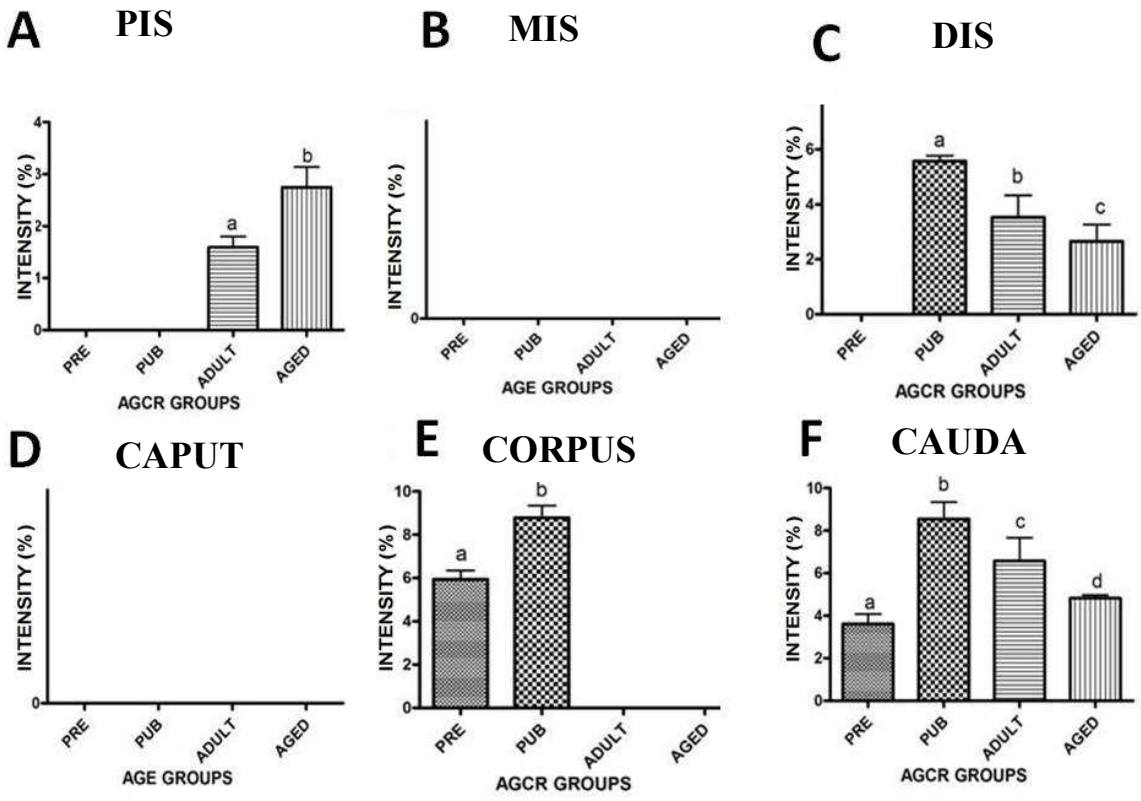

Figure 4.89 A-D. Age-related Changes in Intensity of S-100 Expression in the Epididymal Segments in AGCR. A, B and C (Proximal, middle and distal initial segments); D (Caput); E (Corpus) and F (Cauda). Bars bearing dissimilar alphabet superscripts (a,b, c) are significantly different

4.4.1.2 Histochemical and Immunohistochemical Demonstrations of Nerves and Glial-like Cells (Astrocyte-like) in the Testis and Epididymis using Golgi-silver Techniques, Anti NF 20 and Anti-GFAP

With the use of Golgi-silver technique, both the neuronal and the astrocyte-like structures were demonstrated in the testicular tunica albuginea (Fig. 4.90), interstitium and along the seminiferous tubular boundary (Fig. 4.92) in all the AGCR groups. In nearly all the capsule of all AGCR, twigs of the two structures (neuronal fibres and glial-like cells) were given off to radiate into the testicular parenchyma (Fig. 4.92). Within the segments of the epididymal duct, neuronal and astrocyte-like structures were remarkably observed within the periductal muscle coat and in the epididymal interstitum of middle (MIS) and distal initial segment (DIS), caput, corpus and cauda segments (Figs. 4.95-4.99). Golgi intensity profile in both the testicular capsule (Fig. 4.91) and interstitium (Fig. 4.93) were significantly lower ($p<0.05$) in the prepubertal rat when compared to others. The intensity appeared to increase with age advancement though, an insignificant ($p>0.05$) decline value was displayed by aged AGCR relative to the pubertal and adult values. The intensities of the nerve and glial-like cells of the middle initial segment downwards consistently displayed significantly higher intensity ($p<0.05$) in the pubertal AGCR relative to others (Fig. 4.100 B-F).

Neurofilament (NF)-positive areas for nerve fibre presence in the testes of different age groups of AGCR were localised in the tunica albuginea and peri-albuginea interstitium of the capsule (Fig. 4.101) as well as in the seminiferous tubular interstitium (Fig. 4.103). For the segments of epididymal duct, conspicuous NF positive areas were restricted to the the periductal muscle coat and epididymal ductal interstitium most especially in the perivascular part of the distal initial segment (DIS), caput, corpus and cauda segments of the epididymis in all AGCR groups (Figs. 4.107-110). The intensity of NF expression in the testicular capsules (Fig. 4.102) and interstitium (Fig. 4.104) was observed to be significantly higher in the pubertal and adult AGCR when compared to others and the intensity increases with age with peak shown in pubertal and a subsequent decline. The profile of NF intensity in distal initial segment (DIS) downwards consistently revealed significantly higher intensities in the pubertal and adult rats relative to others (Fig. 4.111 C-F). In general, the trend of NF expression intensity from the distal initial segment to the caudal segment appeared to increase with age.

Positive areas for the presence of astrocyte-like cells on using anti glial fibrillary acid protein (anti GFAP) marker in the testes and epididymis of all AGCR include; the interstitium between seminiferous tubules (Fig. 4.112) and the perivascular part of the epididymal ductal interstitium (Figs. 4.114-119). Regarding the profile of testicular GFAP intensity (Fig. 4.113), significantly higher ($p<0.05$) intensity was noticed in the aged AGCR relative to others. The intensity seems to increase with advancement in age with both pubertal and adult AGCR displaying a non significant difference ($p>0.05$) in the value of their intensities. In the epididymis, similar trend described for the testicular GFAP intensity (Fig. 4.120 C-F) was remarkably observed in the distal initial epididymal segment downwards.

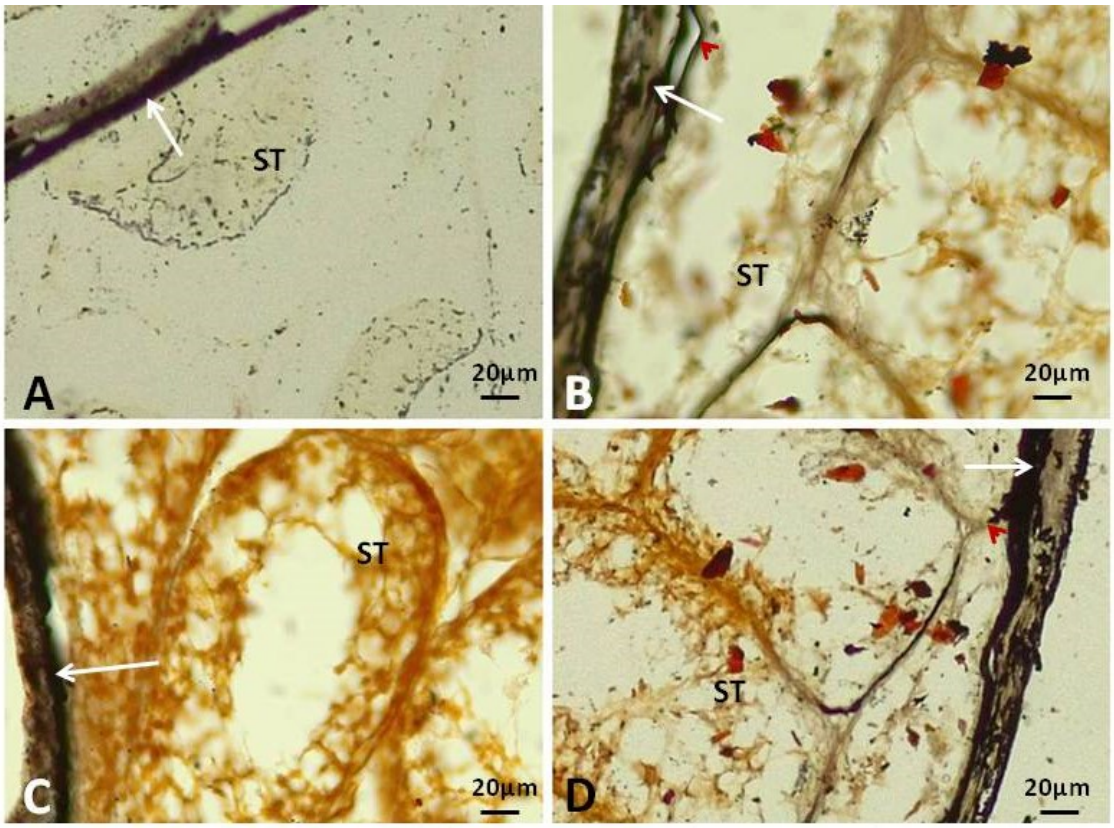

Figure 4.90. Golgi Staining of the Testis of Different Age-Groups of the AGCR. A. Prepubertal B. Pubertal C. Adult and D. Aged. Note the display of nerve fibre in the tunica albuginea (arrow) and twigs radiating from it to parenchyma (arrow head). Scale bar: 20µm

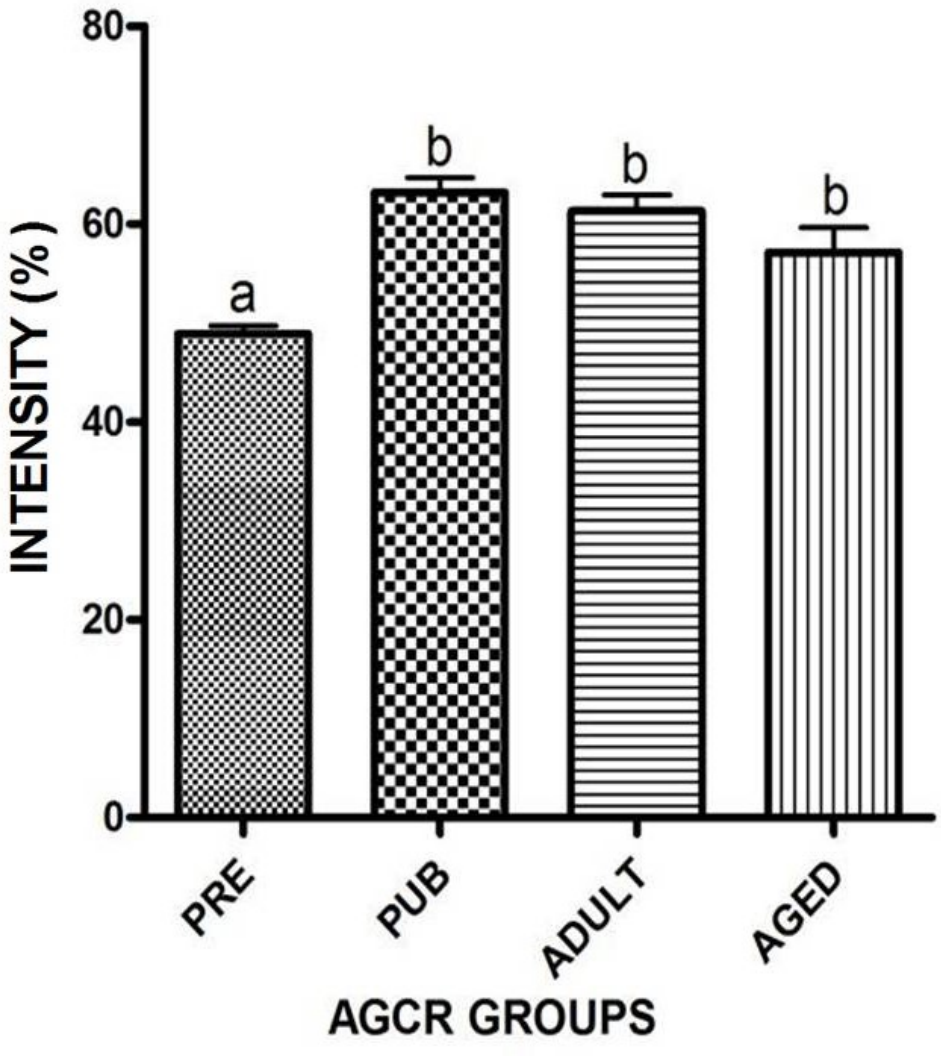

Figure 4.91. Age-related changes in intensity of Golgi-silver staining of the testicular capsule in AGCR. Bars bearing dissimilar alphabet superscripts (a,b) are significantly different.

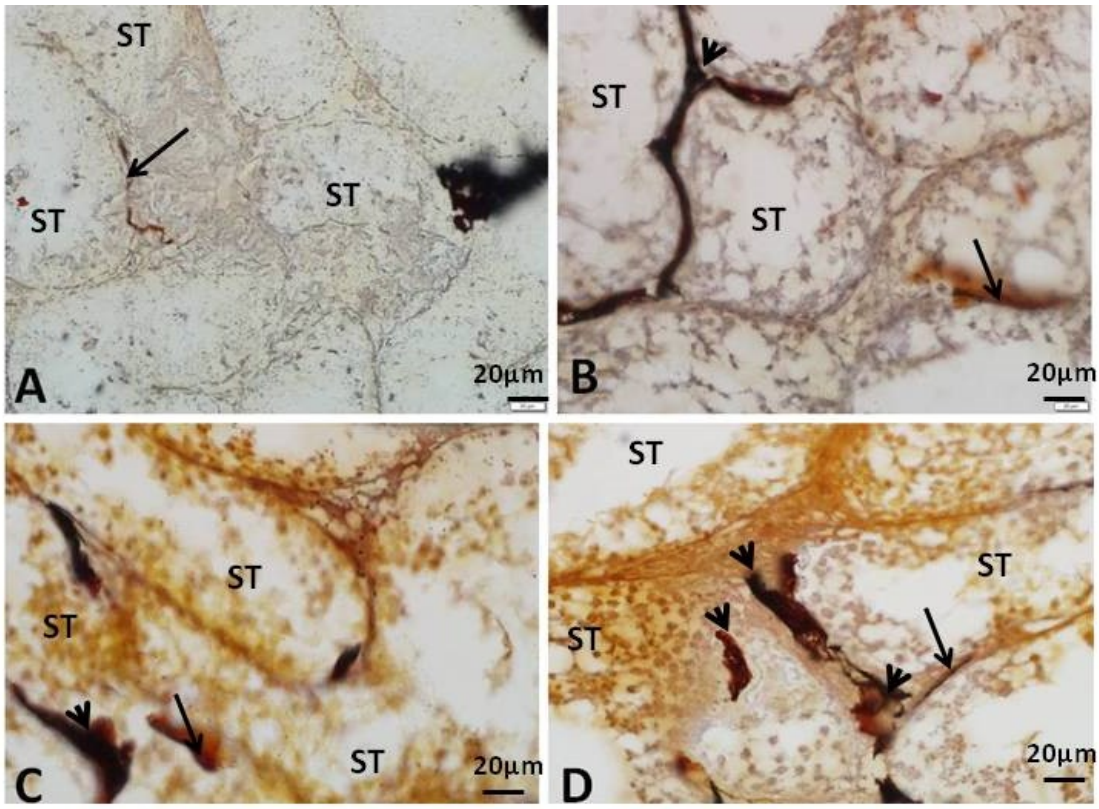

Figure 4.92. Golgi Staining of the Testis of Different Age Groups of AGCR. A. Prepubertal B. Pubertal C. Adult and D. Aged. Note the display of fine nerve fibre (long arrow) between seminiferous tubular (ST) boundary and thick nerve fibre in the ST interstitium (arrow head). Scale bar: 20µm

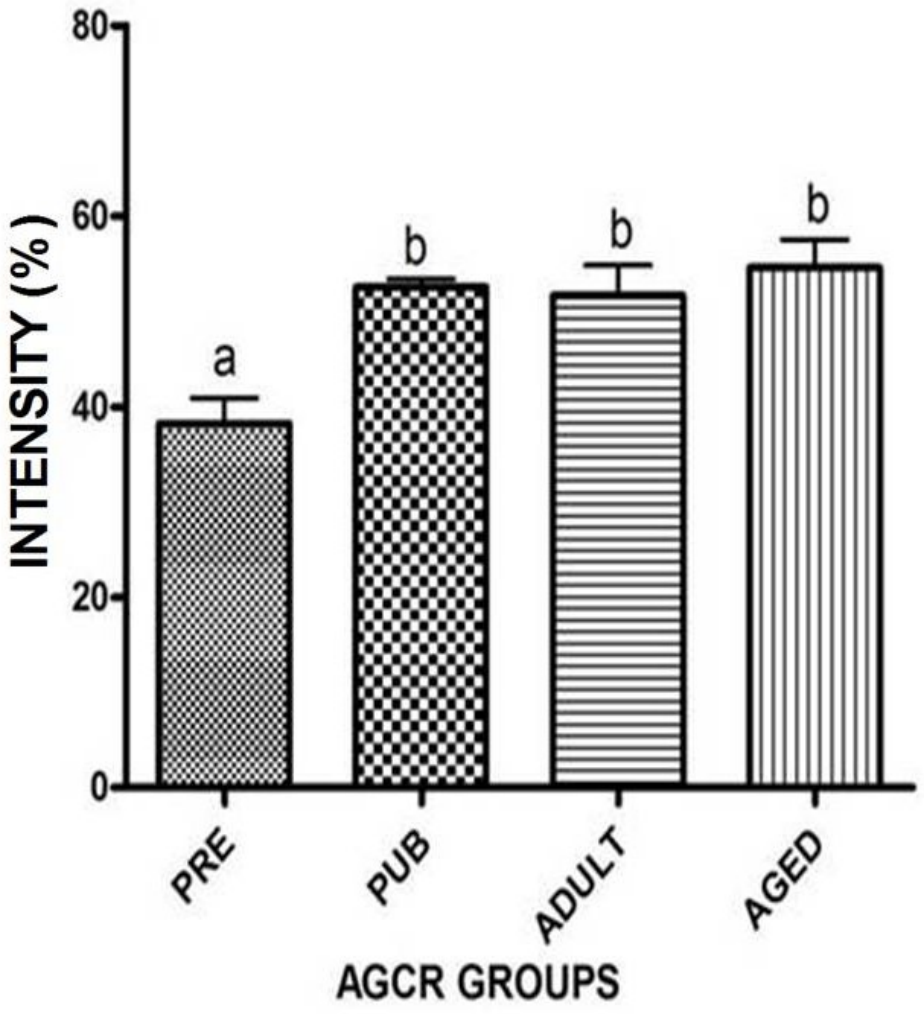

Figure 4.93. Age-related Changes in the Intensity of Golgi-Silver Staining of the Testicular Parenchyma in AGCR. Bars bearing disimilar alphabet superscripts (a,b,c) are significantly different.

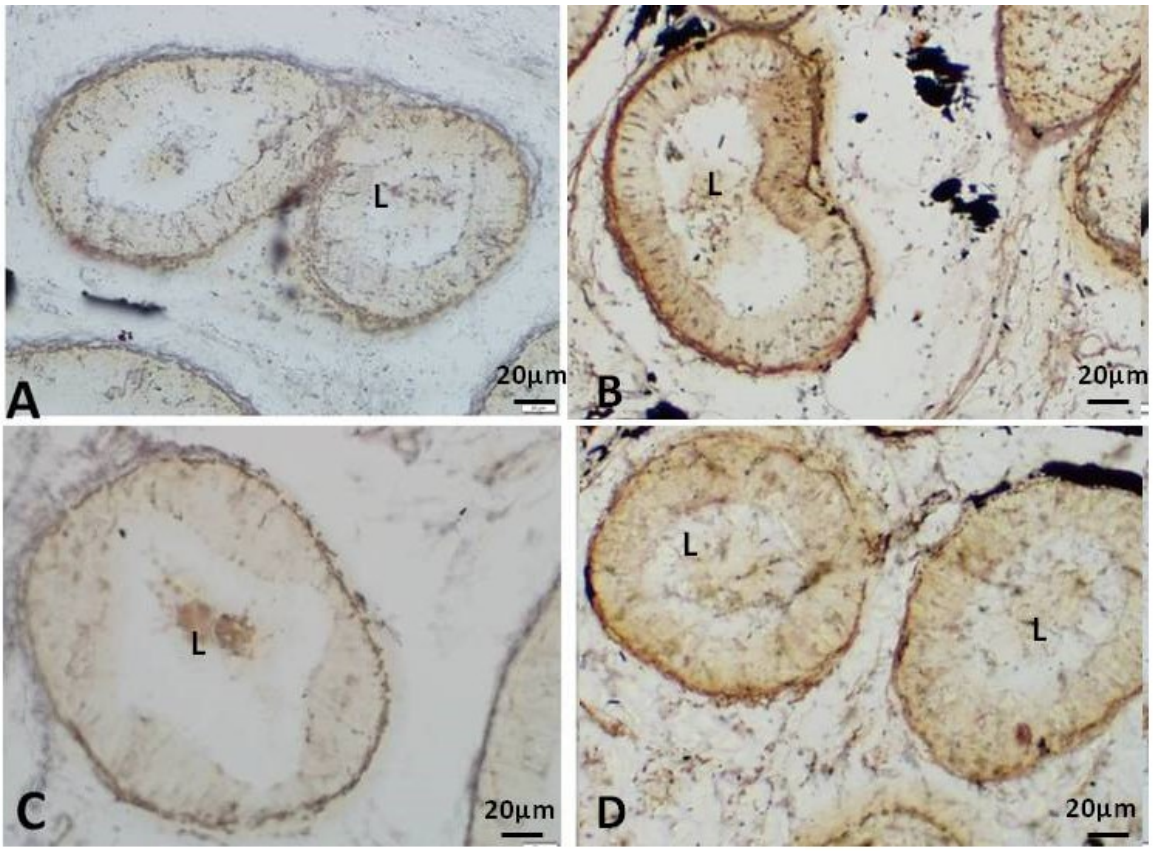

Figure 4.94. Golgi Staining of the Proximal Initial Segment (PIS) of the Epididymis in the Different Age Groups of AGCR. A. Prepubertal B. Pubertal C. Adult D. Aged: No visible nerve fibre across all AGCR group. Stain: Golgi-Silver impregnation.

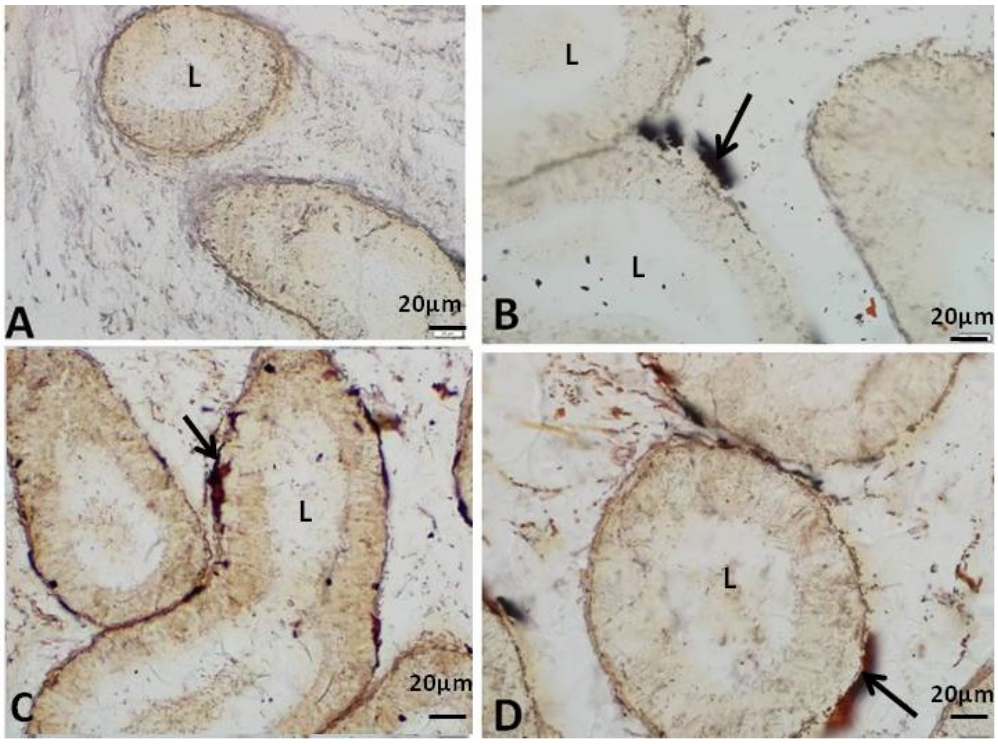

Figure 4.95. Golgi Staining of the Middle Initial Segment(MIS) of the Epididymis in the DifferentAge Groups of AGCR. A. Pre-pubertal: No visible nerve fibre B. Pubertal: C. Adult:D. Aged: presence of nerve fibre (arrow) within periductal muscle coat. Scale bar: 20µm

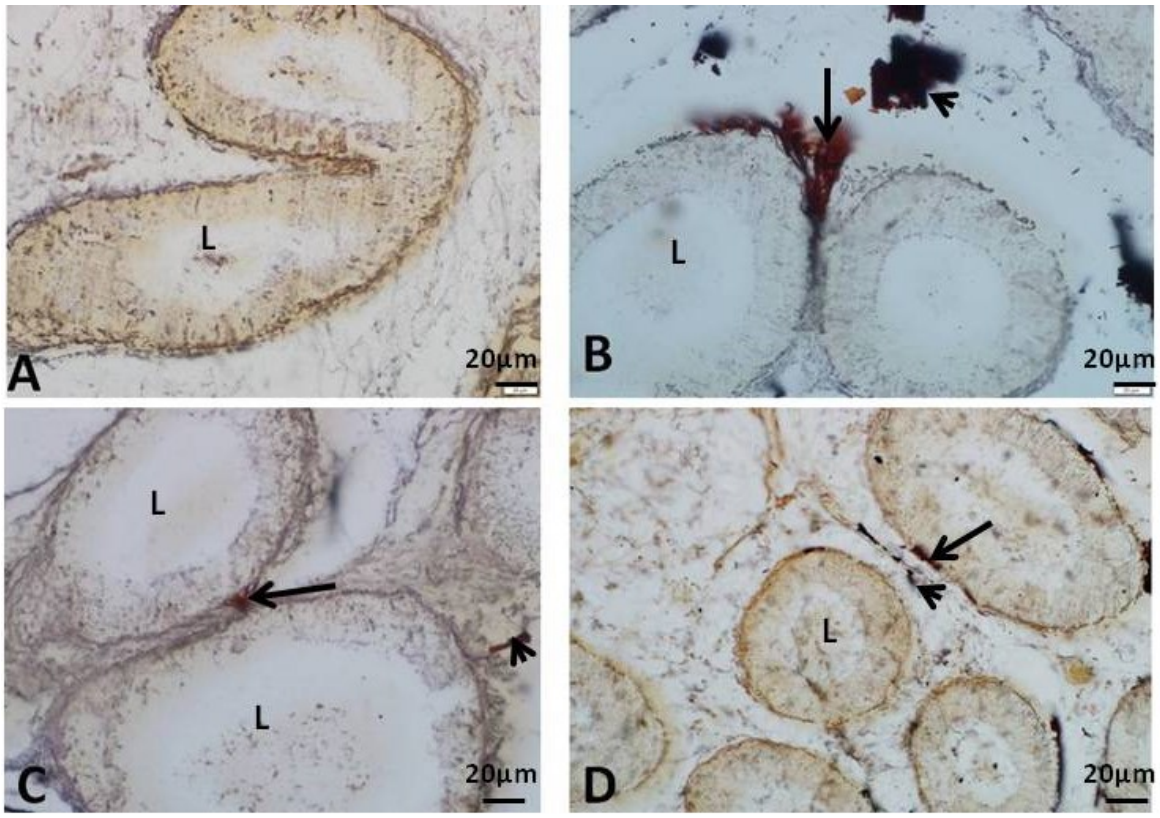

Figure 4.96. Golgi Staining of the Distal Initial Segment (DIS) of the Epididymis in the Different Age Groups of AGCR. A. Prepubertal: No visible NFB. Pubertal: displays thick NF in the interstitium (arrow head) and PMC (long arrow) C. Adult and D. Aged: bear scanty thin NF in the interstitium (arrow head) and periductal muscle coat (long arrow). Scale bar: 20µm

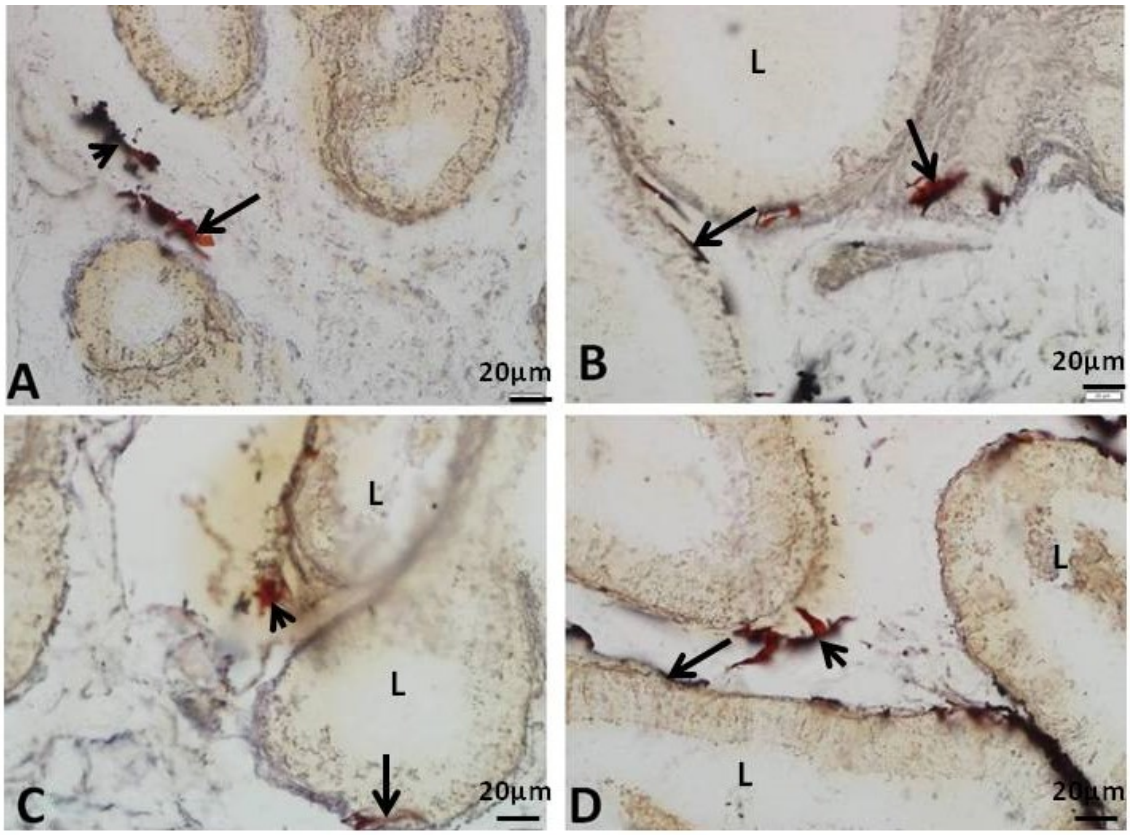

Figure 4.97. Golgi Stainingof the CAPUT Epididymis in the Different Age Groups of AGCR. A. Prepubertal B. Pubertal C. Adult D. Aged. Note the display of nerve fibres within the PMC (long arrow) and the interstitium (arrow head) in all groups.

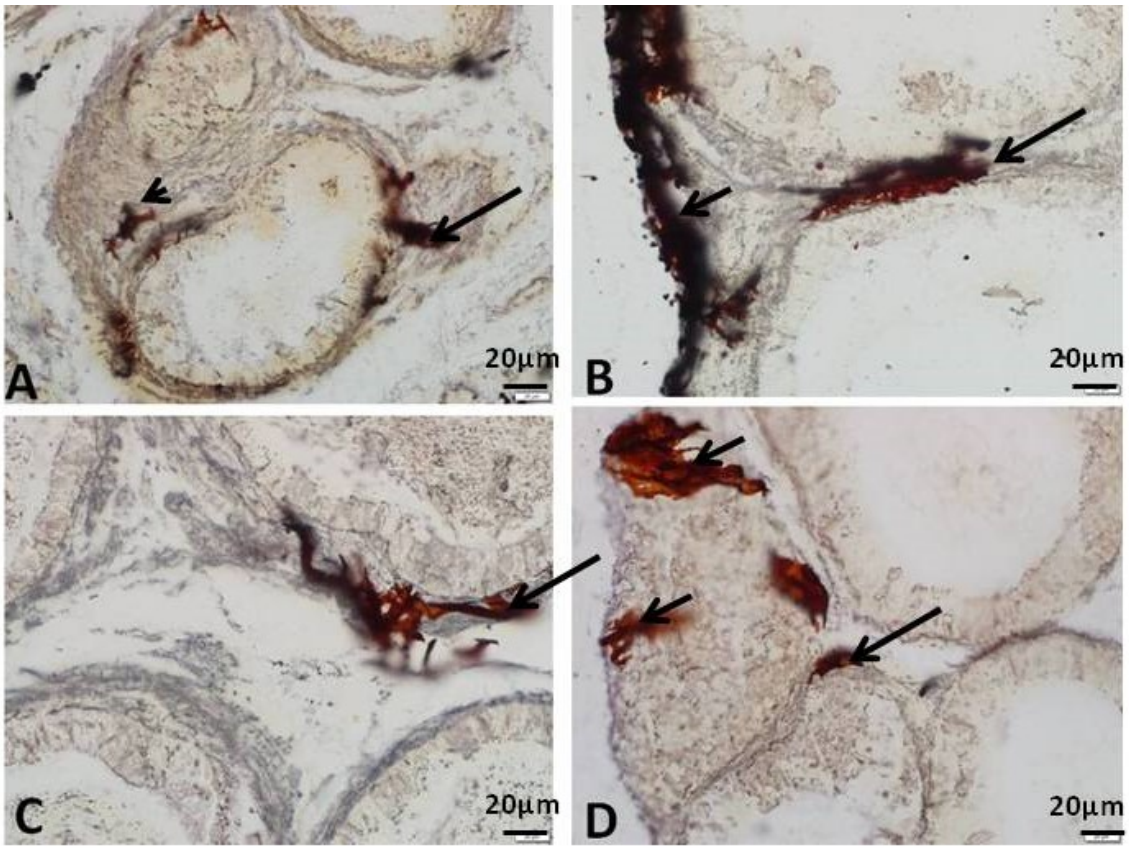

Figure 4.98. Golgi Staining of the CORPUS Epididymis in the Different Age Groups of AGCR. A. Prepubertal B. Pubertal C. Adult D. Aged. Note the display of dense nerve fibres within the PMC (long arrow), the epididymal sheath (short arrow), and the interstitium (arrow head). Scale bar: 20µm

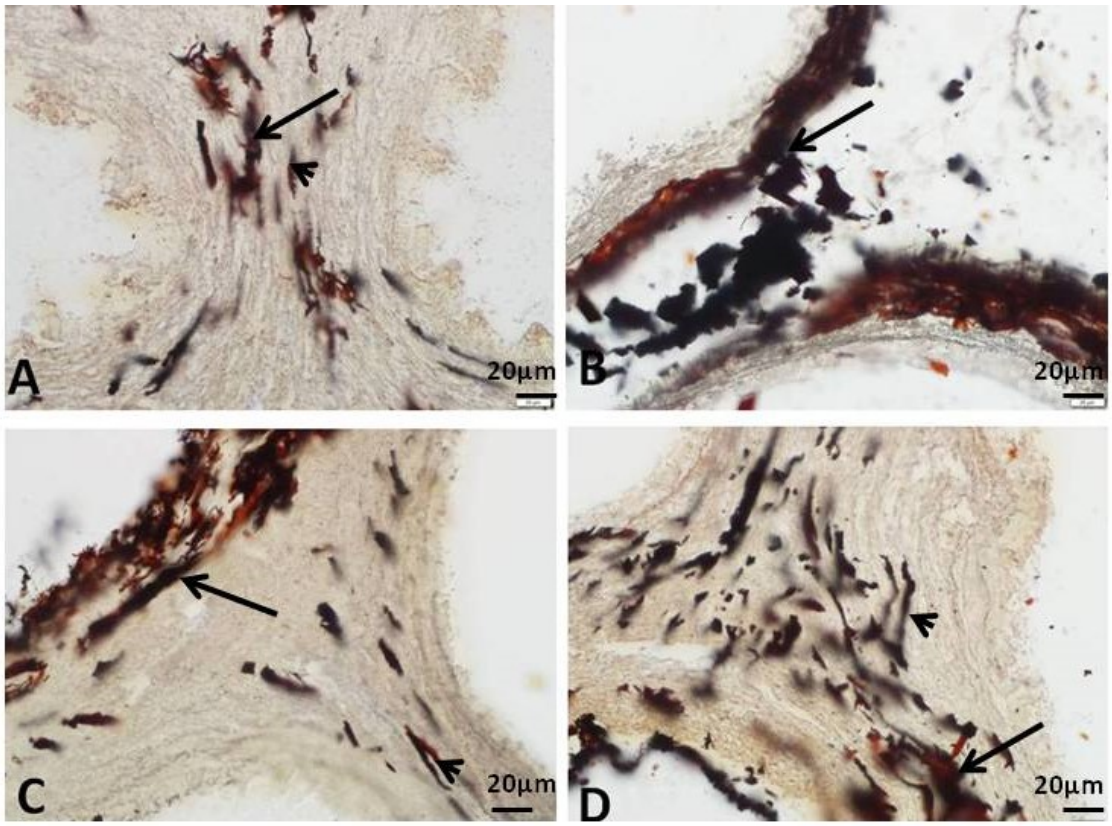

Figure 4.99. Golgi Staining of the CAUDA of the Epididymis in the Different Age Groups of the AGCR. A. Prepubertal: B. Pubertal: C. Adult: D. Aged: Note the display of thick nerve bundles (long arrow) and solitary nerve fibres (arrow head) along the PMC and the epididymal interstitium. Scale bar: 20µm

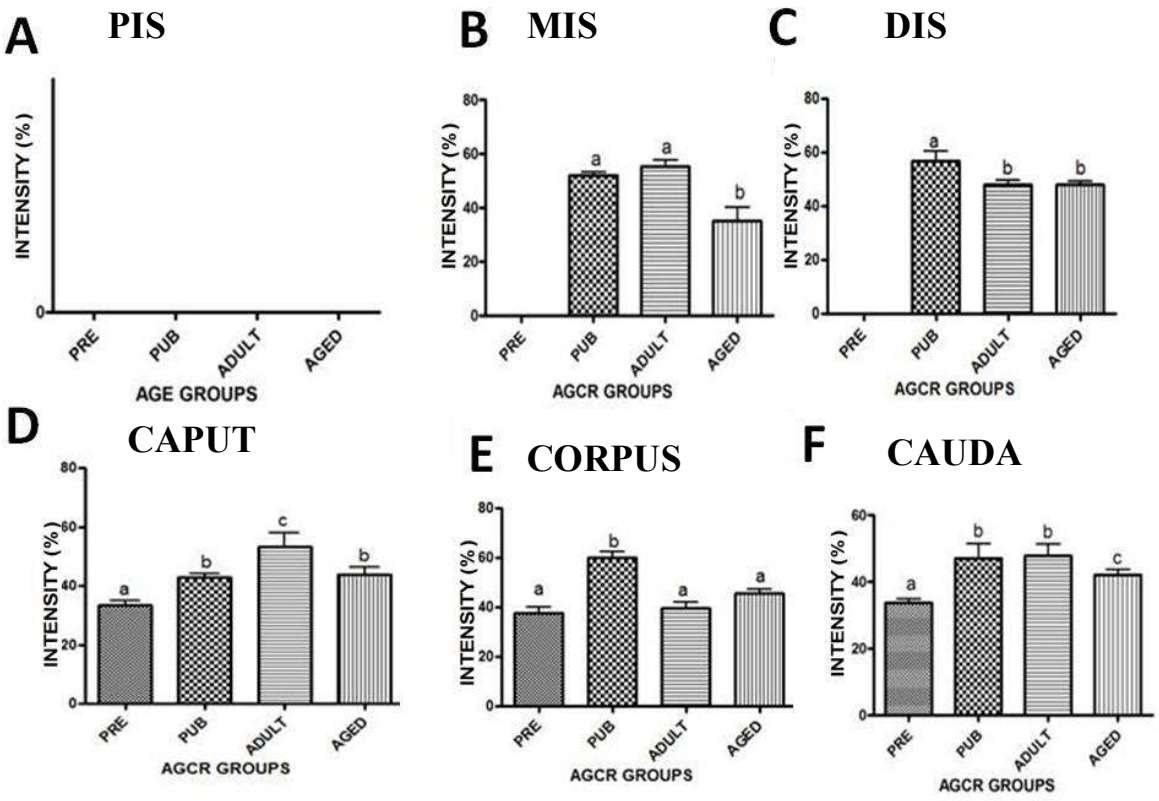

Figure 4.100 A-F. Age-related Changes in Intensity of Golgi-Silver Impregnation Staining of the Epididymal Segments in AGCR. A Proximal initial segment (PIS); B Middle initial segment (MIS); C Distal initial segment (DIS); D. Caput; E. Corpus; F Cauda. Bars bearing dissimilar alphabet superscripts (a,b, c) are significantly different.

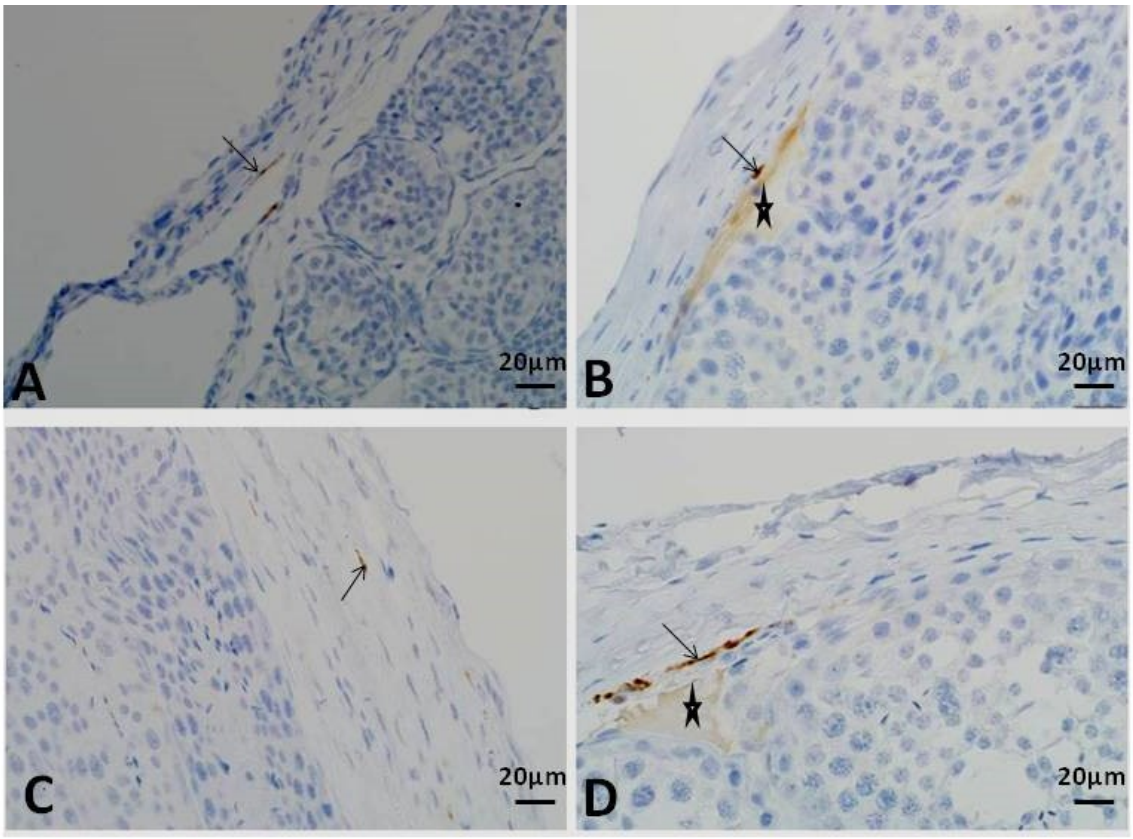

Figure 4.101. Photomicrographs of Neurofilament (NF)Expression in the Testicular Capsule of Different Age Groups of AGCR. A. Prepubertal: B. Pubertal: C. Adult: D. Aged: Note the positive NF staining of nerve structures in the tunica albuginea (arrows) and peri-albuginea interstitium (star). Immunostain: Neurofilament; Scale bar: 20µm

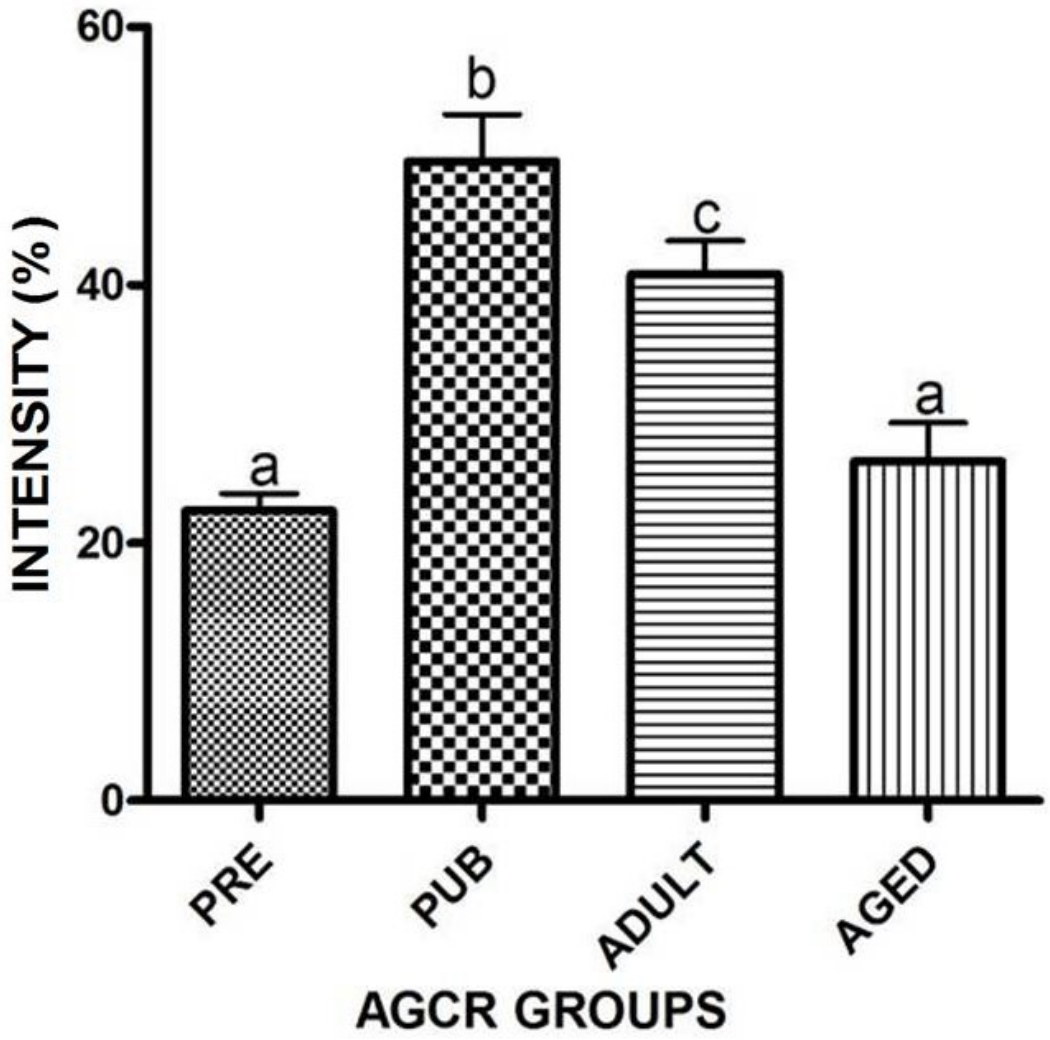

Figure 4.102. Age-related Changes in the Intensity of Neurofilament (NF) Expression in the Testicular Capsule in AGCR. Bars bearing dissimilar alphabet superscripts (a,b,c) are significantly different.

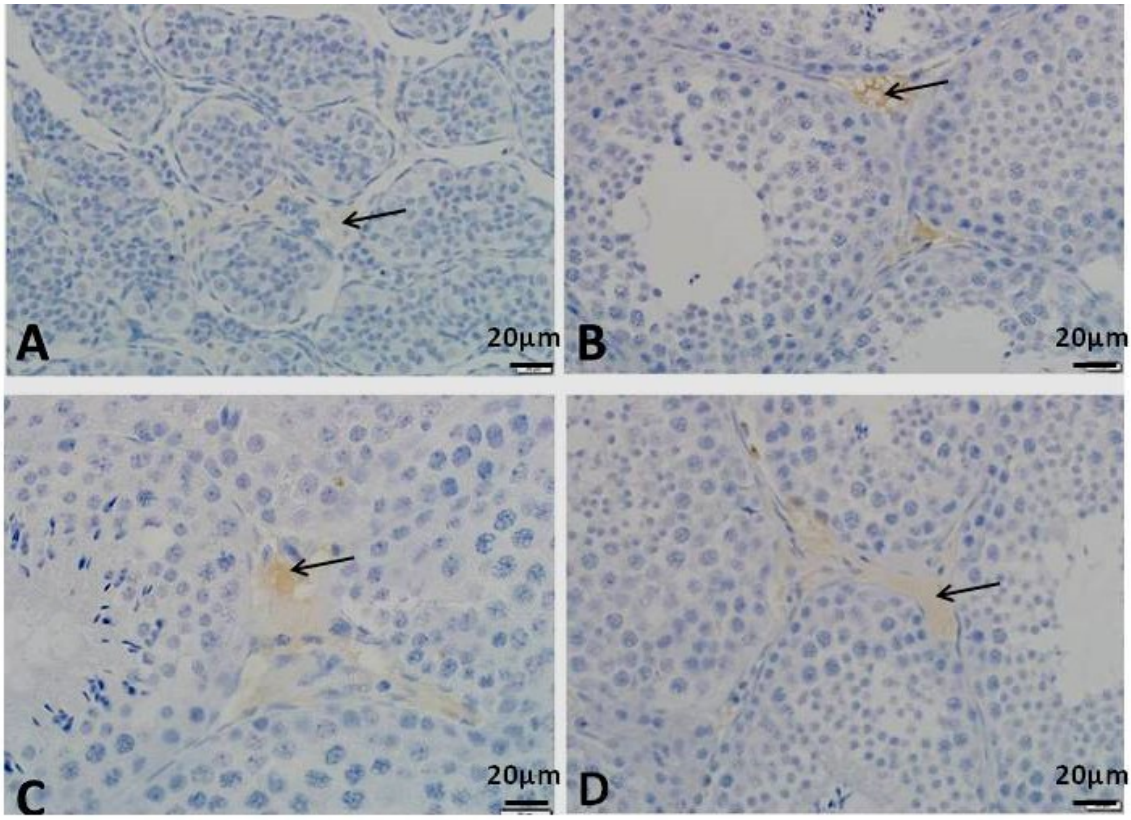

Figure 4.103. Photomicrographs of Neurofilament(NF) Expression in the Testis of Different Age Groups of AGCR. A. Prepubertal: B. Pubertal: C. Adult: D. Aged: Note the positive NF staining of nerve structures in the seminiferous tubular interstitium (arrows). Immunostain: Neurofilament. Scale bar: 20µm

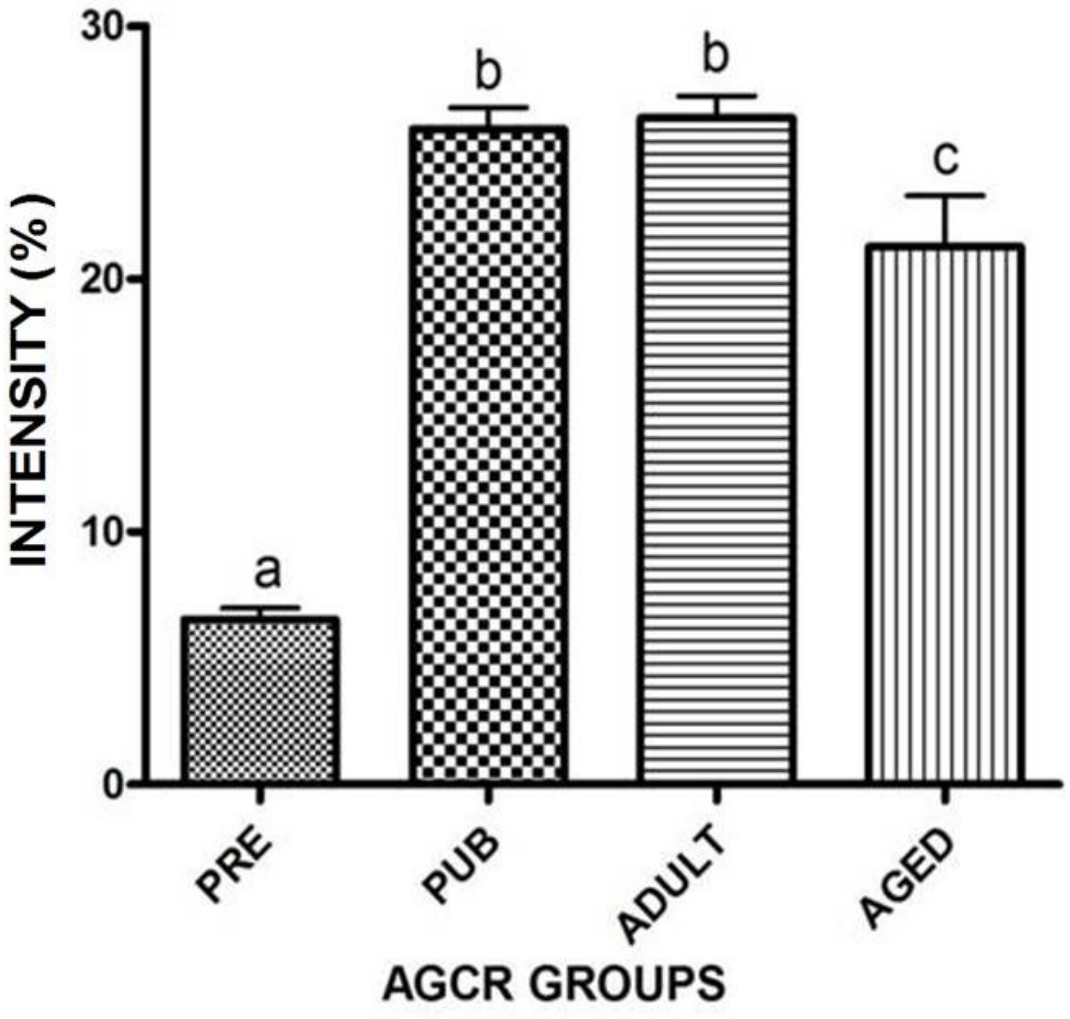

Figure 4.104. Age-related Changes in the Signal Intensity of Neurofilament (NF) Expression in the Testicular Parenchyma in AGCR. Bars bearing dissimilar alphabet superscripts (a,b,c) are significantly different.

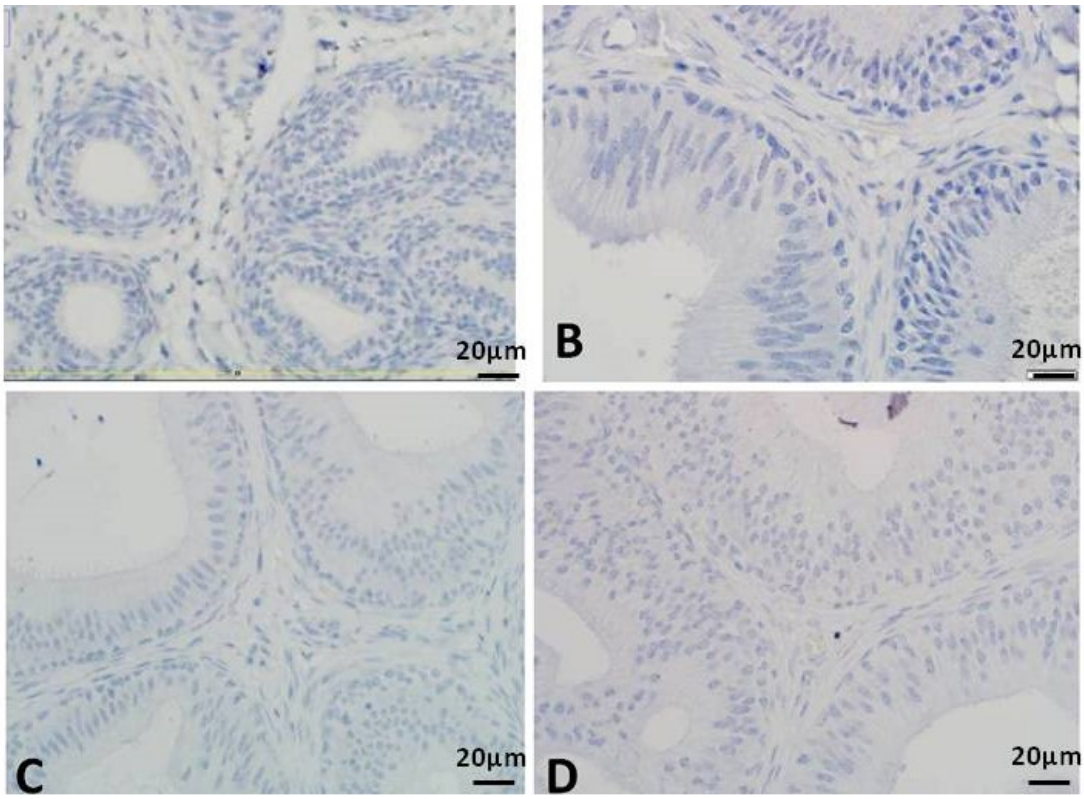

Figure 4.105. Photomicrographs of Neurofilament (NF) Expression in the Proximal Initial Segment (PIS) of Epididymis in AGCR. A. Prepubertal B. Pubertal C. Adult D. Aged. Note the negative staining of the epididymal structures. Scale bar: 20µm

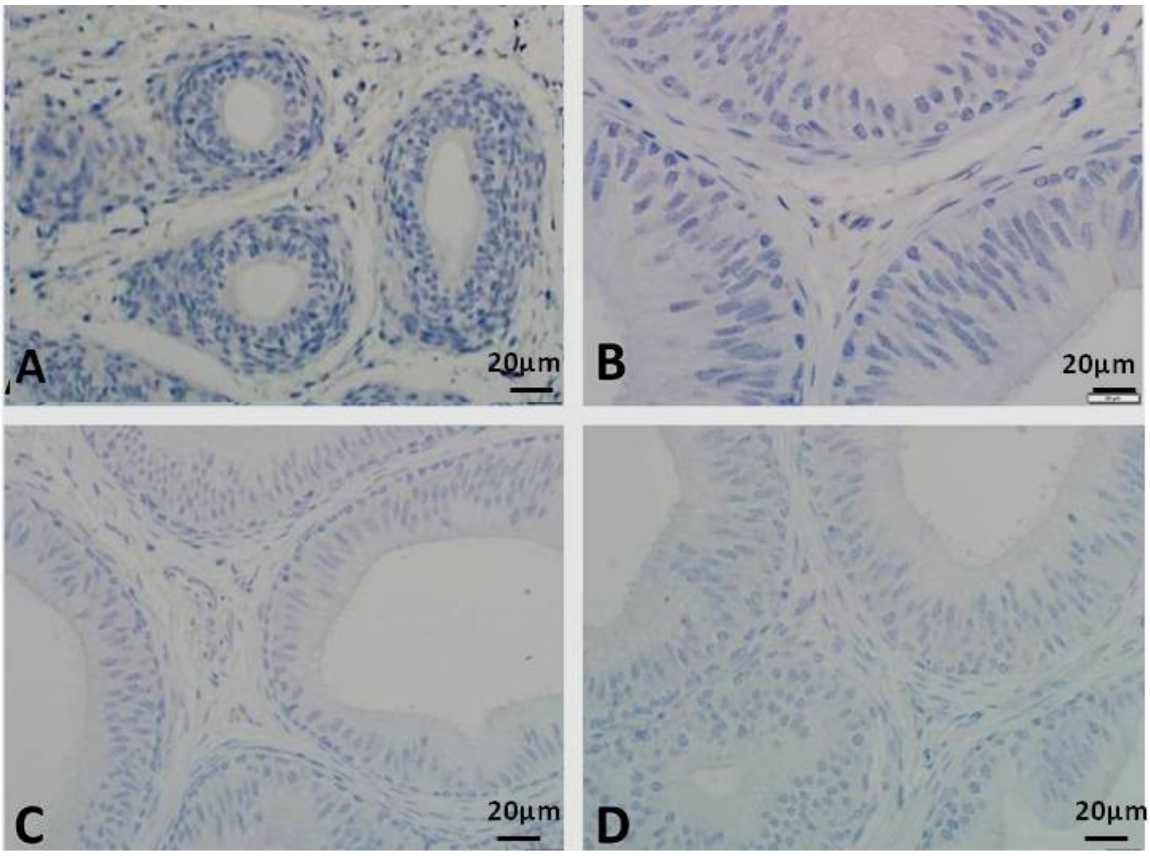

Figure 4.106. Photomicrographs of Neurofilament(NF) Expression in the Middle Initial Segment (MIS) of the Epididymis in AGCR. A. Prepubertal B. Pubertal C. Adult D. Aged. Note the negative staining of the epididymal structures in all groups.

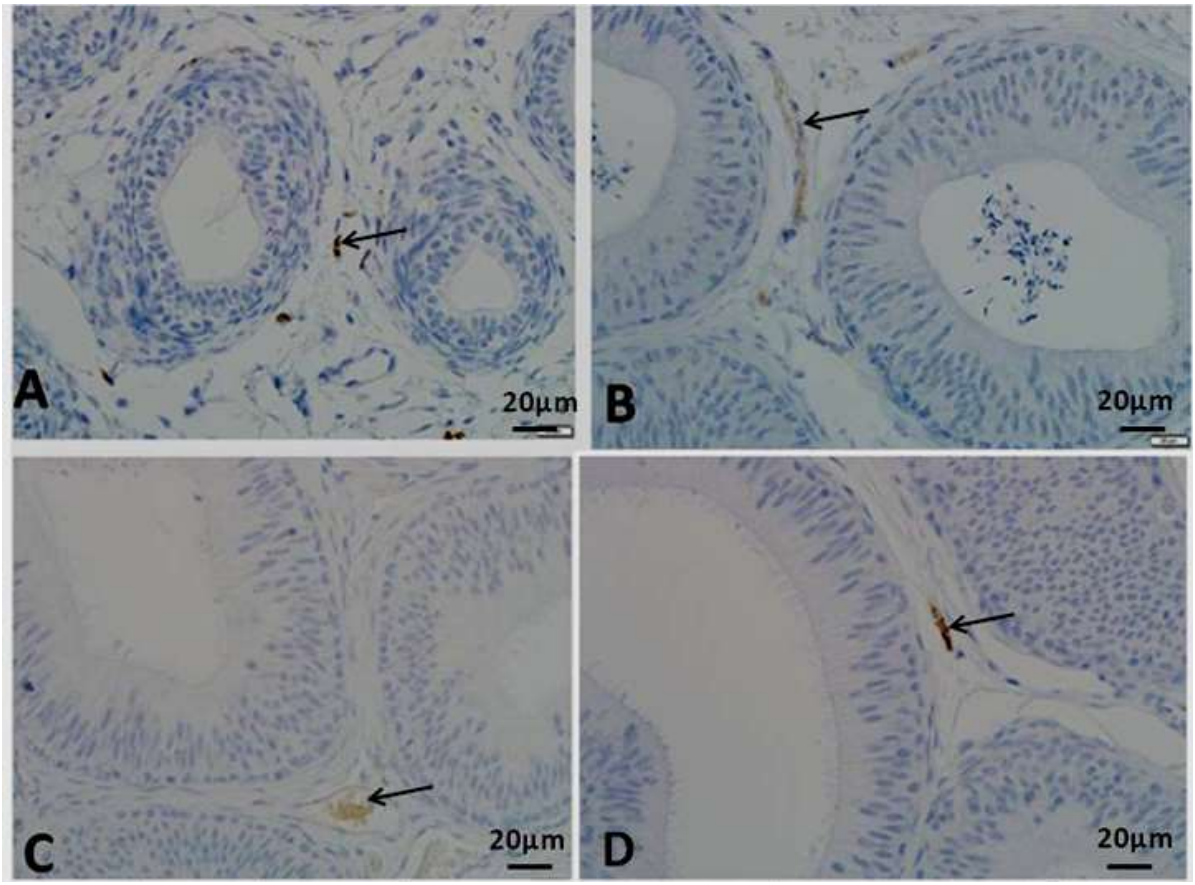

Figure 4.107. Photomicrographs of Neurofilament (NF) Expression in the Distal Initial Segment (DIS) of the Epididymis in AGCR. A. Prepubertal: B. Pubertal: C. Adult: D. Aged: Note the positive NF staining of nerve structures in the epididymal ductal interstitium (arrow).

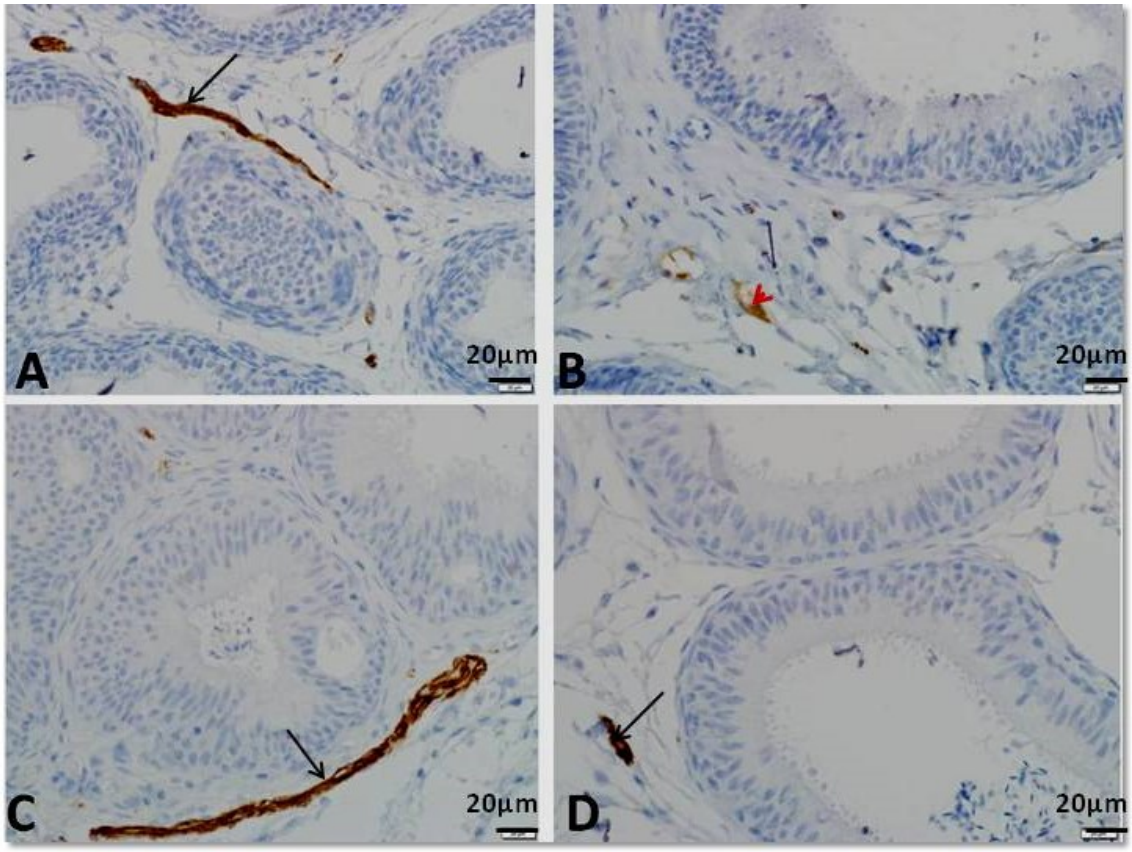

Figure 4.108. Photomicrographs of Neurofilament(NF) Expression in the CAPUT Epididymis in AGCR. A. Prepubertal: B. Pubertal: C. Adult: D. Aged: Note the positive NF staining of nerve structures in the epididymal ductal interstitium (arrow) and in perivascular area (arrow head).

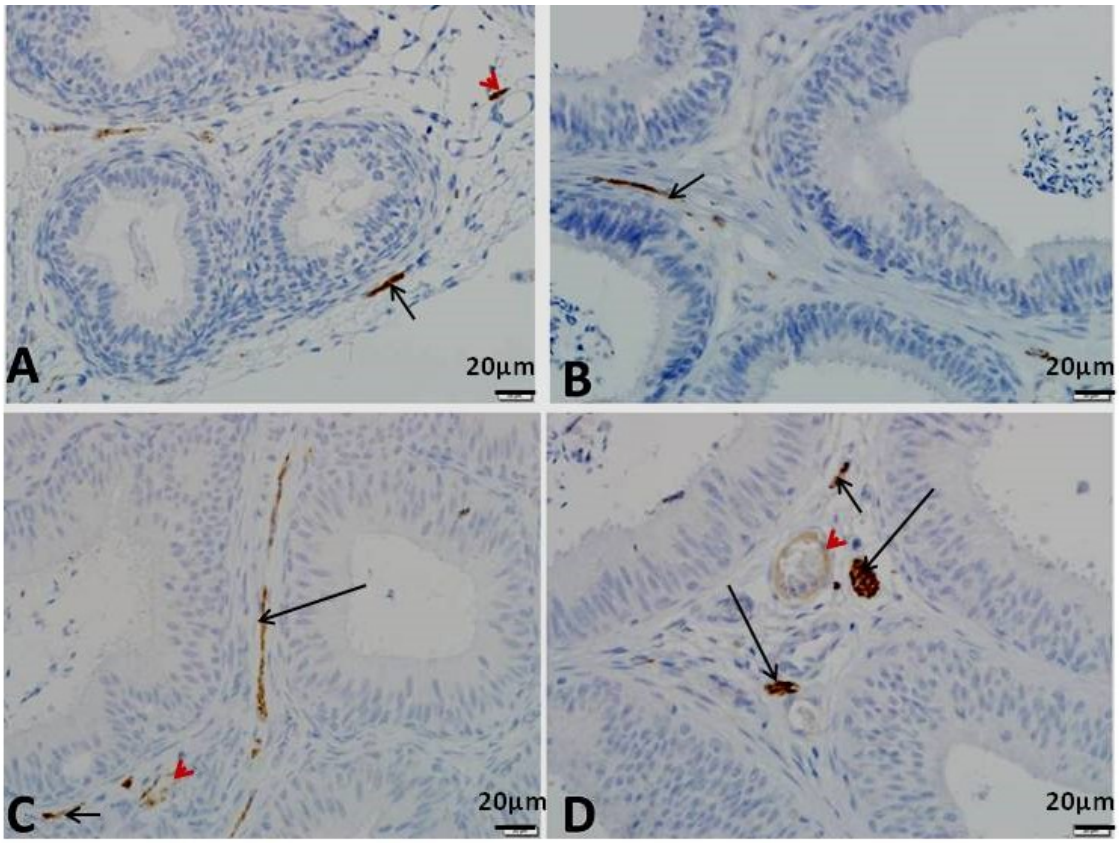

Figure 4.109. Photomicrographs of Neurofilament(NF) Expression in the CORPUS Epididymis in AGCR. A. Prepubertal: B. Pubertal: C. Adult: D. Aged: Note the positive NF staining of nerve structures in the epididymal ductal interstitium (long arrow), perivascular area (arrow head) and periductal muscle coat (short arrow).

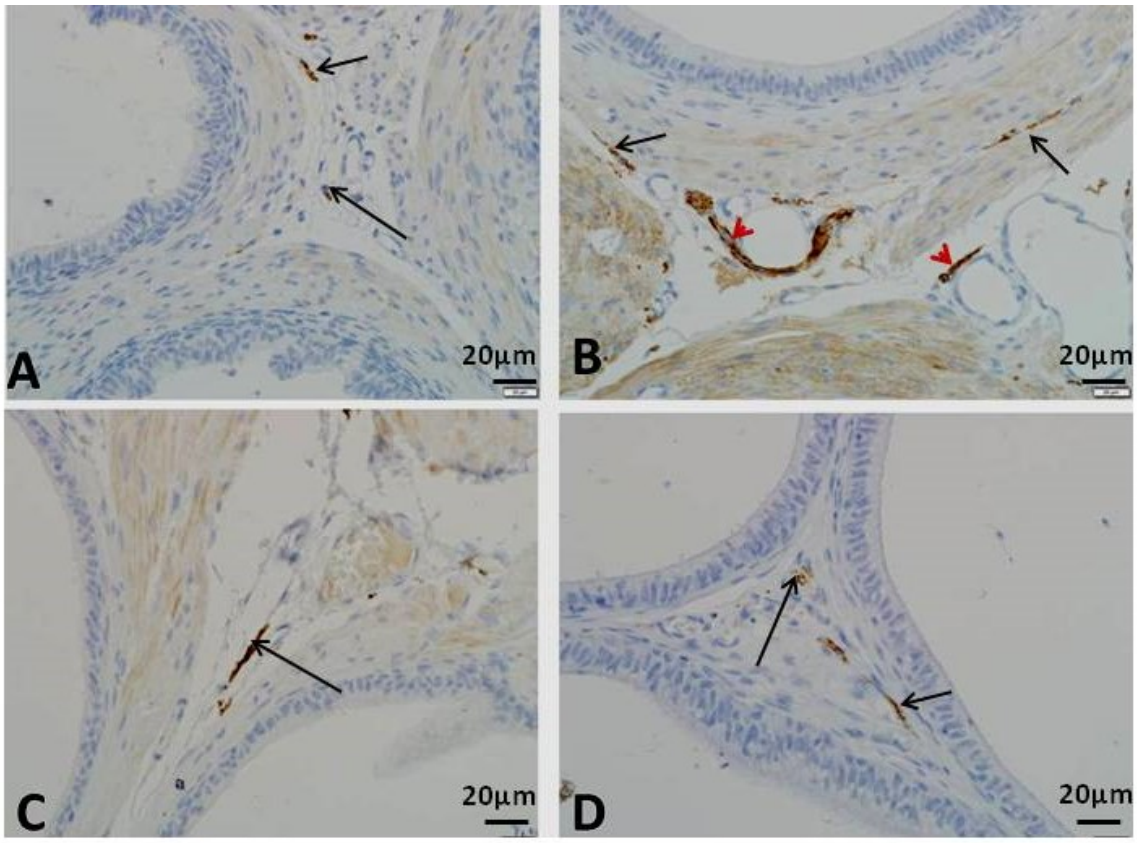

Figure 4.110. Photomicrographs of Neurofilament Expression (NF) in the CAUDASegment of Epididymis in AGCR. A. Prepubertal: B. Pubertal: C. Adult: D. Aged: Note the positive NF staining of nerve structures in the epididymal ductal interstitium (long arrow), perivascular area (arrow head) and periductal muscle coat (short arrow). Scale bar: 20µm

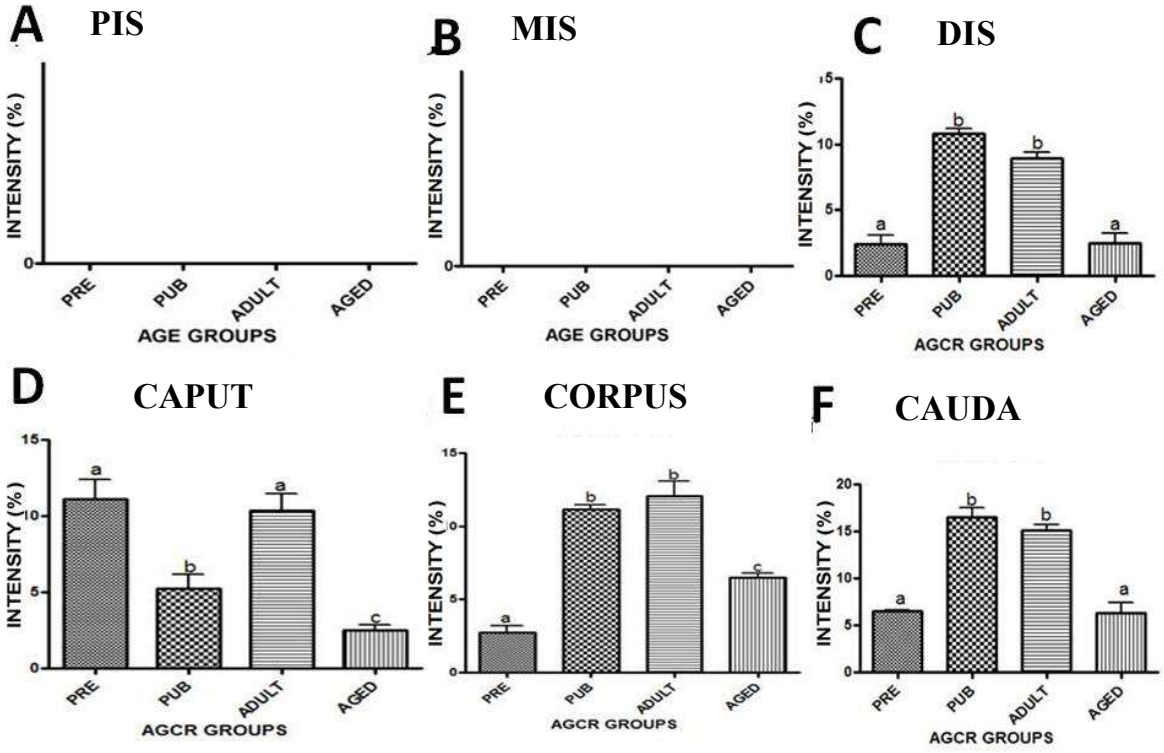

Figure 4.111 A-F Age-related Changes in the Intensity of Neurofilament (NF) Expression in the Epididymal Segments in AGCR. A Proximal initial segment (PIS); B Middle initial segment (MIS); C Distal initial segment (DIS); D. Caput; E. Corpus; F Caudal. Bars bearing dissimilar alphabet superscripts (a,b,c) are significantly different.

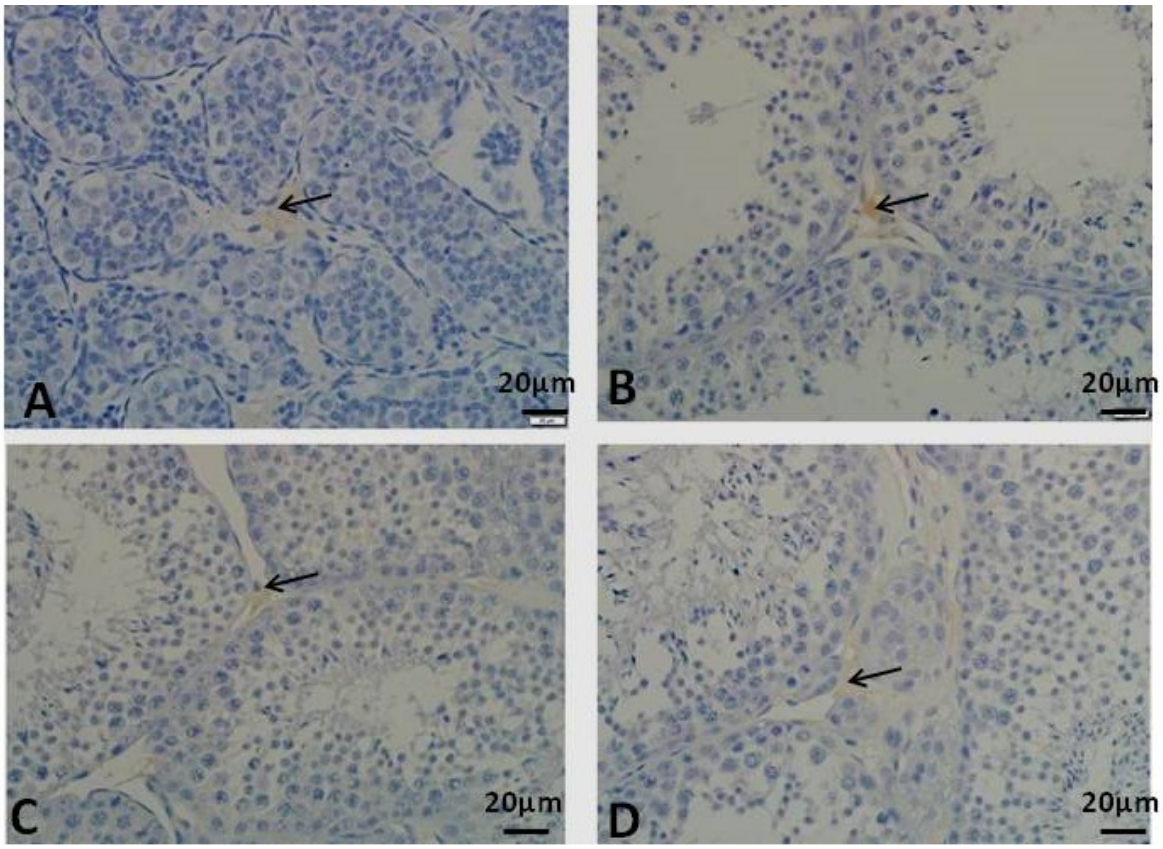

Figure 4.112. Photomicrographs of Glial Fibrillary Acid Protein (GFAP) Expression in the Testis of different Age Groups of the AGCR. A. Prepubertal: B. Pubertal: C. Adult: D. Aged: Note the positive GFAP staining of astrocyte-like cells in seminiferous tubular interstitium (arrow). Scale bar: 20µm.

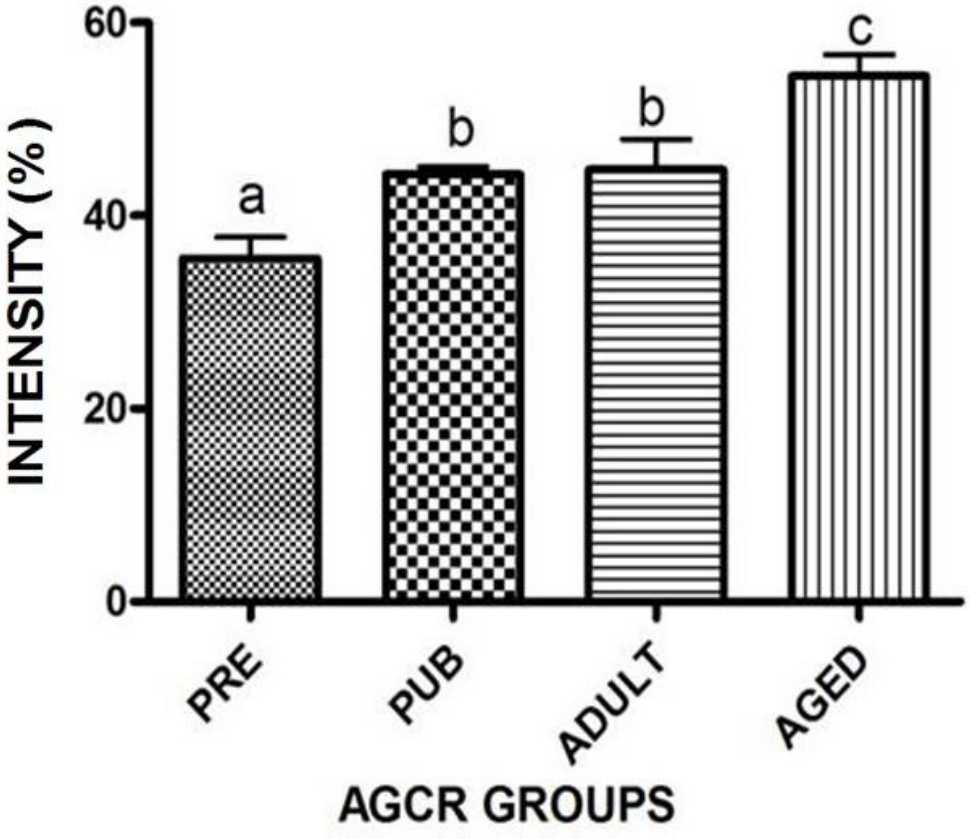

Figure 4.113. Age-related Changes in Intensity of Glial Fibrillary Acid Protein (GFAP) Expression in the Testicular Parenchyma in AGCR. Bars bearing dissimilar alphabet superscripts (a,b, c) are significantly different.

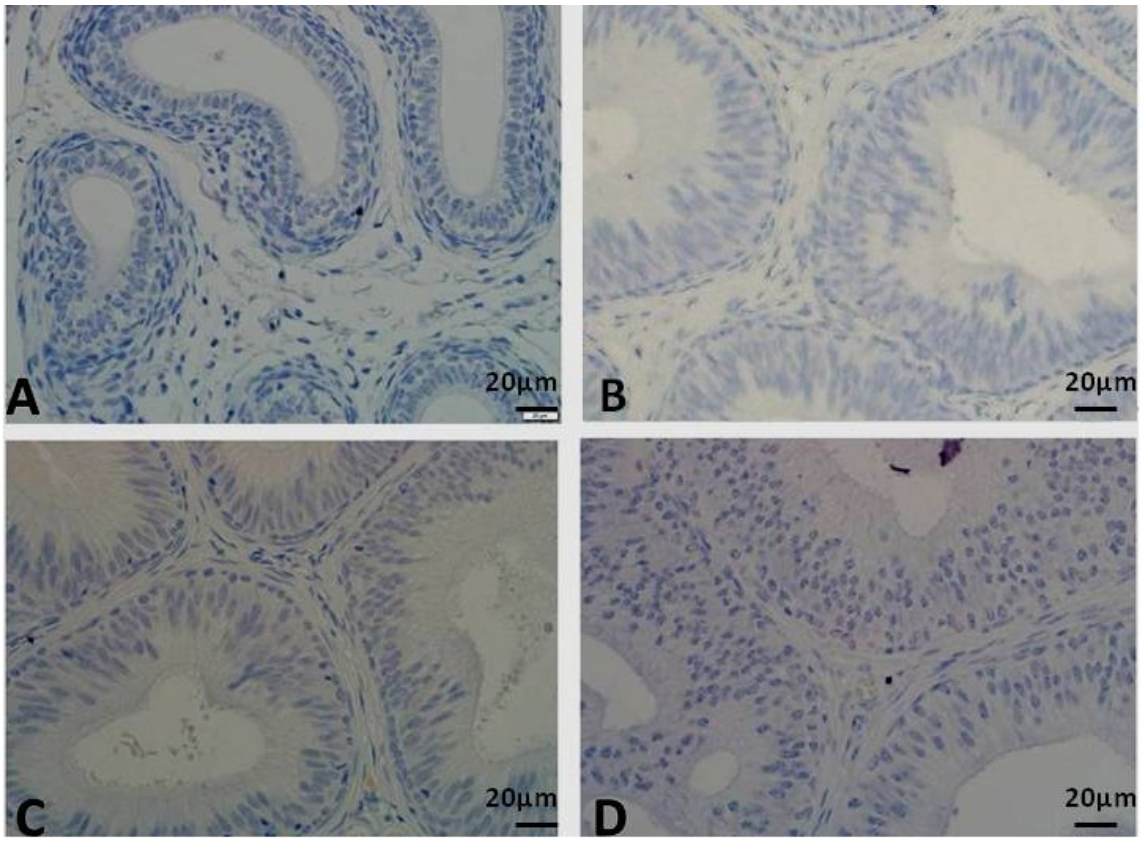

Figure 4.114. Photomicrographs of GFAP Expression in the Proximal Initial Segment (PIS) of theEpididymis in AGCR. A. Prepubertal: B. Pubertal: C. Adult: D. Aged: Note the negative GFAP staining of epididymal structures across all age groups.

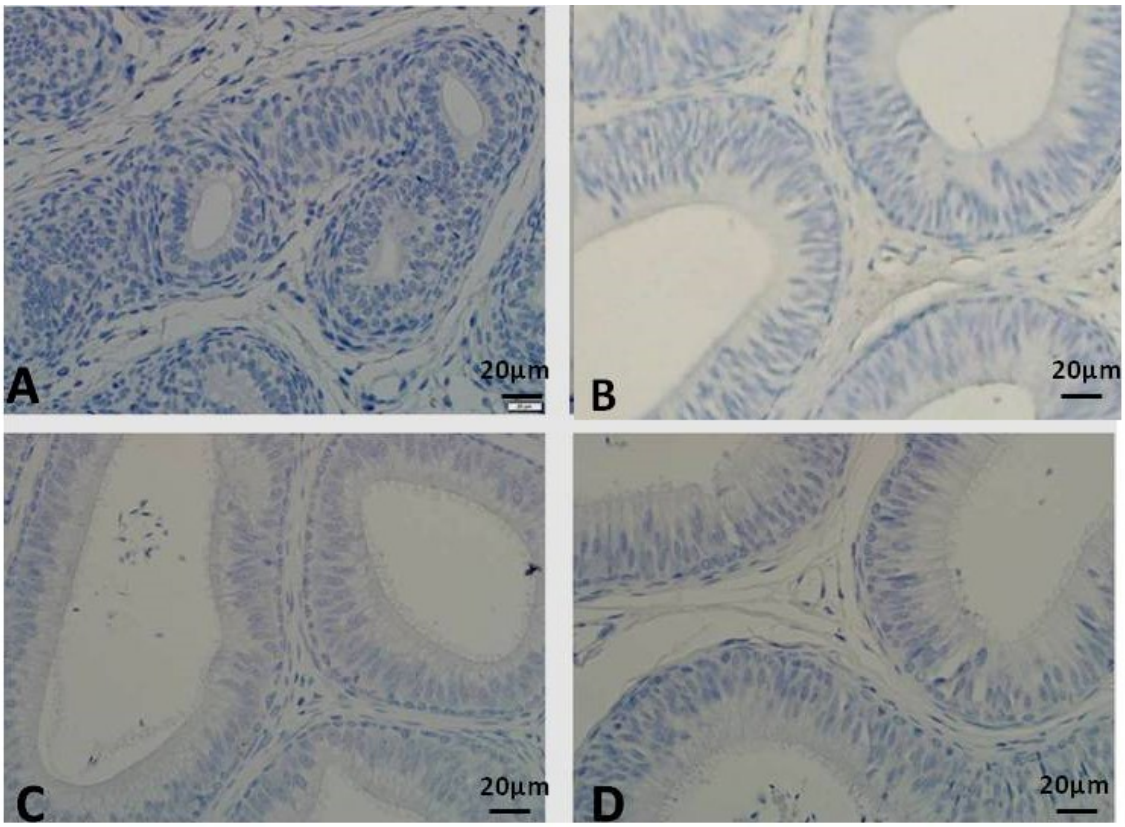

Figure 4.115. Photomicrographs of GFAP Expression in the Middle Initial Segment (MIS) of theEpididymis in AGCR. A. Prepubertal: B. Pubertal: C. Adult: D. Aged: Note the negative GFAP staining of epididymal structures across all age groups.

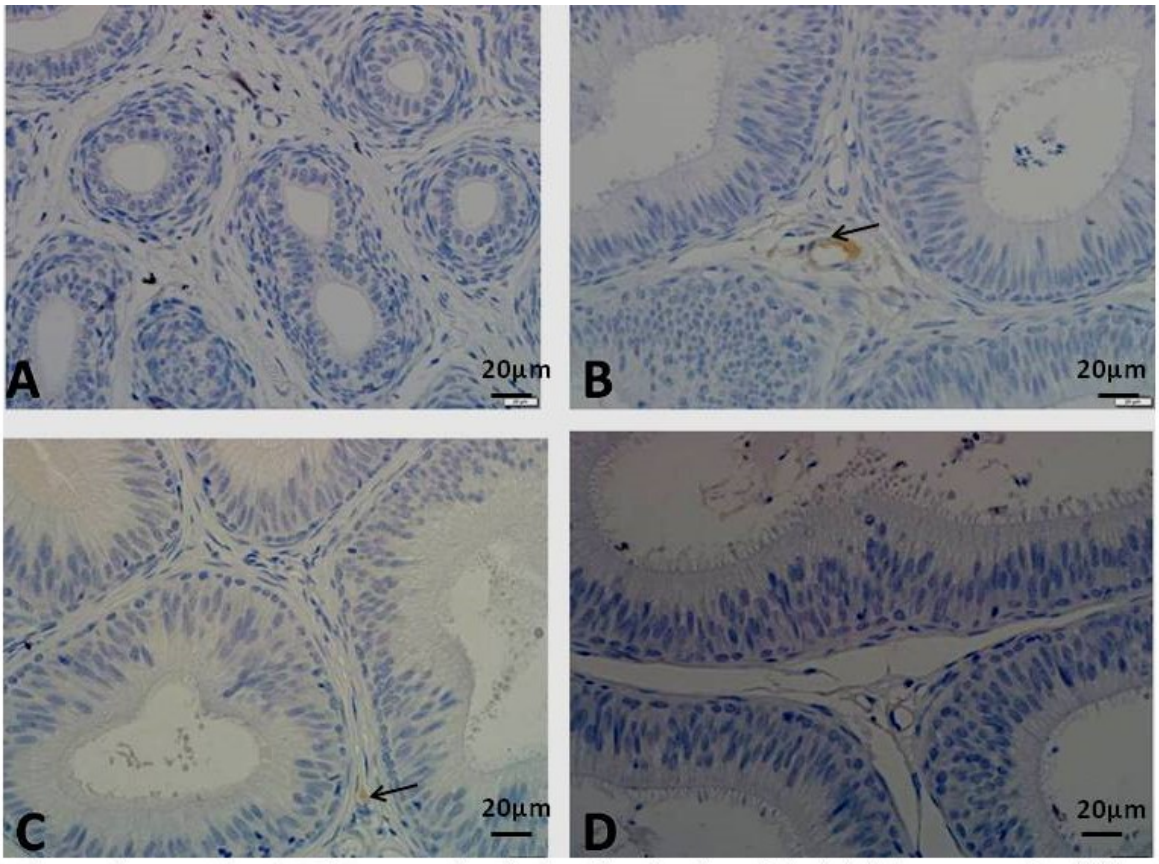

Figure 4.116. Photomicrographs of GFAP Expression in the Distal Initial Segment(DIS) of the Epididymis in AGCR. A. Prepubertal: B. Pubertal: C. Adult: D. Aged: Note the positive GFAP staining of astrocyte-like cells in the perivascular area of ductal interstitium of B and C (arrow). Scale bar: 20µm

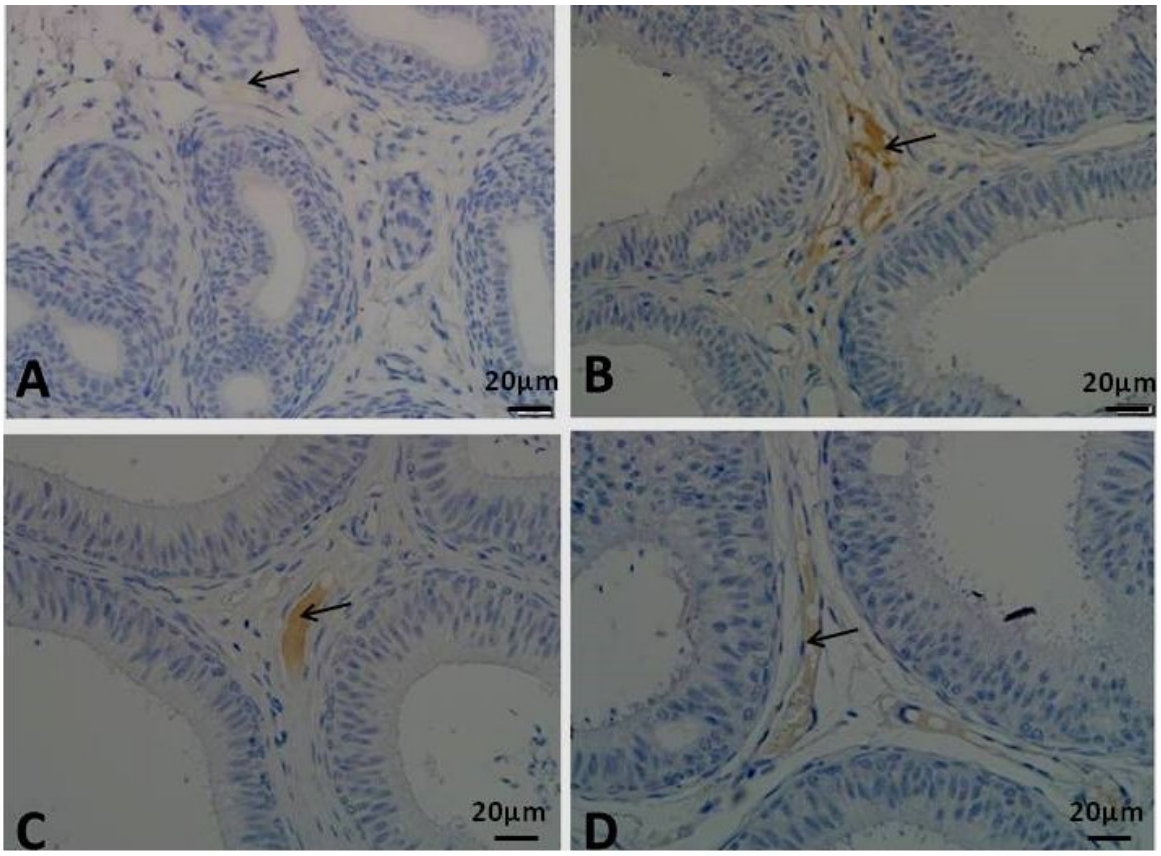

Figure 4.117. Photomicrographs of GFAP Expression in the CAPUT Segment of Epididymis in AGCR. A. Prepubertal: B. Pubertal: C. Adult: D. Aged: Note the positive GFAP staining of astrocyte-like cells in the perivascular area of ductal interstitium (arrow), in all groups.

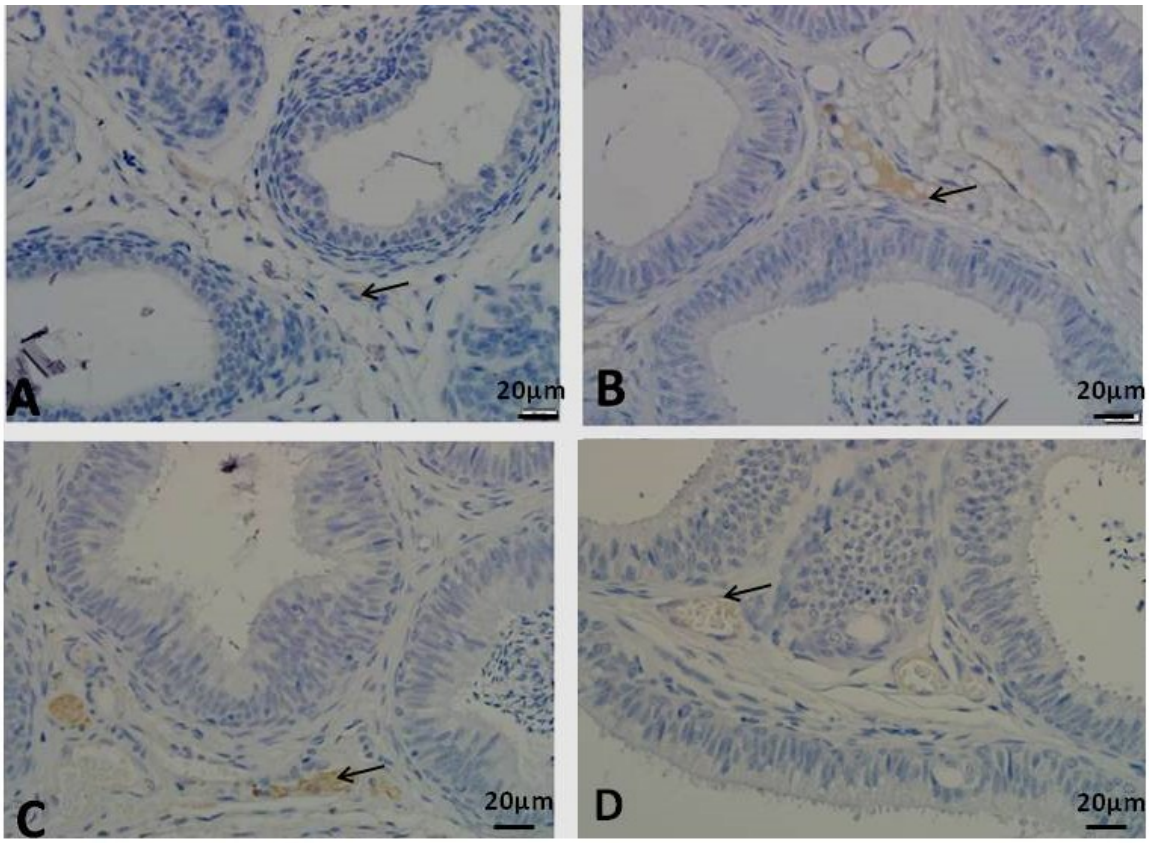

Figure 4.118. Photomicrographs of GFAP Expression in the CORPUS Segment of Epididymis in AGCR. A. Prepubertal: B. Pubertal: C. Adult: D. Aged: Note the positive GFAP staining of astrocyte-like cells in the perivascular area of ductal interstitium (arrow), in all groups.

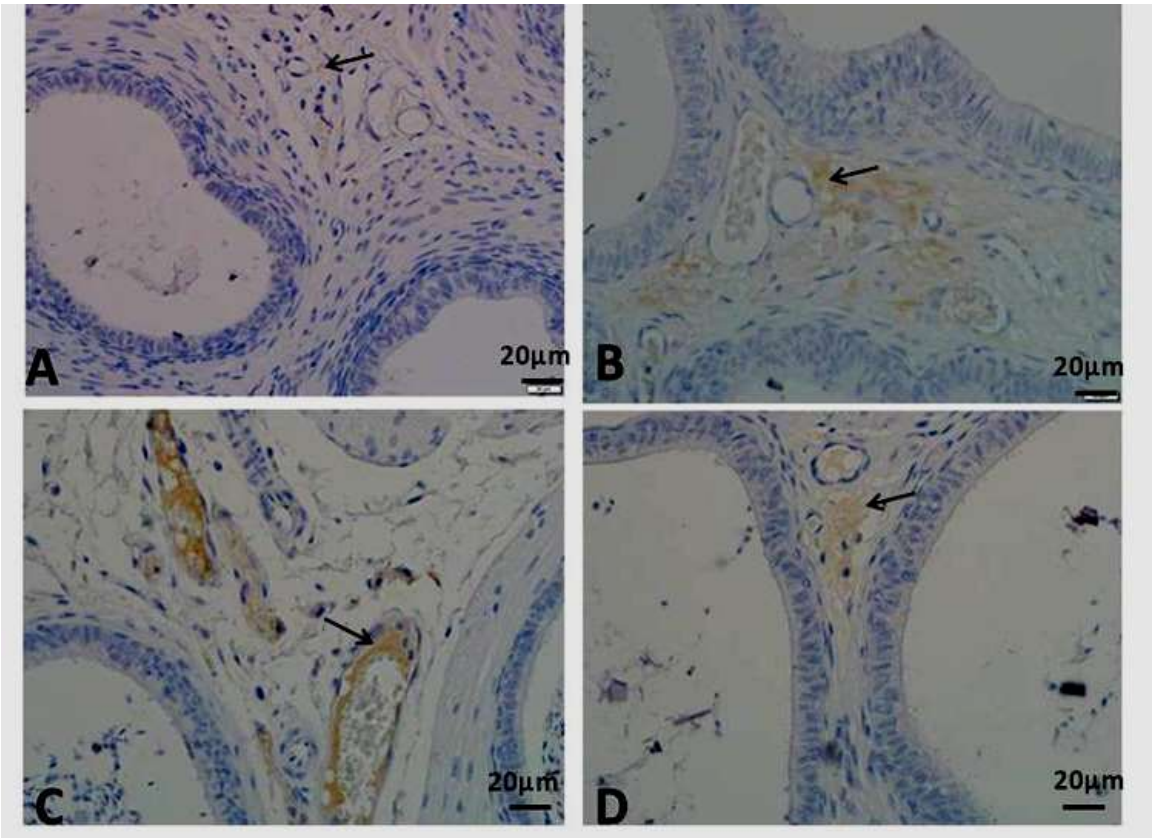

Figure 4.119. Photomicrographs of GFAP Expression in the CAUDAEpididymis in AGCR. A. Prepubertal: B. Pubertal: C. Adult: D. Aged:Note the positive GFAP staining of astrocyte-like cells in the perivascular area of ductal interstitium (arrow), in all groups. Scale bar: 20µm.

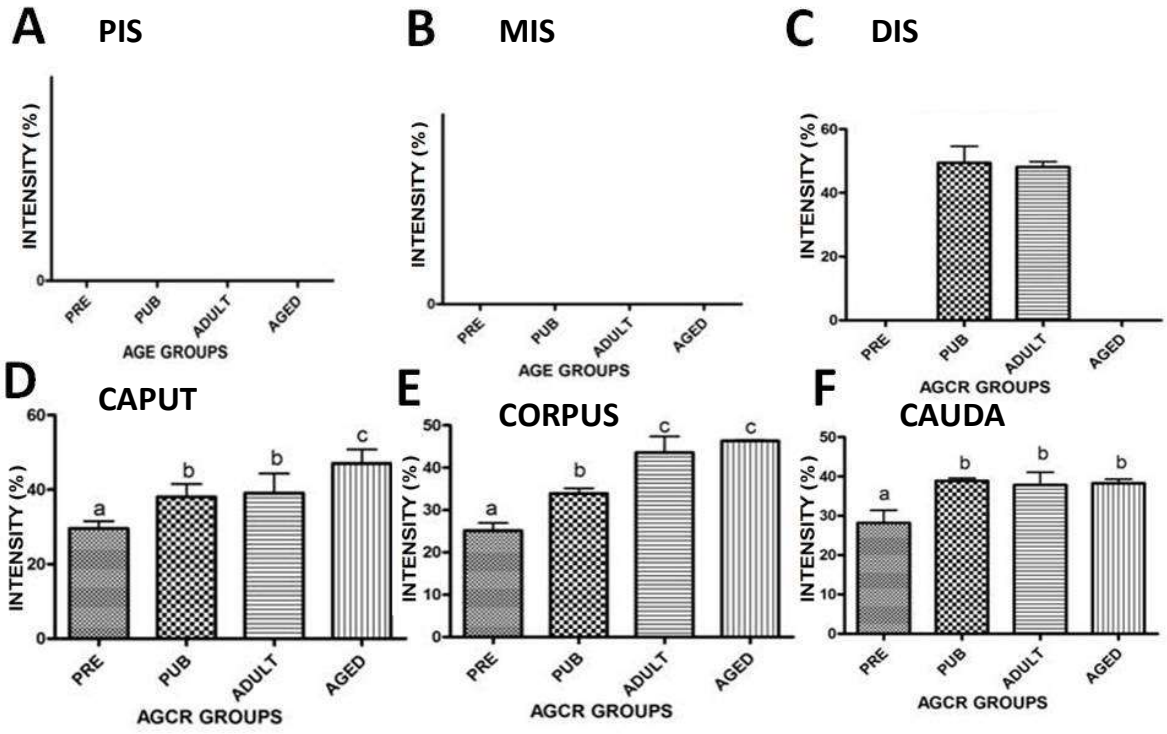

Figure 4.120 A-F. Age-related Changes in Intensity of GFAP Expression in the Epididymal Segments in the AGCR.A Proximal initial segment (PIS); B Middle initial segment (MIS); C Distal initial segment (DIS); D. Caput; E. Corpus; F Cauda. Bars bearing dissimilar alphabet superscripts (a,b,c) are significantly different.

4.5 EXPERIMENT FIVE

4.5.1 Age-related Changes in the Serum Hormonal Profiles of the African Greater Cane Rat

4.5.1.1 Serum Testosterone Level

There was a significant elevation in the serum testosterone level of the adult AGCR when compared to others (Fig. 4.121; Table 4.6). Conversely, serum testosterone level was markedly lower in the prepubertal AGCR relative to other groups (Fig. 4.121;Table 4.6). In this study, serum testosterone profile across the different age group of AGCR appears to progressively increase with age advancement with peak level observed in the adult rat and later followed by an insignificant ($p>0.05$) decline level inthe aged rats.

4.5.1.2 Serum Luteinising Hormone Level

Serum luteinising hormone level was significantly higher ($p<0.05$) in the pre-pubertal AGCR relative other groups (Fig. 4.122;Table 4.6). However, there was no significant difference ($p>0.05$) in the LH levels in both adult and aged AGCR. (Fig. 4.122;Table 4.6). With the exception of the peak level of LH seen in the pre-pubertal AGCR, the profile of LH produced across all AGCR groups seems to decrease with advancing age.

4.5.1.3 Serum Follicle Stimulating Hormone Level

Serum follicle stimulating hormone level was significantly elevated ($p<0.05$) in the pre-pubertal AGCR when compared to other groups (Fig. 4.123;Table 4.6). On the contrary, there was no significant difference ($p>0.05$) in the FSH levels of pubertal, adult and aged AGCR (Fig. 4.123;Table 4.6). The trend of FSH levels across the different AGCR groups appeared to decrease with age variation except for the peak observed in the pre-pubertal AGCR.

4.5.1.4 Serum Estrogen Level

There was a significant increase in the serum estrogen level of the aged AGCR relative to other groups (Fig. 4.124;Table 4.6). In addition, there was no significant difference in the estrogen levels of prepubertal and pubertal AGCR, though; a slight insignificant increase was seen in the estrogen value of the pubertal AGCR (Fig. 4.124;Table 4.6). Interestingly, estrogen hormone level observed in this study progressively increases with age.

4.5.1.5 Serum Progesterone Level

Serum progesterone level was significantly elevated in the pubertal AGCR compared to other groups (Fig. 4.125;Table 4.6). With the exception of the remarkable climax seen in the level of progesterone of pubertal, there was no significant difference in estrogen level of others,

though, an insignificant increase exists in the values of adult and aged over prepubertal (Fig. 4.125;Table 4.6). Thus, a trend of fairly stable level was seen with age advancement.

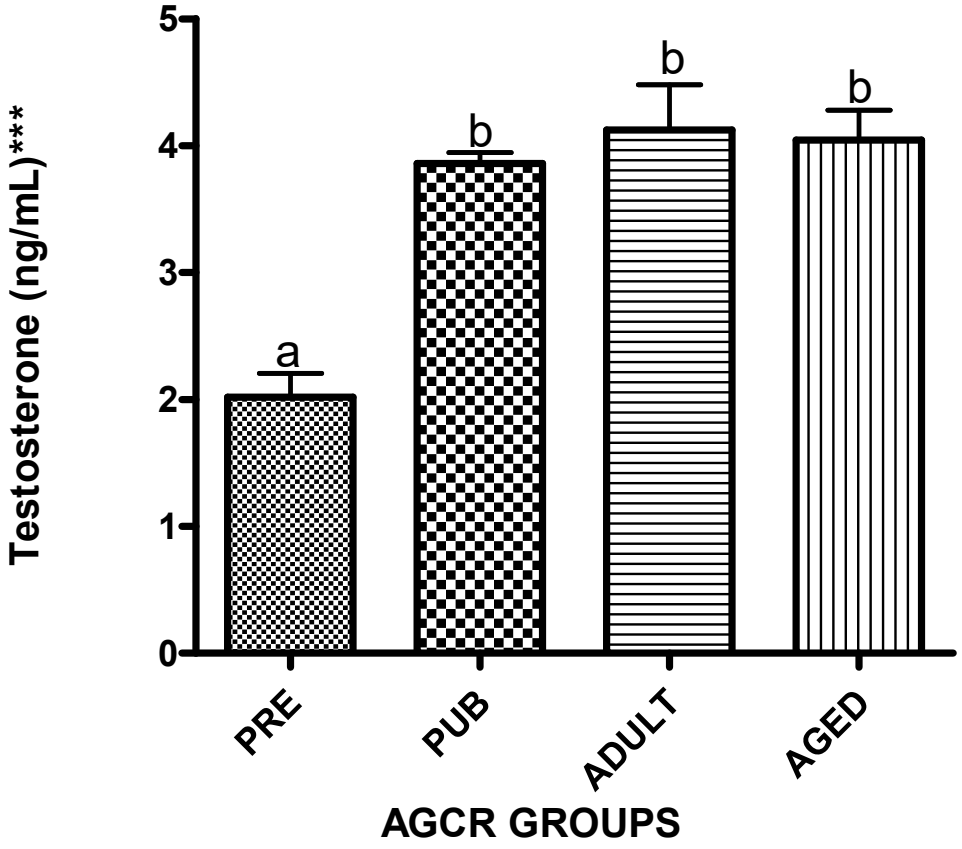

Figure 4.121. Age-related Changes in the Testosterone Level in AGCR. Bars bearing dissimilar superscripts (a,b, c) are significantly different.

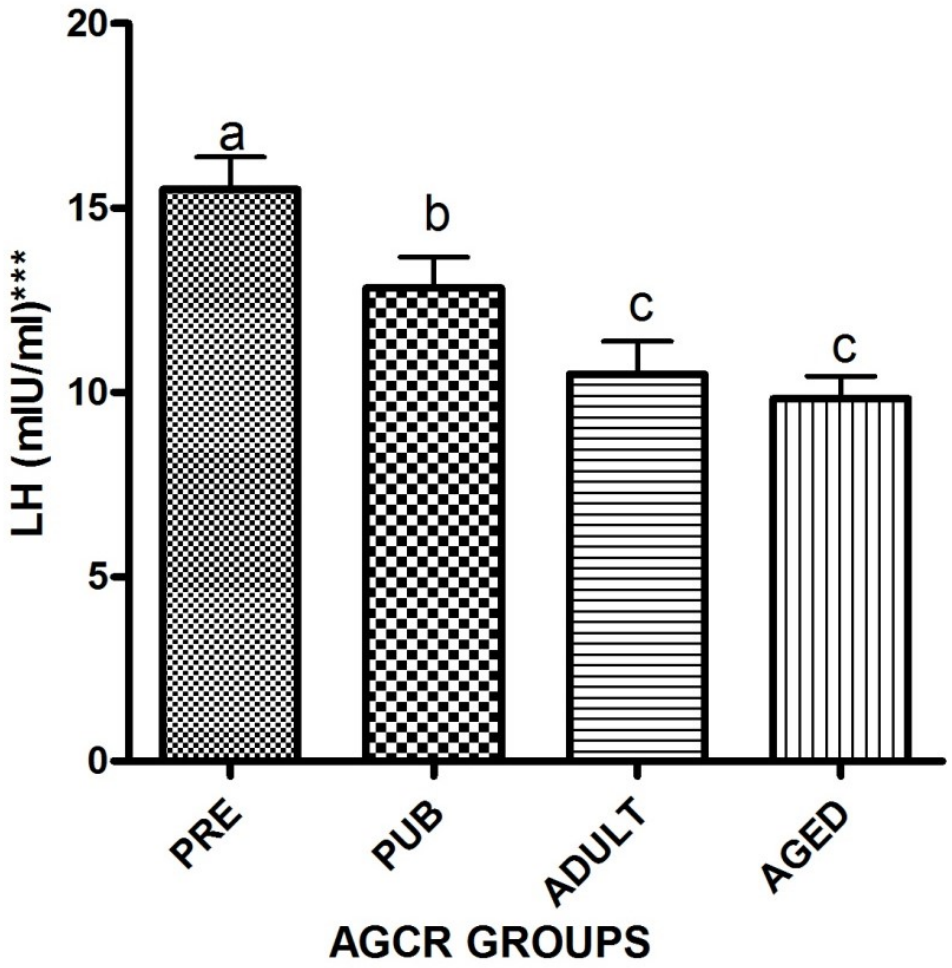

Figure 4.122. Age-related Changes in the Luteinising Hormone Level in AGCR. Bars bearing dissimilar superscripts (a,b, c) are significantly different.

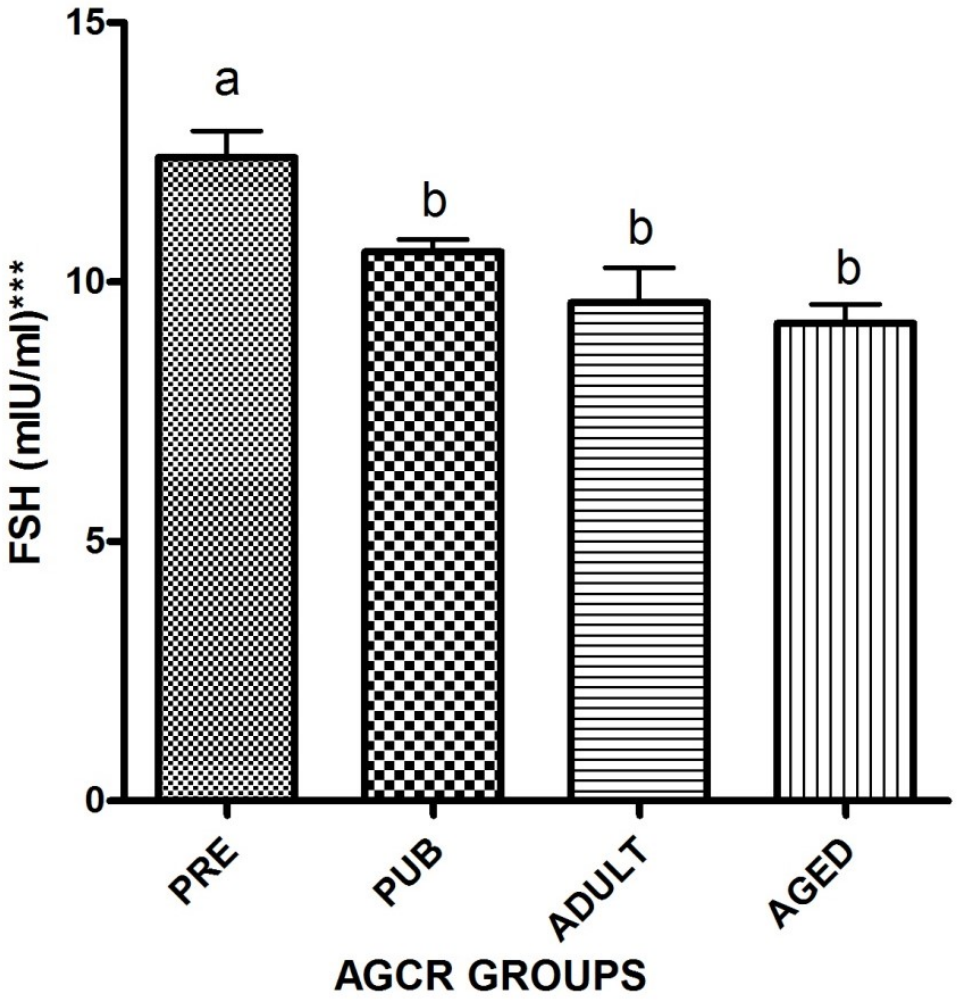

Figure 4.123. Age-related Changes in the Follicle Stimulating Hormone Level in AGCR. Bars bearing dissimilar superscripts (a,b, c) are significantly different.

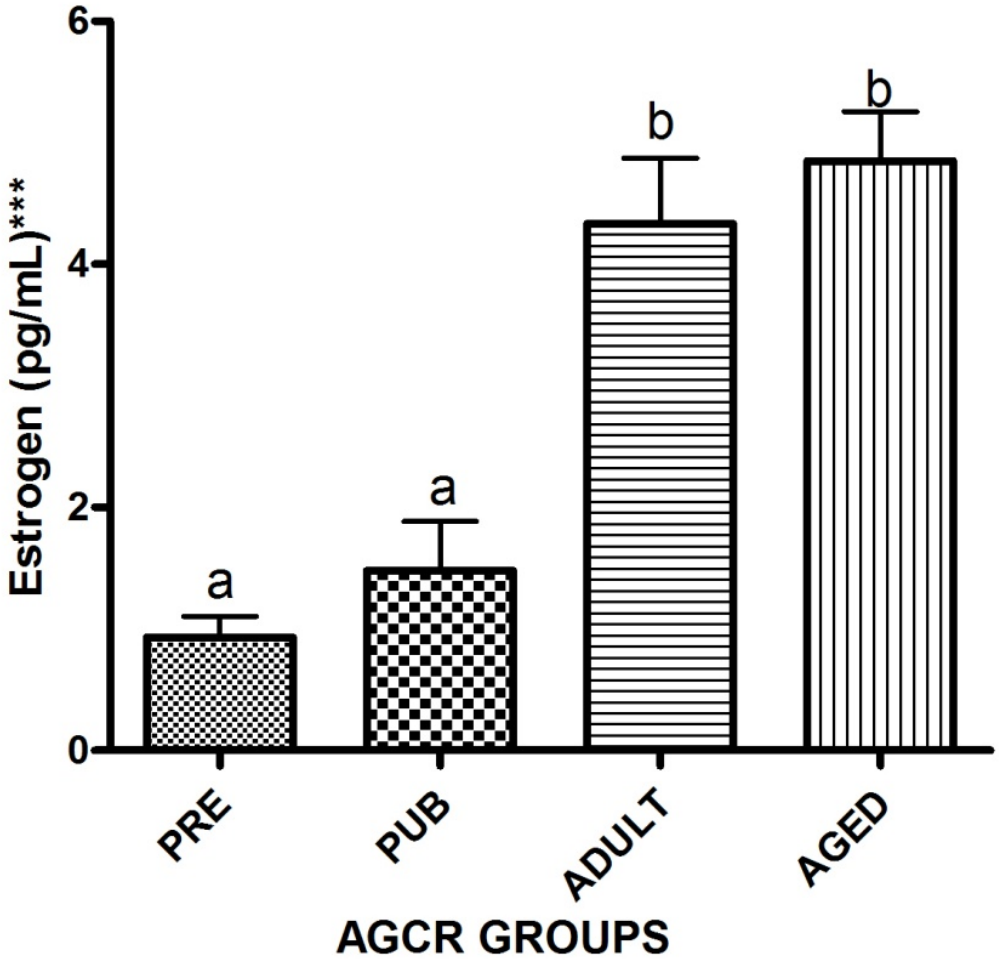

Figure 4.124. Age-related Changes in the Estrogen Level in AGCR. Bars bearing dissimilar superscripts (a,b, c) are significantly different.

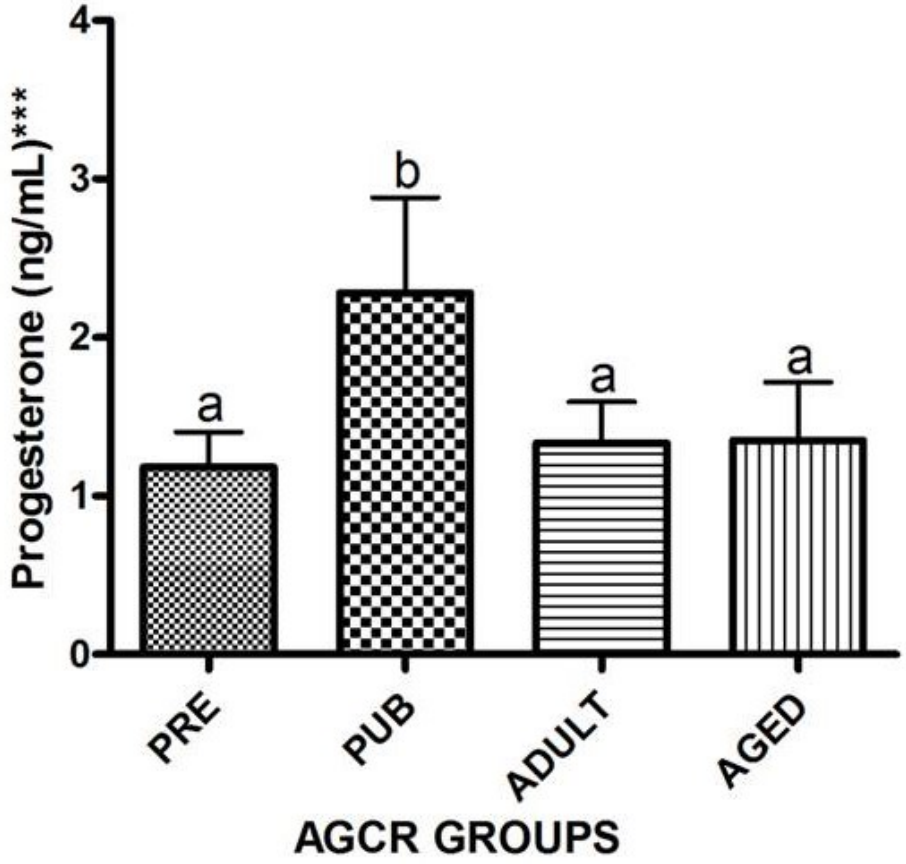

Figure 4.125. Age-related Changes in the Progesterone Level in AGCR. Bars bearing dissimilar superscripts (a,b, c) are significantly different.

Table4.6. Age-related Changes in the Serum Sex Hormone Levels of the African Greater Cane Rat.

	AGCR GROUPS			
HORMONE	**PP**	**PB**	**AD**	**AG**
TESTOSTERONE (ng/ML)	2.02±0.19[a]	3.85±0.29[b]	4.12±0.15[b]	4.07±0.26[b]
PROGESTERONE (ng/ML)	1.10 ± 0.30[a]	1.49±0.49[b]	0.97±0.19[a]	0.99± 0.22[a]
FSH (mIU/ml)	12.33±0.83[a]	10.58±0.95[b]	9.50±0.6[b]	9.25±0.70[b]
LH (mIU/ml)	15.50±0.88[a]	12.83±1.20[b]	10.17±0.83[c]	9.83±0.60[c]
ESTROGEN (pg/ML)	0.94±0.00[a]	1.48±0.40[a]	4.33±0.82[b]	4.85±0.41[b]

Values with different alphabet superscripts (a, b, c) in the same row are significantly different

CHAPTER FIVE

5.0 DISCUSSION

The characteristic cream to milky-white colouration and ellipsoidal shape of the testes observed in the different age groups of the African greater cane rat is consistent with the reports of Olukole *et al*. (2009) on the testicular gross morphologic appearance in the mature adult cane rat. The progressive age-related increase in the testicular weight and the relative testicular weight with maximum testiculo-somatic weight value displayed by the adult group of cane rat implies that with advancement in age, testicular weights increase with increase body weight. The rise in the values of these indices could probably be related to the functional reproductive status of the testicular parenchymal tissue from pubertal age to the aged. The range of the extremes of the relative weights in adult) further tallies with the earlier report of Olukole *et al.* (2009) on the smaller nature of cane rat testes relative to their body size. The measurement of testicular biometric parameters (length, width and circumference) most especially the scrotal circumference has been found to provide an indirect measurement of testicular size, volume and onset of active spermatogenesis (Bongso *et al.,* 1982). Therefore, the significant age-dependent increase in testicular biometric parameters could also be attributed to morphological compensation required to meet up with the varying reproductive functional activities with advancing age. The findings on the weight and biometric parameters concur with reports from similar age-related studies on the goat by Nishimura *et al*. (2000) and Dhabale (2007).

The inverted S-shaped appearance of the epididymis, the visible numerous convolutions of the caput and corpus epididymal segments as well as the slight variations in the colouration of the segments observed in all the different age groups of *Thryonomis swinderianus* is in agreement with the features of epididymis documented by Adebayo *et al*. (2010) in the matured adult greater cane rat. The age-dependent increase in the epididymal weight together with the uniform epididymal somatic weight (0.01 percentage body weight) seen across the different age groups of the cane rat could substantiate the probable compensatory weight gain with advancement in age. However, the postulated theory could not explain the reason for the non significant difference in the relative epididymal weights across the studied animal. The epididymal length and width were also observed to increase with age thereby conforming to the pattern earlier described for the testicular biometric parameters. It is important to mention that the width of the caput segment relative to other

segments was markedly longer in all the groups and this could be connected to the massive convolution of the caput segment. The biometric parameters in this study corroborate the finding of Gupta and Singh (1988a).

The observed testicular capsule composition in the different age groups of the cane rat is consistent with earlier findings on testicular capsule divisions and constituents in mammals (Dyce *et al*., 2002; Konich and Liebich, 2014). In addition, the progressive age-related increase in testicular capsule thickness and the increased percentage tunica albuginea in all AGCR groups corroborate the earlier reports of Sarma *et al*. (2011) in the buck and rat (Lasheen *et al*., 2015). It however disagrees with the report on goat by Kumari (2013) in age-related decrease in capsular thickness in the black Bengal goat. The increase in capsular thickness with age advancement could be linked to the varying functional activity across the groups. Morphologically, the tunica albuginea remains the fibrous component of the testicular capsule while the tunica vaginalis constitutes the serous part that is responsible for the smooth appearance of the testis (Konich and Liebich, 2014). It suffices to suggest that the marked increase in percentage tunica albuginea contribution to capsular thickness in prepubertal rats when compared to others could be due to the significant fortification role of the former in the developmental event of testicular parenchyma in this age group of AGCR.

The absence of patent testicular parenchymal lumen coupled with the reduced interstitial cell components in the testis of the pre-pubertal rat appear to be suggestive of structural proof of the quiescent reproductive status of this age group. Unlike in prepubertal, morphological presence of lumen in seminiferous tubules was evident from pubertal onwards and could be linked to the possible spermiogenetic activities occurring in their seminiferous epithelium The testicular histology observed in pre-pubertal rat in this study is similar to those reported for immature rat (Lasheen *et al*., 2015) and some young avian species (Kannan *et al*., 2015).

The restriction of PAS positive staining to the testicular capsule, basement membrane, interstitum and seminiferous tubular lumen is in agreement with previously recognised glycogen rich regions in the testes (Rajani *et al*., 2008; Sarma *et al*., 2011; Shagufta *et al*., 2012). The marked parenchymal PAS staining intensity in the pubertal cane rat relative to others could be attributed to increase in demands for glycogen to meet up with the energy requirement for reproductive climax and the intiation of spermatogenic activities. This

finding corroborates the report of age-related changes in testicular parenchymal staining in ram by Kishore *et al.* (2012).

The Masson's trichome-positive staining observed in the testicular capsules and interstices of seminiferous tubules suggests that collagen fibres are abundantly present in the highlighted parts of the testes. This finding attests to the earlier reports of collagen expression in the testes of mammals (Shagufta *et al*., 2012; Kumari, 2013). In the same vein, the age-related increase in capsular Masson's trichome staining intensity could be presumed to be due to collagen fibre amplification with advancement in age. While the non-significant difference in the MT staining of seminiferous tubular parenchyma could be ascribed to the uniform distribution of collagen fibres across age groups.

The observed progressive decrease in germinal epithelial heights with concomitant increase in luminal diameter as age advances can be assumed to coincide with decrease in functional activity with ageing. These findings partly agree with the report of Sarma *et al*. (2012) in the goat. The seemingly uniform tubular diameter in the pubertal cane rat onwards in this study corroborates the earlier reports on tubular diameter profile in mammals (Nishimura *et al*., 2000). However, it is at variance with age-related increase in tubular diameter reported by Sarma *et al*. (2012) and Kumari (2013) in goats.

The presence of similar testicular boundary tissue components in all the age categories of cane rat is suggestive of morphophysiological roles of mechanical support, spermatozoa discharge and as barrier for regulating material movements across the parenchyma (Desjardins, 1993; Marettová et al., 2010). The ultrastructural components of testicular boundary tissue observed across all age categories of the cane rat agree with the boundary tissue composition in rodents (Maekawa *et al.*, 1996; Rezigalla *et al*., 2012). However, it is incongruent with reports of numerous myoid cell layerspresent in the boundary tissue described in large animals (Virtanen *et al*., 1986; Maekawa *et al*., 1996) and in avian spps (van Nassauw *et al*. 1993; Aire, 1997; Aire and Ozegbe, 2007).

The roundish shape of the Sertoli cell nucleus observed in the pre-pubertal testes of the cane rat unlike the typical triangular shape in the other groups is supported by the fact that Sertoli cell can assume several different shapes depending on the stage of the seminiferous cycle and the age of development (Russell *et al.,* 1990a; Hess and Franca, 2005). Regarding Sertoli cell nuclear location, the presence of nucleus close to the basal lamina even with aging in different groups of the AGCR is comparable to the Sertoli cell nuclear position in the

Agoutis rodent (Arroyo *et al*., 2015) but is at variance with distant location in Spix's yellow toothed cavyrodent reported by Santos *et al.* (2014). Besides the nuclear profile, the Sertoli cell cytoplasm especially in the adult AGCR was remarkably observed to contain abundant SER which has been previously postulated by Hess and Franca (2005) to have functional correlation with lipid or steroid metabolism.

The consistent flanking of the Sertoli cells by other spermatogenic lineage cells in the entire rat groups forms interactive contacts and such interactions have been suggested to provide enabling physical and functional support for spermatogenesis (Kerr, 2000). The presence of tight junctions between Sertoli cells in all age groups has been suggested to be necessary for forming haematotesticular barrier (Byers *et al.* 1993*).*

The identification of three distinct spermatogonia types (Type A, Intermediate and B) in proliferative phase of spermatogenesis close to the basal lamina in the prepubertal group onwards could be linked to the essential role of spermatogonia in reproduction. Spermatogonia are recognised stem cells that are important in the preservation of spermatogenetic process through its proliferative potential that culminate in the production of numerous spermatozoa (Phillips *et al*., 2010). Hence, the occurrence of spermatogonia across all age groups underscores the above highlighted function. This finding is in agreement with reports from similar age- related studies (Assis-Neto *et al.,* 2003; Arroyo *et al.*, 2015). The consistent observation of euchromatic nuclear type in the spermatogonia of pre-pubertal rat could be indicative of active transcription activity (Feher, 2012). In addition, the presence of numerous mitochondria in the cytoplasm of different spermatogonia types of the pre-pubertal rat could be suggestive of high metabolic activities.

The identification of five spermatocyte types; Pre-leptotene, leptotene, zygotene, pachytene and diplotene characterized by progressive increase in nuclear size, synaptonemal formation and chromatin condensation in the meiotic phase of spermatogenesis in different cane rat groups is consistent with spermatocyte types described in mammals (Hunter, 2003; Page and Hawley, 2004; Beguelini *et al*., 2011) and in age-related study by Arroyo *et al*. (2015). The irregular nuclear and cytoplasmic shapes that typify the prepubertal spermatocytes could be associated with rapid meiotic cellular activity in this age group. The observed ultrastructural alteration in the prepubertal spermatocyte morphology concurs with the report of Bellve *et al.* (1977) on prepubertal mouse.

The observed lower Leydig cell population and fewer mitochondria in the pre-pubertal rat compared to others are suggestive of less reproductive activity in this age group and with advancement in age remarkable features of active reproduction would be evident. These findings are similar to the reports of Tripepi *et al*. (2000) in pigs and Lasheen *et al*. (2015) in rats. The remarkable increase in the amount of lipid droplets and SER observed in the Leydig cell cytoplasm of adult AGCR could be associated and consistent with the expected high steroidogenic activity. These findings corroborate the morphological features reported for ground squirrel at full spermatogenesis (Pudney *et al*., 1985; Pudney, 1986).

The epididymis in the different age groups AGCR is divided into four segments of six distinct zones; zone I, zone II, zone III (initial segment), zone IV (caput), zone V (corpus) and zone VI (cauda) based on histological, histomorphometrical and histochemical characteristics that include epithelial height, distribution pattern of different types of epithelial lining cells, luminal diameter and shape, stereocilia height and peritubular muscle coat thickness. This observed epididymal division is in agreement with the reports of 4 segment and six zones by Adebayo *et al*. (2016) in adult cane rat as well as in boar (Wrobel and Fallenbacher, 1974). It however, contrasted the observations of; 3 segments in dog and camel (Chandler *et al*., 1981; Ruhl, 2001), 4 segments in other mammals such as rat and cat (Hamilton, 1975; Sanchez, 1998) and 5 segments in hamster, mouse, African giant rat and buck (Flickinger *et al*., 1978; Takano, 1980; Oke *et al*., 1989; Goyal and Williams, 1991).

The simple cuboidal to columnar epididymal epithelial lining of the pre-pubertal unlike the classical pseudostratified stereociliated columnar epithelium observed in other groups is in conformity with earlier reports on epididymal epithelial lining in immature and mature mammals (Oke, 1982; Adebayo and Olurode, 2010; Olukole *et al*., 2010).

The observed progressive age-related increment in epididymal histomorphometric parameters in the different age groups of cane rat as well as cranio-caudal alterations (increase or decrease) to some of the parameters along epididymal duct in this study partly agree with the trend of the histomorphometric parameters reported by Olukole *et al*. (2010) in adult cane rat and wholly concur with the pattern reported by Kishore *et al*. (2012) on similar age-related study in goat. The variations noticed in the histomorphometric parameters between the segments and within cane rat groups might be to accommodate the varied physiological activities of the different segment of the epididymis across age groups. For instance, the increase in stereocilia height of the initial segment functionally has been

attributed to an additional resorptive ability of the epithelium in this segment (Alkafafy, 2005).

The increase in periductal muscle coat thickness towards the caudal segment in each group of cane rat is in accord with the pattern previously reported for the epididymal segments in most mammals (Delhon and Lawzewitsch, 1994; Sanchez *et al.*, 1998, Ruhl, 2001; Calvo *et al.,* 1999). The functional implication of periductal smooth muscular coat presence along the epididymal segments has been suggested to be essential in the movement of the sperm toward the terminal segment (Goyal, 1985; Zayed *et al*., 2012). The pronounced thickness of the PMC in the cauda epididymis could be linked to ejaculation. In addition, the presence of age-dependent increase in the thickness of epididymal coat of the different groups of the cane rat more particularly in the cauda segment of the pubertal group could be suggestive of morphological compensation needed for the initiation of ejaculatory activity of the rats in this group.

The observation of round ductal luminal shape in all the epididymal segments of prepubertal rat as well as the display of variable luminal shape (stellate to roundish) in other rat groups partly agree with the numerous reports of round luminal shape in the lower segments of the epididymal duct of most mammals (Sanchez *et al*., 1998; Alkafafy, 2005; Kumari, 2013). The roundish shape has been attributed to the regular nature of the epithelium in lower segments especially the cauda segment where epithelium is uniformly low and luminal diameter is at maximum thereby favouring adaptation for sperm storage and maturation (Goyal, 1985; Alkafafy, 2005). However, the irregularly long nature of the epithelium in the initial segments has been suggested to contribute to the stellate shape of their lumen (Sanchez *et al*., 1998; Alkafafy, 2005). Based on the above morpho-functional assumptions regarding the ductal luminal shape, it is understandable to attribute the fairly uniform epididymal epithelium height in prepubertal rat to their roundish ductal luminal shape.

The presence of positive PAS staining in the epidididymal interstitium, lamina propria, peri-nuclear region of the epithelium, ductal stereocilia and lumen of different age groups of cane rat is consistent with glycogen rich parts of the epididymis previously reported in most mammals (Goswami and Singh,1988; Oke *et al*., 1988; Kishore, 2012; Kumari, 2013). The significantly higher PAS staining intensity observed in all the epididymal segments of pubertal cane rat relative to others imply the active functional status of this age

group. The demonstration of intense PAS staining in pubertal rat is consistent with the reports of Kishore (2012) and Kumari (2013) on similar age-related studies in goats.

The demonstration of positive MT staining in the epididymal duct interstices and in the smooth muscles surrounding the epididymal ducts is consistent with the reported sites of collagen fibre in the epididymis (Shagufta *et al*., 2012). Owing to the resilience of collagen fibres (Bacha and Bacha, 2000), it suffices to assume that its presence in the epididymal interstices and periductal muscle coat correlates with its functional roles of maintaining ductal architecture. The demonstration of exceptionally high MT intensity in nearly all the epididymal segments of the pubertal rat further confirms the reproductive activeness of this age group.

The numerous mitochondria displayed in the basal and the perinuclear part of principal cells of caput epididymis in pre-pubertal rat is suggestive of increased metabolic activities within the caput of this age group. Increased mitochondria have been suggested to be part of cellular provision needed for marked absorptive function that is peculiar to caput epididymis (Adebayo *et al*., 2016). In addition, the abundant long rough endoplasmic reticulum (RER) and Golgi apparatus seen in the adult and aged rats are presumed to be morphological indicators of protein synthesis. This finding especially in the adult group concurs with report of Adebayo *et al*. (2016).

The progressive accumulation of lysosomal and lipofuschin granules as well as mitochondria degeneration in the principal cell of both corpus and cauda epididymis of aged rat could be attributed to the aging process (Hart and Schoning, 1984; Serre and Robaire, 1998; Calvo *et al*., 1999). As lysosome is known for housing hydrolytic enzymes which are important in phagocytosis of both damaged cellular organelles and extracellular products as well as storage of lipofuscin, the major undigested material (Ivy *et al*., 1996). Therefore, the progressive accumulation of lipofuschin in the principal cell of aged rat could functionally impair the intracellular trafficking through combined oxidative damage and decline of the degradative pathways which are reputed causative factors in aging (Sohal and Brunk, 1990; Tabatabaie and Floyd, 1996).

The age-dependent nuclear indentation observed in the principal cell of corpus and cauda epididymis in pubertal to aged cane rats might be correlated with increased metabolic and synthetic activities (Ramos and Dym, 1977). This finding is consistent with indented nuclear shape reported in the Macaque monkey (Ramos and Dym, 1977), brown rat (Serre

and Robaire (1998), ram (Elzoghby *et al*., 2014) and in adult AGCR (Adebayo *et al*., 2016). The consistent observation of spermatozoa in both corpus and cauda epididymal lumen in pubertal AGCR onwards and the filling of the epididymal lumen of prepubertal rat with cellular debris provide structural evidences of reproductive activeness and quiescence respectively.

Sperm morphological characteristics are essential parameters that reveal the extent of normality and maturity of the sperm population in the ejaculate and could as well correlate with fertility status of a mammalian spp (Memon *et al.,* 1986). The shape of spermatozoon head in the different age groups of African greater cane rat observed in this study is in agreement with the report of Olukole *etal*. (2014) and also concurs with spermatozoa head of mammals (Villalpando *et al*., 2000; Breed, 2005; Oyeyemi and Babalola, 2006). The absence of acrosomal hook on the sperm head in all the age groups also confirms the earlier report of Olukole *et al*. (2014). This observation distinguished it from the other rodents in which sperm head folds back onto itself to give a "hook"-like appearance (Blandau, 1951; Breed *et al*., 2005).

The non significant difference in the linear dimensions; sperm head length and width, mid-piece length, tail length and the complete spermatozoa lengths observed in the pubertal to aged rats is similar to the sperm morphometric data reported in age-related study conducted in boar (Quintero-Moreno *et al.,* 2009; Banaszewska *et al.,* 2011). Although insignificant increment occurred in the sperm dimensions with increasing age it was not enough to conclude that there was an age-related alteration in sperm morphometrics. The age of a male animal has been identified as an important cause of variation in spermatozoa morphometric dimensions (Gregor and Hardge, 1995, Kondracki *et al.* 2005, Quintero-Moreno *et al.* 2009).

The observed uniformly low percentage (roughly 15%) of abnormal sperm cells in both testes and epididymis of the different age groups of cane rat concurs with the normal acceptable range reported for mammals (Moss *et al*., 1979; Wilde *et al*., 1999). Bearing this in mind, the level of these abnormalities might not affect the breeding soundness of pubertal to aged AGCR. Also, the higher proportions of the curve and bent mid-pieces as well as bent tail defects displayed across all age groups has been suggested to be due to the disorganisation of structural components of the tail with resultant weakness of the structure and folding of the flagellum (Briz *et al*., 1996). The finding on the percentage abnormal spermatozoa is similar

to the report of Olukole *et al*. (2014) on matured adult of this rodent species and also agrees partially with the report of Varesi *et al.* (2013) on canine spermatozoa.

The percentage motility of live spermatozoa has been reported to positively correlate with the fertilizing capability of sperm cells (Oyeyemi and Ubiogoro, 2005). Therefore, the significantly increased motility observed in the epididymis of the pubertal and adult cane rats more remarkably in the adult could be suggested to reflect the excellent fertilizing ability of this age group. Conversely, the reduced percentage sperm motility displayed by the aged cane rat could be linked to the progressive ageing process within the epididymal segments more particularly the cauda segment and could as well account for most of the reduction in the fertility potential of most aged animals. The profile of sperm motility seen in this study corroborates the pattern documented in similar age-related study in hamster rat (Calvo *et al*., 1999) and in man (Kidd *et al*., 2001; Jung *et al*., 2002).

The non-significant difference in the testicular and epididymal percentage sperm livability from the pubertal to aged rats implies that the ratio of the live spermatozoa to dead counterparts in the ejaculate of each group was uniformly higher across the groups. The picture above is expected because the groups of the cane rat studied were not exposed to toxicant that could have markedly disrupted the balance in the livability ratio.

Furthermore, the marked increased testicular and epididymal sperm concentrations observed in the pubertal and adult cane rat, more particularly in the latter age group, could be attributed to the morpho-physiological activeness of this group. However, the markedly decreased gonadal and extragonadal sperm concentrations shown by aged AGCR is consistent with the widely documented decline profile of sperm concentration in aged animal (Humphrey and Ladds, 1975; Lamano-Carvalho *et al*., 1988; Calvo *et al*., 1999) and in man (Neaves *et al*., 1985).

The expression of vimentin in the testicular Sertoli and Leydig cells as well as in the peritubular coat and interstitium (stroma and perivascular) in all the epididymal segments of the different cane rat groups further substantiates the earlier reported vimentin enriched regions in the mammalian testis and epididymis (Bilinska, 1989; Sasaki *et al*., 2010; Moustafa, 2012). The structural support and functions of vimentin in the testis are believed to include; the anchorage and translocation of spermatids in preparation for spermiation (He *et al*., 2007; Lie *et al*., 2010; Sasaki *et al.,* 2010). Therefore, the increased testicular vimentin intensity in the adult rat could reflect its reproductive activeness. Vimentin has also been

found to be widely distributed in cells of mesenchymal origin (Kameda, 1995). Thus, it suffices to attribute the increased intensity observed in all the epididymal segments of prepubertal rats to the presence of higher population of relatively undifferentiated cells when compared to other groups of cane rat.

Saturated (S)-100 is a structural protein with unclear biological function though available reports have shown that it may be involved in establishing the blood-testis barrier (Czykier *et al.,* 2000; Cruzana *et al.,* 2000; Cruzana *et al.,* 2003; Abd-Elmaksoud *et al*., 2014). Considering the age-related increase in the intensity of S-100 expression in the testes of cane rat from pubertal to aged, it could be suggested that the intensity seems to correlate with maturity. Also, it could be deduced that the intensity is indicative of striking secretory and absorptive processes as well as blood- testis barrier strengthening which are peculiar to these age groups. However, the negative immunolocalisation of S-100 in prepubertal testis is difficult to explain for now. Subsequent study that will incorporate prenatal testis along with the present prepubertal data is recommended to further unravel the S-100 profile in immature testes of African greater cane rat.

The observed positive immunoreactivity to S-100 proteins in the periductal muscle coat, interstitial stroma and perivascular part of the epididymal segments in all AGCR is consistent with reports of the distribution of S-100 in mammalian epididymis (Czykier *et al*., 1999; Czykier *et al*., 2000). The strong intensity found in the corpus and cauda epididymal segments of pubertal AGCR especially in the interstitial vascular endothelium can be linked to S-100 involvement in transcytotic movement of materials within the interstitium (Czykier *et al*., 1999; Czykier *et al*., 2000).

The nervous system has been implicated in the extrusion of spermatozoa from the seminiferous tubules of some mammalian spps (rat, dog and rabbit) that possess smooth muscle cells in their capsules (Davies *et al*., 1970). Therefore, the age-related increase in the intensities of neurofilament and Golgi expressed capsular nerve fibres in cane rats seem to justify the functional need of innervation with age advancement. In addition, the strong neurofilament and golgi intensities expressed in the testicular interstitum of both pubertal and adult groups moderately correlate well with the marked testosterone secretions and sperm parameters values obtained in this study. In the same vein, it is logical to assume that the conspicuous reduction in the intensities of expression of both in prepubertal rat could be connected to the low reproductive activity. These findings agree with the report of Falade *et*

al. (2017) in the African giant rat but contrast the reports of Prince (1996) in man and Wrobel and Brandl (1998) in pig.

The intense NF and Golgi expressions in the interstitium and periductal muscle coat aspects of the caput and corpus epididymal segments in pubertal and adult cane rats could be suggested to correlate with the developmental and functional states of the epididymal ducts more particularly the adult group with active reproductive activity. The progressive segment-related increased neuronal fibre expressions observed along the epididymal segments in all the age groups corroborates the pattern documented in rats (Kempinas *et al.*, 1998), rabbits (Sienkiewicz *et al.*, 2015) and camel (Liguori*et al*., 2013). In addition, the marked NF expression in the cauda epididymis of the adult rat relative to others could be presumed to mediate the neuromuscular events needed to transport spermatozoa through the duct. Several studies have equally associated the presence of certain neurotrasmitters in the nerve fibres supply to the epididymis in regulating certain epithelial cell functions which include electrolyte transport (Chan *et al*, 1994) and protein processing (Ricker *et al*, 1996).

The positive immunolocalisation of glial fibrillary acid protein (GFAP) in the interstitium of seminiferous tubules of all cane rat groups is in agreement with previous reports of interstitial Leydig cell being immunopositive for astrocyte marker (GFAP) (Maunoury *et al*., 1991; Holash *et al*., 1993; Davidoff *et al*., 2002; Falade *et al*., 2017). The functional implication of the localisation of astrocyte-like cells in the interstium has been suggested to be involved in blood- testis barrier (BTB) formation, a prototype of the blood-brain barrier formed by astrocytes in the brain (Holash *et al*., 1993). In respect of the highlighted function, the increased testicular GFAP expression intensity with age advancement might be correlated with the strengthening of BTB. This finding concurs with the increased testicular GFAP intensity reported by Falade *et al*., (2017) in the African giant rat but contrasts the reports of decrease GFAP profile especially in CNS tissues of man (Davidoff *et al*., 2002) and African greater cane rat (Olude *et al.*, 2015).

GFAP localisation in perivascular regions has been assumed to regulate blood pressure and permeability of vascular walls (Buniatan *et al*., 1998). Therefore, the consistent demonstration of a varying levels of strong positive GFAP immunulocalisation arround the vascular components of the epididymal ductal interstitium in all segments of all rat groups could be connected to the marked exchange of materials between interstitial vessels and the epithelial components in these segments. In addition, the observed age-dependent increase in

intensity of GFAP expression in the epididymal segments (caput, corpus and cauda) of the cane rat further substantiates the need for the proportionate increase in the permeability regulation with ageing.

The peak serum testosterone level observed in adult rat with subsequent decline with age advancement suggests the age maximum active reproductive activity. In addition, it has been speculated that testosterone peak may be triggered by a complementaryLeydig cell hypertrophy and proliferative germ cell activity (Choi and Smitz, 2014). The trend of serum testosterone in this study concurs with the reports of Wang *et al*. (1993) and Vom Saal *et al.* (1994). It however contradicts the decrease and stable levels reported by Horn *et al.* (1996), Calvo *et al.* (1999) and Travison *et al.* (2007).

The reduced LH level observed in the older rats especially in the adult group relative to others provides a remarkable suggestive evidence of functional pituitary-gonadal relationship. The peak testosterone level is presumed to provide a consequential triggering of luteinising hormone release which is on decline in this group. Interestingly, studies have shown that moderate or extreme testosterone decline in a male subject with intact hypothalamic-pituitary relationship may or may not be compensated with LH climax (Bagatell and Bremnar, 1996; Feldman *et al.,* 2002; Woerdeman *et al.,* 2010).

Follicle stimulating hormone is important in the regulation of spermatogenesis (Kumar, 2009; Peltoketo *et al*., 2010; Araujo and Wittert, 2011). Thus, the increasedFSH level observed in pre-pubertal rats could be attributed to the initiation of the seminiferous epithelium maturation in this group while the decline in the other groups of cane rats suggests an already intact, matured seminiferous epithelium ready to exert a feedback influence on FSH secretion.

The observed estrogen level increase with advancement in age could be associated with increased body fat as well as increase in aromatase activity that usually accompanies ageing (Leder *et al*., 2004). In addition, the suggested elevated level of the aromatase activity could affect the feedback for testosterone synthesis which might result in a consequential decline in its level. Contrary to the age-related elevation observed in this study, trends of estrogen levels with advancing age have been variously reported to either decline or remain steady (Orwoll *et al*., 2006; Araujo *et al.,* 2008; Araujo and Witter, 2011).

Progesterone is believed to play a role in activating sperm in the female reproductive tract and as a modulator of male sexual response and behaviour (Oettel and Mukhopadhyay, 2004). Hence, the progesterone peak observed in pubertal rat suggests that maximum sexual response and behaviour is attainable at this age.

5.1 CONCLUSION

This study has demonstrated the presence of;

i. Similar gross testicular and epididymal features in all the age-groups of AGCR, while, morphometric parameters (testicular and epididymal weights, lengths and circumferences) were conspicuously reduced in prepubertal AGCR.

ii. Patent Seminiferous tubular lumen in the testes of the late pre-pubertal age (4 months) to aged AGCR and presence of simple cuboidal to columnar epithelial lining in pre-pubertal epididymal duct relative to the classical pseudostratified ciliated columnar epithelium in pubertal to aged AGCR.

iii. Sperm motility and concentration were markedly increased in the caudal epididymis of the adult cane rat.

iv. Vimentin and S-100 (Structural protein markers), neurofilament (neuronal element marker) and GFAP (glial or astrocyte-like marker) were intensily expressed in the testis and epididymis of the adult AGCR.

v. The principal male androgen (testosterone) was remarkably elevated in the adult AGCR

5.2 CONTRIBUTION TO KNOWLEDGE

1. The results from the histology, histochemistry, ultrastructure, hormonal profiles and sperm parameters showed that maximum functional reproductive activeness is in adult cane rat (12-30 months) which favourably positioned it as a good candidate for breeding programme

2. The first report of seminiferous tubular lumen canalization, a pointer to initiation of spermatogenic activities during post natal development in AGCR with the first evidence at late pre-pubertal (4months).

3. The presence of abundant lysosomal and lipofuschin granules found only in aged AGCR which is indicative of ageing

4. The abundance of nerve fibres in the testes and epididymis of the adult AGCR can be associated with increased reproductive activities

5. The marked expression of Vimentin in the testes of adult AGCR can be attributed to optimum anchorage of spermatids an important factor in spermiation

5.3 Further Research

As part of my future research plan, I hope to unravel age-related changes in the morphophysiology of the accessory sex glands (prostate, seminal vesicle, bulbourethral and coagulating glands), pituitary gland and brain centres involved in the regulation of reproduction in African greater cane rats.

REFERENCES

Abd-Elmaksoud, A., 2005. Morphological, glycohistochemical, and immunohistochemical studies on the embryonic and adult bovine testis [dissertation]. Munich: Institute of Veterinary Anatomy II, Faculty of Veterinary Medicine.

Abd-Elmaksoud, A., Shoeib, M.B. and Marei, H.E.S., 2014. Localisation of S-100 proteins in the testis and epididymis of poultry and rabbits. *Anatomy and Cell Biology* 47:180-187

Addo, P., Dodoo, A., Adjei, S., Awumblla, B. and Awotwi, E., 2002. Determination of the ovulatory mechanism of the grasscutter (*Thryonomys swinderianus*). *Journal of Animal Reproduction Science* 71(1-2): 125-37.

Adebayo, A., Akinloye, A., Olukole, S., Ihunwo, A.O. and Oke, B., 2014a. Anatomical and immunohistochemical characteristics of the prostate gland in the greater cane rat (Thryonomys swinderianus). *Anatomia Histologia Embryologia*, 42 (2): 1 - 8.

Adebayo, A., Akinloye, A., Olukole, S., Oyeyemi, M., Taiwo, O., Ihunwo, A.O. and Oke, B., 2014b. Gross histological and ultrastructural features of the bulbourethral gland in the greater cane rat (*Thyonomys swinderianus*). *Anatomia Histologia Embryologia*, 43 (1): 1 - 7.

Adebayo, A.O. and Olurode, S.A., 2010. The morphology and morphometry of the epididymis in the greater cane rat *(Thryonomys swinderianusTemmincks).Folia Morphologia* 69(4): 246–252.

Adebayo, A.O., Akinloye, A.K., Olukole, S.G., Ihunwo, A.O and Oke, B.O., 2014. Structural, ultrastructural and immunohistochemical analysis of the vesicular gland in the male greater cane rat (*Thryonomys swinderianus*). *European Journal of Anatomy* 18 (4): 317-325.

Adebayo, A.O., Oke, B.O. and Akinloye, A.K., 2009. The gross morphometry and histology of the male accessory sex glands in the greater cane rat (*Thryonomys swinderianus* Temminck). *Journal of Veterinary Anatomy* 2 (2): 41-51.

Adebayo. A.O., Akinloye, A.K., Ihunwo, A.O. and Oke, B.O., 2015. The coagulating gland in the male greater cane rat (*Thryonomys swinderianus*): morphological and immunohistochemical features. *Folia Morphologia* 74 (1): 25–32.

Adebayo, A.O., Akinloye, A.K.., Ihunwo, A.O., Taiwo, V.O. and Oke, B.O., 2016. Zonal changes in the ultrastructure of the epididymal principal cell of the greater cane rat (*Thryonomys swinderianus*). *Alexandria Journal of Veterinary Science* 48 (1): 99-106

Adebayo, A.O., Akinloye, A.K.., Ihunwo, A.O., Taiwo, V.O. and Oke, B.O., 2019. Ultrastructural studies of acrosomal formation in the male greater cane rat (*Thryonomys swinderianus*). *Journal of Microscopy and Ultrastructure* 7(1): 14-8

Adekola, A. G. and Ogunsola, D. S.,2009. Determinants of productivity level of commercial grasscutter farming in Oyo State. *Proceeding International Conference on Global Food Crisis*. *19th - 24th April,* Owerri, Nigeria. pp 15 - 21.

Adjanahoun, E., 1989. Contribution to the development of the livestock of the grasscutter (*Thryonomys swinderianus*, Temminck 1827) and al'etude its reproduction. Doctoral Thesis, Maisons-Alfort, Paris.

Adoun, C., 1993. Place de l'aulacode (*Thryonomys swinderianus*) dan's le regne animal et sa repartition geographique. *Proceedings of the Conference Internationale, L'Aulacodiculture: Acquis ET Perspective*. (CIA'93), Cotonou, Benin, 1993, p. 35-40.

Adu, E.K., Otsyina, R.H. and Agyei, A.D., 2005. The efficacy of different dose levels of albendazole for reducing fecal worm egg count in naturally infected captive grasscutter (*Thryonomys swinderianus*, Temminck). *Livestock Resources for Rural Development* 17 (128).

Agnes, V. F. and Akbarsha, M. A., 2001. Pale vacuolated epithelial cells in the epididymis of aflatoxin-treated mice. *Reproduction* (formerly *J Reprod Fertil*) 122:629–41.

Aire, T. A. and Ozegbe, P. C., 2007. The testicular capsule and peritubular tissue of birds: morphometry, histology, ultrastructure and Immunohistochemistry. *Journal of Anatomy* 210: 731–740

Aire, T.A., 1997. The structure of the interstitial tissue of the active and resting avian testis. *Onderstepoort Journal of Veterinary Research* 64: 291–299.

Aire, T.A. and van der Merwe, M., 2003. The ductuli efferentes of the greater cane rat (*Thryonomys swinderianus*). *Anatomy and Enbryology* 206: 409-417.

Akbarsha, M. A. and Averal, H. I., 1999b. Epididymis as a target for the toxic manifestation of vincristine: Ultrastructural changes in the clear cell. *Biomedicine Letter* 59:149–59.

Akbarsha, M. A., Faisal, K. and Rasha, A., 2015. The epididymis: structure and function, mammalian endocrionology and male reproductive biology. 10.1201/b18900-7, 115-166.

Akhmerova, L.G. 2006. Leydig cell development. Usp. *Fiziologicheskikh Nauk* 37 (1): 28–36.

Alkafafy, M., 2009. Some Immunohistochemical Studies on the Epididymal Duct in the Donkey
(*Equus asinus*).*Journal Veterinary Anatomy* 2 (2): 23 – 40

Alkafafy, M., 2005. Glycohistochemical, immunohistochemical and ultrastructural studies of the
bovine epididymis [dissertation]. Munich: Institute of Veterinary Anatomy II, Faculty of Veterinary Medicine, LMU.

Alkafafy, M., Elnasharty, M., Sayed-Ahmed, A. and Abdrabou, M., 2011. Immunohistochemical
studies of the epididymal duct in Egyptian water buffalo (*Bubalus bubalis*). *Acta Histochemica* 113:96-102.

Aluko, F. A., Salako, A. E., Ngere, L. O. and Awojobi, H. A., 2014. Reproductive history of cane rat: A review of the reproduction and reproductive performance. *Journal of Agriculture and Social Research* 14 (1): 109-115.

Amman, R.P., 1981. A critical review of methods for evaluation of spermatogenesis from seminal characteristics. *Journal of Andrology* 2:37-58.

Amselgruber, W.M., Sinowatz, F., Schams, D. and Lehmann, M., 1992. S-100 protein

immunoreactivity in bovine testis. *Andrologia* 24:231-5.

Amselgruber, W.M., Sinowatz, F. and Erhard, M., 1994. Differential distribution of immunoreactive S-100 protein in mammalian testis. *Histochemistry,* 102:241-5.

Andres, T.L., Trainer, T.D. and Lapenas, D.J., 1981. Small vessel alterations in the testes of infertile men with varicocele. *American Journal of Clinical Pathology* 76: 378-384.

Andrew, W., 1971. *The anatomy of aging in man and animals*. New York and London, Grune and Stralton Co, .Pp 1983 – 193.

Araujo, A.B., Travison, T.G., Leder, B.Z. and Mckinlay, J.B., 2008. Correlations between serum testosterone, estradiol and sex hormone-binding globulin and bone mineral density in a diverse sample of men. *Journal of Clinical Endocrinology and Metabolism* 93(6): 2135-2141.

Araujo, A.B. and Witter, G.A., 2011. Endocrinology of the aging male. *Best Practice Research: Clinical Endocrinology and Metabolism* 25 (2): 303-319.

Arcuri, C., Giambanco, I., Bianchi, R. and Donato, R., 2002. Subcellular localisation of S100A11 (S100C, calgizzarin) in developing and adult avian skeletal muscles. *Biochim Biophys Acta* 1600:84-89.

Arrotéia, K.F., Garcia, P.V., Barbieri, M.F., Justino, M.L. and Pereira, L.A.V., 2012. The epididymis: embryology, structure, function and its role in fertilization and infertility in: Embryology – *Updates and Highlights on Classic Topics,* Prof Luis Violin Pereira (Ed.), ISBN: 978-953-51-0465-0, In-Tech, Available from: http://www.intechopen.com/books/embryology-updates-and-highlightson-classic-topics/the-epididymis-embryology-structure-function-and-its-role-in-fertilization-and-infertility.

Arroyo, M. A. M., Silva, F. F. S., Santos, P. R. S., Silva, A. R. Oliveira, M. F. and Assis Neto, A. C., 2015. Ultrastructure of spermatogenesis and spermatozoa in agoutis during sexual development. *Reproduction, Fertility and Development* 29(2): 383-393.

Aruldhas, M. M., Subramanian, S., Sekhar, P., Vengatesh, G., Govindarajulu, P. and Akbarsha, M. A., 2006. In vivo spermatotoxic effect of chromium and the consequent

responses in the epididymal epithelial basal cells and intraepithelial macrophages: Study in a non-human primate (*Macaca radiata* Geoffroy). *Fertility and Sterility* 86:1097–105.

Asibey, E. O. A., 1974. The grasscutter (*Thryonomys swinderianus* Temminck) in Ghana. *Symposium of Zoological Society London* 34: 161-170.

Asibey, E. O. A. and Addo, P. G., 2000. The grasscutter, a promising animal for meat production. In: African perspective, practices and policies supporting sustainable development (Turnham, D., ed). Scandinavian Seminar College, Denmark, in association with Weaver Press Harare. Zimbabwe. www.cdr.dk/sscafrica/asad-gh.ht.m

Asibey, E. O. A. and Eyeson, K. K., 1973. Additional information on the importance of wild animals as food source in Africa south of the sahara. *Bongo Journal of the Ghana Wildlife Society* 1(2): 13 - 17.

Assis-Neto, A. C., Carvalho, M. A. M., Melo, M. I. V., Miglino, M. A., Oliveira, M. F. and Mariana, A. N. B., 2003b. Phases of the development and testicular differentiation in agoutis (*Dasyprocta aguti*) raised in captivity. *Brazillian Journal of Veterinary Research in Animal Science* 40: 71–79.

Ayad, B.M., 2018. Basic semen parameters assisted by computer-aided sperm analysis (CASA) and their correlations with advanced semen parameters in normozoospermic men with different abstinence periods. Dissertation presented for the degree of Doctor of Philosophy (Medical Physiology) in the Faculty of Medicine and Health Sciences, Stellenbosch University.

Bacha, W. J. and Bacha. L.M., 2000. Colour atlas of veterinary histology. 2nd Edn. Lippincott, Williams and Wilkins, Philadelphia. pp. 203-219.

Bagatell, C.J. and Bremnar, W.J. , 1996. Androgens in men – uses and abuses. *New England Journal of Medicine*, 334 (11): 707-714.

Bakst, M.R., Akuffo, V., Trefil, P. and Brillard, J.P., 2007. Morphological and histochemical characterization of the seminiferous epithelial and Leydig cells of the turkey. *Animal Reproductive Science* 97: 303–313.

Banaszewska, D., Kondracki, S. and Wysokińska, A., 2011. Effect of age on the dimensions and shape of spermatozoa of large White Polish boars *Archiv fur Tierzucht* 54 (5): 504-514

Banks, F.C.L., Knight, G.E. and Calvert, R.C., 2006. Smooth muscle and purinergic contraction of the human, rabbit, rat, and mouse testicular capsule. *Biology and Reproduction* 74: 473–480.

Banks, J.W., 1993. Applied veterinary histology. 3rd ed. Mosby Year Book. Inc. St. Louis,

Baltimore, Boston, Chicago, London, Philadelphia, Sydney, Toronto.Baptist, R. and Mensah, G. A., 1986. Benin and West Africa: The cane rat farm animal of the future. *World Animal Review* 60: 2 - 6.

Barratt, C.L.R., 1995. Spermatogenesis. In Cambridge reviews in human reproduction gametes. The spermatozoon. J.G Grudzinskas and JL YOvich Eds. Cambridge University Press, Cambridge. Pp.250-267.

Barth, A. D. and Oko, R. J., 1989. Abnormal morphology of bovine spermatozoa. Ames: Iowa State University Press; 1989.

Batalha, L. M. and Oba E., 2006. Morphometrical and morphological characterization of capybara (*Hydrochoerus hydrochaeris*) spermatic cells). *Archives of Veterinary Science* 11: 66-72.

Bedford, J.M., 1978. Anatomical evidence for the epididymis as the prime mover in the evolution of the scrotum. *Developmental Dynamics* 152(4): 483-507.

Beguelini, M.R., Moreira, P.R.L., Faria, K.C., Marchesin, S.R.C. and Morielle-Versute, E., 2009. Morphological characterization of the testicular cells and seminiferous epithelium cycle in six species of Neotropical bats. *Journal of Morphology* 270: 943–953.

Beguelini, M. R., Puga,C.C. I.,Taboga, S.R. and Morielle-Versute, E., 2011. Ultrastructure of spermatogenesis in the white-lined broad-nosed bat, *Platyrrhinus lineatus (Chiroptera: Phyllostomidae). Micron* 42: 586–599.

Bellve, A.R., Cavicchia, J.C., Millette, C.F., O'Brien, D.A., Bhatnagar, Y.M. and Martin, D.Y.M., 1977. Spermatogenic cells of the prepuberal mouse. Isolation and morphological. The *Journal of Cell Biology* 74: 68-85.

Bergh, A., 1987. Treatment with HCG increases the size of Leydig cells and testicular macrophages in unilaterally cryptorchid rats. *International Journal of Andrology* 10:765-772.

Bernard, R.T.E., 1984. The occurrence of spermiophagy under natural conditions in the cauda epididymis of the Cape horseshoe bat *(Rhinolophus capensis). Journal of Reproduction and Fertilit*y 71:539-543.

Bilin´ska, B., 1989. Visualization of the cytoskeleton in Leydig cells *in vitro*. Effect of luteinising hormone and cytoskeletal disrupting drugs. *Histochemistry* 93: 105-110.

Bilin´ska, B., 1994. Staining with ANS fluorescent dye reveals distribution of mitochondria and lipid droplets in cultured Leydig cells. *Folia Histochemica* 32(2): 21-24.

Bishop, I., 1984. Macdonald, D. The encyclopedia of mammals. New York: Facts on file. p.703.

Bishop, M.W.H., 1970. Aging and reproduction in the male. *Journal of Reproduction and Fertility* 12: 65-87.

Blandau, R. J., 1951. Observations on the morphology of rat spermatozoa mounted in media of different refractive indices and examined with the phase microscope. *The Anatomical Record* 109: 271-275.

Bloom, E., 1973. The ultrastructure of some characteristic sperm defects. *Nordisk Veterinary Medicine* 25: 283.

Boni, R., Burg, G., Doguoglu, A., Ilg, E.C., Schafer, B.W., Muller, H.C.W., 1997. Immunohistochemiacal localisation of the Ca2+ binding S100 proteins in normal human skin and melanocytic lesions. *British Journal of Dermatology* 137:39-43.

Bongso, T.A., Jainudeen, M.R. and Zahrah, A. S., 1982. Relationship of scrotal circumference to age, body weight and onset of spermatogenesis in goats. *Theriogenology*18 (5): 513-524

Böttiger, B.W., Möbes, S., Glätzer, R., Bauer, H., Gries, A., Bärtsch, P., MotschJ. and Martin,

E., 2001. Astroglial protein S100 is an early and sensitive marker of hypoxic brain damage and outcome after cardiac arrest in humans.*Circulation* 103, 2694-2698.

Bradford, M.M., McRorie, R.A. and Williams, W.L., 1976. Involvement of esterases in sperm penetration of the corona radiate of the ovum. *Biology of Reproduction* 15: 102-106.

Breed, W.G., 2005. Evolution of the spermatozoon in muroid rodent. *Journal of Morphology* 265 (3):271-290.

Brito, L. F. C., 2007. Evaluation of stallion sperm morphology. *Clinical technique in equinepractice* 6: 249-264.

Brito, L. F., Sertich, C. P. L., Stull, G. B., Rives, W. and Knobbe, M., 2010. Sperm ultra-structure, morphometry, and abnormal morphology in American black bears (*Ursus americanus*). *Theriogenology* 74(8): 1403-1413.

Briz, M. D. and Fabrega, A., 2013. The boar spermatozoa. In: Bonet, S., Casas, I., Holt, W.V. and Yeste, M. (ed.), Boar reproduction: fundamentals and new biotechnological trends. Springer Science & Business Media, New York, 1-48

Briz, M.D., Bonet, S., Pinart, B. and Camps, R., 1996. Sperm malformations throughout the boar epididymal duct. *Animal Reproductive Science* 43:221–239.

Brunk, U.T., Jones, C.B. and Sohal, R.S., 1992. A novel hypothesis of lipofuscinogenesis and cellular aging based on interactions between oxidative stress and autophagocytosis. *Mutation Research* 275:395-403.

Brüntup, M. and Aïna, M., 1999. La commercialisation de l'aulacode et de sa viande. Rapport d'étude,GTZ/PPEAu, Cotonou(Bénin), 53p.

Buniatan, G., Traub, P., Albinus, M., Beckers, G., Buchmann, A., Gebhardt, R. and Osswald, H., 1998. The immunoreactivity of glial fibrillary acidic protein in mesangial cells and podocytes of the glomeruli of rat kidney in vivo and in culture. *Biology of Cell* 90: 53–61

Bush, T.G., Savidge, T.C., Freeman, T.C., Cox, H.J., Campbell, E.A., Mucke, L., Johnson, M.H. and Sofroniew, M.V., 1998. Fulminant jejuno-ileitis following ablation of enteric glia in adult transgenic mice. *Cell* 93:189–201

Byanet, O., Nzalak, J.O., Salami, S.O., Nwaogu, I.C., Bosha, J.A., Umosen, A.D., Ojo, S.A. and Obadiah, H.I., 2008. Macroscopic studies of the gastrointestinal tract of the African grasscutter (*Thryonomis swinderianus*). *Veterinary Research* 2(2): 17-21

Byanet, O., Onyeanusi, B.I. and Ibrahim, N.D.G., 2009. Sexual dimorphism with respect to the macro-morphometric investigations of the forebrain and cerebellum of the grasscutter (Thryonomys swinderianus). *International Journal of Morphology* 27(2): 361-365.

Byers, S., Jegou, B., Mac-Calman, C. and Blaschuk, O., 1986. Sertoli cell adhesion molecules and the collective organisation of the testis. In: Russel, L.D., Griswold, M.D and Clearwater, F.L. (eds) the Sertoli cell, Cache River, pg 461-476.

Byers, S., Pelletier, R. M. and Sua´rez-Quian, C., 1993. Sertoli cell junctions and the seminiferous epithelium barrier. In 'The Sertoli Cell'. (Eds L. Russell and M. Griswold.) pp. 431–446. Casher River Press:Clearwater.

Byskov, A., Andersen, C. and Westergaard, L., 1983. Dependence of theonset of meiosis on the internal organisation of the gonad. In*Current Problems in Germ Cell Differentiation*(eds McLaren A,Wylie CC), pp. 215–224. Cambridge, UK: Cambridge UniversityPress.

Byskov, A. G., 1986. Differentiation of mammalian embryonicgonad. *Physiol Rev* 66, 71–117. O'Callaghan J.P. and Sriram, K., 2005. Glial fibrillary acidic protein and related glial proteins as biomarkers of neurotoxicity. *Expert Opinion on Drug Safety* **4**(3):433-442

Calvo, A., Pastor, L. M., Martinez, E., Vazquez, J. M. and Roca, J., 1999. Age-related changes in the hamster epididymis. *Anatomical Record* 256: 335–346.

Campos, M. B., Vitale, M. L., Calandra, R. S. and Chiocchio, S. R, 1990. Serotonergic innervation of the rat testis. *Journal of Reproductive Fertility* 88: 475-479

Carreau S., Bois, C., Zanatta, L., Silva, F.R.M.B., Bouraima-Lelong, H. and Delalande, C., 2011. Estrogen signaling in testicular cells. *Life Sciences* 89: 584-587.

Chan, H.C., Fu, W.O., Chung, Y.W., Thou, T.S. and Wong, P.Y.D., 1994. Adrenergic receptors on cultured rat epididymal cells: regulation of chloride conductances. *Biology and Reproduction* 51:1040-1045.

Chandler, J. A., Sinowatz, F. and Pierrepoint, C. G., 1981. The ultrastructure of dog epididymis. *Urology Research* 9 (1): 33-44.

Chatchavalvanich, K., Thongpan, A. and Nakai, M., 2005. Ultrastructure of spermiogenesis in a freshwater stingray, Himantura signifier. *Ichthyological Research* 52: 379–385.

Chaves, E.M., Aguilera-merlo, C., Crucen, O.A., Fogal,T., Piezzi, R.,Scardapene, L. and Dominiguez, S., 2012. Seasonal morphological variation and age-related changes of the seminal vesicle of Viscacha (*Lagostomus maximus maximus*): An Ultrastructural and Immunohistochemical Study. *Anatomical Record* 295: 886-895.

Cheng, C.Y. and Mruk, D.D., 2002. Cell junction dynamcs in the testis: Sertoli-germ cell interactions and male contraceptive development. *Physiological Review* 82: 825-874.

Choi, J. and Smitz, J., 2014. Luteinising hormone and human chorionic gonadotropin: distinguishing unique physiologic roles. *Gynecology and Endocrinology* 30 (3): 174-181.

Christensen, A.K., 1975. Leydig cells. In: Handbook of physiology V. Male reproductive system. Eds E.B. Ashwood and R.O Greep. The American Physiological Society, Washington, 57-94.

Christensen, A.K. and Fawcett, D.W., 1977. The structure of testicular interstitial cells in mice. *American Journal of Anatomy* 118: 551-572.

Clermont, Y., 1962. Quantitative Analysis of spermatogenesis of the rat: a revised model for the renewal of spermatogonia. *The American Journal of Anatomy*111: 111-129.

Clermont, Y., 1963. The cycle of seminiferous epithelium in man. *The American Journal of Anatomy* 112: 35-51.

Clermont, Y., 1972. Kinetics of spermatogenesis in mammals: Seminiferous epithelial cycle and spermatogonial renewal. *Physiological Reviews* 52:198-236.

Clottey, J. A., 1981. Relation of physical body composition to meat yield in the grasscutter (*Thryonomys swinderianus* Temminck). *Ghana Journal of Science* 21: 1-7.

Cool, J. and Capel, B., 2009. Mixed signals: development of the testis. *Seminars in Reproductive Medicine* 27: 5–13,2009.

Cool, J., DeFalco, T. and Capel, B., 2012. Testis formation in the fetal mouse: dynamic and complex de novo tubulogenesis. *Wiley Interdisciplinary Review in Developmental Biology* 1: 847–859.

Cooper, T.G. and Hamilton, D.W., 1977. Observations on destruction of spermatozoa in the cauda epididymis and proximal vas deferens of nonseasonal male mammals. *American Journal of Anatomy* 149:93-110.

Cornwall, G. A., 2009. New insights into epididymal biology and function. *Human Reproduction Update* 15 (2): 213–227.

Costa, D. S., Henry, M. and Paula, T. A. R., 2004. Espermatogeˆnese de Catetos (*Tayassu tajacu*). *Arquivo Brasileiro Medicina Veterinaria e Zootecnia* **56**, 46–51.

Costa, D.S., Paula, T.A.R. and Matta, S.L.P., 2006. The intertubular compartment morphometry in Capibaras (*Hydrochoerus hydrochaeris*) testis. *Animal Reproductive Science* 91: 173-179.

Courot, M., Hochereau-de Reviers, M-T. and Ortavant, R., 1970. Spermatogenesis. In the testis. Vol. 1. A.D Johnson, WR Gomes and NL Vandemark Eds. Academic Press, New York. pp.339-432.

Cran, D. G. and Jones, R., 1980. Aging of male reproductive system: changes in the epididymis. *Experimental Gerontology* 15:93-101.

Cruzana, B. C., Hondo, E., Kitamura, N., Matsuzaki, S., Nakagawa, M. and Yamada, J., 2000. Differential localisation of immunoreactive alpha- and beta-subunits of S-100 protein in feline testis. *Anatomia Histologia Embryologia* 29:83-6.

Cruzana, M.B., Budipitojo, T., De Ocampo, G., Sasaki, M., Kitamura, N. and Yamada, J., 2003. Immunohistochemical distribution of S-100 protein and subunits (S100-alpha and S100-beta) in the swamp-type water buffalo (*Bubalus bubalis) testis. Andrologia35:142-5.*

Cummins, J.M., 1983. Sperm size, body mass and reproduction in mammals. In the sperm cell. André, J (eds). Martinus Nijhoff, The Hague, 1983, p. 395-398.

Curry, M.R. and Watson, P.F., 1995. Sperm structure and function. Gametes—the spermatozoon. Cambridge University Press, Cambridge, 45-69.

Czykier, E., Sawicki, B. and Zabel, M., 1999. Immunocytochemical localisation of S-100 protein in the European bison testis and epididymis. *Folia Histochemica Et Cytobiologica* 37:83-84.

Czykier, E., Sawicki, B. and Zabel, M., 2000. S-100 protein immunoreactivity in mammalian testis and epididymis. *Folia Histochemica Et Cytobiologica* 38:163-6.

Czykier, E., Zabel, M., Surdyk-Zasada, J., Lebelt, A. and Klim, B., 2010. Assessment of S100

protein expression in the epididymis of juvenile and adult European bison. *Folia histochemica Et cytobiologica* 48 (3): 333-338.

Dacheux, J.- L., Gatti, J.L. and Dacheux, F., 2003. Contribution of epididymal secretory proteins for spermatozoa maturation. *Microscopic Research Technique* 61: 7-17

Dacheux, J.- L. and Dacheux, F., 2014. New insights into epididymal function in relation to sperm maturation. *Reproduction* 147: R27-R42

Dacheux, J.- L., Castella, S., Gatti, L.J. and Dacheux, F., 2005. Epididymal cell secretory activities and the role of the proteins in boar sperm epididymis. *Theriogenology* 63 (2): 319-341

Davidoff, M. S., Middendorff, R., Köfüncü, E., Müller, D., Jezek, D. and Holstein, A. F., 2002. Leydig cells of the human testis possess astrocyte and oligodendrocyte marker molecules. *Acta Histochemica* 104 (1): 39-49.

Davis, J.R., Langford, G.A. and Kirby, P.J., 1970. The testicular capsule. In *The Testis. development, anatomy and physiology* eds Johnson AD, Gomes R, Vandemark NL), pp. 281–337. London: Academic Press.

de Krester, D.M., 1969. Ultrastructural features of human spermiogenesis. *Zeitschrift fur Zellforschung und mikroskopische Anatomie* 98: 477-505.

de Krester, D.M. and Kerr, J.B., 1994. The cytology of the testis. In the physiology of reproduction 2nd Ed. Vol. 1. E Knobil and J.D Neill Eds. Raven Press, New York. pp.1177-1290.

de Kretser, D.M. and Kerr, J.B., 1988. The cytology of the testis. In *ThePhysiology of Reproduction* (eds Knobil E, Neill J, et al.), pp. 837– 932. New York: Raven Press.

de Rooij, D.G., 1983. Proliferation and differentiation of undifferentiated spermatogonia in the mammalian testis. In Stem Cells: Their identification and characterisation. CS Potten Ed. Churchill-Livingstone, Edinburgh. pp. 89-117.

Desjardins, C., 1993. Design and function of the microcirculationIn: Cell and molecular biology of the testis; Desjardins, C. and Ewing, L.L. (Editors). New York. Oxford University Press. Pp: 127–136.

Delhon, G. and von Lawzewitsch, I., 1994. Ductus epididymidis compartments and morphology of epididymal spermatozoa in llamas. *Anatomia Histologia Embryologia* 23 (3): 217-225.

Demoulin, A., Koulischer, L., Hustin, J., Hazee-Hagelstein, M.T., Lambotte, R. and Franchimont, P., 1979. Organ culture of mammalian testis III. Inhibin secretion. *Hormone Research*, 10: 117-190.

Dhabale, R.B., 2007. Studies on post-natal developmental changes in reproductive organs and effects of gonadotrophin releasing hormone on spermatogenesis in native buck (*Bidri, Capra hircus*). Thesis Submitted to the Sri Venkateswara Veterinary University in Partial Fulfilment of the Requirements for the Award of the Degree of Doctor of Philosophy in the Faculty of Veterinary Science.

Dierichs, R., Wrobel, K.H. and Schilling, E., 1973. Licht- und elektronenmikroskopisch Untersuchungen an den Leydigzellen des Schweines wiihrend der postnatalen Entwicklung. *Z Zellforsch* 143: 207-227.

Donato R., 1999. Functional roles of S100 proteins, calcium-binding proteins of the EF-hand type. *Biochim Biophys Acta* 1450:191-231.

Donato, R., 2001. S100: a multigenic family of calcium-modulated proteins of the EF-hand type with intracellular and extracellular functional roles. *International Journal of Biochemistry and Cellular Biology* 33:637-68.

Don White, J., Berardinelli, J.G. and Aune, K.E., 2005. Age Variation in gross and histological characteristics of the testis and epididymis in Grizzly bears. *Ursus* 16 (2): 190-197.

Dunn, K.W. and Maxfield, F.R., 1992. Delivery of ligands from sorting endosomes to late endosomes occurs by maturation of sorting endosomes. *Journal of Cell Biology* 117:301-310.

Dwarikas, S., Maseko, B.C., lhunwo, A.O., Fuxe, K. and Manger, P.R., 2008. Distribution and morphology of putative catecholaminergic and serotonergic neurons in the brain of the greater cane rat, *Thryonomys swinderianus*. *Journal of Chemical Neuroanatomy,* 35: 108-122.

Dyce, K.M., Sack, W.O. and Wensing, C.J.G., 2002. *Text book of veterinary anatomy,* 3rd edition, Suanders, Pennsylvania. 183-192.

Eddy, E.M. and O'Brien, D., 2006. The spermatozoon. Knobil and Neill's physiology of reproduction. Academic Press. San Diego, 3-54.

Ehlers, K. and Halvorson, L.M., 2013. Gonadotropin-releasing hormone (GnRH) and the GnRH receptor (GnRHR). *Glob. Libr. womens's med*. DOI 10.3843/GLOWM.10285.

El–Desouki, N.I., El-Refaiy, A.I., Afifi, D.F. and Talaat, H., 2017.Changes in the cytoskeletal intermediate filaments of testicular tissues of rabbits related with age and the prophylactic role of vitamin E. *International Journal of Scientific & Engineering Research* 8 (6): 260-270.

El-Gehani F, Tena-Sempere M. and Huhtaniemi, I., 1998. Vasoactive intestinal peptide is an important endocrine regulatory factor of fetal rat testicular steroidogenesis. *Endocrinology* 139: 1474–1480.

Elston, G.N. and Manger, P., 2014. Pyramidal cells in VI of African rodents are bigger, more branched and more spiny than those in primates. *Frontier in Neuroanatomy* 8: 4.

Elzoghby, I.M.A., Sosa, G.A., Mona, N. A. H. and Manshawy, A.A., 2014. Postnatal development of the epididymis in the sheep. *Benha Veterinary Medical Journal* 26 (1): 67-74.

Ewing, L. and Zirkin, B., 1983. Leydig cell structure and steroidogenic function. *Recent Progress in Hormone Research,* 39: 599–635.

Falade, T.E., Olude, M.A., Mustapha, O.A., Mbajiorgu, E.F., Ihunwo, A.O., Olopade, J.O. and Oke, B.O., 2017. Connective tissue, glial and neuronal expressions in testis of African giant rat (Cricetomys gambianus). *Journal of Morphological Science* 34 (3): 186-193.

Fawcett, D.W., 1970. A comparative review of sperm ultrastructure. *Biology of Reproduction* 2: 90-127.

Fawcett, D.W., 1975b. The mammalian spermatozoon. *Developmental Biology* 44:394-436.

Fawcett, D. and Phillips, D.M., 1969a. Observation on the release of spermatozoa and on changes in the head during passage through the epididymis. *Journal of Reproduction and Fertility Supplemen* 6: 405-418.

Fawcett, D.W., Anderson, W.A. and Phillips, D.M., 1971. Morphogenic factors influencing the shape of the sperm head. *Developmental Biology* 26: 220-251.

Fayenuwo, J. O., Akande, M., Taiwo, A. A. and Adebayo, A. O., 2003. *Guidelines for grasscutter rearing*. Technical Bulletin, IAR & T.,Ibadan. p. 38.

Feher, J., 2012. Quantitative human physiology: an introduction Waltham, MA: Elsevier/Academic Press. p. 170.

Feldman, H.A., Longcope, C., Derby, C.A. and Johannes, C.B., 2002. Age trends in the level of serum testosterone and other hormones in middle-aged men: longitudinal results from the Massachusetts male aging study. *Journal of Clinical Endocrinology and Metabolism* 87 (2): 589-598.

Flickinger, C. J., Howards, S. S. and English, H. F., 1978. Ultrastructural differences in efferent ducts and several regions of the epididymis of the hamster. *American Journal of Anatomy* 152 (4): 557-585.

Franca, L.R., Avelar, G.F. and Almeida, F.F.L., 2005. Spermatogenesis and sperm transit through the epididymis in mammals with emphasis on pigs. *Theriogenology* 63:300–318.

Freneau, G.E., Chenoweth, P.J., Ellis, R. and Rupp, G., 2010. Sperm morphology of beef bulls evaluated by two different methods. *Animal Reproductive Science* 118 (2/4):176-81

Frenette, G., Thabet, M. and Sullivan, R., 2006. Polyol pathway in human epididymis and semen. *Journal of andrology* 27(2): 233-239.

Frungieri, M.B., Urbanski, H.F., Hohne-Zell, B. and Mayerhofer, A., 2000. Neuronal elements in the testis of the Rhesus monkey: Ontogeny, characterization and relationship to testicular cells. *Neuroendocrinology* 71:43-50

Gage, M. J. G., 1998. Mammalian sperm morphometry. *Proceeding of Royal Society London* vol. 265, 1998, p. 97-103.

Gage, M. J. G. and Morrow, E. H., 2003. Experimental evidence for the evolution of numerous, tiny sperm via sperm competition. *Current Biology* 13: 754-757.

Gayton, F., Bellido, C., Aguilar, E. and van Rooijen, N., 1994. Requirement for testicular macrophages in Leydig cell proliferation and differentiation during prepubertal development in rats. *Journal of Reproduction and Fertility* 102: 393-399.

Goeritz, F., Quest, M., Wagener, A., Fassbender, M. and Broich, A., 2003. Seasonal timing of sperm production in roe deer: Interrelationship among changes in ejaculate

parameters, morphology and function of testis and accessory glands. *Theriogenology* 59: 1487-1502.

Gong, Y-G., Feng, M-M., Hu, X-N., Wang, Y-Q., Gu, M., Zhang, W. and Ge, R-S., 2009. Peptidergic not monoaminergic fibers profusely innervate the young adult human testis. *Journal of Anatomy* 214: 330–338

Gore, A.C., 2002a. GnRH: The master molecule of reproduction. Norwell, MA Kluver Academic Publishers.

Goswami, S.K. and Singh, Y., 1988. Regional histochemistry of the ductus epididymis in camel. National symposium on recent advances in Anatomy of ruminant's reproduction and III convention. pp: 32.

Goyal, H. O., 1985. Morphology of the bovine epididymis. *AmericanJournal of Anatomy* 172(2): 155-172.

Goyal, H. O. and Williams, C. S., 1991. Regional differences in the morphology of the goat epididymis: A light microscopic and ultrastructural study. *American Journal of Anatomy* 190:349–69.

Gregor, G. and Hardge, T., 1995. The influence of gene variants at the Ryanodine-receptor on sperm quality of boars. *Archiv fur Tierzucht* 38: 527-538

Griswold, M.D., 2016. Spermatogenesis: The commitment to meiosis. *Physiological Review* 96: 1–17.

Grunewald, S., Paasch, U., Glander, H.J. and Anderegg, U., 2005. Mature human spermatozoa do not transcribe novel RNA. *Andrologia* 37(2-3): 69-71.

Gupta, A. N. and Singh, Y., 1988a. Post-natal development of the testis in goat. National Symposium on Recent Advances in Anatomy of ruminants Reproduction and IIIrd Convention June 23–25, 1988, pp.20.

Guzick, D.S., Overstreet, J.W., Factor-Litvak, P. and Brazil, C.K., 2001. Sperm morphology, motility, and concentration in fertile and infertile men. *New England Journal of Medicine* 345(19): 1388-1393.

Hafez, B. and Hafez, E.S.E., 2000. Reproduction in farm animals. 7th ed. New York. Lippincott Williams & Wilkins, USA.

Haidl, G., Jung, A. and Schill, W.B., 1996. Aging and sperm function. *Human Reproduction* 11:558–560.

Haimoto, H., Hosoda, S. and Kato, K., 1987. Differential distribution of immunoreactive S100-
alpha and S100-beta proteins in normal nonnervous human tissues. *LaboratoryInvestigation* 57:489-98.

Hall, J.E. and Gill, S., 2001. Neuroendocrine aspects of aging in women. *Endocrinology and Metabolism Clinics of North America* 30: 631-646.

Hamilton, D. W., 1975.Structure and function of the epithelium lining the ductuli efferentes, ductus epididymis, and ductus deferens in the rat. In: Handbook of Physiology Vol. 5: Male Reproductive System. (Eds. Greep RO, EB Astwood,), American Physiology Society, Washington, DC. pp 259-301.

Hannema, S.E. and Hughes, I.A., 2006. Regulation of Wolffian duct development. *Hormone Research* 67 (3): 142-151

Happold, D. C. D., 1987.*The mammals ofNigeria*.ClarendonPress.Oxford. pp. 10-16.

Hart, L. and Schoning, P., 1984. Age-related changes in the cat testis and epididymis. *American Journal of Veterinary Research* 45:2380–2384.

Hardy, M., Gelber, S. and Zhou, Z., 1991. Hormonal control of Leydig cell differentiation. *Annals of NewYork Academicof Science* 637:152–163.

Hargrove, J.L., MacIndoe, J.H. and Ellis, L.C., 1977. Testicular contractile cells and sperm transport. *Fertility and Sterility* 28: 146–1157.

He, D., Zhang, D., Wei, G., Lin, T. and Li, X., 2007. Cytoskeleton vimentin distribution of mouse Sertoli cells injured by nitrogen mustard in vitro. *Journal of Andrology* 28: 389–396.

Heizmann, C.W. and Cox, J.A., 1998. New perspectives on S100 proteins: a multi-functional Ca(2+)-, Zn(2+)- and Cu(2+)-binding protein family. *Biometals* 11:383-97.

Heizmann, C.W., Fritz, G. and Schafer, W., 2002. S100 Proteins: Structure, Functions and Pathology. *Frontiers in Bioscience* 7:1356-68.

Hejmej, A., Kotula-Balak, M., Sadowska, J. and Bilin´ska, B., 2007. Expression of connexin 43 protein in testes, epididymides, and prostates of stallions. *Equine VeterinaryJournal* 39: 122-127.

Hermo, L., 1995. Structural features and functions of principal cells of the intermediate zone of the epididymis of adult rats. *Anatomical Record* 242:515–30.

Hermo, L., Green, H. and Clermont, Y., 1991a. Golgiapparatus of epithelial principal cells of the epididymal initial segment of the rat: Structure, relationship with endoplasmic reticulum, and role in the formation of secretory vesicles. *Anatomical Record* 229:159–76.

Hess, R. A. and Franca, L. R., 2008. Spermatogenesis and cycle of the seminiferous epithelium. *Advanced Experimental Medical Biology* 636: 1–15.

Hess, R.A. and Franca, L.R., 2005. Structure of the Sertoli cell. In Sertoli cell biology edited by Griswold M and Skinner M. Elservier Academic Press. Pp. 19-40.

Hess, R.A., 1990. Quantitatve and qualitative characteristics of the stages and transitions in the cycle of the rat seminiferous epithelium: light microscopic observations of perfusion-fixed and plastic embedded testes. *Biology of Reproduction* 43: 525-542.

Hess, R.A., 2003. Estrogen in the adult male reproductive tract: a review. *Reproductive Biology and Endocrinology* 1:52.

Heyn, R., Makabe, S. and Motta, P. M., 2001. Ultrastructural morphodynamics of human Sertoli cells during testicular differentiation. *Italian Journal of Anatomy and Embryol*ogy 106: 163–171.

Hodges, R.D., 1974. *The Histology of the fowl*. London: Academic Press.pp. 300-326.

Hoffman, M., 2008. *Thryonomis swinderianus*. IUCN red list of threatened Species. Version 2013. International Union for Conservation of Nature. Retrieved 2013-09-08

Holash J.A., Harik, S.I., Perry, G. and Stewart, P.A., 1993. Barrier properties of testis microvessels. *Proceeding of National Academic of Science USA,* 90: 11069–11073

Holstein, A.F., 1976. Ultrastructural observations on the differentiation of spermatids in man. *Andrologia* 8: 157-165

Holstein, A. F., Roosen-Runge, E.C. and Schirren, C., 1988. Spermiogenesis in aging testis. In: *Illustrated Pathology of Human Spermatogenesis*, Eds: A. F. Holstein, E.C. Roosen-Runge and C. Schirren, Grosse Verlag, Berlin. pp 195-238.

Holstein, A.F. and Weiss, C., 1967. On the effect of the smooth musculature in thetunica albuginea in the testes of rabbits; measurement of the interstitial pressure.*Journal of Experimental Medicine*142: 334–337.

Horn, R., Pastor, L.M., Moreno, E., Calvo, A., Canteras, M. and Pallares, J., 1996. Morphological and morphometric study of early changes in the ageing golden hamster testis. *Journal of Anatomy* 188: 109-117.

Huhtaniemi, I. and Pelliniemi, L., 1992. Fetal Leydig cells: cellular origin, morphology, life span, and special functional features. *Proceeding of the Society for Experimental Biology and Medicine* 201, 125–140.

Humphrey, J. D. and Ladds, P. W., 1975. A quantitative histological study of changes in the bovine testis and epididymis associated with age. *Research in Veterinary Science*19: 135–141.

Hunnicutt, G.R., Mahan, K., Lathrop, W.F., Ramarao, C.S., Myles, G. and Primakoff, P., 1996b. Structural relationship of sperm soluble hyaluronidase to the sperm membrane protein PH-20. *Biology of Reproduction* 54: 1343-1349.

Hunter, N.,2003. Synaptonemal complexities and commonalities. *Molecular Cell* 12: 533–535.

Ichihara, I. and Pelliniemi, L.J., 2007. Morphometric and ultrastructural analysis of stage specific effects of Sertoli and spermatogenic cells seen after testosterone treatment on young adult rat testis, *Annals of Anatomy* 189: 413-426.

Igbokwe, C.O., 2010**.** Gross and microscopic anatomy of thyroid gland of the wild African grasscutter (*Thryonomys swinderianus*, Temminck) in Southeast Nigeria. *European Journal of Anatomy* 14 (1): 5-10

Immler, S., Pryke, S. R., Birkhead, T. R. and Griffith, S. C., 2010. Pronounced with in-individual plasticity in sperm morphometry across social environments. *Evolution* 64 (6): 1634-1643.

Ivy, G.O., Roopsingh, R., Kanai, S., Ohta, M., Sato, Y. and Kitani, K., 1996. Leupeptin causes an accumulation of lipofuscin substances and other signs of aging in kidneys of young rats: further evidences for the protease inhibitor model of aging. *Annals of New York Academic Science* 786:12-23

Jamieson, B.G.M., 2007. Avian spermatozoa: structure and phylogeny. In: Jamieson, BGM, editor. Reproductive biology and phylogeny of birds Part A. Jersey: Science Publishers. p.349–511

Johnson, A. K. and Gross, P. M., 1993. Sensory circumventricular organs and brain homeostatic pathways. FASEB J 7: 678-686..

Johnson, L. and Neaves, W.B., 1981. Age-related changes in the Leydig cell population, seminferous tubules and sperm production in stallion. *Biology of Reproduction*, 24:703-12

Jones, R., 2004. Sperm survival versus degradation in the mammalian epididymis: A hypothesis. *Biology of Reproduction* 71:1405–11.

Jones, R., Hamilton, D. W. and Fawcett, D. W., 1979. Morphology of the epithelium of the extratesticular rete testis, ductuli efferentes and ductus epididymidis of the adult male rabbit. *Journal of Anatomy* 156:373–400.

Jones, R.C., 1974. The ultrastructure of spermatozoa from some hystricomorph rodents. In The functional anatomy of the spermatozoon, Ed. Afzelius, B. A. Pergamon Press, Oxford, 1974, p. 251-258.

Jori, F., Mensah, G.A. and Adjanohoun, E., 1995. Grasscutter farming: an example of rational utilization of wildlife. *Biodiversity and Conservation* 4: 257-265.

Jung, A., Schuppe, H. C. and Schill, W. B., 2002. Comparison of semen quality in older and younger men attending an andrology clinic. *Andrologia* 34:116–122

Junqueira, L.C. and Carneiro, J., 2005. Basic histology. Textbook and atlas. 10th ed (in Croatian Z Bradamante. Lj. Kostovic-Knezevic. Eds). Skolska knjiga Zagreb.

Juste, J., Fa, J. E., Perez Del Val, J. and Castroviejo, J., 1995. Market dynamics of bushmeat species in Equatorial Guinea. *Journal of Applied Ecology* 32 (3): 454-467.

Kaleczyc, J., Majewaski, M., Calka, J. and Lakomy, M., 1993. Adrenergic innervation of the epididymis, vas deferens, accessory genital glands and urethra in the boar. *Folia Histochemistry Cytobiology* 31(3):117- 123.

Kaler, L.W. and Neaves, W.B., 1978. Attrition of the human Leydig cell population with advancing age. *Anatomical Research* 192:513-18.

Kaler, L.W. and Neaves, W.B., 1981. The androgen status of aging male rats. *Endocrinology* 108(2):712-9.

Kameda, Y., 1995. Co–expression of vimentin and 19S-thyroglbulin in follicular cells located in the C- cell complex of dog thyroid gland. *Journal of Histochemistry and Cytochemistry* 43 (11):1097-1106.

Kanchev, L.N., Konakchieva, R., Angelova, P.A. and Davidoff, M.S., 1995. Substance P modulating effect on the binding capacity of hamster Leydig cell LH receptors. *Life Science* 56: 1631–1637.

Kangawa, A., Otake, M., Enya,S., Yoshida, T. and Shibata, M., 2016. Histological development of male reproductive organs in Microminipigs. *Toxicologic Pathology* 44(8): 1105-1122.

Kannan, T.A., Ramesh, G. and Sivakumar, M., 2015. Age-related changes in the gross and histoarchitecture of testis in Japanese Quails (*Coturnix coturnix japonica*). *International Journal of Livestock Research* 5(6): 26-33.

Karmore, S.K., Dalvi, R. S., Meshram, B. and Deshmukh, S. K., 2015. Age-related changes in ultrastructure and histoenzymic distribution of epididymis in goat (*Capra hircus*). *Indian Journal of Veterinary Anatomy* 27(2): 47-51.

Kempinas, W.D., Suarez, J.D., Roberts, N.L. and Strader, L.F., 1998. Fertility of rat epididymal sperm after chemically and surgically induced sympathectomy. *Biology of Reproduction* 59:897-904.

Kerr, J.B. and de Krester, D.M., 1974. The role of the Sertoli cell in phagocytosis of the residual bodies of spermatids. *Journal of Reproduction and Fertility* 36:439-440 (abstract).

Kerr, J.B. and Knell, C.M., 1988. The fate of fetal Leydig cells during the development of the fetal and postnatal rat testis. *Development* 103: 535–544.

Kerr, J. B., 2000. Male reproduction system. In 'atlas of functional histology'. (Ed. J. B. Kerr.) pp. 339–358. Mosby International Limited:New York.

Kidd, S. A., Eskenazi, B. and Wyrobek, A. J., 2001. Effects of male age on semen quality and fertility: A review of the literature. *Fertility and Sterility* 75:237–248.

Kolodzieyski, L. and Danko, J., 1995. A histological, histochemical and immunohistochemical picture of the ovary of a hermaphrodite goat. *Folia Veterinarian* 39: 107-110.

Kishore, P.V.S., Geetha, R. and Sabiha, H., 2012. Postnatal differentiation and regional histological variations in the ductus epididymis of rams. *Tamilnadu Journal of Veterinary and Animal Science* 8(3): 145-151.

Kizawa, K., Uchiwa, H. and Murakami, U., 1996. Highly-expressed S100A3, a calcium-binding protein, in human hair cuticle. *Biochim Biophys Acta* 1312:94-98.

Kobayashi, A. and Behringer, R. R., 2003. Developmental genetics of the female reproductive tract in mammals. *Nature Review of Genetics* 4: 969-980

Kondracki, S., Banaszewska, D. and Mielnicka, C., 2005. The effect of age on the morphometric sperm traits of domestic pig (*Sus scrofa domestica*). *Cellular and Molecular Biology Letter* 10: 3-13.

König, H.E. and Liebich, H-G., 2014. Veterinary anatomy of domestic mammals: Textbook and color atlas. In: Endocrine gland (*Glandulae endocrinae*), Third Edition eds. König, H.E and Liebich, H-G Schattauerr Press, Stuttgart New York. Pp 561-569.

Kopecky, M., Semecky, V. and Nachtigal, P., 2005. Vimentin expression during altered spermatogenesis in rats. *Acta histochemica* 107: 279—289

Kotula-Balak, M., Hejmej, A., Sadowska, J. and Bilin´ska, B., 2007. Connexin 43 expression in human and mouse testes with impaired spermatogenesis. *European JournalofHistochemistry* 51: 261-268.

Krähn, G., Kaskel, P., Sander, S., Pereira, J., Waizenhöfer, Y., Wortmann, S., Leiter,U. and Peter, R.U., 2001. S100b is a more reliable tumor marker in peripheral blood for patients with newlyoccurred melanoma metastases compared with MIA, albumin and lactate-dehydrogenase. *Anticancer Res* 21, 1311-1316.

Kulkarni, S.A., Garde, S.V. and Sheth, A.R., 1992. Immunocytochemical localisation of bioregulatory peptides in marmoset testes. *Archives of Andrology* 29:87– 102.

Kumar, T.R., 2009. FSH beta knockout mouse model: a decade ago and into the future. *Endocrine* 36 (1): 1-5.

Kumanov, P., Nandipati, K.C., Tomova, A., Robeva, R. and Agarwal, A., 2005. Significance of inhibin in reproductive pathophysiology and current clinical applications. *Reproductive Biomedicine Online* 10(6):786–812.

Kumari, P., 2013. Gross, histomorphoiogicai and histochemical changes in testis, epididymis, vas, and seminal vesicles of developing (post-natal) kids of Black Bengal *goats.(Capra hircus)*. A thesis submitted to West Bengal University of animal and fishery sciences in partial fulfilment of the requirements for the degree of Doctorate of Veterinary Science.

Kuntz, A. and Morris, R.E., 1946. Components and distribution of the spermatic nerves and the nerves of the vas deferens. *Journal of Comparative Neurology* 85: 33–44.

Kuopio, T., Tapanainen, J., Pelliniemi, L. and Huhtaniemi, I., 1989. Developmental stages of fetal-type Leydig cells in prepubertal rats. *Development* 107: 213–220.

Lakomy, M, Kaleczyc, J. and Majewski, M., 1997. Noradrenergic and peptidergic innervation of the testis and epididymis in the male pig. *Folia HistochemCytobiologie* 35:19–27.

Lamano-Carvalho, T. L., Favaretto, A. L. V., Komesu, M. C. and Lopes, R. A., 1988. Influence of age on the production of rat spermatozoa, on their concentration in the cauda epididymis, and on FSH, LH and testosterone plasma levels. *Histology and Histopathology* 3: 413–417.

Laing, J.A., 1979. Fertility and Infertility in domestic animals. Third Edition, Pg. 261.

Lasheen, S.S., Refaat, S.H., EI-Nefiawy, N.E. and Abd-Elgawad, R.A., 2015. Developmental characteristics of rat testicular tissue and the impact of chronic noise stress exposure in the prenatal and postnatal periods. *Anatomy and Physiology* 4 (4):1-15.

Lasserre, A., Barrozo, R., Tezón, J. G., Miranda, P. V. and Vazquez-Levin, M. H., 2001. Human epididymal proteins and sperm function during fertilization. *Biological Research* 34:165–78.

Lauriola, L., Michetti, F., Maggiano, N. and Galli, J.,2000. Prognostic significance of the Ca2+

binding protein S100A2 in laryngeal squamous-cell carcinoma. *Int J Cancer (Pred Oncol)* 89, 345-349.

Leblond, C. P. and Clermont, Y., 1952. Spermiogenesis of rat, mouse, hamster and guinea pig as revealed by the periodic acid fuschin sulphurous acid technique. *American Journal of Anatomy* 90(2): 167-215.

Leder, B.Z., Rohrer, J.L., Rubin, S.D., Gallo, J. and Longcope, C., 2004. Effects of aromatase inhibition in elderly men with low or borderline-low serum testosterone levels. *Journal of Clinical Endocrinology and Metabolism* 89 (3): 1174-1180.

Leung, G. P., Cheung, K. H., Leung, C. T., Tsang, M. W. and Wong, P. Y., 2004. Regulation of epididymal principal cell functions by basal cells: Role of transient receptor potential (Trp) proteins and cyclooxygenase-1 (COX-1). *Molecular Cell Endocinology* 216:5–13.

Lie, P. P., Mruk, D. D., Lee, W. M. and Cheng, C. Y., 2010. Cytoskeletal dynamics and spermatogenesis. *Philosophical Transactions of the Royal Society B: Biological Sciences* 365 (1546):1581-1592

Liguori, G., Paino, S., Squillacioti, C. and De Luca, A., 2013. Innervation and Immunohistochemical Characteristics of Epididymis in Alpaca Camelid (Vicugna Pacos), *Italian Journal of Animal Science* 12:1, e15

Lim, M.C., Maubach, G. and Zhuo, L., 2008. Glial fibrillary acidic protein splice variants in hepatic stellate cells–expression and regulation. *Molecular Cells* 25:376–384

Lording, D. and De Kretser, D., 1972. Comparative ultrastructural and histochemical studies of the interstitial cells of the rat testis during fetal and postnatal development. *Journal of Reproduction and Fertility* 29, 261–269.

Lodish, H., Berk, A., Matsudaira, P., 2005. Molecular Cell Biology, 5th ed. WH Freeman & Co, Nova Iorque

Lowseth, L.A., Gerlach, R.F., Gillett, N.A. and Muggenburg, B.A., 1990. Age-related changes in the prostate and testes of the Beagle dogs. *Veterinary Pathology* 27: 347-353.

Lumpkin, M., Negro-villar, A., Franchimont, P. and McCann, S., 1981. Evidence for a hypothalamic site of action of inhibin to suppress FSH release. *Endocrinology* 108: 1101-1104.

Lydka, M., Kotula-balak, M., Kopera-sobota, I.,Tischner, M. and Bilin´ska, B., 2011. Vimentin expression in testes of Arabian stallion. *Equine Veterinary Journal* 43 (2): 184-189.

Maekawa, M., Kamimura, K. and Nagano, T., 1996. Peritubular myoid cells in the testis: their structure and function. *Archive of Histology and Cytology* 59: 1–13.

Manandhar, G., Sutovskya, P., Joshib, H. C., Stearnsc, T. and Schattena, G., 1998. Centrosome reduction during mouse spermiogenesis. *Developmental Biology*203: 424–434.

Manandhar, G., Simerly, C., Salisbury, J. L. and Schatten, G., 1999. Centriole and centrin degeneration during mouse spermiogenesis. *Cell Motil. Cytoskeleton* 43: 137–144.

Manandhar, G., Simerly, C. and Schatten, G., 2000. Highly degenerated distal centrioles in rhesus and human spermatozoa. *Human reproduction*, 15(2): 256-263.

Manandhar, G. and Sutovsky, P., 2007. Comparative histology and subcellular structure of mammalian spermatogenesis and spermatozoa. In 'Comparative reproductive biology'. (Eds H. Schattenand G. M. Constantinescu.). pp. 81–95. Blackwell Publishing Professional:Carlton, Ames.

Marchese-Ragona, S.P. and Johnson, K.A., 1990. Structural and biochemical studies of the dynein ATPase. In Gagnon, C. (ed.), *Controlsof Sperm Motility: Biological and Clinical Aspects*. CRC Press, Boca Raton, pp. 203–217.

Maree, L., Du Plessis, S.S., Menkveld, R. and Van der Horst, G., 2010. Morphometric dimensions of the human sperm head depend on the staining method used. *Human Reproduction* 25(6): 1369-1382

Marettová, E., Maretta, M. and Legáth, J., 2010. Changes in the peritubular tissue of rat testis after cadmium treatment. *Biology of Trace Elements Research* 134:288–295.

Marinoni, E., Di Iorio, R., Gazzolo, D., Lucchini, C. and Michetti, F., 2002. Ontogenic localisation and distribution of S-100 beta protein in human placentaltissues. *Obstetric andGynecology* 99:1093-1099.

Martínez, A. I P., 2004. Canine fresh and cryopreserved semen evaluation. *Animal Reproductive Science* 82: 209-24.

Matsumoto, A.M., 2001. The testis. In: Felig P, Frohman, L.A., eds. Endocrinology and Metabolism, 4th ed. New York: McGraw-Hill. Pp. 635-705.

Maunoury, R., Portier, M-M., Léonard, N. and McCormick, D., 1991. Glial fibrillary acidic protein in adrenocortical and Leydig cells of the Syrian golden hamster (Mesocricetus auratus). *Journal of Neuroimmunology* 35: 119–129

Mayerhofer, A., Amador, A.G., Steger, R.S. and Bartke, A., 1990. Testicular function after local injection of 6hydroxydopamine or norepinephrine in the golden hamster (Mesocrisetusauratus). *Journal of Andrology* 11: 301–311.

McCarrey, J.R., 2013. Toward a more precise and informative nomenclature describing fetal and neonatal male germ cells in rodents. *Biology of Reproduction* 89: 47.

McLaren, A., 1998. Gonad development: assembling the mammalian testis. *Curriculum Biology* 8: 175–177.

Meachem, S.J., Nieschlag, E. and Simoni, M., 2001. Inhibin B in male reproduction: pathophysiology and clinical relevance . *European Journal of Endocrinology* 145: 561-71

Meisner, A. D., Klaus, A. V. and O'leary, M. A., 2005. Sperm head morphology in 36 species of artiodactylans, periodactylans, and cetaceans (Mammalia). *Journal of Morphology* 263: 179-202.

Memon, M. A., Bretzlaff, R. N. and Ott, R. S., 1986. Comparison of semen techniques in goats. *Theriogenology* 26: 823-827.

Mendis-Handagama, S.M.L.C., Risbridger, G.P. and de Kretse, D.M., 1987. Morphometric analysis of the components of the neonatal and the adult rat testis interstitium. *International Journal of Andrology* 10: 525–534

Mendis-Handagama, S.M.L.C.H. and Ariyaratne, H.B.S., 2001. Differentiation of the adult Leydig cell population in the postnatal testis. *Biology of Reproduction* 65: 660–671.

Menkveld, R., Oettlé, E. E., Kruger, T. F., Swanson, R. J., Acosta, A. A. and Oehninger, S., 1991. Atlas of human sperm morphology. Baltimore: Williams & Wilkins; 1991.

Mestrich, M.L., 1993. Nuclear morphogenesis during spermiogenesis. In molecular biology of the male reproductive system. D de Krester Ed. Academic Press, San Diego. pp. 67-97.

Michetti, F., Lauriola, L, Rende, M, and Stolfi, V.M., 1985. S-100 protein in the testis. An immunochemical and immunohistochemical study. *Cell Tissue Research* 240:137-42.

Miyake, K., Yamamoto, M., Narita, H., Hashimoto, J. and Mitsuya, H., 1986. Evidence for contractility of the human seminiferous tubule confirmed by its response to noradrenaline and acetylcholine. *Fertility and Sterility* 46: 734-737

Molenaar, G. J., Sienkiewicz, W., Lakomy, M. and Meloen, R.H., 1997. New data on the nervous influence on male fertility and testis functions - inverse relation between nervous and endocrine activities. *Annals of Anatomy* [*Suppl*] 179: 10-11

Monadjem, A., Taylor, P. J., Denys, C. and Cotterill, F. P., 2015. Rodents of sub-Saharan Africa: a biogeographic and taxonomic synthesis. Walter de Gruyter GmbH, Berlin, Germany, 2015. pp. 1102.

Monesi, V., 1965. Synthetic activities during spermatogenesis in the mouse. RNA and protein. *Experimental Cell Research* 39: 197-224.

Moniem, K.A., Tingari, M.D. and Kunzel, E., 1980. The fine structure of the boundary tissue of the seminiferous tubules of the camel (*Camelus dromedarius*). *Acta Anatomica* 107:169-76.

Monteiro, J.C., Pinto da Matta, S. L., Predes, F. S. and Rego de Paula, T. A., 2012. Testicular morphology of adult Wistar rats treated with *Rudgea viburnoides* (Cham.) Benth. Leaf Infusion. *Brazillian Archives Biology Technology* 55 (1): 101-105.

Moore, H.D.M., 1990a. The development of sperm-egg recognition processes in mammals. *Journal of Reproduction and Fertility Supplement* 42:71-78.

Moore, K.L. and Persaud, T.V.N., 2003. Urogenital system. In: *The developing human: clinical* o*riented embryology*, Saunders Elsevier, (Ed.), pp. 246-285, Elsevier, ISBN: 978-85- 352-2662-1, Philadelphia: Saunders.

Morales, E. H. R., Pastor, L.M., Santamaria, L., Pallarés, J., Zuasti, A., Ferrer, C. and Canteras, M., 2004. Involution of seminiferous tubules in agedhamsters: an ultrastructural, immunohistochemicaland quantitative morphological study. *Histology Histopathology* 19: 445-455.

Mortimer, D., 1994. Practical laboratory andrology. Oxford University Press on Demand, New York, 13-36.

Mortimer, S.T., 1997. A critical review of the physiological importance and analysis of sperm movement in mammals. *Human reproduction update* 3(5): 403-439.

Moore, B.W., 1965. A soluble protein characteristic of the nervous system. *Biochemical Biophysical Research Communications* 9:739-44.

Moss, J.A., Melrose, D.R., Reed, H.C.B. and Vandeplassche, M., 1979. Semen and artificial inseminaton. In: Fertilty and infertility in domestic animals. Laing, J.A (eds) 3rd, London, Bailliere Tindal. p.57.

Mostaghel, E.A., 2013. Steroid hormone synthetic pathways in prostate cancers. *Translational Andrology and Urology* 2(3): 212-227.

Motoc, A., Rusu, M.C. and Jianu, A. M., 2010. The spermatic ganglion in humans: an anatomical update. *Romanian Journal of Morphology and Embryology* 51(4):719–723.

Moustafa, A.M., 2012. Age-related changes in the immunohistochemical localisation pattern of α-smooth muscle actin and vimentin in rat testis. *The Egyptian Journal of Histology* 35:412-423.

Muller-Esterl, W. and Fritz, H., 1981.Sperm acrosin. *Methods Enzymology* 8: 621-632.

Myster, S.H., Knott, J.A., Wysocki, K.M., O'toole, E., and Porter, M.E., 1999. Domains in the 1α dynein heavy chain required for inner arm assembly and flagellar motility in Chlamydomonas. *The Journal of cell biology* 146(4): 801-818.

Nadir, F., Khavanin, A., Mazaheri, Z. and Soleimanian, A., 2016. Effect of noise pollution on male fertility (Review). *Journal of occupational health and epidemiology* 5 (1): 53-62.

Naftolin, F., Garcia-Segura, L.M., Hovath, T.L., Zsarnovsky, A., Demir N., Fadiel, A., 2007. Estrogen-induced hypothalamic synaptic plasticity and pituitary sensitization in the control of the estrogen-induced gonadotropin surge. *Reproductive Sciences* 14(2): 101-116.

NagDas, S.K., Winfrey, V.P. and Olson, G.E., 1996.Identification of hydrolase binding activities of the acrosomal matrix of hamster spermatozoa. *Biology of Reproduction* 55: 1405-1414.

Nakagawa, T., Nabeshima, Y. and Yoshida, S., 2007. Functional identification of the actual and potential stem cell compartments in mouse spermatogenesis. *Developmental Cell* 12: 195–206.

Nallella, K.P., Sharma, R.K., Aziz, N. and Agarwal, A., 2006. Significance of sperm characteristics in the evaluation of male infertility. *Fertility and sterility* 85(3): 629-634.

Neaves W.B., Johnson, L. and Petty, C.S., 1985. Age-related changes in numbers of other Interstitial cells in testes of adult men: evidencing bearing on the fate of Leydig cells lost with increasing age. *Biology of Reproduction* 33:259-69.

Neesen, J., Kirschner, R., Ochs, M.and Schmiedl, A., 2001. Disruption of an inner arm dynein heavy chain gene results in asthenozoospermia and reduced ciliary beat frequency. *Human molecular genetics* 10(11): 1117-1128.

Nicander, L. and Glover, T. D., 1973. Regional histology and fine structure of the epididymal duct in the golden hamster (*Mesocricetus auratus*). *Journal of Anatomy* 114:347–64.

Nie, R., Zhou, Q., Jassim, E., Saunders, P.T. and Hess, R.A., 2002. Differential expression of estrogen receptors alpha and beta in the reproductive tracts of adult male dogs and cats. *Biology of Reproduction* 66:1161-1168.

Nilsson, S. and Gustafsson, J.A., 2002. Estrogen receptor action. *Critical Review in Eukaryotic Gene Expression* 12: 237-258.

Ninomiya, I., Ohta, T. Fushida, S. Endo, Y. Hashimoto, T. and Yagi, M., 2001. Increased expression of S100A4 and its prognostic significance in esophageal squamous cell carcinoma. *International Journal of Oncology* 18: 715-720.

Nipken, C. and Wrobel, K. H., 1997. A quantitative morphological study of age-related changes in the donkey testis in the period between puberty and senium. *Andrologia* 29 149-161.

Nishimura, S., Okano, K., Yasukouchi, K., Gotoh, J., Tabata, S. and Iwamoto H., 2000. Testis developments and puberty in the male Tokara (Japanese native) goat. *Animal Reproductive Science* 64: 127–131.

Nistal, M., Paniagua, R. and Asuncion-Abaurrea, M., 1982. Varicose axons bearing synaptic vesicles on the basal lamina of the human seminiferous tubules. *Cell Tissue Research* 226: 75-82.

Nojima, D., Linck, R.W. and Egelman, E.H., 1995. At least one of the protofilaments in flagellar microtubules is not composed of tubulin. *Curriculum in Biology* 5: 158-167.

Ntiamoa-Baidu, Y., 1998. Sustainable use of bush meat. Wildlife development plan: 1998–2003. Wildlife Department, Accra. 6: 78.

Oakberg, E.F., 1956a. A description of spermiogenesis in the mouse and its use in analysis of the cycle of the seminiferous epithelium and germ cell renewal. *The AmericanJournal of Anatomy* 99:391-413

O'Donnel, L., Nicholis, P.K.., O'Bryan, M.K., McLachlan, R.I. and Stanton, P.G., 2011. Spermiation: The process of sperm release. *Spermatogenesis* 1(1): 14-35.

Oduwole, O.O., Peltoketo, H. and Huhtaniemi, I.T., 2018. Role of Follicle-Stimulating Hormone in Spermatogenesis.Role of Follicle-Stimulating Hormone in Spermatogenesis. *Frontiers in Endocrinology* 9: 763

Oettel, M. and Mukhopadhyay, A.K., 2004. Progesterone: the forgotten hormone in men? *The aging mal*e, 7: 236-257.

Ogwuegbu, S. O., Oke, B. O., Akusu, M. O. and Aire, T. A., 1985. Gonadal and extragonadal sperm reserves of the Maradi (Red Sokoto) Goat. *Bulletin of Animal Health and Productionin Africa* 33: 139-141

Oke, B.O., 1982. Some studies on the reproductive organs of the African giant rat (*Cricetomys gambianus*, Waterhouse) during the climatic seasons at Ibadan. MSc. Thesis, Department of Veterinary Anatomy, University of Ibadan, Nigeria.

Oke, B. O., Aire, T. A., Adeyemo, O. and Heath, E., 1988. The structure of the epididymis of the giant rat (Cricetomys gambianus, Waterhouse): histological, histochemical and microstereological studies. *Journal of Anatomy* 160: 9-19.

Oke, B.O., Aire, T.A., Adeyemo, O. and Heath, E., 1989. The ultrastructure of the epididymis of the African giant rat (*Cricetomys gambianus*, Waterhouse). *Journal of Anatomy* 165:75-89.

Oloye, A.A., Oyeyemi, M.O., Ola-Davies, O.E. and Innamah, O.A., 2011. Effect of aqueous extracts of *Spondias monbin* on the spermiogram of Wistar rats. *Bulletin of Animal Health and Production African* 59: 95-99

Olude, M.A., Mustapha, O.A., Aderounmu., O.A., Olopade, J.O. and Ihunwo, A.O., 2015. Astrocyte morphology, heterogeneity and density in the developing African giant rat (*Cricetomys gambianus*). *Frontiers in Neuroanatomy* 9: 1-10

Olude, M.A., Mustapha, O.A., Sonubi, A.C., Falade, T.E., Ogunbunmi, T.K., Adebayo, A.O. and Akinloye, A.K., 2014. Morphometric study of the skull of the greater cane rat (*Thryonomys swinderianus,* Temmnick). *Nigeria Veterinary Journal* 35(3): 1026-1037

Olukole, S. G., Oyeyemi, M.O. and Oke, B. O., 2014. Semen characteristics and spermiogram of the African greater cane rat (*Thryonomys swinderianus,* Temminick). *Slovak Journal of Animal Science* 47 (3): 125-131.

Olukole, S.G., Oyeyemi, M.O. and Oke, B.O., 2009. Biometrical observations on the testes and epididdymis of the domesticated adult African greater cane rat (*Thryonomys swinderianus*). *European Journal of Anatomy* 13 (2): 71-75.

Olukole, S.G., Oyeyemi, M.O. and Oke, B.O., 2010. Gonadal and extragonadal sperm reserves of the domesticated adult African greater cane rat (*Thryonomys swinderianus*). *Reproductive biology* 10 (2): 155-158

Olukole, S.G., Madekurozwa, M-C. and Oke, B.O., 2018. Spermiogenesis in the African sideneck turtle (*Pelusios castaneus*): Acrosomal vesicle formation and nuclear morphogenesis. *Journal of King Saud University - Science.*30 (3): 359-366

Opara, M.N., Ike, K.A. and Okoli, I.C., 2006. Haematology and plasma biochemistry of the wild adult African grasscutter (*Thryonomis swinderianus*. Temminck). *Journal of American Science* 2(2):17-22

Opara, M.N., 2010. The grasscutter I: The livestock of tomorrow. *Research Journal of Forestry* 4(3):119-135.

Orgebin-Crist, M.-C., 1962. Recherches expérimentales sur la durée de passage des spermatozoïdes dans l'épididyme du taureau. *Annals of Biology Animal Biochemistry and Biophysiology* 2, 51–108.

Orwoll, E., Lambert, L.C., Marshall, L.M., Phillips, K., Blank, J. and Barrett-Connor E. ,2006. Testosterone and estradiol among older men. *Journal of Clinical Endocrinology and metabolism* 91 (4): 1336-1344.

Owen, O. J. and Dike, U. A., 2012. Grasscutter (*Thyonomys Swinderianus*) husbandry in Nigeria: A review of the potentialities, opportunities and challenges. *Journal of Environmental Issues and Agriculture in Developing Countries* 4 (1): 104-11

Oyeyemi, M.O., Oke, A.O., Ajala, O.O. and Idehen, C.O., 2002. Differences in testicular parameters and morphological characteristics of spermatozoa as related to age of West African Dwarf bucks. *Tropical Journal of Animal Science* 5:99-107.

Oyeyemi, M.O. and Ubiogoro, O., 2005. Spermiogram and morphological characterstics in testicular and epididymal spermatozoa of large boar in Nigeria. *International Journal of Morphology* 23 (3): 235-23

Oyeyemi, M.O. and Babalola, E. T., 2006. Testicular parameters and morphological characteristics of testicular and epididymal spermatozoa of white Fulani bulls in Nigeria. *International Journal of Morphology* 24(2): 175-180.

Oyeyemi, M.O., Olukole, S.G., Taiwo, B. and Adeniji, D.A., 2009. Sperm motility and viability in West African dwarf rams treated with *Euphorbia hirta*. *International Journalof Morphology* 27(2): 459-462.

Page, S.L. and Hawley, R.S., 2004. The genetics and molecular biology of the synaptonemal complex. *Annual Review of Cell and Developmental Biology* 20: 525–558.

Parkinson, T., 2001. Fertility and infertility in male animals.In: *Arthur's Veterinary Reproduction and Obstetrics* (Eds.: Noakes, D. E., Parkinson, T. J. and England, G. C. W.) 8th edition. Saunders Publishers, Edinburgh. 2001, p. 695-750.

Paniagua, R., Codestal, J., Nistal, M., Rodriguez, M.C. and Santamaria, L., 1987a. Quantification of cell types throughout the cycle of the human seminferous epithelium and their DNA content. *Anatomy and Embryology* 176:225-230.

Paniagua, R., Nistal, M., Amat, P., Rodriguez, M.C. and Martin, A., 1987. Seminiferous tubule involution in elderly men. *Biology of Reproduction* 36: 939-947.

Parés-Casanova, P. M., Samuel O. M. and Olopade J. O., 2015. Non-functional sexually dimorphic mandibular differences in the African rodent *Thryonomys swinderianus(*Temminck, 1827). *Annals of Biological Research* 6 (10): 26-31

Parkinson, T., 2001. Fertility and infertility in male animals. Pages 695 – 750. In: Noakes, D. E., Parkinson, T. J. and England, G. C. W. (Eds.). *Arthur's Veterinary Reproduction and Obstetrics*. 8th Edition, Saunders Publishers, Edinburgh.

Pastor, L.M., Zuasti, A., Ferrer, C., Bernal-Ma~nas, C. M., Morales, E., Beltr_an-Frutos E. and Seco-Rovira, V. 2011. Proliferation and apoptosis in aged and photoregressed mammalian seminiferous epithelium, with particular attention to rodents and humans. *Reproduction in Domestic Animal* 46:155–164.

Pasquini, C., Spurgeon, T. and Pasquini, S. 1997. *Anatomy of domestic animals: systemic and regional approach*. 9th ed. Sudz publishing.

Paulsen, F., Hallmann, U., Paulsen, J. and Thalr, A. 2000. Innervation of the cavernosus body of

the human efferent tear ducts and function in tear outflow mechanism. *Journal of Anatomy* 197:177-187.

Păunescu, T. G., Shum, W. W., Huynh, C., Lechner, L., Goetze, B., Brown, D. and Breton, S., 2014. High-resolution heliumion microscopy of epididymal epithelial cells and their interaction with spermatozoa. *Molecular Human Reproduction* 20:929–37.

Peltoketo, H., Rivero-Muller A., Ahtiainen, P., Poutanen, M. and Huhtaniemi, I. 2010. Consequences of genetic manipulations of gonadotropins and gonadotropin receptors in mice. *Annales d endocrinology* 71 (3): 170-176.

Pérez-Armendariz, E.M., Romano, M.C., Luna, J., Miranda, C., Bennett, M.V. and Moreno A.P. 1994. Characterization of gap junctions between pairs of Leydig cells from mouse testis. *American Journal of Physiology* 267(2 pt 1):570–580.

Phillips N.J., McGowan M.R., Johnston S.D. and Mayer D.G., 2004. Relationship between thirty post-thaw spermatozoal characteristics and the field fertility of 11 high-use Australian dairy AI-sires. *Animal Reproductive Science* 81(1/2):47-61.

Phillips, B.T., Gassei, K. and Orwig, K.E., 2010. Spermatogonial stem cell regulation and spermatogenesis. *Philosophical Transactions of the Royal Society B*, 365: 1663–1678

Ploen, L., 1971. A Scheme of rabbit spermateliosis based upon electron-microscopical observations. *Zeitschrift fur Zellforschung und mikroskopische Anatomie* 115: 553-564.

Prince, F.P., 1992. Ultrastructural evidence of indirect and direct autonomic innervation of human Leydig cells: Comparison of neonatal, childhood and pubertal ages. *Cell Tissue Research* 269:383-390.

Prince, F.P., 1996. Ultrastructural evidence of adrenergic, as well as cholinergic, nerve varicosities in relation to the lamina propia of the human seminiferous tubules during childhood. *Tissue cell* 28: 507-513.

Pudney, J., 1986. Fine structural changes in Sertoli and Leydig cells during the reproductive cycle of the ground squirrel, *Citellus lateralis*. *Journal of Reproduction and Fertility* 77: 37-49

Pudney, J., Canick, J.A., Clifford, N.M., Knapp, J. and Callard, G.V., 1985. Location of enzymes of androgen and estrogen biosynthesis in the testis of the ground squirrel (*Citellus lateralis*). *Biology and Reproduction* 33: 971-980.

Quintero-Moreno, A., Gonzalez-Villalobos, D., Lopez-Brea, J. J. G., Esteso, M. C., Fernandez-Santos, M. R., Carvalho-Crociata, J. L., Mejia-Silva, - W. and Leon-Atencio, G., 2009. Morphometric evaluation of sperm head of domestic pig according to their Age. *Revista Cientifica* FCV-LUZ, 19: 153-158.

Rajani, C., Ramesh, G. and Vijayaragavan, C., 2008. Histoenzymic studies of the epididymis in rat (*Rattus norwegicus*). *Indian Journal of Animal Research* 42: 291-293.

Ramos, A. S. and Dym, M., 1977a. Fine structure of the monkey epididymis. *American Journal of Anatomy*, 149 (4) 501.

Ramos-Ibeas, P., Pericuesta, E., Fernández-González, R., Ramírez, M. A and Gutierrez-Adan, A. 2013. Most regions of mouse epididymis are able to phagocytose immature germ cells. *Reproduction* 146:481–89.

Rauchenwald M., Steers, W.D. and Desjardins, C., 1995. Efferent innervation of the rat testis. *Biology of Reproduction* 52: 1136–1143.

Rezigalla, A.A., Makawi, S.A. and Tingari, M.D., 2012. Rabbit seminiferous tubules morphological observations on the boundary tissue. *Professional Medical Journal* 19(5): 742-746.

Ricci, G., Andolfi, L., Zabucchi, G., Luppi, S., Boscolo, R., Martinelli, M., Zweyer, M. and Trevisan, E., 2015. Ultrastructural morphology of sperm from human globozoospermia. *BioMedical Research International* 2015(6): 1-8.

Ricker D.D., Chamness, S.L., B.T. and Chang, T.S.K., 1996. Changes in luminal fluid protein composition in the rat cauda epididymis following partial sympathetic denervation. *Journal of Andrology* 17:117-126.

Robaire, B. and Hermo, L., 1988. Efferent ducts, epididymis, and vas deferens: Structure, functions and their regulation. In *The physiology of reproduction,* eds. E. Knobil and J. D. Neill, 999–1080. Raven Press, New York.

Robaire, B., Syntin, P. and Jervis, K., 2000. The coming of age of the epididymis. In: *Testis, Epididymis and Technologies in the Year 2000*, Jégou B, Pineau C, Saez J, (Ed.), pp. 229- 262, Springer: Hildenberg, ISBN 978-3-540-67345-3, New York, EUA.

Robaire, R., Hinton, B. T. and Orgebin-Crist, M. C., 2006. The epididymis. In Physiology of Reproduction, eds. E. Knobil and J. D. Neill, 3rd edn., 1071–147. Elsevier, New York.

Rodríguez, C. M., Labus, J. C. and Hinton, B. T. , 2002. Organic cation/carnitine transporter, OCTN2, is differentially expressed in the adult rat epididymis. *Biology of Reproduction,* 67:314–19.

Roosen-Runge, E.C. , 1973. Germinal cell loss in normal metazoan spermatogenesis. *Journal of Reproduction and Fertility* 35: 339-348.

Rothwell, B. and Tingari, M.D., 1973. The ultrastructure of the boundary tissue of the seminiferous tubule in the testis of the domestic fowl (*Gallus domesticus*). *Journal of Anatomy* 114: 321–328.

Rowlands, I.W., 1994. Capacity of hyaluronidase to increase the fertilizing power of sperm. *Nature (London)* 154: 323-333.

Ruhl, S., 2001. Immunohistochemische Lokalisation von Spermadhesinen im Hoden and Nebenhoden des Hundes (*Canis familiaris*). Vet. Med. Diss., Tierärztliche Fakultät, LMU, München, Deutschland.

Russell, L., 1977. Desmosome-like junctions between Sertoli and germ cells in the rat testis. *American Journal of Anatomy,* 148, 301–312.

Russell, L. and Frank, B., 1978. Characterization of rat spermatocytes after plastic embedding. *Archiveof Andrology* 1(1):5-18.

Russell, L. D., Ren, H. P., Sinha, H. I., Schulze, W. and Sinha, H. A., 1990. A comparative study in twelve mammalian species of volume densities, volumes, and numerical densities of selected testis components, emphasizing those related to the Sertoli cell. *American Journal of Anatomy*188: 21–30.

Russell, L. and Clermont, Y., 1976. Anchoring device between Sertoli cells and late spermatids in rat seminiferous tubules. *Anatomical Record,* 185, 259–278.

Russell, L.D., 1977a. Movement of spermatocytes from the basal to the adluminal compartment of the rat testis. *The American Journal of Anatomy* 148:313-328.

Russell, L.D., 1978. The blood-testis barrier and its formation relative to spermatocyte maturation in the adult rat: A lanthanum tracer study. *The Anatomical Record* 190:99-112.

Russell, L.D., 1979b. Further observations on tubulobulbar complexes formed by late spermatids and Sertoli cells in the rat tests. *The Anatomical Record* 194: 213-232.

Russell, L.D., 1993. Form, dimensions, and cytology of mammalian Sertoli cells. In The Sertoli Cell. L.D Russell and M.D Griswold Eds. Cache River Press, Clearwater. pp. 1-37.

Russell, L.D. and Malone, J.P., 1980. A study of Sertoli-spermatid tubulobulbar complexes in selected mammals. *Tissue and Cell* 12: 263-285.

Russell, L.D., Ettlin, R.A., Sinha Hikim, A.P. and Clegg, E.D., 1990b. Histological and histopathological evaluation of the testis. Cache River Press, Clearwater.

Samuelson, D.A., 2007. Textbook of veterinary histology. (ed.). Saunders Elservier, St. Louis Missouri 63146. 418-441.

Santos, P.R.S., Oliveira, M. F., Arroyo, M. A. M., Silva, A. R., Rici, R. E. G., Miglino, M. A. and Assis Neto, A. C., 2014. Ultrastructure of spermatogenesis in Spix's yellow-toothed cavy (*Galea spixii*). *Reproduction* 147: 13–19

Sànchez, B., Flores, J. M., Pizarro, M. and Garcia P., 1998. Histological and immunohisto-chemical study of the cat epididymis. *Anatomia Histologia Embryologia* 27 (2): 135-140.

Sapsford, C.S., Rae, C.A. and Cleland, K.W., 1969. The fate of residual bodies and degenerating germ cells and the lipid cycle in Sertoli cells in the bandicoot (*Parameles nasuta*). *Australian Journal of Zoology* 17: 195-292.

Sarrna, K., Kalita, S.N. and Devi, J., 2011. Age-related changes in the cytomorphology of the seminiferous epithelium in Assam goat (Capra hircus) from birth to 10 month.. *Folia Veterinaria* 55(1): 45-49.

Sasaki, M., Endo, H., Kimura, J., Rerkamnuaychoke, W., Hayakawa, D., Bhuminand, D., Kitamura, N. and Fukuta, K.. 2010. Immunohistochemical localisation of the cytoskeletal proteins in the testes of the lesser mouse deer (*Tragulus javanicus*) *Mammal Study* 35(1):57-64.

Sasaki, M., Yamamoto, M., Arishima, K. and Eguchi, Y., 1998. Effects of follicle-stimulating hormone on intermediate filaments and cell division of Sertoli cells of fetal rat testis in culture. *Journal of Veterinary Medical Science* 60: 35–39.

Sathananthan, A.H., Ratnam, S.S., Ng, S.C., Tarin, J.J., Gianaroli, L. and Trounson, A., 1996. The sperm centriole: its inheritance, replication and perpetuation in early human embryos. *Human Reproduction* 11(2): 345-356.

Schäfer, B.W and Heizmann, C.W. (1996). The S100 family of EF-hand calcium-binding proteins: functions and pathology. *Trends in Biochemical Sciences*, 21:134-40.

Schimming, B.C., Pinheiro, P.F.F., Vicentini, C.A. and Domeniconi, R.F., 2012. Ultrastructure of the epithelium lining of cauda epididymidis in mongrel dog. *Pesquisa Veterinaria Brasileira* 32(Supl.1): 32-36.

Schulster, M., Bernie, A.M. and Ramasamy, R., 2016. The role of estradiol in male reproductive function. *Asian Journal of Andrology* 18: 435-440.

Scott, H.M., Manson, J.I. and Sharpe, R.M., 2009. Steroidogenesis in the fetal testis and its susceptibility to disruption by exogenous compounds. *Endocrine Reviews* 30 (7): 883-925.

Seiler, P., Cooper, T. G. and Nieschlag, E., 2000. Sperm number and condition affect the number of basal cells and their expression of macrophage antigen in the murine epi-didymis. *International Journal of Andrology* 23:65–76.

Serre, V. and Robaire, B., 1998. Segment-Specific Morphological Changes in Aging Brown Norway Rat Epididymis‘. *Biology of Reproduction*58: 497-513.

Setchell, B.P., 1978. The mammalian Testis. Paul Elek, London.

Setchell, B.P., 1980. The functional significance of blood-testis barrier. *Journal of Andrology* 1: 3-10.

Setchell, B.P., Maddocks, S. and Brooks, D.E., 1994. Anatomy, vasculature, innervations and fluids of the male reproductive tract. In physiology and reproduction 2nd Ed. E. Knobil and J.D Neil Eds. Raven Press, New York. pp 1068-1176.

Setchell, B.P., 1998. The Parkes lecture. Heat and the testis. *Journal of Reproduction and Fertility* 114: 179-194.

Setchell BP, Maddocks S. and Brooks D., 1994. Anatomy, vasculature, innervation and fluids of the male reproductive tract; in Knobil E, Neill JD (eds): The Physiology of Reproduction. New York, Raven Press, vol 1, pp 1063–1176.

Shackleton, C. and Manulowicz, E., 2003. Apparent pregnene hydroxylation deficiency (APDH); seeking the percentage of an orphan metabolome. *Steroids* 68:707-17.

Shagufta, B., Sharma, K., Suri, S. and Devi, J., 2012. Histochemical studies on the testis of adult Bakerwali goat (Capra hircus). *Indian Journal of Veterinary Anatomy* 24(1): 50-51.

Sharma, R. and Agarwal, A., 2011. Spermatogenesis: an overview. In: Zini A., and Agarwal A. (ed.), Sperm chromatin: Biological and clinical applications in male. Springer, New York, 19-44.

Sharpe, R.M., 1994. Regulation of spermatogenesis. In the physiology of reproduction. 2nd Ed. E. Knobil, J.D Neill Eds. Raven Press, New York. pp. 1363-1434.

Show, M.D., Anway, M.D., Folmer, J.S. and Zirkin, B.R., 2003. Reduced intratesticular testosterone concentration alters the polymerization state of the Sertoli cell intermediate filament cytoskeleton by degradation of vimentin. *Endocrinology* 144: 5530-5536.

Sienkiewicz, W., Szczurkowski, A., Dudek, A. and Kaleczyc, J., 2015. Innervation of the chinchilla testis, epididymis, and vas deferens. *Bulletin of the Veterinary Instute Pulawy*, 59: 547-555.

Simões L.S., Rici R.E.G., Favaron P.O., Sasahara T.H.C., Barreto R.S.N., Borghesi J. and Miglino, M.A., 2016. Ultrastructural analysis of the spermatogenesis in the guinea pig(*Cavia porcellus*).*Pesquia Veterinaria Brasileira* 36(1):89-94

Singh, I., 2011. Textbook of human histology with colour atlas and practical guide. Sixth edition. Jaypee Brothers Medical Publishers Ltd, New Delhi.

Skinner, J.D. and Smithers. R.H.N. , 1990. The mammals of the southern African subregion. Pretoria Univ. Press. Pretoria.

Sofroniew, M.V. and Vinters, H.V., 2010. Astrocytes: biology and pathology. *ActaNeuropathology* 119:7–35

Sohal, R.S. and Brunk, U.T., 1990. Lipofuscin as an indicator of oxidative stress and aging. In: Porta EA (ed.), Lipofuscin and Ceroid Pigments. New York: Plenum Press. p. 17-26.

Solari, A.J. and Tres, L., 1967. The ultrastructure of the human sex vesicle. *Chromosoma* 22: 16-31.

Soley, J.T., 1992. A histological study of spermatogenesis in the ostrich (*Struthio camelus*). Ph.D. Thesis, University of Pretoria, Pretoria.

Soro D., Karamoko Y., Kimse M. and Fantodji, A., 2014. Study of basic haematological parameters: indicators of the general state and immune competence in the male grasscutter (Thryonomys swinderianus, Temminck, 1827) bred in captivity in Côte d'Ivoire. *Journal of Animal and Plant Sciences*, 22 (1): 3379-3387.

Sosa, Z.Y., Palmada, M.N., Fóscolo, M.R., Capani, F., Conill, A. and Cavicchia, J.C., 2009. Administration of noradrenaline in the autonomic ganglia modifies the testosterone release from the testis using an ex vivo system. *International Journal of Andrology* 32(4):391–398.

Sousa, P. C., Santos, E. A. A., Souza, A. L.P., Lima, G. L., Barros, F. F. P. C.,Oliveira, M. F. and Silva, A. R., 2013. Sperm morphological and morphometric evaluation in captive collared peccaries (*Pecari tajacu*). *Pesquisa Veterinária Brasileira* 33(7): 924 – 930.

Speroff, L. and Fritz, M.A., 2005. Hormone biosynthesis, metabolism and mechanism of action. Weinberg, R.W., Murphy, J. and Pancotti, R. Clinical gynecologic endocrinology and infertility. 7th ed. Philadelphia, PA: Lippincolt Williams & Wilkins. p. 77-81.

Sprando, R.L. and Russell, L.D., 1987. Comparative study of cytoplasmic elimination in spermatids of selected mammalian species. *The American Journal of Anatomy* 178: 72-80.

Spruston, N., 2008. Pyramidal neurons: dendritic structure and synaptic integration. *Nature Review Neuroscience* 9(3): 206-221.

Steinberger, A. and Steinberger, E., 1976. Secretion of a FSH-inhibiting factor by cultured Sertoli cells. *Endocrinology* 99: 918-921.

Steinberger, E. and Steinberger, A., 1975. Spermatogenic function of the testis. In handbook of physiology. Vol. V. Endocrinology. Section 7, Male reproductive system. R.O Greep and E.B Astwood Eds. American Physiological Society, Washington, DC. pp. 1-19.

Steinert, P.M., Jones, J.C.R. and Jones, R.D., 1984. Intermediate filaments. *The Journal of Cell Biology* 99: 22-27.

Sullivan, R., Saez, F., Girouard, J. and Frenette, G., 2005. Role of exosomes in sperm maturation during the transit along the male reproductive tract. *Blood Cells, Molecules,and Diseases* 35(1): 1-10.

Tabatabaie, T. and Floyd, R. A., 1996. Protein damage and oxidative stress. In: Holbrook N, Martin, G.R, Lockshin, R.A (eds.), *Cellular Aging and Cell Death*. New York: Wiley-Liss. pp35-49.

Takano, H., 1980. Qualitative and quantitative histology and histogenesis of the mouse epididymis, with special emphasis on the regional difference. *Acta Anat (Nippon)* 55: 575-587.

Tamura, R., Mizumura, K., Sato, J., Kitoh, J. and Kumazawa, T., 1996. Segmental distribution of afferent neurons innervating the canine testis. *Journal of Autonomic Nervous System* 58:101–107.

Tegelenbosch, R. A. and de Rooij, D. G., 1993. A quantitative study of spermatogonial multiplication and stem cell renewal in the C3H/101 F1 hybrid mouse. *Mutation Research* 290: 193–200.

Teixeria, R.D., Veira, G.H.C., Colli, G.R. and Bao, S.N., 1999. Ultrastructural study of spermatozoa of the neotropical lizards, *Tropidurus semitaeniatus,* and *Tropidurus torquatus* (Squamata, Tropiduridae). *Tissue and Cell* 31 (3): 308-317.

Temminck, C.J., 1827.On a new species of the rodent family, forming the type of the genus. In: Dufour G. and d'Ocagne E (ed):*Monographs of some kinds of mammals, the species of which have been observed in the different museums of Europe*. Seventh Monograph, volume 1. Paris. Pp. 245-248, pl. XXV.

Toghyani, S., Dashti, G.R., Roudbari, N.H., Rouzbehani, S and Monajemi, R., (2013). Lithium carbonate inducing disorders in three parameters of rat sperm. *Advanced Biomedical Research* 2 (55): 1-6.

Toran-Allerand, C.D., Tinnikov, A.A., Singh, R.J., Nethrapalli, I.S., 2005. 17alpha-estradiol: a brain-active estrogen? *Endocrinology* 146(9):3843-50

Toshimori, K., 2009. Dynamics of the mammalian sperm head: modifications and maturation events from spermatogenesis to egg activation (Vol. 204). Springer Science & Business Media, Berlin Heidelberg, 11-39.

Toshimori, K. and Eddy E., 2014. The Spermatozoon. In: Plant, T.M. and Zeleznik, A.J. (ed.), Knobil and Neill's physiology of reproduction. Academic Press, San Diego, 99-136. Mortimer, 1997

Travison, T.G., Araujo, A.B., Kupelian, V., O'Donnell, A.B. and Mckinlay, J.B., 2007. The relative contributions of aging, health, and lifestyle factors to serum testosterone decline in men. *Journal of Clinical Endocrinology and Metabolism* 92 (2): 549-555.

Tripepi, S., Carelli, A., Perrotta, E., Brunelli, E., Tavolaro, R., Facciolo, R.M. and Canonaco, M., 2000. Morphological and functional variations of Leydig cells in testis of the domestic pig during the different biological stages of development.*Journal of Experimental Zoology* 287:167–175

Uboh, F. E., Akpanabiatu, M. I., Ekaidem, I. S., Ebong, P. E. and Umoh, I. B., 2007. Effect of inhalation exposure to gasoline on sex hormones profile in wistar albino rats.*Acta endocrinologica (buc)* 3(1): 23 -30

van der Merwe, M., 1999. Breeding season and breeding potential of the greater cane rat *(Thryonomys swinderianus)* in captivity in South Africa. Breeding season and breeding potential of the greater cane rat (*Thryonomys swinderianus*) in captivity in South Africa, *South African Journal of Zoology* 34:2, 69-73,

van Nassauw, L., Harrison, F. and Callebaut, M., 1993. Smooth muscle cells in the peritubular tissue of the quail testis. *European Journal of Morphology* 31, 60–64.

Varesi, S., Vernocchi, V., Faustini, M. and Luvoni, G.C., 2013. Morphological and acrosomal changes of canine spermatozoa during epididymal transit. *Acta Veterinaria Scandinavica.* 55:17

Villalpando, I., Villafan-Monroy, H., Aguayo, D., Zepeda-Rodriguez, A.,. Espitia, H.G. and Chavez-Olivares, A., 2000. Ultrastructure and motility of the caudal epididymis spermatozoa from the volcano mouse (*Neotomodon alstoni* Merriam, 1898). *The Journal of Experimental Zoology* 287 (4): 316-326.

Virtanen, I., Kallajoki, M., Närvänen, O., Paranko, J., Thornell, L.E., Miettinen, M. and Lehto, V.P., 1986. Peritubular myoid cells of human and rat testis are smooth muscle cells that contain desmin-type intermediate filaments. *Anatomical Record* 215: 10-20.

Vogl, T., Propper, C., Hartmann, M., Strey, A., Strupat, K., van den Bos, C., Sorg, C and Roth J. 1999. S100A12 is expressed exclusively by granulocytes and acts independently from MRP8 and MRP14. *Journal of Biological Chemistry* 274:2591-2596.

Vom Saal, F.S., Finch, C.E. and Nelson, J.F., 1994. The natural history of reproductive aging in humans, laboratory rodents, and selected other vertebrates. *In* E. Knobil (ed.), *Physiology of Reproduction.* 2nd ed. Chapter 61, Vol. 2, pp. 1213-1314. Raven Press, New York.

Wang, Y. F. and Holstein, A. F., 1983. Intraepithelial lymphocytes and macrophages in the human epididymis. *Cell Tissue Research* 233:517–21.

Wang, C., Leung, A. and Sinha-Hikim., A.P., 1993. Reproductive aging in the male Brown Norway rat: a model for the human. *Endocrinology* 133: 2773-2781

Wang, C., Sinha-Hikim., A.P., Lue, Y.H., Leung, A., Baravarian, S. and Swerdloff, R.S., 1999. Reproductive aging in the Brown Norway rat is characterized by accelerated germ cell apoptosis and is not altered by luteinising hormone replacement. *Journal of Andrology* 20 509–518.

Wang, E., Fischman, D., Liem, R. and Sun, T., 1985. Intermediate filaments. *Annals of New York Academy Science* 455: 635-648

Weber, J.E., Russell, L.D., Wong, V. and Paterson, R.N., 1983. Three-dimensional reconstruction of a rat stage Sertoli cell II. Morphometry of Sertoli and Sertoli-germ cell relationships. *American Journal of Anatomy* 167: 163-179.

Weiss, L., 1983. Histology, cell and tissue biology 5th edition. Elservier Science Publishing Co. inc, New York 10017, pp 1001-1053.

Wells, M. E. and Awa, O. A., 1970. New technique for assessing acrosomal characteristics of spermatozoa. *Journal of Diary Science* 53: 227.

Welsh, M., Saunders, P.T., Atanassova, N., Sharpe, R.M. and Smith, L.B., 2009. Androgen action via testicular peritubularmyoid cells is essential for male fertility. *FASED J*ournal 23: 4218- 4230.

Wheater, P.R., Burkitt., H.G. and Danels, V.G., 1990. Male reproductive system. In: Functional histology. A text and colour atlas. ELBS (2nd) edition, 18: 277-288.

Wicki, R, Schafer, B.W., Erne, P. and Heizmann, C. W. 1996. Characterization of the human and mouse cDNAs coding for S100A13, a new member of the S100 protein family. *Biochemical and BiophysicalResearch Communication* 227:594-599.

Wildt, D.E., Brown, J.L. and Swanson, W.F., 1999. Cats. In: Knobil E, Neill J (eds.), Encyclopedia of Reproduction, vol. 1. New York: Academic Press p. 497–510.

Woerdeman, J., Kaufman, J.M. and de Ronde, W., 2010. In young men, a moderate inhibition of testosterone synthesis capacity is only partly compensated by increased activity of the pituitary and the hypothalamus. *Clinical Endocrinology* 72 (1): 76-80.

Woods, C.A. and Kilpatrick, C.W., 2005. "Infraorder Hystricognathi". *In* Wilson, D.E.*;* Reeder, D.M (eds.). *Mammal Species of the World: A Taxonomic and Geographic Reference* (3rd ed.). Johns Hopkins University Press. p. 1545.

Wrobel, K.H. and Abu-Ghali, N., 1997. Autonomic innervation of the bovine testis. *Acta Anatomia* 160: 1-14.

Wrobel, K.H. and Fallenbacher, E., 1974.Histologische und histochemische untersuchungen am nebenhodenepithel erwachsener Eber. *Zuchthyg* 9: 20-31

Wrobel, K.H. and Bergmann, M., 2006. In: Eurell, J.A and Frappier, B.L. Dellmann's textbook of histology, 6th Ed. Blackwell Publishing Ltd. Iowa. 233-255.

Wrobel, K.H. and Moustafa, M.N.K. , 2000. On the innervation of the donkey testis. *Annals of Anatomy* 182:13-22.

Wrobel, K.H. and Schenk, E., 2003. Immunohistochemical investigations of the autonomous innervation of the cervine testis. *Annals of Anatomy* 185: 493-506.

Wrobel, K.H. and Brandl, B., 1998. Autonomous innervation of the porcine testis in the period from birth to adulthood. *Annals of Anatomy* 180: 145-156.

Wrobel, K.H., Schilling, E. and Dierichs, R., 1973. Enzymhistoche-mischeUntersuchungenan den Leydigzellen des Schweinesw~ihrend der postnatalenOntogenese. *Histochemie* 36: 321- 333

Wrobel K.H., Schilling, E. and Dierichs, R., 1974. Die Histochemie der Zwischenzellen im Schweinehoden wahrend der postnatalen Entwicklung. *Verhandlungen der Anatomischen Gesellschaft* 68: 247-249.

Yanagimachi, R., Kamiguchi, Y., Mikamo, K., Suzuki, F. and Yanagimachi, H., 1985. Maturation of spermatozoa in the epididymis of the Chinese hamster. *The American Journal of Anatomy*, 172: 317-330.

Yeboah, S. and Adamu, E.K. 1995. The cane rat. *Biologist*42: 86-87

Yeung, C. H., Cooper, T. G., Oberpenning, F., Schulze, H., and Nieschlag, E. 1993. Changes in movement characteristics of human spermatozoa along the length of the epididymis. *Biology of Reproduction* 49: 274–280.

Yeung, C. H., Nashan, D., Sorg, C., Oberpenning, F., Schulze, H., Nieschlag, E. and Cooper. T. G., 1994. Basal cells of the human epididymis- antigenic and ultrastructural similarities to tissue-fixed macrophages. *Biology of Reproduction* 50:917–26.

Yeung, C. H., Morrell, J. M., Cooper, T. G., Weinbauer, G. F., Hodges, J. K. and Nieschlag, E., 1996. Maturation of sperm motility in the epididymis of the common marmoset (*Callithrix jacchus*) and the cynomolgus monkey (*Macaca fascicularis*). *International. Journal of Andrology* 19: 113–121.

Yonemura, Y., Endou, Y., Kimura, K., Fushida, S.,Bandou, E., Taniguchi, K.,Kinoshita, K., Ninomiya, I., Sugiyama, K., Heizmann, C.W., Schafer, B.W. and Sasaki, T., 2000. Inverse expressionof S-100A4 and E-cadherin is associated with metastatic potential in

in gastric cancer. *Clinical Cancer Research* 6: 4234-4242

Young, B., Lowe, J.S., Stevens, A. and Health, J.W., 2006. Wheater's functional histology: A text and colour atlas. Fifth Edition, Churchill Livingstone, Elservier Limited. pp. 346-358.

Zamboni, Z., 1992. Sperm structure and its relevance to infertility: an electron microscopic study. *Archive of Pathology and Laboratory Medicine*, 116: 325-44.

Zayyed, A.E., Aly, K.H., Ibrahim, I.A. and Abd El-maksoud, F. M., 2012. Morphological studies on the seasonal changes in the epididymal duct of the one-humped camel (*Camelus dromedarius*). *Veterinary Science Development* 2(1): e3-e3.

Zemjanis, R.,1970. Collection and evaluation of semen. In: Diagnostics and Therapeutic techniques in animal reproduction, 2nd edition, Williams and Wilson Company. Baltimore, MD. pp. 139-156.

Zhang, L., Yang, P., Bian, X.and Zhang, Q., (2105). Modification of sperm morphology during long-term sperm storage in the reproductive tract of the Chinese soft-shelled turtle, *Pelodiscus sinensisScientific Report.* **5**: 16096

Zhao, L. and Burt, A.D., 2007. The diffuse stellate cell system. *Journal of Molecular Histology* 38:53–64

Zhu, L. J., Zong, S. D., Phillips, D. M., Moo-Young, A. J. and Bardin C. W., 1997. Changes in the distribution of intermediate filaments in rat Sertoli cells during the seminiferous epithelium cycle and postnatal development. *Anatomical Record* 248: 391–405.

Zirkin, B., Ewing, L., Kromann, N. and Cochran, R., 1980. Testosterone secretion by rat, rabbit, guinea pig, dog, and hamster testes perfused *in vitro*: correlation with Leydig cell ultrastructure. *Endocrinology* 107: 1867–1874